The role of Mef2 in *Drosophila* muscle development

Daniel H. Hancock

PhD Thesis

School of Biosciences
Cardiff University

ProQuest LLC
789 East Eisenhower Parkway
P.O. Box 1346
Ann Arbor, MI 48106-1346

DECLARATION

The work described in this dissertation was carried out in the Department of Biosciences, Cardiff University between October 2005 and September 2009. This work has not previously been accepted in substance for any degree and is not being concurrently submitted in candidature for any degree.

Signed ..... Date 30/09/09

STATEMENT 1

This thesis is being submitted in partial fulfilment of the requirements for the degree of Doctor of Philosophy (PhD).

Signed ..... Date 30/09/09

STATEMENT 2

This thesis is the result of my own independent work and investigation, except where otherwise stated. Other sources are acknowledged by explicit references.
This dissertation contains approximately 50,000 words, excluding references.

Signed ..... Date 30/09/09

STATEMENT 3

I hereby give consent for my thesis, if accepted, to be available for photocopying and for inter-library loan, and for the title and summary to be made available to outside organisations.

Signed ..... Date 30/09/09

Acknowledgements

Firstly, I would like to thank Dr.Taylor for his guidance and support throughout my time in his lab - he was always there for me when needed and I am very grateful for that. I would also like to thank him for all the interesting and enjoyable discussions we have had over the years, where he has always been encouraging of new ideas.

I would like to thank everyone in the lab past and present - Jun Han, Karen Wessel, Cedric Soler, Stuart Elgar and David Liotta you have all made the lab an enjoyable place to work; thank you for all the good times we have shared and also importantly your patience in answering my unending string of questions.

I would also like to thank all my friends in Cardiff who have all made my time here an especially happy one; Nick, Cathal, Mostyn, Lizzie, Rhodri, Kate, Gwen, Tom, Jude, Ced, Gav, Anna, Wendy D, Wendy F, Heather, Mark and Jade – thanks for all the good times.

Particular thanks to Tom, Mark, Wendy D and Wendy F for their help and support when I needed it most and especially to Olivia, who has been very supportive and understanding during all of these final stages of finishing my PhD.

Finally, I would like to thank my family, who have always supported me in whatever I have done. This thesis is for them.

Contents

List of Abbreviations

AMP : Adult Muscle Precursor

BDGP : Bloomington *Drosophila* Genome Project

bHLH : basic Helix Loop Helix

BLAST : Basic Local Alignment Search Tools

CDD : Conserved Domain Database

DGRC : *Drosophila* Genetic Resource Centre

DLM : Direct Longitudinal Muscle

DN : Dominant Negative

DNA : Deoxyribonucleic Acid

FCM : Fusion Competent Myoblast

FRT : Flippase Recognition Target

HEI : Hybrid Element Insertion

HTH : Helix Turn Helix

GFP : Green Fluorescent Protein

MADF : Myb-like domain found in Adf1

MADS : MCM1, Agamous, Deficiens and SRF

NEB : New England Biolabs

OR : Oregon R (wild type fly strain)

PCR : Polymerase Chain Reaction

RNAi : Ribonucleic Acid Interference

SANT : Swi3, Ada2, N-CoR, TFIIIB

SDM : Site Directed Mutagenesis

UAS : Upstream Activation Sequence

VDRC : Vienna *Drosophila* RNAi Centre

Genes

Act57B : Actin 57B

Ada2 : Adapter Protein 2

ap : apterous

Bap : Bagpipe

Duf : Dumbfounded

Dpp : Decapentaplegic

EcR : Ecdysone Receptor

Eve : Even-Skipped

hh : Hedgehog

Him : Holes in Muscle

Kr : Kruppel

l(1)sc : Lethal of Scute

Mef2 : Myocyte Enhancer Factor 2

Meso18E : Mesodermal gene in region 18E

MCM1 : Mini Chromosome Maintenance 1

MHC / Mhc : Myosin Heavy Chain

Msh : Muscle Segment Homeobox

N-CoR : Nuclear Receptor Co-Repressor

Slp : Sloppy-Paired

sns : sticks and stones

SRF : Serum Response Factor

Su(H) : Suppressor of Hairless

Swi3 : Switching Defective Protein 3

TFIIIB : Transcription Factor III B

Tin : Tinman

Wg : Wingless

Zfh1 : Zinc Finger Homeodomain 1

Summary

Muscle differentiation is a complex process involving the transition from undifferentiated mesoderm to a final functional musculature. Mef2 is an essential positive regulator central to the co-ordination of this process. It targets a plethora of key genes both early and late in the differentiation program and its activity must be tightly controlled (Pothoff and Olson, 2007).

The aim of my research was to investigate the role of Mef2 in orchestrating *Drosophila* muscle differentiation. I did this by analysing the formation of the larval somatic musculature under conditions that either increased or decreased Mef2 activity using gain and loss-of –function of either; Mef2 itself, Him, a repressor of Mef2 activity (Liotta et al, 2007) or of Zfh1, a potential regulator of *Mef2* expression (Postigo et al, 1999). Part of this investigation involved the generation and characterisation of Mef2 dominant negative proteins and isolation of a *Him* mutant.

Detailed analysis revealed a distinct subset of somatic muscles that are missing when Mef2 activity is reduced and another subset of muscles that are duplicated when Mef2 activity is increased. This suggests a role for Mef2 in patterning of the musculature that has not been established previously. In addition, I identified a role for Mef2 in the regulation of *Him* expression, revealing a mechanism whereby Mef2 could be involved in its own repression.

I also investigated the role of *meso18E* in muscle differentiation; a previously uncharacterised novel gene identified as an early target of Mef2 (Taylor, 2000). I found this to be a Myb-like domain containing protein that is a direct target of Mef2. Over-expression caused a severe disruption to the somatic musculature, revealing a potential role for meso18E in muscle guidance. Generation of *meso18E* mutant alleles by FRT element mediated recombination showed the gene to be essential for development.

Introduction

1.1 *Drosophila* as a model organism.

I have used genetics and molecular biology techniques to study muscle development in the fruit fly, *Drosophila melanogaster.*

Drosophila was first used as a model organism for scientific research 100 years ago (Morgan, 1910), and during this period its use led to many of the key principles of classical genetics being first established (Ashburner et al, 2004).

Drosophila is a small, yet fascinatingly complex organism, which is fecund, fertile all year round, cheap to maintain and has a temperature dependent life cycle of around twelve days. The life cycle is shown in FIG 1.1. Male and female adult flies are clearly distinguishable and after mating the females lays the fertilised embryos externally. The embryo then undergoes embryogenesis; the development of all the structures required for larval life. As the embryo is external to the female parent each of the stages of embryogenesis can be easily studied as development occurs. At the final stage of embryogenesis the newly formed larva is ready to hatch and after doing so undergoes three growth cycles; passing through three larval instar stages. During these instar stages the larva undergoes considerable growth and a build up of energy stores until it is ready to undergo pupation, where it will metamorphose and finally eclose, emerging as an adult fly.

These aspects of *Drosophila* biology make it attractive for use as a laboratory organism, but it is the genetics, the genetic manipulability and the number of techniques established over these last 100 years that truly makes *Drosophila* a super model organism for scientific research.

D.melanogaster has a relatively small genome of around 180Mb, consisting of approx 13,600 genes which are divided among four chromosomes; the X chromosome, two main

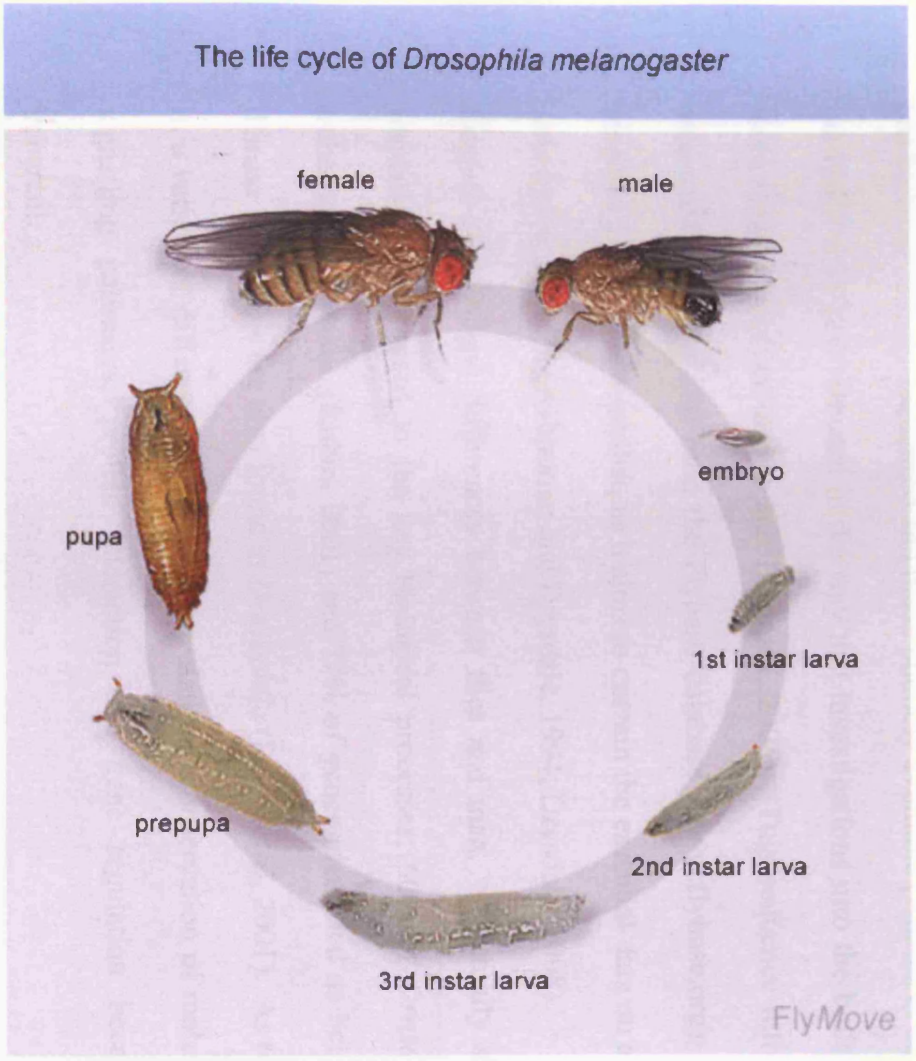

FIG 1.1 The life cycle of *Drosophila melanogaster*

Image taken from flymove (Weighmann et al, 2003)

autosomes (II and III) and an additional small autosome (IV) (Adams et al, 2000; Greenspan, 1997). Through the use of well-established collections of visible markers and balancer chromosomes, which prevent recombination from occurring, the inheritance of these chromosomes can be traced from parent to progeny in each generation and so particular genes of interest can be traced (Ashburner et al, 2004).

Along with other *Drosophila* species, the euchromatic genome of *Drosophila melanogaster* has been completely sequenced and made publicly available (Adams et al, 2000) and this marked a huge step forward in the way that investigations into the biology of *Drosophila* were approached (Ashburner and Bergman, 2005). This sequence information has been annotated and collected onto the Flybase database (www.flybase.org), which is the key resource for any Drosophilist, as it aims to contain the essential data on all the genes in the *Drosophila* genome (Ashburner and Drysdale, 1994; Drysdale, 2008).

Despite the obvious differences between flies and man, we actually share considerable similarity with regard to the key biological processes; 60% of *Drosophila* genes have orthologs in humans (Rubin, 2001) and 77% of genes identified as being responsible for disease in humans are also found in *Drosophila* (Reiter et al, 2001). As research progresses in a variety of different organisms the evolutional conservation of molecular components, signalling pathways, protein interaction and gene regulation becomes increasingly apparent.

Drosophila is an organism of great genetic manipulability. As an invertebrate it generally has only one copy of each gene in its genome and thus it has proven relatively straight forward in achieving large numbers of gene deletion mutants, be this through large scale screens for a particular phenotype, where random mutagenesis is achieved through the use of chemical or ionising damage or through the action of transposable elements, or through

the direct targeted deletion of a known gene of interest. The generation of gene deletions in vertebrate models, which not only is more difficult than gene deletion in *Drosophila* is also repeatedly problematic due to the fact that often a gene has multiple copies, with degrees of functional redundancy between them.

1.2 Techniques in *Drosophila* research.

Throughout its period of study a number of key techniques for investigating the function, significance, interaction and regulation of a gene have been developed. Outlined below are key experimental techniques that have been essential to my PhD.

1.2.1 Gene Over-expression / Gain-of-Function :

Of particular note is the Gal4 UAS expression system (Brand and Perrimon, 1993), which allows the ectopic expression of a transgene construct in any specific pattern in the organism to investigate the role of a gene. FIG 1.2 shows a schematic of how the Gal4 UAS system works. It enables the researcher to ectopically express any gene with both spatial and temporal control and also control of the levels of the protein being over-expressed and the significance of this technique cannot be stressed enough. For a review of Gal4 UAS applications see Duffy, 2002.

1.2.2 Gene Expression pattern visualisation:

The localisation of either the RNA transcript of a particular gene or the protein product of a gene can be traced and visualised through the use of RNA in-situ hybridisation (Lehmann and Tautz, 1994) or protein immuno-histochemistry using specific antibodies (Lang et al,

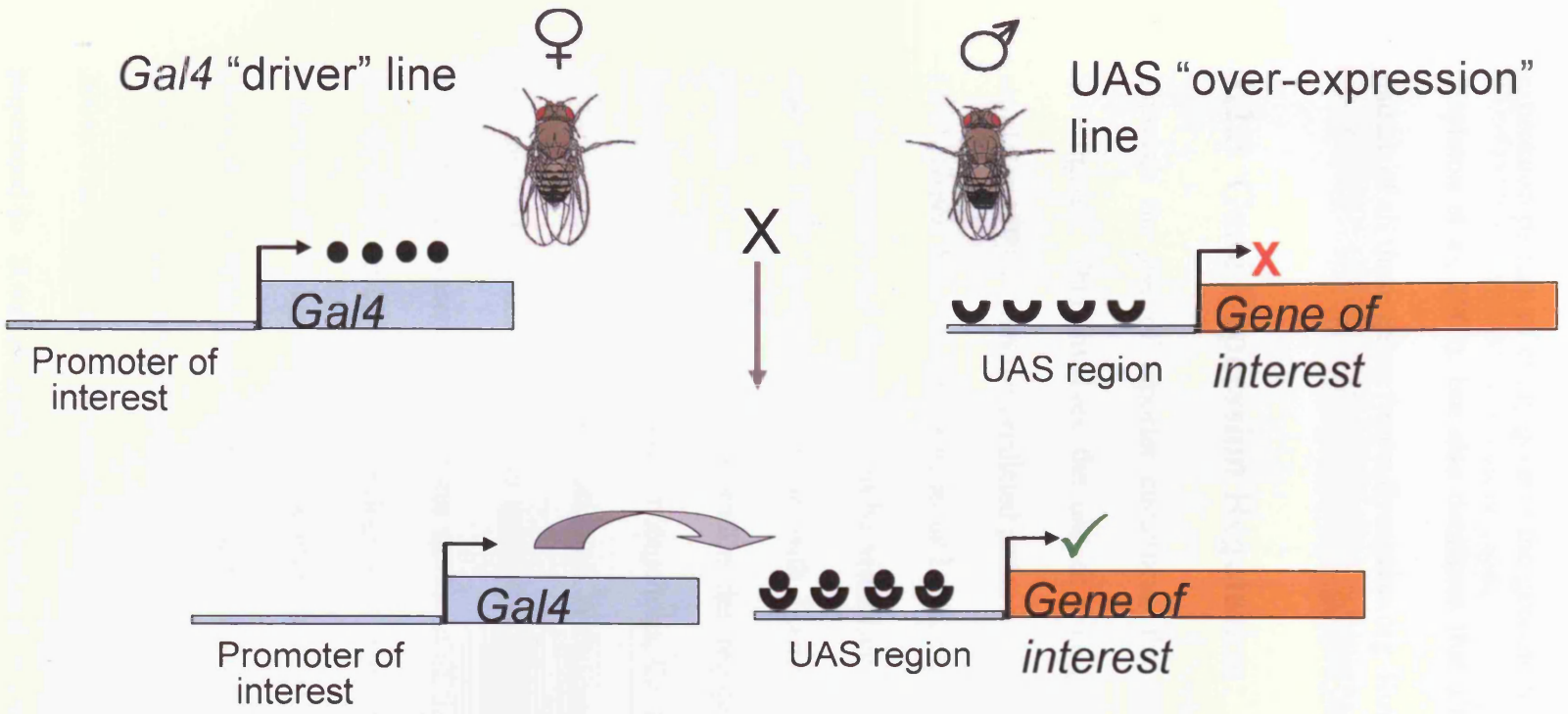

FIG 1.2 The Gal4 UAS expression system in *Drosophila*

By using the Gal4 UAS system, gene expression can be targeted to specific regions at any place or time within the flies' development.

The system makes use of two yeast (*S.cerevisiae*) specific components that are introduced into the fly transgenically; the transcription factor Gal4 and the sites that the Gal4 transcription factor binds to – the Upstream Activation Sequence (UAS). Through these factors any gene of interest can be expressed in any pattern of interest.

The system works through two indivdual trangenic lines that must be brought together in a genetic cross to activate. One line, the Gal4 driver line, contains the promoter of gene interest which will drive the Gal4 transcription factor in the promoter's specific pattern. The other line, the UAS over-expression line, contains the gene of interest to be over-expressed. The gene of interest contains a series of Gal4 binding sites upstream of it and will only be expressed in the presence of the Gal4 protein. Consequently the gene of interest is only expressed in the pattern of the promoter of interest.

The Gal4 UAS system is temperature sensitive, with more Gal4 protein being expressed at higher temperatures and consequently the level of expression of the gene of interest can be controlled.

(Figure adapted from Brand and Perrimon, 1993 and Duffy, 2002)

1980). Through RNA in-situ hybridisation the expression pattern of a gene can be traced and there exists databases that aim to not only provide the appropriate cDNA to allow the expression pattern of every gene in the genome to be traced in this way (www.fruitfly.org, Stapleton et al, 2002), but also databases that aim to provide images for the expression pattern of all these genes (www.flyexpress.org Kumar, 2009).

1.2.3 Gene Expression Regulation:

Through the use of reporter constructs, the expression regulation of a gene can be investigated. This involves the use of transgenic constructs which place a region of regulatory DNA from the predicted promoter of a gene upstream of a reporter gene such as *GFP (Green Fluorescent Protein)* or *LacZ*; the promoter sequence then drives expression of the reporter and this can then be visualised by either immuno-histochemistry or in the case of GFP direct visualisation with fluorescence (Ashburner et al, 2004). Through analysis of transcription sites within the regulatory region and manipulation through techniques such as site directed mutagenesis, the key transcription factors involved in the expression of a gene can be elucidated. A further aspect of the study of gene expression regulation is the use of *in-silico* transcription factor binding site searches within areas of phylogenetic conservation to form the basis of this reporter construct design (see Zhang and Gerstein, 2003 review). Phylogenetic footprinting to identify sequence conservation makes use of the complete genomic sequences established for a number of distantly-related *Drosophila* species and through alignment and comparison of equivalent DNA regions across these species regions can be identified that are evolutionarily conserved (Grad et al, 2004). The evolutionary distance between even the most closely related *Drosophila* species sequenced to *D.melanogaster* (*D.simulans*) is around 3 million years (Russo et al, 1995), whereas the most distantly related species to *D .melanogaster* sequenced (*D. mojavensis*) is

around 50 million years or (Russo et al, 1995), or the equivalent evolutionary distance between mouse and man (Hartl and Lozoskaya, 1994) and as a result of this any conservation in non-coding DNA sequence (where there is a greater degree of tolerated mutation and sequence variation than coding DNA), suggests that this site may be of particular importance, and as such is often indicative of the sites of key transcription factor binding sites involved in the regulation of the gene. The Vista tools website is a key program for phylogenetic footprinting in *Drosophila* (Frazer et al, 2004).

1.2.4 Gene Loss-of-Function :

In genetics, the classical way of understanding the function of a gene is through the isolation and characterisation of a mutant. Traditionally this was achieved through the random mutagenesis of the whole genome using either ionising radiation, chemicals or the mobilisation of transposable elements, followed by the subsequent screening of all the mutant lines for an effect upon a particular process (see St.Johnson, 2002 for review). Though such techniques have identified a large number of key developmental genes (for example, Nüsslein-Volhard and Wieschaus, 1980) and provided huge advances in the understanding of developmental biology, these forward genetics screens are laborious and as time goes on the same mutants are repeatedly isolated instead of novel genes of interest being hit.

Consequently with the advent of both the annotated genome sequence (Adams et al, 2000; Drysdale, 2008) and recent advances in molecular recombination techniques such as FRT element mediated recombination (Parks et al, 2004; Ryder et al 2005) and homologous recombination (Rong and Golic, 2000) a gene that is already known to be of interest (for example due to its expression pattern or a phenotype associated with its over-expression) can be specifically targeted for deletion. Such targeted deletion, or reverse genetics, marks

a significant step forward for the relatively straight forward generation of specific mutants (Adams and Sekelsky, 2002; Venken and Bellen, 2005).

In addition to this, the technique of RNAi (RNA interference), that was first discovered in *C.elegans* (Fire et al, 1998), can be used in *Drosophila* (Reichhart et al, 2002; Kavi et al, 2008) to knock down the RNA transcripts of a specific targeted gene, and consequently reduce that genes RNA and subsequent protein levels. This technique can be used as part of the Gal4 UAS system (Brand and Perrimon, 1993), such that a gene can have its expression levels reduced in a spatial and temporal manner as well as increased in this way through use of a regular UAS construct (Duffy, 2002). Recently, large scale projects have been undertaken which aim to provide stocks containing RNAi transgenic lines corresponding to every gene in the genome (Dietzl et al, 2007 and NIG-FLY, Japan).

As part of my PhD thesis I generated and characterised mutations in specific genes of interest using P-element mediated recombination and characterised other mutant lines that were generated by homologous recombination in collaboration with another lab.

These two techniques are outlined below.

1.3 Transposable Elements

Transposable elements are autonomous mobile units that mediate their transposition through the enzyme transposase. They are parasites of DNA which can cause mutation and genome change and are capable of both vertical (from parent to offspring) and horizontal (from one organism to another, sometimes one species to another) transmission (Engels, 1983; Kidwell, 1983; Kidwell,1985).

P elements are a Type II Transposon family which only invaded *Drosophila* around 200yrs ago but has now eventually spread through all populations (entering *Drosophila melanogaster* only around 100yrs ago). Because the invasion has been relatively recent, there exist original laboratory strains of *Drosophila melanogaster* (M strain) which contain no P-elements (Kidwell 1983; Engels, 1992).

The isolation and manipulation of P-elements have allowed them to be developed as a geneticist's tool for generating gene mutation. By combining an immobile transposase enzyme with a mobile non-autonomous element, one single element put into an M strain fly can be allowed to make one jump to a region at random within the genome. In doing so this element may land in a gene and disrupt its function. That element can then be mapped to determine its new position in the genome (Spradling et al, 1995; Castro and Carareto, 2004). This has been the basis for a number of forward genetics screens using P elements and other types of transposable element to generate new mutants (for review see Bellen et al, 2004).

The transposition of an element in the genome is not entirely random; there is an apparent preference for particular regions of DNA, and certainly an avoidance of heterochromatin, which may reflect the accessibility of the DNA (Berg and Spradling, 1991). To try to maximise the number of different insertions a large number of transposition events have been performed using different types of element starting from a number of various initial positions to transpose from (Bellen et al, 2004).

Recently a number of key efforts have been made to generate transposable element stocks that will achieve an insertion in every gene in the genome. The three main insertion projects are The Berkeley *Drosophila* Genome Project (Bellen et al, 2004), the European DrosDel project kept at Cambridge and Szeged (Ryder et al, 2004), and the Exelixis collection kept at Harvard Medical School (Thibault et al, 2004) .With a screen specific to

the X chromosome (Beinert et al, 2004) and the *Drosophila* Genetic Resource Center (Kyoto Japan) also making contributions.

It was initially observed that it is possible to achieve transposition between the 5' end of one element and the 3' end of another which was adjacent to it. Such Hybrid Element Insertion (HEI) allows for the transposition of the endogenous DNA between the elements (Grey et al, 1996).

The subsequent development of a technique that used the basis of this observation to allow for a combination of elements on different copies of a chromosome, *trans* – heterozygous P-element deletion (Gubb et al, 1997) opened up the potential for achieving deletion of a gene region between two elements, by simply crossing two lines together, instead of the previous complicated process of acquiring the elements on the same chromosome first for HEI (Ryder and Russell, 2003 review).

A significant development involving the DrosDel and Exelixis collections is that the element they used were designed in a way that allows for detectable trans- recombination between two different elements (Golic and Golic, 1996; Thibault et al, 2004). This achieves a deletion of the DNA between two elements mediated by recombination through appropriately orientated FRT sites within the element (Ryder and Russell, 2003).

Consequently through the combination of two different pre-established single insertion lines, a vast number of deletions become possible (Ryder et al, 2004; Parks et al, 2004). These can generate anything from a partial deletion of a gene to the removal of large portions of a chromosome, causing the deletion of hundreds of genes at one time. The main limiting factor is that the FRT sites in the elements must be in the same orientation to be compatible for a recombination event between them. This is not always the case, as when an element jumps it can land in either orientation in the genome.

1.4 Homologous Recombination.

For the maintenance and viability of a genome it is essential that the DNA repair and recombination machinery of a cell acts to repair any double strand breaks it detects in the DNA. It achieves this in part through using the intact homologous DNA on the other chromosome as a template. The occurrence of this defence process can be exploited to achieve targeted gene deletion, duplication or disruption through the introduction of open ended DNA containing regions of homology to the gene of interest.

Such gene targeting through homologous recombination has been welcomed in the field of genetics, as it allows for the specific deletion of a gene already established to be of interest (reverse genetics), when previously a mutant could only be achieved through laborious screens using chemicals, radiation or transposable elements (forward genetics) (reviews Adams and Sekelsky, 2002; Venken and Bellen, 2005).

This technique had been well established in a number of model systems such as mouse and yeast (Orr-Weaver et al, 1981; Jasin and Berg, 1988) but proved more difficult in *Drosophila*. Only recently has it been successfully achieved (Rong and Golic, 2000), after finding difficulties in efficiency when using the male germline (Bellaiche et al, 1999). It has subsequently been developed in different ways as a means of generating gene deletion, duplication or point mutation (Rong and Golic, 2001; Rong et al, 2002; Gong and Golic, 2003; Xie and Golic, 2004) and shown to be capable of generating targeted deletions as large as 47Kb (Gong and Golic, 2004).

There are two established approaches for homologous recombination; Ends In and Ends Out. Ends In results in a gene duplication, which can subsequently be reduced to a single copy through *CreI* activity (Xie and Golic, 2004). Ends Out achieves gene deletion through

replacement with a marker gene (Gong and Golic, 2003). The nomenclature refers to the direction the arms of the construct point when the recombination event occurs (FIG 1.4.1). Briefly, the Ends Out gene replacement technique (FIG 1.4.2) involves the use of an introduced construct which contains FRT sites (for mobilising the injected construct once in the genome), an *I-SceI* cut site (for generating a double strand break in the mobilised construct), and a *w+* marker gene flanked by two arms of homology. These arms are homologous to the regions of endogenous DNA flanking the gene you want to delete. The FRT site and *I-SceI* site are specific to the yeast, *Saccharomyces cerevisiae* and are activated or cut through the Flp recombinase (Flippase) and I-SceI enzymes respectively; both of which are heat-shock inducible and introduced into the genome by appropriate crossing (see Materials and Methods). When a successful recombination event occurs the endogenous gene is deleted, being replaced with a *w+* marker gene from the construct (see FIG 1.4.2). The event is traced by following the effect of the *w+* marker on eye colour and then confirmed by PCR or Southern blot hybridisation to the gene region.

It is these techniques for gene deletion and those outlined above for gene functional and transcriptional analysis that I will use to investigate the roles of two novel genes involved in muscle differentiation in *Drosophila.*

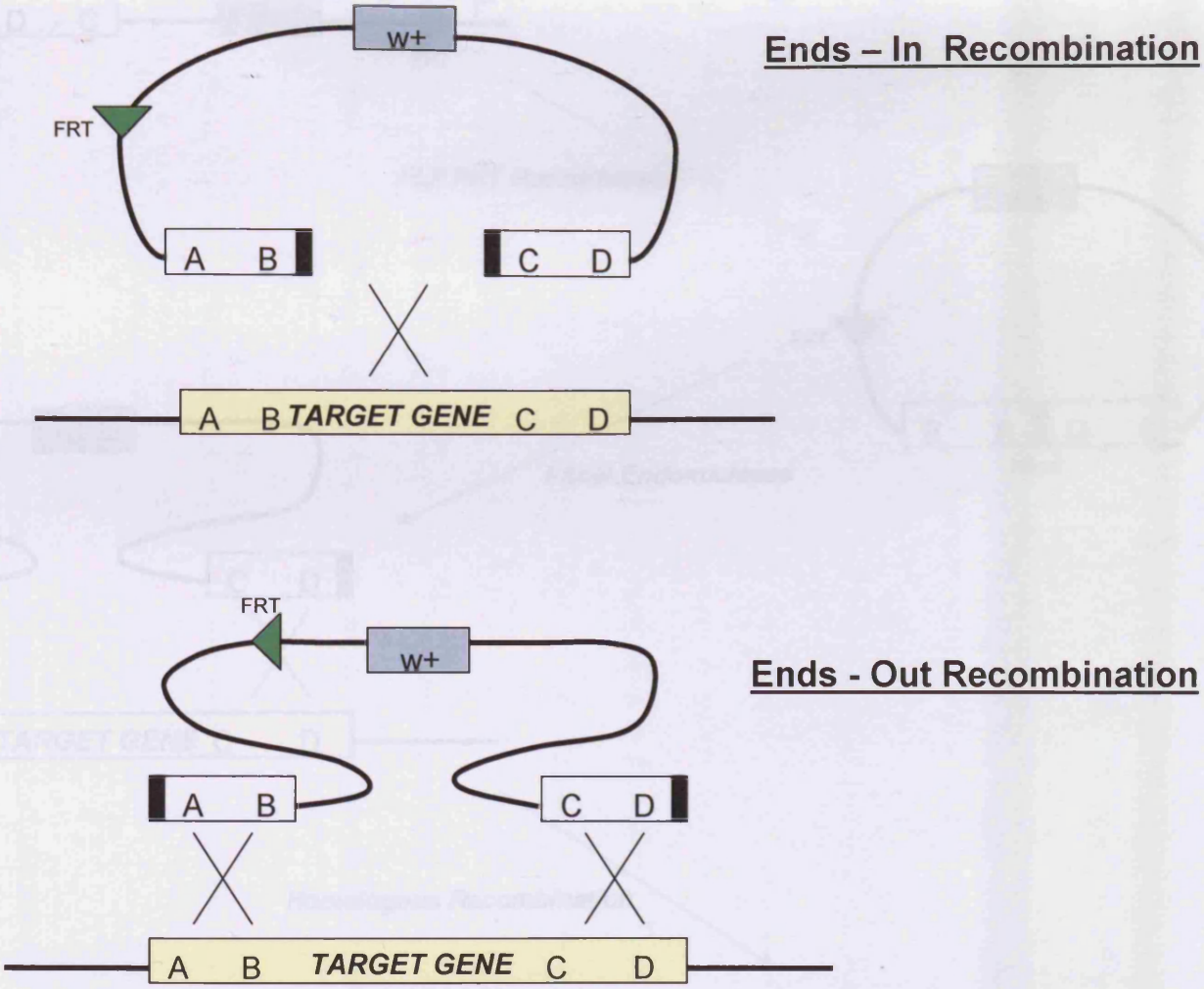

FIG 1.4.1 Ends In and Ends Out Targeting in Homologous Recombination

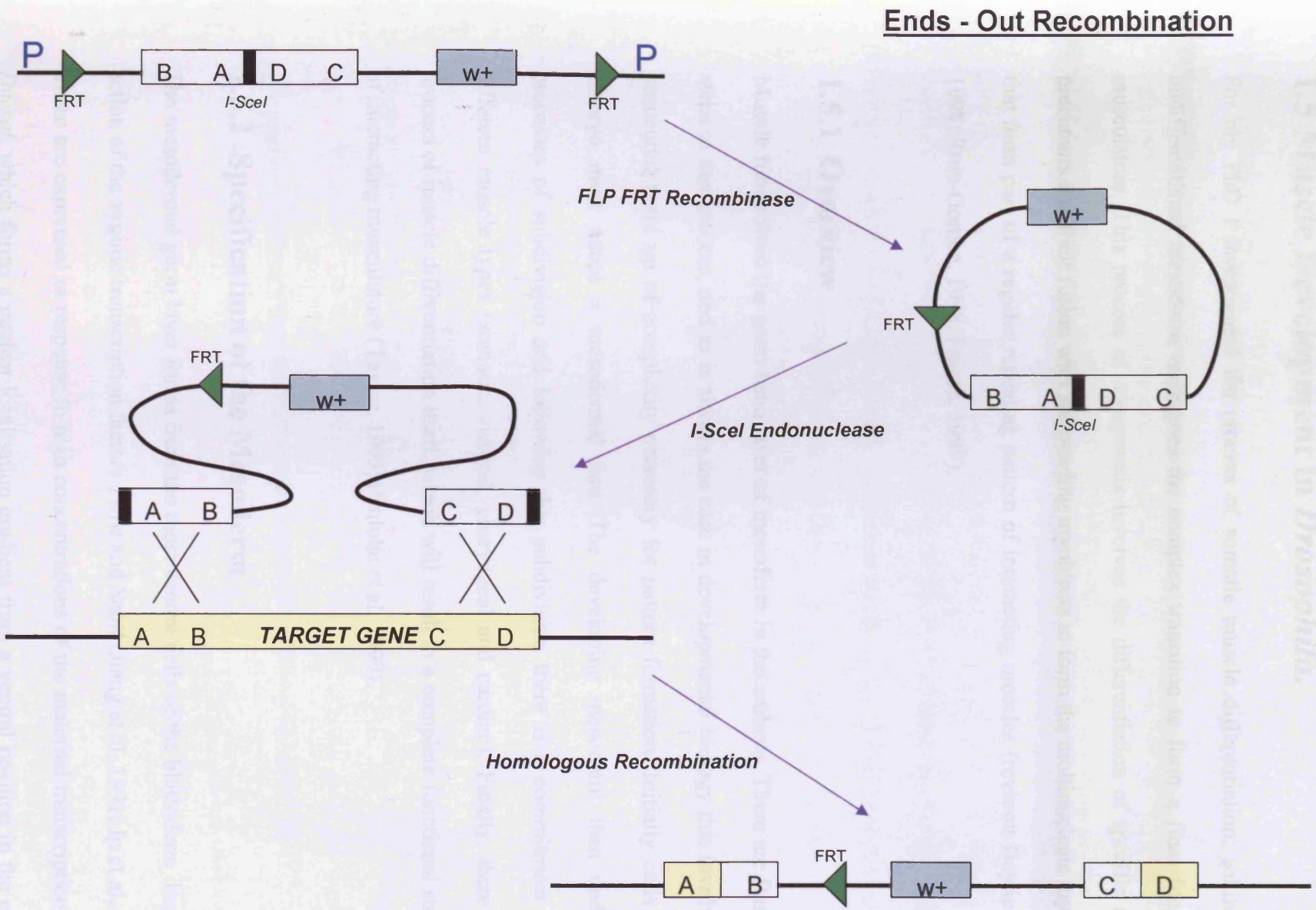

FIG 1.4.2 Homologous Recombination by the Ends Out method

1.5 Muscle Development in *Drosophila.*

For my PhD I investigated the process of somatic muscle differentiation; asking how undifferentiated mesoderm undergoes the complex transition to form a final functional musculature. This process of myogenesis involves the differentiation of specific muscle precursors and their fusion with surrounding myoblasts to form the multinucleate myotubes that form part of a regular repeating pattern of interacting muscles (reviews Baylies et al, 1998; Ruiz-Gomez, 1998; Frasch, 1999).

1.5.1 Overview

Muscle forms from the germ band layer of mesoderm in the embryo. There are four main steps to this process, and as is always the case in developmental biology this involves the sequential build up of complexity necessary for pattern formation. Initially cells in the embryo must adopt a mesodermal fate. The developing mesoderm then undergoes processes of subdivision and following this subdivision there is a commitment of the different muscle types (somatic, visceral, pharyngeal and cardiac). Finally, there is the process of muscle differentiation itself, which will result in a complete functional structure of interacting musculature (Taylor, 1995; Paululat et al, 1999).

1.5.2 Specification of the Mesoderm

The mesodermal germ layer forms from the most ventral cells of the blastoderm due to the action of the zygotic transcription factors *Twist* and *Snail* (Jiang et al, 1991; Ip et al, 1992). These are expressed in response to high concentrations of the maternal transcription factor *Dorsal,* which forms a nuclear localisation gradient from a ventral position in the embryo

(Jiang et al, 1991; Pan et al, 1991). Both *Twist* and *Snail* are essential for the formation of the mesoderm (Leptin, 1992) and *Twist* is expressed in all the cells of the mesoderm and its derivatives (Thisse et al, 1988). During gastrulation these *Twist* expressing cells invaginate along the ventral midline then migrate dorsally forming a monolayer just beneath the overlying ectoderm (Leptin and Grunewald, 1990).

Initially the mesoderm at this stage is uniform, with all cells expressing the bHLH transcription factor *Twist* at the same level (Thisse et al, 1987) and also as a result expression of the direct Twist targets; the muscle specific transcription factors Mef2 and Tinman which are now activated is also uniform (Lilly et al, 1995; Taylor et al, 1995; Azpiazu and Frasch, 1993). Subsequently there is a subdivision to the mesoderm that causes the levels of *Twist* expression in the mesoderm to become modulated, which has a crucial effect on the assignment of cells in adopting different muscle types (Baylies and Bate, 1996; Taylor, 1996 review).

1.5.3 Subdivision of the mesoderm.

The subdivision of the mesoderm results from a combination of regulatory factors which are extrinsic and intrinsic to the mesoderm (Baylies and Bate, 1996). This subdivision occurs along both the dorsal-ventral axis and the anterior-posterior axis. The ectoderm overlying the dorsally-located mesodermal monolayer secretes a series of extrinsic signals which effect cell fate and pattern the mesoderm, Decapentaplegic (Dpp), Wingless (Wg) and Hedgehog (hh) signalling molecules are all secreted in this way and these factors are conserved in both their form and function in mesoderm specification in vertebrates and invertebrates (review Baylies et al, 1998). Dpp in this manner plays a role in subdivision of

the dorsal-ventral axis through maintenance of *Tinman* expression dorsally (Frasch, 1995; Maqbool and Jagla, 2007 review).

Additionally, a subdivision of the mesoderm occurs along the anterior posterior axis through the action of the pair rule genes *Even-skipped (Eve)* and *Sloppy Paired (Slp)* which are both intrinsic to the mesoderm. *Eve* is required for the formation of the anterior mesodermal derivatives; visceral muscle and fat body - *Eve* mutants fail to form these structures (Azpiazu et al, 1996) and *Slp* is required for the formation of the posterior mesodermal structures; the somatic and heart muscle – which *Slp* mutants fail to form (Riechmann et al, 1997). The action of these factors is associated with a modulation of *Twist* expression; high levels of Twist are maintained in the Slp domain and low levels of Twist occur in the Eve domain (Dunin-Borkowski et al, 1995).

As mentioned above, extrinsic Dpp signalling maintains Tinman signalling dorsally (Frasch, 1995) in addition Hh signalling acts upon the anterior region of the embryo maintaining *Bagpipe* (*Bap*), a gene required for visceral muscle formation (Azpiazu et al, 1996) and Wg reinforces the difference between the Eve and Slp domains through maintaining high levels of Twist in the Slp domain (Reichmann et al, 1997).

It is this combination of D/V and A/P mesodermal subdivision that allows the specification of the three different muscle types; somatic, visceral, and cardiac and also the fat body according to the four domains in a segment. Cells which are in the Slp domain express high levels of *Twist* and if they are also positioned dorsally and receive sufficient Tinman signals from the overlying ectoderm, they will adopt a cardiac fate. Cells in the Slp domain that are positioned more ventrally and do not receive the Tinman signal adopt a somatic muscle fate. Similarly cells in the Eve domain are divided by their dorsal and ventral position; dorsally positioned cells in this domain will become visceral muscle, whereas those located ventrally will become fat body (Reviewed Maqbool and Jagla, 2007).

1.5.4 Somatic muscle development

It is from this point of D/V and A/P mesodermal subdivision that the somatic muscle begins to be specified. The larval somatic musculature consists of a regular, repeating pattern of thirty interacting individual muscles in each abdominal hemi-segment (Bate, 1990). These muscles are multinucleate myotubes which are attached to the cuticular exoskeleton at points specific to each individual muscle (Bate, 1990; Frasch 1999 review). Though each individual somatic muscle is similar with respect to physiological and structural characteristics (Bate and Rushton, 1993) there are distinct morphological differences between each individual muscle in terms of shape and size, position and orientation within the abdomen, attachment sites and motorneuron innervation (Bate, 1993; Ruiz-Gomez, 1998; Frasch, 1999). It is through analysis of these characteristics that an assessment of correct somatic muscle differentiation can be made. FIG 1.5.1 and FIG 1.5.2 shows the somatic musculature with a figure from Bate, 1993 showing each of the 30 individual somatic muscles.

The formation of an individual somatic muscle from the specified somatic mesoderm can be divided into a number of key stages;

- specification of a muscle progenitor cell from a uniform population of cells within the "somatic muscle domain" by lateral inhibition
- asymmetric division of the progenitor to form at least one muscle founder cell
- the recruitment of fusion competent myoblasts (FCMs) to a single founder cell, their fusion to the founder cell and the subsequent development of a multinucleate myotube
- extension of this developing myotube towards tendon cell attachment sites in the epidermis

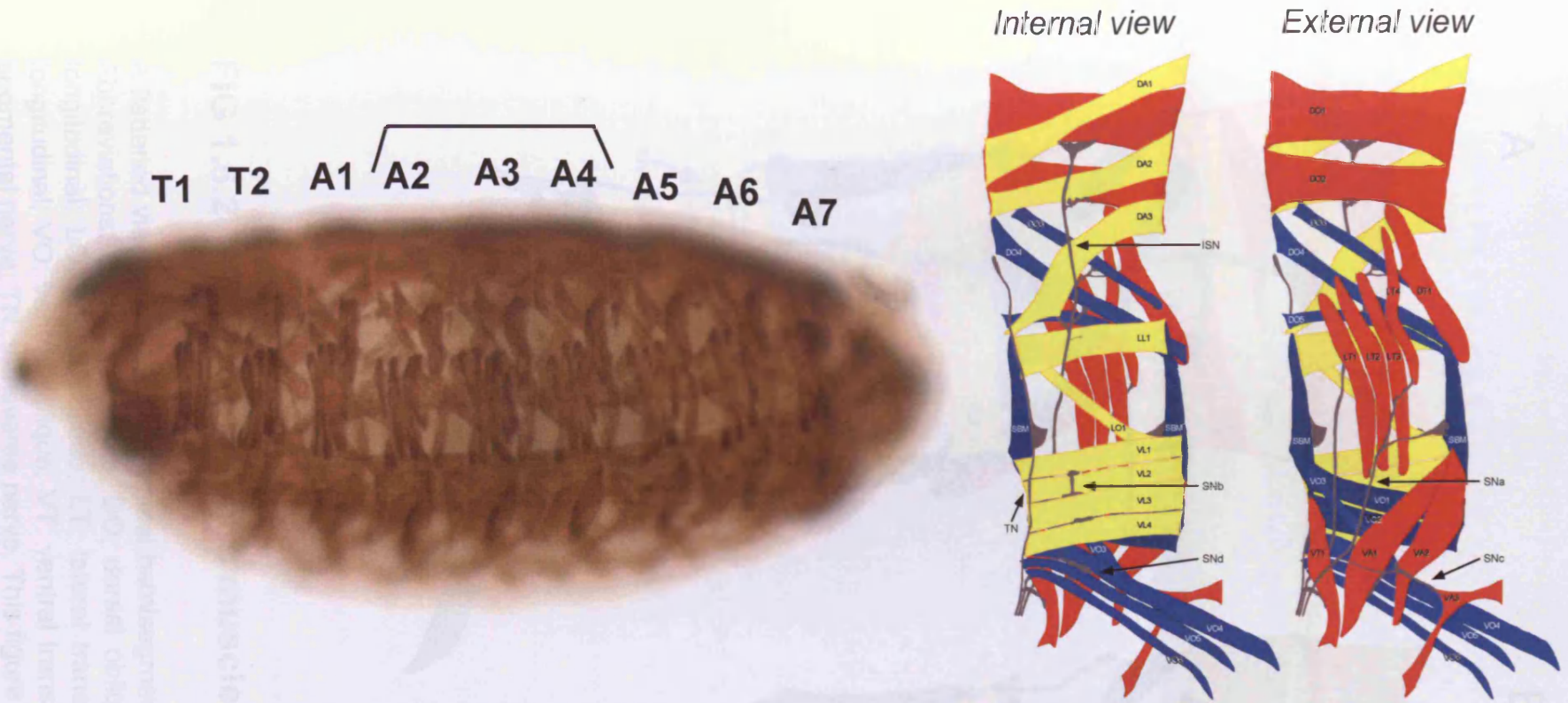

A) Stage 17 embryo (anti β3 tubulin)

B) Abdominal hemi-segment (30 muscles)

FIG 1.5.1 Somatic musculature of the St17 embryo

A) Stage 17 wild type embryo stained with anti-β3 tubulin antibody to visualise the somatic musculature. Embryo is viewed laterally and muscles focussed in an external plane. The embryo is divided into thoracic and abdominal hemi-segments. Abdominal hemi-segments A2-A7 contain the same pattern of 30 individual muscles, a schematic of which are shown in B)

B) Schematic of the 30 individual muscles of an abdominal hemisegment (A2-A7) showing an internally focussed and an externally focussed view of the muscles. Each muscle has a unique shape, size, position, attachment and innervation characteristics which are specific to that muscle type (Image from Bate, 1993).

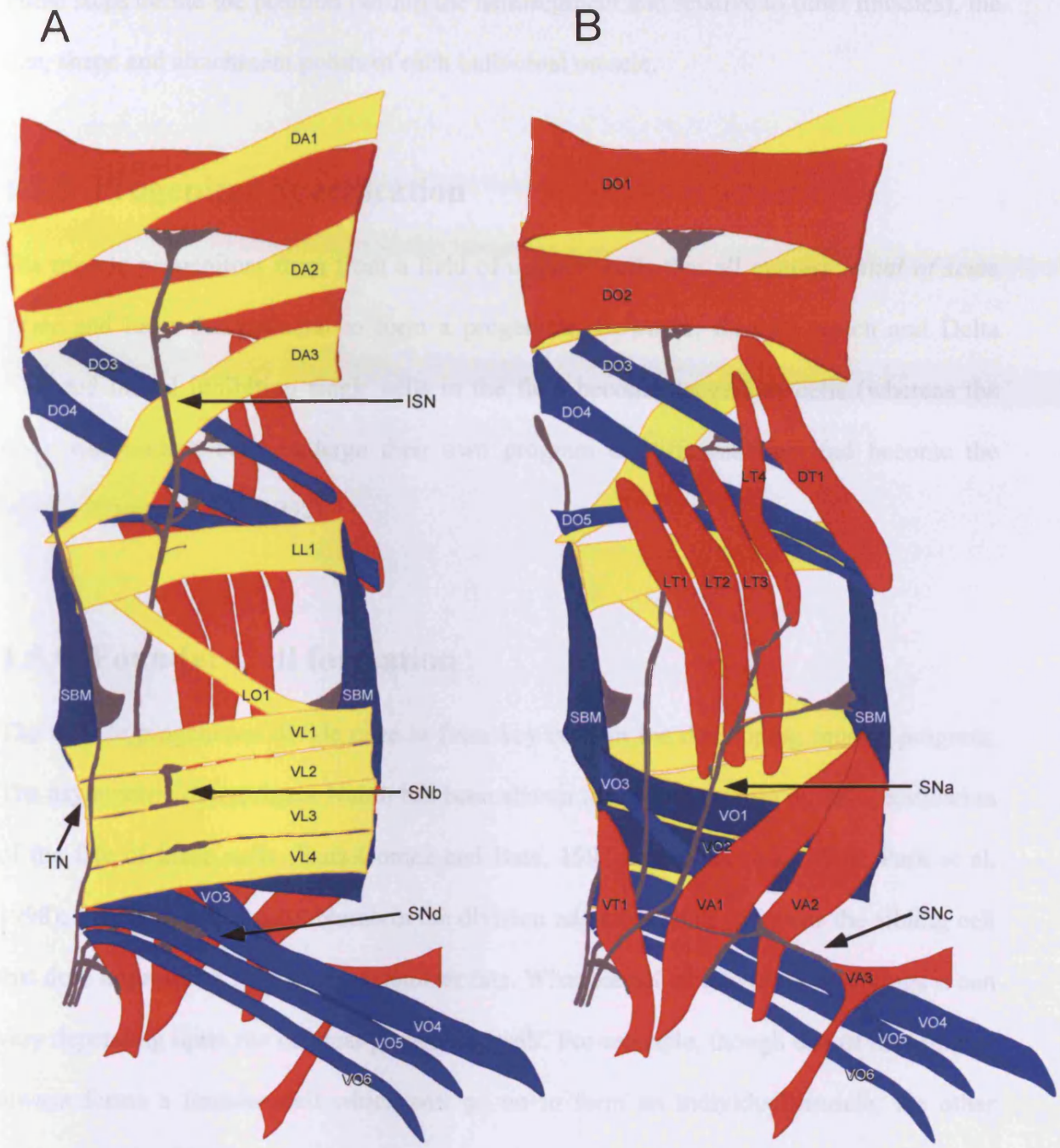

FIG 1.5.2 Wild-type somatic muscle pattern in *Drosophila*.

A flattened view of an A2-7 abdominal hemisegment. **(A)** Internal view. **(B)** External view. Abbreviations: DA: dorsal acute; DO; dorsal oblique; DT; dorsal transverse; LL: lateral longitudinal; LO: lateral oblique; LT: lateral transverse; VA: ventral acute; VL: ventral longitudinal; VO: ventral oblique; VT: ventral transverse; ISN: intersegmental nerve; SN: segmental nerve; TN: transverse nerve. This figure is from Bate,1993.

These steps define the position (within the hemisegment and relative to other muscles), the size, shape and attachment points of each individual muscle.

1.5.5 Progenitor Specification

The muscle progenitors form from a field of uniform cells that all express *lethal of scute l(1)sc* and have the potential to form a progenitor. However, through Notch and Delta mediated lateral inhibition single cells in the field become progenitor cells (whereas the other surrounding cells undergo their own program of differentiation and become the FCMs) (Carmena et al, 1995).

1.5.6 Founder Cell formation

The muscle progenitors divide once to form key cells in the developing muscle program. The asymmetric determinant Numb has been shown to play a key role in the specification of the fate of these cells (Ruiz-Gomez and Bate, 1997; Carmena et al, 1998; Park et al, 1998); the cell that acquires Numb in the division adapts one fate, whereas the sibling cell that does not acquire Numb adopts another fate. What the actual fate of these siblings is can vary depending upon the original progenitor itself. For example, though one of the siblings always forms a founder cell which will go on to form an individual muscle, the other sibling can be an adult muscle precursor (AMP) (Bate, 1990), a heart pericardial cell (Carmena et al, 1998) or another founder cell which will become a different adjacent individual muscle (Ruiz-Gomez and Bate, 1997). However, there is no variation in the fate of the cells that each individual progenitor will produce; for example the progenitor that forms the DA1 muscle founder always also gives a daughter that forms a pericardial cell

(Su et al, 1999) and the progenitor that forms the VA1 muscle founder always also gives a daughter that forms the VA2 muscle founder (Ruiz-Gomez et al, 1997).

When there are errors in the distribution of Numb at this stage of division the fate of the sibling cells can be affected. For example there is a progenitor that gives rise to the VA3 muscle founder and an AMP, and the sibling cell of the pair that acquires Numb will always adopt the VA3 fate whereas the sibling cell that does not acquire Numb will adopt the AMP fate. However when *Numb* is over-expressed so that it is acquired by both of the daughter cells on division of the progenitor, both of the siblings adopt the VA3 fate. Alternatively, in a *Numb* mutant, neither of the daughter cells can acquire Numb on division of the progenitor, and consequently both adopt an AMP fate (Ruiz-Gomez and Bate, 1997).

This would manifest itself in the St17 embryo as a duplication of the VA3 muscle (and loss of AMP) in the UAS-Numb condition and loss of the VA3 muscle (with duplication of the AMP) in the *Numb* mutant condition. In a similar manner, if a particular progenitor normally gives rise to two muscle founders rather than a muscle founder and an AMP (as is the case with the VA1 and VA2 muscles), then this would show itself in the St17 embryo as a transformation of muscle fate between the two. (Ruiz-Gomez and Bate, 1997).

Each individual muscle is derived from a single founder cell and these founder cells form in a stereotypic pattern within the hemi-segment (Bate, 1990; Bate, 1993) and then remain in a fixed position relative to each other during development until the final muscle pattern is formed (Beckett and Baylies, 2007).

Each founder cell expresses a combination of transcription factors which define it and the subsequent individual muscle that will form from it, and consequently these transcription factors are sometimes known as muscle identity genes (Baylies et al, 1998; Frasch, 1999 reviews). Examples of genes expressed in specific progenitors are *Kruppel* (Ruiz-Gomez et

al, 1997), *apterous* (Bourgouin et al, 1992), *S59/slouch* (Dohrmann et al, 1990; Knirr et al, 1999), *even-skipped* (Frasch et al, 1987) *muscle segment homeobox (msh)* (Nose et al, 1998), *nautilus* (Keller et al, 1997), *ladybird* (Jagla et al, 1998), *vestigial (vg)* (Williams et al, 1991), *collier* (Crozatier and Vincent, 1999; Dubois et al, 2007), *toll* (Halfon et al, 1995) and *connectin* (Nose et al, 1992) (Baylies et al, 1998; Ruiz-Gomez, 1998; Frasch, 1999; Maqbool and Jagla, 2007 reviews) and some of these transcription factors are necessary and sufficient for the formation of a specific individual muscle type. FIG 1.5.2 is a schematic taken from Baylies et al 1998 which shows some of these identity gene expression patterns in the individual muscles of the final somatic musculature.

In a similar manner to the Numb experiments, altering the acquisition of certain identity genes also causes a change in fate, for example in *apterous* mutants a loss of the LT muscles is seen, whereas when *apterous* is over-expressed LT muscle duplication occurs (Bourgouin et al, 1992), which is indicative of the way that Numb is required for the maintenance of identity gene expression in certain situations (Ruiz-Gomez and Bate, 1997; Park et al, 1997; Carmena et al, 1998).

1.5.7 Founder cell and Fusion Competent Myoblast fusion

Once a founder cell has formed it must begin the process of myoblast fusion in order to grow into the multinucleate myotube that forms an individual muscle. As mentioned above, the founder cells and FCMs derive from the same initial population of cells, but due to lateral inhibition the founder cells adopt a different fate. The founder cell and FCMs surrounding it express a distinct combination of proteins which mean that fusion is always asymmetric; it can only be between a founder and a FCM not between two founders or two FCMs (Reviewed in Taylor, 2000; Taylor, 2002; Dworak and Sink 2002; Taylor, 2003).

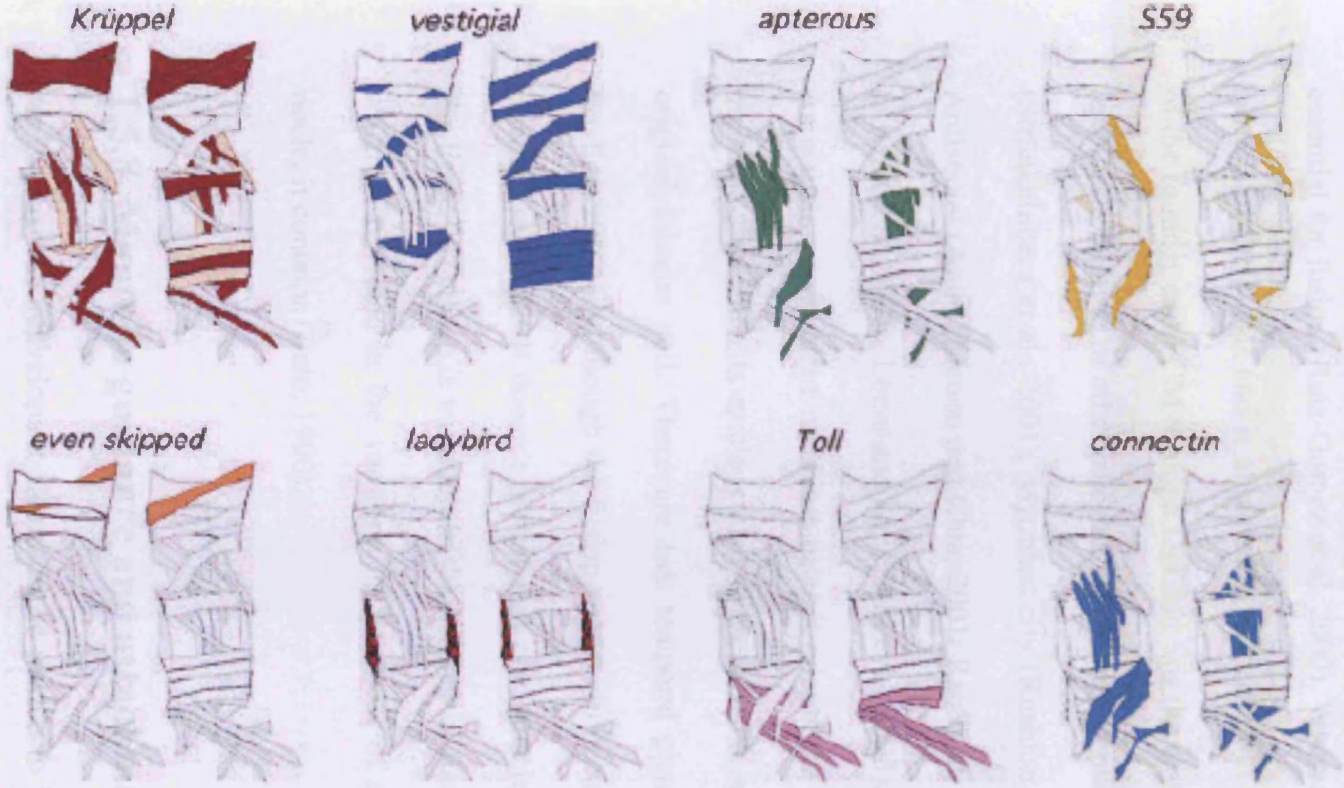

FIG 1.5.3 Expression pattern of identity genes in somatic muscle

Figure taken directly from (Baylies et al, 1998) shows how identity genes are expressed in the somatic muscles of the embryo.

Some factors are common to both types of cell but there are others that are specific to just one type. Dumbfounded (Duf) and sticks and stones (sns) are two such cell-type specific proteins. *Duf* is expressed specifically in the founder cells and is a myoblast attractant essential for fusion (Ruiz-Gomez et al, 2000). Whereas *sns* is specifically expressed on the surface of the FCMs and is attracted to Duf (Bour et al, 2000). After the initial recognition of the founder and FCM through Duf and Sns the rest of the fusion process can occur. This involves a number of other proteins which are essential for the process, including Roughest (Strünkelnberg et al., 2001), Myoblast city (Rushton et al, 1997), Rolling pebbles (Rols) / Antisocial (Ants) (Menon and Chia, 2001; Rau et al, 2001; Chen and Olson, 2001), Hibris (Artero et al, 2001), Loner and Arf (Chen et al, 2003).

As a fusion competent myoblast fuses it adopts the fate of the founder cell / developing myotube and thus its nucleus also expresses the specific muscle identity genes of the original founder cell. There are two temporal phases to myoblast fusion (Beckett and Baylies, 2007) and though the fusion appears to occur at similar times for each developing muscle (such that it doesn't appear that one muscle forms before another) (Beckett and Baylies, 2007) there is variation in the number of fusion events for each individual muscle which is reflected in the variation its final size of a final and is seen by the number of nuclei it contains (Bate, 1990).

1.5.8 Myotube guidance and attachment

As the myotube develops it also must be guided to its appropriate attachment sites in the epidermis so that the final muscle will be positioned correctly within the embryo so that it can function as a unit as part of the working musculature (Volk, 1999; Schnorrer and Dickson, 2004). This is achieved through cross talk between the extending myotube and the

tendon cell attachment sites. And as fusion events are still occurring between FCMs and this extending and growing myotube, this means that there are two intercellular communication events occurring simultaneously during this time (Schnorrer and Dickson, 2004).

The myotube projects filipodia in the direction of nearby tendon cells and on reaching the destination they stop extending and form a stable connection through adhesion molecules such as integrin (Schnorrer and Dickson, 2004). This adhesion allows the muscle to contract from this position; flies that are null for *integrin* form their muscles properly and have them reach the attachment sites appropriately but the muscle does not cope with contraction, and the muscle consequently balls up due to not being able to maintain its attachment (Brown et al, 2000).

The tendon cells are positioned at stereotypic positions within the epidermis and their initial formation occurs independently of muscle formation; tendon cells form normally even in *Twist* mutants which have no mesoderm (Becker et al, 1997). The Zinc finger transcription factor Stripe is an early marker of the tendon cells (Volk and VijayRaghavan, 1994), and is essential for their correct function. In *Stripe* mutants muscles fail to reach their attachment sites (Frommer et al, 1996), whereas over-expression of stripe at ectopic sites in the epidermis causes the formation of ectopic tendon cells in these positions to which the myotubes migrate to, consequently disturbing the final musculature pattern (Vorbruggen and Jackle, 1997). Despite tendon cells being able to form independently of the mesoderm initially, they subsequently require muscle; the EGF receptor on the surface of the tendon cell requires a signal in the form of the ligand Vein to be secreted from the extending myotube in order for the tendon cell to correctly differentiate (Yarnitzky et al, 1997).

1.5.9 Mef2 and Orchestration of the Muscle Differentiation process

Mef2 (Myocyte enhancer factor2) is a key promoting factor in the orchestration of muscle differentiation in invertebrates and vertebrates (Taylor, 1995; Pothoff and Olson, 2007). It is a MADS box (MCM1, Agamous, Defeciens and SRF) containing transcription factor (Shore and Sharrocks, 1995; Molkentin et al, 1996) which is essential for somatic muscle development.

Due to the occurrence of two genome duplications there are four copies of Mef2 in vertebrates, A,B,C and D (Yu et al, 1992; Edmondson et al, 1994) and as a result, studying the role of Mef2 in vertebrate differentiation proves difficult due to a degree of redundancy between the different copies (Black and Olson, 1998). However, *Drosophila* has only one copy of *Mef2* (Lilly et al, 1994; Nguyen et al, 1994; Taylor et al, 1995), and so it is has been possible to generate null and hypomorphic mutant lines for this gene (Bour et al, 1995; Lilly et al, 1995; Ranganayakulu et al, 1995) which have revealed a great deal about its significance in muscle development. A *Mef2* null mutant embryo forms no somatic muscle, showing that is necessary for the formation of the somatic muscle in invertebrates (Bour et al, 1995; Lilly et al, 1995). The *Mef2* hypomorphic mutants show a series of varying degrees of severity on the formation of muscle; from the vast majority of somatic muscles being missing in $Mef2^{113}$ mutants, to only a few muscles being affected in the weak hypomorph mutant $Mef2^{65}$. $Mef2^{424}$ shows an intermediate phenotype to these (Ranganayakulu et al, 1995). The different hypomorphic mutants produce different amounts of Mef2 and have been used to show that Mef2 levels have various effects on the timing and occurrence of gene activation to influence muscle differentiation in embryogenesis (Gunthorpe et al, 1999; Elgar et al, 2007). *Mef2* is expressed throughout all

the muscle types (somatic, visceral, pharyngeal and the contractile cardiac) and is present from early mesoderm going from the uniform field of high expression Twist cells in the mesoderm to the complex structure of the final regular repeating musculature at the end of embryogenesis (Nguyen et al, 1994; Lilly et al, 1994; Taylor et al, 1995). As mentioned previously, Twist is responsible for this early *Mef2* expression (Taylor et al, 1995), acting directly upon its regulatory sequence (Cripps et al, 1998).

Mef2 has been shown to bind to the consensus regulatory sequence YTAWWWWTAR (Andres et al, 1995) and a number of key genes associated with muscle structure have been identified as direct Mef2 targets; for example, *Tropomyosin* (Lin et al, 1996), *β3-tubulin* (Damm et al, 1998) and *Paramyosin* (Arrendondo et al, 2000). In addition, more recently a number of key large-scale studies have shown that Mef2 binds to the regulatory region of a large number of genes essential for many aspects of muscle differentiation and plays a role in their expression either directly or indirectly (Junion et al, 2005; Sandmann et al, 2006; Elgar et al, 2008).

A number of mechanisms exist to ensure that the regulation of Mef2 itself is correct and its activity is restrained until the appropriate times during development. The co-repressor, Him (Holes in Muscle) was recently shown to repress Mef2 activity in embryogenesis acting through the conserved repressor Groucho (Liotta et al, 2007; Liotta PhD thesis, 2005) and also in the adult musculature (Soler and Taylor, 2009). Over-expression of Him causes a severe inhibition of somatic muscle differentiation in a manner that mimics the *Mef2* loss-of-function alleles (Liotta et al, 2007).

In addition the conserved repressor Zfh1 (Zinc finger homeodomain 1) (Lai et al, 1993) shows evidence of *Mef2* repression (Postigo et al, 1997) and like Him, its over-expression

also causes an inhibition to somatic muscle differentiation (Postigo et al, 1997; Postigo et al, 1999).

Another means of regulation is the tight control of Mef2 activity throughout development as Mef2 levels have a direct effect upon muscle differentiation (Gunthorpe et al, 1999). There are genes that have a low requirement of Mef2 activity in order to be expressed and other genes that have a high requirement of Mef2 activity in order to be expressed. Such low requirement genes are expressed earlier in embryogenesis, whereas the high requirement genes are expressed later (Elgar et al, 2008) and this observation reveals a general way in which Mef2 can act upon a number of transcriptional targets over time.

In addition to this Mef2 can bind to the DNA as a homodimeric or heterodimeric protein (Black and Olson, 1998; Pothoff and Olson 2007) and a range of bHLH proteins can act as the binding partner in this Mef2 heterodimer (Black and Olson, 1998). Variation in the Mef2 binding partner also provides another possible means of Mef2 regulation in activating targets. In addition, Mef2 has been shown to be capable of auto-regulation (Cripps et al, 2004) and thus can provide a way of rapidly upregulating its activity at the appropriate time.

All of these mechanisms provide a means of Mef2 activity to be tightly regulated over time such that its plethora of targets can be activated in the appropriate place and the appropriate time to ensure the correct differentiation of the musculature. However, though it is known that *Mef2* is expressed in the majority of key cells throughout muscle development and that Mef2 is essential for somatic muscle differentiation itself, the exact involvement of Mef2 in these different stages is poorly understood.

At the early stages of the muscle differentiation program Mef2 is expressed but its role is not understood. For example, at the stage of progenitor formation, *Mef2* is expressed in the muscle progenitor and subsequently maintained in the founder cell but lost in the

pericardial cell (Su et al, 1999). And at the fusion stage, *Mef2* is expressed in both the fusion cell and the FCMs (Taylor, 2003 review), targets many of the genes involved in the fusion process (Sandmann et al, 2006), but must oversee the differential expression programs that distinguish the founder cell and the FCM in some way.

Initially it was thought that Mef2 acted later in somatic muscle differentiation, as the majority of its established targets were structural genes expressed towards the end of myogenesis (Lin et al, 1996; Damm et al, 1998; Arrendondo et al, 2000). However, when it was shown that it played a part in the regulation of the novel mesodermal gene *meso18E*, Mef2 was established to have a role early in development as well (Taylor, 2000). Subsequent evidence that Mef2 regulated another early gene, *Actin57B* (Kelly et al, 2002), combined with the recent data from global analyses of Mef2 action (Junion et al, 2005; Sandmann et al, 2006; Elgar et al, 2008) which reveal a number of genes involved in the early differentiation stages to be potential Mef2 targets, means that Mef2 plays an active role throughout the stages of myogenesis. What the specific roles are for Mef2 in these stages of myogenesis is an important question for understanding the process of muscle differentiation.

Though the *Mef2* hypomorphic alleles have provided insight into the importance of Mef2 they are limited in their use for studying the different stages of muscle differentiation. In alleles that cause a large decrease in Mef2 activity (such as in the $Mef2^{22.21}$ null mutant or the $Mef2^{113}$ hypomorph) the detrimental effect of an event early in myogenesis may mask a role that Mef2 plays later in embryogenesis. Conversely with alleles that cause a milder decrease in Mef2 activity, (such as the $Mef2^{65}$ allele) the embryo may be able to pass through such earlier developmental stages but as a result the drop in Mef2 activity is not significant enough to determine an effect in other stages. Consequently, alternative approaches for investigating Mef2 function in myogenesis are required.

1.6 Main Aims for my PhD

The main aims of my PhD are to investigate the roles of Mef2 and genes that are involved in regulation of its activity during the muscle differentiation programme.

I have done this in the following main ways;

- Generation and characterisation of a Mef2 dominant negative construct that can be used with the Gal4 UAS system to allow the controlled reduction of Mef2 activity in a spatial and temporal manner during the different stages of muscle differentiation.

- Investigation into the expression regulation of the *Him* gene.

- Generation and characterisation of mutant alleles in *Him* to further assess the role of this gene in muscle differentiation and Mef2 repression

- Characterisation and comparison of the gain-of-function and loss-of-function phenotypes associated with the *Zfh1* and *Him* genes.

- Investigation of the early Mef2 target and potential Mef2 effector *meso18E,* through bioinformatics, transcriptional regulation studies and gain-of-function experiments and the generation of loss-of-function alleles.

Materials and Methods

2.1 Molecular Biology

2.1.1 Agarose gel Electrophoresis

DNA fragments were separated by size using electrophoresis on agarose gels.

1% (w/v) agarose with 1x TBE (90mM Tris-Borate, 2mM EDTA) gels used with 1ul per 10ml molten gel of ethidium bromide solution (10mg/ml) added. DNA loaded on the gel and intercalated with ethiduim bromide was visualized with a UV transilluminator.

Lambda HindIII DNA and 1Kb Plus (Invitrogen) ladder were used as molecular weight markers.

2.1.2 DNA gel extraction

DNA fragments were purified by running on an agarose gel, extracting the fragment with a clean scalpel whilst visualising it under a low frequency UV light source and using a gel extraction kit (Qiagen) in accordance to the manufacturers' instructions.

2.1.3 DNA Precipitation with ethanol.

DNA was precipitated by the addition of 2 volumes of ice cold ethanol after the salt concentration was adjusted with 1/10 volume of 3M sodium acetate. The mixture was incubated for 20-30 minutes at -80°C (or o/n at -20°C) and the DNA was recovered by centrifugation at 13.000 rpm in a microfuge for 20 minutes. The pellet was washed with 70% ethanol, air dried and resuspended in a suitable volume of double distilled H_2O.

2.1.4 Phenol chloroform extraction

DNA was purified of proteins and salts using phenol chloroform and washing with ethanol as follows. dH2O was added to take the volume up to 100ul and then 100ul of phenol chloroform (Sigma) was added. This mixture was vortexed at centrifuged at r.t at 13000rpm for 10mins. The upper, DNA-containing phase, was collected and DNA precipitation performed to concentrate it.

2.1.5 Restriction digests

All restriction digests were performed in a total volume of 50ul and the incubation performed at 37°C for 2hrs. Buffers and enzymes used were NEB. Double digests were either performed simultaneously or sequentially in accordance with enzyme buffer compatibility. Where appropriate enzyme activity was stopped by heat inactivation (65°C, 20mins), phenol chloroform purification or DNA gel extraction (Qiagen).

2.1.6 Blunt ends

If blunt ends were required after a restriction enzyme cut, the DNA was purified then the ends were filled in with T4 DNA polymerase (NEB), supplemented with dNTPs (100uM) and BSA in an appropriate buffer (NEB). The reaction was carried out at 37°C for 35mins, then the T4 DNA pol was heat inactivated at 75°C for 20mins.

2.1.7 Vector dephosphorylation

To prevent unwanted recircularisation of prepared vectors the ends were dephosphorylated using Calf Intestinal Phosphatase (CIP) (NEB). Vector purified by phenol chloroform

extraction and DNA precipitation was resuspended in diH20 and dephosphorylated in a total volume reaction of 30ul at 37°C for 20mins. The vector would then be purifed by gel extraction (Qiagen).

2.1.8 Ligation

Ligation was performed in a 10ul total volume reaction, using T4 DNA Ligase (NEB) and the prepared insert with appropriately cut and dephosphorylated vector in a ratio of 3:1. Ligations were performed either at room temperature for 1hr followed by 1hr on ice, or at 16°C overnight (12°C o/n if the ligation involves an EcoRI site).

Ligations using pGEM-T (Promega) were performed using the provided kit in accordance to manufacturers instructions.

2.1.9 Genomic DNA Extraction

Approx. 15-20 flies were collected, anaesthetised, kept on ice and homogenised in a 1.5ml Eppendorf using rapid strokes with a DNase-free plastic grinding pestle and 100ul of Buffer A (100mM TrisHCl pH7.7, 100mM EDTA, 100mM NaCl, 0.5% SDS). An additional 200ul of Buffer A is added along with 3ul Proteinase K (15.6mg/ml) and incubated in 65°C water bath for 1hr. 2ul of RNAse A (10mg/ml, Qiagen) is added and incubated at 37°C for 20mins. 100ul of 5M KOAc is added and the mixture voretexed and incubated on ice for 5mins before centrifuging using a microfuge at 13000rpm for 25mins. The supernatant is transferred to a fresh tube, mixed with 450ul of ice cold isopropanol and centrifuged at 13000rpm for 5mins. The recovered DNA pellet is washed in 70% ethanol, air dried and resuspended in an appropriate volume of dH2O (Sigma).

2.1.10 PCR – Polymerase Chain Reaction

Standard PCR reactions were carried out for the generation of the various constructs using the DyNAzyme EXT high fidelity DNA Polymerase (Finnzymes). Reactions were carried out in a 50µl volume, containing 5µl of optimised DyNAzyme EXT buffer (containing 1.5mM $MgCl_2$), 1µl of 10mM dNTPs (Promega), 1µl of 25µM forward oligonucleotide primer (MWG), 1µl of 25µM reverse oligonucleotide primer (MWG), 5µl of 100ng/µl template DNA (plasmid or genomic) and 1µl of DNA polymerase. The volume was then adjusted with distilled H_2O (Sigma). The DNA templates were amplified using 20-30 cycles in a Peltier thermal cycler (MJ Research) equipped with a heated lid.

In general the following program was used:

- Initial denaturation: 95°C, 5 minutes
- Denaturation: 95°C, 1 minute
- Annealing: 55-65°C, 1 minute
- Extension: 72°C, 1 minute/Kb of template sequence
- Final extension: 72°C, 5-10 minutes

2.1.11 Site Directed Mutagenesis

Site Directed Mutagenesis of circular DNA was performed according to the Quik Change Site Directed Mutagenesis Protocol (Stratagene). Mutagenesis primers were designed using the Stratagene website tool.

2.1.12 Bacterial Cultures and agar plates

Bacteria were grown either in liquid culture in Luria-Bertani (LB) medium (per Litre: 10g Bacto-tryptone, 5g yeast extract, 5g NaCl, pH 7.0) at 37°C with continuous shaking at 300rpm, or on LB-agar (LB plus 15g/L Bacto-Agar) plates at 37°C. Ampicillin, at a final concentration of 100μg/ml was used as a selector where appropriate.

2.1.13 Transformation of Competent Cells

5-10ul of ligation mixture is incubated on ice for 15mins with 50ul of *E.coli* DH5α competent cells (Invitrogen) and then heat shocked in a 42°C bath for 45 seconds for the cells to take up the DNA. The cells are given 2mins on ice to recover then given 450ul of prewarmed SOC medium (2% Tryptone, 0.5% Yeast Extract, 10mM NaCl, 10mM KCl, 10mM $MgCl_2$, 10mM $MgSO_4$, 20mM Glucose) and incubated at 37°C for 45min with shaking.

Cells that took up the DNA are selected by plating out 100ul / 250ul of the mixture onto LB Agar / Antibiotic plates and incubated at 37°C o/n. For all the plasmids I have used the selective antibiotic has been ampicillin.

2.1.14 Plasmid Preparation from bacterial culture.

1.5ml of o/n bacterial culture was centrifuged at 13000rpm for 5 mins to pellet cells. The supernatant was removed and an additional 1.5ml centrifuged. The plasmid Spin Mini Prep protocol (Qiagen) was then performed according to the manufacturers instructions. For larger plasmid preparations 50ml of o/n bacterial culture was used with the Midi prep kit (Qiagen).

2.1.15 Preparation of Digoxigenin-labelled RNA probe for RNA in-situ hybridisation

Prior to transcription, DNA templates were linearised with appropriate restriction enzymes and were then purified by gel extraction.

Transcription reactions were carried out in 50µl containing approximately 500ng of linearised template DNA, 1µl of 10X transcription buffer (Roche), 1µl of DIGNTP mix (Roche), 0.5µl of RNAse inhibitor (Roche) and 1µl of T7 RNA polymerase (Roche). The volume was then adjusted to 10µl with RNAse free H_2O (Sigma). Reactions were incubated at 37°C for 2 hours. After transcription, the DNA template was removed by the addition of 1µl of DNAseI buffer, 6µl of H2O and 3µl of DNAseI RNase free (10U/µl; Roche). This was incubated at 37°C for 15 minutes. The RNA probes were then fragmented with 80µl of 125mM sodium carbonate (pH 10.2) at 60°C for 15minutes. The alkaline hydrolysis of the probes was stopped by adding of 50µl 7.5M ammonium acetate. RNA was precipitated with isopropanol, washed with 70% ethanol, air dried and resuspended in TE:formamide (1:1).

The yield of DIG-labelled RNA was estimated in a spot test using a DIG-labelled control (Roche). The test was performed following the manufacturer's instructions. Briefly, dilutions of both the control and the probes (all in RNase free double distilled H_2O) to be tested were spotted and cross-linked to a positively-charged nylon membrane (Roche). The spots were then colorimetrically detected and the comparison of the intensities of the spot allowed an estimation of labelling yield. Probes were diluted with TE:formamide (1:1) to 25ng/µl and 5µl was used for *in situ* hybridisation

2.2 Cell Biology

2.2.1 Immunohistochemistry

Fixed embryos (See 2.3.3 for embryo fixation method) stored in methanol were stained with a single antibody as follows.

Embryos were washed in 1x PBS-TX (PBS buffer with 0.3% Triton X-100) and then blocked in PBS-TX BSA (PBS-TX with 0.5% bovine serum albumin (Sigma)) at room temp for 3x10mins. Preabsorbed primary antibody was diluted in PBS-TX, added to the embryos and incubated overnight at 4°C with gentle shaking. Primary antibody is removed and embryos washed in PBS-TX before adding biotinylated secondary antibody to whichever animal the antibody was raised in (here anti-mouse or anti-rabbit (Vector Laboratories)) and incubating at room temp for 1hr. After removal of antibody and washing with PBS-TX the signal is amplified using Vectastain Elite ABC Kit (Vector Laboratories) The stain was then developed with 0.5mg/ml diaminobenzadine (DAB) (Sigma) and 0.02% hydrogen peroxide. Embryos were mounted either in 80% glycerol or in an acetone: araldite mixture (1 :1 ratio) after a serial dehydration in ethanol. Mounting in glycerol allowed rotation of the embryos with gently pressure on the cover slip, enabling observation of all the musclulature and this method was generally preferred.

Embryos were viewed on a *Zeiss Axioskop* microscope in bright field or nomarski settings and photographed using the *axiovision* software and Axiocam digital camera.

2.2.2 Antibody double labelling

Double antibody stainings were performed essentially as described in 2.2.1 with the main difference being the addition of Nickel salts on visualisation of one antibody to ensure a black colouring develops, as opposed to the usual brown.

When primary antibodies were raised in different species, both were added at the same time and developed sequentially. After the overnight incubation, embryos were washed, the first secondary antibody was added and the stain developed using nickel salts (which gives a black colour). Embryos were then washed and blocked with 0.5% BSA and incubated for one hour at room temperature with the second secondary antibody. This was developed without nickel salts to give a light brown precipitate.

When primary antibodies were raised in the same animal, embryos were incubated overnight at 4°C with gentle shaking with the first antibody and developed using nickel salts. Embryos were then washed, blocked with 0.5% BSA and incubated overnight at 4°C with gentle shaking with the second primary antibody. This was developed the next day without nickel salts.

2.2.3 RNA in-situ hybridisation

In situ hybridisations were carried out essentially as described by Kopczynski et al, 1998 with the use of Digoxigenin-labelled RNA probes. Fixed embryos were rehydrated in MeOH: 4% paraformaldehyde/PBS before fixing for a further 10 minutes in 4% paraformaldehyde/PBS. After 3 washes in 1X PBS containing 0.1% tween-20 (PBT), embryos were prehybridised at 55°C for 1 hour in hybridisation buffer (50% formamide (Fluka), 4X SSC (Sigma), 1X Denhardt's solution (Sigma), 250µg/ml yeast tRNA (BRL), 250µg/ml salmon testis DNA (Sigma), 50µg/ml heparin (Sigma), 0.1% Tween-20). Embryos were then hybridised overnight at 55°C with 0.125µg of DIG-labelled RNA probe in 0.5ml hybridisation buffer. The next morning, embryos were washed with 4 changes of washing solution at 55°C (50% formamide, 2X SSC, 0.1% tween-20) during the day, the last wash was overnight .For the detection, embryos were incubated for 90 minutes at room temperature with anti-DIG antibody (Roche) in PBT (1:2000). The stain was developed in

the dark at room temperature by incubation in colour solution: 9µl/ml NBT and 7µl/ml BCIP (both Roche) in 0.3ml detection buffer (100mM Tris pH 9.5, 100mM NaCl, 50mM $MgCl_2$, 0.1% Tween-20). Embryos were mounted in 80% glycerol and analysed using an image grabbing system and processing set up (Axiocam digital camera + *Axiovision* software) linked to a *Zeiss Axioskop* microscope.

2.2.4 Somatic muscle scoring analysis

For muscle phenotype assessment, the somatic muscles of St17 embryos were analysed by scoring each of the 30 muscles (Bate, 1993) for muscle loss, duplication, shape defects and attachment defects in abdominal hemi-segments A2-A4 (a total therefore of 90 muscles per embryo). Unless stated otherwise, 20 separate embryos were scored for this analysis. Embryos were generally stained with anti-β3 tubulin antibody for muscle visualisation.

2.2.5 Hatching and Survival tests

In general females homozygous for different GAL4 drivers were crossed with males homozygous for each UAS construct (the main exception to this being Mef2-En (X) in which case, females of the UAS line were used) and laying pots kept at the appropriate experimental temperature (usually, 18°C, 21°C, 25°C or 29°C) from an appropriately timed lay, fertilised embryos of around St14 were selected on the basis of gut autoflorescence under a florescence microscope (and also absence of any GFP balancer if the cross required it e.g Mef2 mutants). These were then transferred to the dry half of an apple juice plate containing a thin layer of fresh yeast on the other half. These plates were then returned to the experimental incubating temperature and embryos allowed to hatch overnight. Percentage of hatching was scored and 2nd instar larva were transferred to tubes as they

emerged over the next few days. The percentage of transferred larvae that survived to white pupae, black pupae and adult stages were then scored. A minimum of 200 embryos were aligned for each experiment and a limit of 100 embryos per apple juice plate and 35 larvae per tube was imposed when transferring the animals.

2.2.5 Adult muscle DLM dissection

For analysis of the direct longitudinal muscles (DLMs) in adult flies, black pupae were selected, carefully removed from their pupal case and fixed in 17.4% parafomaldehyde (diluted in PBS from 37% stock) for a minimum of overnight. Fixed flies were then washed in PBS quickly then again, with shaking for 20mins, then dissected by pinning the head and lower abdomen, removing wings and legs and making a transverse cut section between the second and third pairs of legs. Two further transverse cuts were made, one beneath the head and one a the lower half of the abdomen which results in two transverse sections of the thorax which were stained in hematoxylin solution for 5 mins, washed twice in PBS for 2mins min each and then once in 80% glycerol / PBS for 2mins. Hemi-thoraces were then mounted in glycerol, coverslips sealed with nail polish and then imaged using the Zeiss Axioskop microscope.

2.3 Fly and embryo work:

2.3.1 Fly Husbandry

Fly stocks were maintained on a medium containing 6.77% cornmeal, 7.26% dextrose, 1.45% yeast, 0.68% agar, 2.26% nipagin and 0.32% propanoic acid. The majority of the

stocks were kept at 18°C and changed every four weeks. When making stocks, crosses were kept at 25°C.

When collecting virgins for UAS/GAL4 experiments or crosses, the stocks were amplified and kept at 25°C during the day and 18°C during the night to optimise virgin females collection, which was usually performed first thing in the morning and twice again during the day as needed.

New stocks received from the *Drosophila* stock centre (Bloomington), Exelixis (Harvard Medical School) or DrosDel (Szeged University, Hungary) or other researchrers were kept in quarantine for at least three generations and inspected for mite infection before being brought into the laboratory's fly room.

2.3.2 Fly Stocks

The following stocks have been used for my PhD :

Oregon R (OR) flies were used as a standard wild-type stock.

Transgene constructs were initially injected into *yw* flies and subsequently balanced using FM7 (y,ct/ FM7, ftz lacZ) X chromosome balancer or If / Cyo ; TM3 / TM6b or 3703 CyO/Sco; MKRS/TM6B autosomal balancer lines.

2057 Sequencing strain flies (Bloomington) were used to extract genomic DNA for *Dmeso18E* and *Him* reporter construct generation.

yw flies were used to generate genomic DNA for the homologous recombination construct arms.

Mutant Stocks Table 2.3.1

Gal4 Lines Table 2.3.2

UAS Lines Table 2.3.2

UAS Mef2 Dominant Negative Lines Table 2.3.4

Reporter constructs and GFP fusion stocks Table 2.3.5

Transposable Element lines used in mutant generation Table 2.3.6

2.3.4 Generation of new stocks

Table 2.3.7 shows the new experimental stocks I generated through crossing previously established stocks appropriately.

The general crossing schemes I used for the combination of either a homozygous viable line on the second and third chromosomes, X and second chromosomes and X and third chromosomes are shown in FIG. 2.3.1, 2.3.2 and 2.3.4.

The combinations that contain a lethal allele, such as the *Zfh1*^{2} mutant, require more care in the cross due to the necessity of marked balancer chromosomes. FIG 2.3.5 shows the scheme that was used to generate the *Him Del* ; *Zfh1*^{2} / TM3 ftz LacZ double mutant.

Stock	Chromosome	Comment	Origin	Reference
Him52 ; + ; +	X	P-element deficieny	D.Hancock	-
Him74; + ; +	X	Homologous recombination	Z.Han	-
Him195; + ; +	X	Homologous recombination	Z.Han	-
meso18E Del-6 / FM7; + ; +	X	P-element deletion	D.Hancock	-
meso18E Del-8 / FM7; + ; +	X	P-element deletion	D.Hancock	-
meso18E Dup-11 / FM7; + ; +	X	P-element duplication	D.Hancock	-
+ ; $Mef2^{65}$/ CyO; +	III	EMS induced	R.Schulz	Ranganayakulu et al, 1995
+ ; $Mef2^{424}$/ CyO; +	III	EMS induced	R.Schulz	Ranganayakulu et al, 1995
+ ; $Mef2^{113}$ / CyO; +	III	EMS induced	R.Schulz	Ranganayakulu et al, 1995
+ ; $Mef2^{22.21}$/ CyO; +	III	EMS induced	B.Bour	Bour et al, 1995
+ ; + ; $Zfh1^{2}$/ TM3	III	EMS induced	M.Bate	Lai et al, 1993

Table 2.3.1 Mutant Lines used.

Stock	Chromosome	Comment	Origin	Reference
Twist ; Twist Gal4	X ; II			Baylies and Bate, 1996
Mef2 Gal4	III			Ranganayakulu et al, 1996
24B Gal4	II			Brand and Perrimon, 1993
69B Gal4	III			Brand and Perrimon, 1993
rP298 Gal4	X	Founder cell driver		Menon and Chia, 2001
1151 Gal4	X	Adult muscle driver		Anant et al, 1998
UAS Dicer ; Mef2 Gal4	II ; III	Mef2 Gal4 with UAS Dicer to enhance the effects of RNAi		Ranganayakulu et al, 1996 Schnorrer et al, 2004

Table 2.3.2 Gal4 Lines used.

Stock	Chromosome	Comment	Origin	Reference
UAS Him	II	Homozygous viable.	M. Taylor	Liotta et al, 2007
UAS Zfh1	III	Homozygous viable.		
UAS Mef2 High	III	Homozygous viable. Strong expression line. Also called UAS Mef2 "Nguyen" in lab.	B.Bour	Bour et al, 1995
UAS Mef2 Low	III	Homozygous viable. Weaker expression line. Also called UAS Mef2 10T4A.	K. Beatty	Gunthorpe et al, 1999
UAS meso18E 29T1	II	Homozygous viable. Weaker expression line.	M.Taylor	-
UAS meso18E 29T24	II	Homozygous viable. Weaker expression line.	M.Taylor	-
UAS meso18E 20T2	III	Homozygous viable. Strong expression line.	M.Taylor	-
UAS meso18E 1-125	II	N terminal truncation of meso18E	D.Hancock	-

Table 2.3.3 UAS Lines used (for UAS Mef2 dominant negatives see Table 2.3.4).

Stock	Chromosome	Comment	Origin	Reference
Mef2-En L10-1	X	Homozygous viable. Stronger line. Used in this study.	D.Hancock	-
Mef2-En L2-1	II	Homozygous viable. Strong line. Used in this study and Blanchard et al.	D.Hancock	Blanchard et al, 2009
Mef2-En L5-1	II	Homozygous lethal. Over CyO. Weak stock.	D.Hancock	Blanchard et al, 2009
Mef2-En L6-1	II	Homozygous lethal. Over CyO. Weak stock.	D.Hancock	-
Mef2-En L3-1	III	Homozygous lethal. Used in Blanchard et al.	D.Hancock	-
Mef2-Stop L2-1	X	Homozygous viable.	D.Hancock	-
Mef2-Stop L6-1	II	Homozygous viable.	D.Hancock	-
Mef2-Stop L1-1	III	Homozygous lethal. Over TM6B. Weak stock	D.Hancock	-
Mef2-Stop L4-1	III	Homozygous viable.	D.Hancock	-
Mef2-Stop L6-1 ; L4-1	II ; III	Homozygous viable. Used in this study	D.Hancock	-

Table 2.3.4 UAS Mef2 Dominant Negative Lines generated

Stock	Comment	Origin	Reference
Him Eco/Xba 3.8KB GFP fusion	"Mini-gene" fusion construct. The 3.8KB Him regulatory region driving the Him gene fused to GFP at its C terminus	D. Liotta	Liotta et al, 2007
Him Eco/Xba 3.8KB GFP pStinger	The Him 3.8Kb region in a GFP reporter.	D. Hancock	-
Him Eco/Xho 2.8Kb GFP pH Stinger	Also called p43 in the lab	S. McConnell	-
Him Xho/ Xba 1Kb T GFP pStinger	1Kb region upstream of gene, including TATA box	D. Hancock	-
Him Xho/ Xba 1Kb NT GFP pHStinger	1Kb region upstream of gene, excluding TATA box	D. Hancock	-
Him Posakony 3.6Kb GFP pStinger		J. Posakony	Rebeiz et al, 2002
Him Posakony 2.2Kb GFP pStinger		J. Posakony	Rebeiz et al, 2002
Him 1KB NT Mef2 SDM pHStinger	Deletes Mef2 site in 1Kb NT GFP	D.Hancock	-
Him 3.8KB Twi OL SDM pStinger	Deletes overlapping Twist sites in 3.8Kb GFP	D.Hancock	-
Meso18E C GFP pStinger	1Kb region upstream of gene in a GFP reporter	D.Hancock	-
Meso18E D GFP pStinger	Region in first intron in a GFP reporter	D.Hancock	-
Meso18E C Mef2 SDM GFP pStinger	Deletes Mef2 site in meso18E C GFP	D.Hancock	-

Table 2.3.5 Reporter constructs and GFP fusion stocks

Stock	Chromosome	Comment	Origin	Reference
pBacWH f04435	X	pBacWH FRT element just downstream of *Upd2*. Used for *Him52* deficiency.	Harvard Medical School (Exelixis)	Thibault et al, 2004
pBacWH f06349	X	pBacWH FRT element just upstream of ari1 Used for *Him52* deficiency.	Harvard Medical School (Exelixis)	Thibault et al, 2004
pBacWH e02398	X	pRB (RazorBac FRT element) in the third intron of *meso18E*. Used for *meso18E* deletion / duplication.	Harvard Medical School (Exelixis)	Thibault et al, 2004
pRS-UM-8195-3 pRS3	X	pRS element just upstream (54bp) from the start of *meso18E*. Used for pRS-UM-8195-3 pRS3r generation. *W+*	DrosDel, Cambridge	Ryder et al, 2004
pRS-UM-8195-3 pRS3r	X	The "flipped out" version of the above element. Used for *meso18E* deletion / duplication. *W-*	DrosDel,Cambridge / D.Hancock	-
w^{1118}iso ;2iso ;3iso	-	White insertion line DSK001	DrosDel, Cambridge	Ryder et al, 2004
w^{1118}iso ;Sco/SM6B,70FLP ;3iso	II	Heat-shock Flippase on 2nd Chrmosome DSK001	DrosDel, Cambridge	Ryder et al, 2004
FM7h/P{RS3}l(1)CB-6411-3[1]; 2_{iso}; 3_{iso}	X	X Balancer DSK014	DrosDel, Cambridge	Ryder et al, 2004
P{w[+mC]=XP}l(1)XPG-L[1], $w^{[1118]}$/FM7c	X	Exelixis Balancer D Stock 7756	Harvard Medical School (Exelixis)	Parks et al, 2004

Table 2.3.6 P-Element lines used in mutant generation.

Stock	Chromosomes
Mef2-En Rescue	
Mef2-En (X) ; UAS Mef2 Low	X ; III
Mef2-En (X) ; UAS Mef2 High	X ; III
Mef2-En (II) ; UAS Mef2 Low	II ; III
Mef2-En (II) ; UAS Mef2 High	II ; III
Him mutant Combinations	
Him 52 ; Zfh1-2 / TM3 ftz LacZ	X ; III
Him 52 ; Him GFP fusion	X ; III
Him 52 ; GroBX22	X ; III
Him 74 ; Zfh1-2 / TM3 ftz LacZ	X ; III
Him 74 ; Him GFP fusion	X ; III
Him 74 ; Mef2 Gal4	X ; III
Him 195 ; Zfh1-2 / TM3 ftz LacZ	X ; III
Him 195 ; UAS Mef2 Low	X ; III
Him 195 ; Mef2 Gal4	X ; III
Meso18E functional analysis	
UAS meso18E 29T24 ; UAS Mef2 Low	II ; III
UAS meso18E 29T24 ; UAS Mef2 High	II ; III
UAS meso18E 29T1 ; UAS Mef2 Low	II ; III
UAS meso18E 29T1 ; UAS Mef2 High	II ; III
UAS Him ; UAS meso18E 20T2	II ; III

Table 2.3.7 Generation of new stocks.

Him Del (X) ; Zfh1 Del (III) double

1A) ♀ FM6 / N ; TM2 / MKRS x x / Y ; Zfh1-2 / TM6B dfd YFP Sb ♂

↓

Collect ♀ FM6 / x ; Zfh1-2 / TM2

1B) ♀ Him Del ; + x x / Y ; Zfh1-2 / TM3 ftz LacZ ♂

↓

Collect ♂ Him Del / Y ; TM3 ftz LacZ / +

2) ♀ FM6 / x ; Zfh1-2 / TM2 x Him Del / Y ; TM3 ftz LacZ / + ♂

↓

Collect ♀ FM6 / Him Del ; Zfh1-2 / TM3 ftz LacZ (TM2 / TM3 ftz LacZ is ubx pheno)

and ♂ FM6 / Y ; Zfh1-2 / TM3 ftz LacZ

3) ♀ FM6 / Him Del ; Zfh1-2 / TM3 ftz LacZ x FM6 / Y ; Zfh1-2 / TM3 ftz LacZ ♂

↓

Collect ♀ FM6 / Him Del ; Zfh1-2 / TM3 ftz LacZ

♂ Him Del / Y ; Zfh1-2 / TM3 ftz LacZ

4) ♀ FM6 / Him Del ; Zfh1-2 / TM3 ftz LacZ x Him Del / Y ; Zfh1-2 / TM3 ftz LacZ ♂

↓

Collect ♀ Him Del / Him Del ; Zfh1-2 / TM3 ftz LacZ

♂ Him Del / Y ; Zfh1-2 / TM3 ftz LacZ and cross for STOCK

FIG 2.3.5 Crossing Scheme for Him Del and Zfh12 / TM3 ftz LacZ double mutant.

2.3.3 Embryo Collection and Fixation

Embryos were collected on apple juice-agar plates supplemented with fresh yeast. Collections were made according to the stage at which the embryos were required and the temperature at which the flies were kept.

For fixation, embryos were transferred from the apple juice-agar plate to a basket with a wire mesh base, washed with water and placed in 50% bleach until the chorion membrane was removed (approximately 2 minutes). Dechorionation was monitored under a dissecting microscope. Dechorionated embryos were rinsed, dried and transferred into a 2ml tube containing 1ml heptane. They were then fixed for 20 minutes in heptane: 4% paraformaldehyde/PBS (1:1), and the vitelline membrane removed by vortexing in a mix of heptane and methanol (1/1). The embryos were then washed and stored in methanol at -20°C until required.

2.3.4 Transgenic construct injection

The injection mix was prepared in 1X Spradling buffer (1mM Sodium Phosphate buffer pH6.8, 0.5mM KCl) with the DNA to be injected at a final concentration of 1μg/μl and the helper DNA (which is a source of transposase that will promote the mobilisation of the constructs from the plasmid into the genome) at a final concentration of 0.25μg/μl. The mix was spun for 10 minutes at full speed and 0.5-1μl was loaded into the injection needles prepared by pulling capillaries (1.0mm x 0.78mm, Harvard Apparatus) with a needle puller (KOPF Instruments).

Embryos for injection were obtained from young *yellow-white* females. The *yw* stock was expanded to obtain as many young flies as possible. A minimum of 150 young females and approximately 50 males were placed into laying pots and allowed to lay eggs onto apple

juice-agar plates for few days until they reached their "laying peak" (usually 3-4 days). On the day of injection, plates were changed 3-4 times before the injection and then every 30 minutes during injection.

Embryos from the 30 minutes lays were collected into a mesh basket and dechorionated in 50% sodium hypochlorite (Sigma). They were then aligned onto a coverslip, covered with glue (prepared by placing double side Scotch TM tape in 50-100ml of heptane), posterior end at the edge. Aligned embryos were dessicated for approximately 10 minutes, by placing them in a pot containing Silica-gel 6-16 mesh self-indicating (Fisher), and then covered with halocarbon oil (Voltalef, H10S). They were injected using a micromanipulator connected to a pump (Narishige) and a Nikon microscope.

Coverslips with injected embryos were placed into a humidified chamber (apple juice-agar plate supplemented with fresh yeast and fixed with damp Whatman paper) at 18°C. Embryos were allowed 48 to 50 hours to recover and hatch. Each single newly hatched first instar larva was then collected and transferred into a vial containing fly medium. Vials were placed at 25°C until F_0 adults emerged.

F_0 males were individually mated with three virgin *yw* females. The F_1 generation was then screened for transformants by looking for the emergence of red eye colour. (F_0 females were only crossed to male yw flies if there were insufficient F_0 males that emerge).

Red eyed F1 offspring indicate the successful emergence of a transformant line which was then balanced with FM7 (if on X) or #3703 (if an autosomal insertion) to generate balanced homozygous stock.

2.4 Construct generation:

2.4.1 *Mef2* Dominant Negative

The aim of this was to generate a construct that retains the DNA binding domain (MADS) and Mef2 dimerisation domain, but excludes the transactivation domain of the Mef2 protein. This would then act as a dominant negative protein, capable of binding to sites on the DNA but not activating the genes it would normally once bound.

The MADS and Mef2 domains of Mef2 are conserved among vertebrates and invertebrates and found at the N terminus of the protein. The C terminus contains the transactivation domain. In *Drosophila* Mef2 the MADS and Mef2 domain are situated at amino acids 1-86 of the protein (Taylor et al, 1995). The sizes of previous successful dominant negative proteins that removed the C terminus in vertebrates are shown below :

Mef2A, amino acids 1-131: Ornatsky et al, 1997 (from a study by Yu, 1996)

Mef2C, amino acids 1-109: Krainc et al, 1998

Mef2C, amino acids 1-105 : Okamoto et al, 2000

Mef2D, amino acids 1-153: Shin et al, 1999 (from a study by Molkentin, 1996)

Based on this information I selected a size of 128 amino acids for the Mef2 dominant negative truncation, this ensured the MADS and Mef2 domain was included, was in the same size range and previous constructs and fit conveniently with primer design.

I made two Dominant Negative constructs; one, named Mef2-Stop, which was just a truncation of the Dmef2 protein, consisting of the first 1-128 amino acids and removing the C terminus. The other, named Mef2-En consisted of this truncation fused to the Engrailed

repressor domain. Such Engrailed fusions had been used previously for a number of successful dominant negative proteins (e.g Tinman and Pannier in *Drosophila* Han and Olson 2002; Klinedinst and Bodmer, 2003).

I used DMef2 Isoform III cDNA (clone10 CsCl purified from MVT 31/03/94), as template for generating PCR fragments with appropriate restriction sites for the Mef2 region. (For the purposes of this construct though it does not matter which Dmef2 isoform was used though, as our fragment is amino acids 1-128. The first splice event occurs at amino acid 186). I used the engrailed repressor region in pLit28 (a gift from Cyrille Alexander, NIMR) as template for the Engrailed 2-298 fusion.

Nomenclature:

1. Mef2-Stop:

Describes the truncated protein alone; Mef2 1-128 with a Stop introduced.

2. Mef2-En :

Describes truncation plus engrailed repressor fusion; Mef2 1-128, (no stop), BglII linker, EnR 2-298, (stop).

Mef2-Stop

The Mef2-Stop construct is simply these 128 amino acids with an additional Stop codon at the end.

Primers:

Dmef2 fwd EcoRI – GAA TTC ATG GGC CGC AAA AAA ATT CAA ATA TC

Dmef2 rev STOP BglII – AGA TCT TTA GCG CTG CAT CAT GTT CTG G

Underlined shows restriction site. Red highlights introduced stop codon.

The PCR fragment was amplified using Dynazyme EXT (Finnzymes) using Mef2 cDNA as template, ligated into pGEMT (Promega), sequenced (Lark) and cloned into pUAST (Brand and Perrimon 1993) using EcoRI and BglII (NEB).

Mef2-En

The Mef2-En construct is these 128 amino acids without the additional Stop codon, but instead a BglII linker and amino acids 2-298 of the Engrailed repressor domain. A Stop codon was introduced at the end of the repressor domain.

Primers:

Dmef2 fwd EcoRI – GAA TTC ATG GGC CGC AAA AAA ATT CAA ATA TC

Dmef2 rev GO BglII - AGA TCT GCG CTG CAT CAT GTT CTG G

EnR fwd BglII – AGA TCT GCC CTG GAG GAT CGC TG

EnR rev XhoI - CTC GAG TTA GGA TCC CAG AGC AGA TTT CTC

Underlined shows restriction site. Red highlights introduced stop codon.

The Dmef2 1-128 fragment was amplified by PCR using Mef2 cDNA as template, ligated into pGEMT and sequenced. The EnR 2-298 domain was also amplified by PCR, using EnR in pLit28 as template (a gift from Cyrille Alexandre, NIMR)., This fragment was then ligated into pGEMT and sequenced.

The Mef2 1-128 fragment was then cloned into pUAST using EcoRI and BglII. This construct was subsequently reopened with BglII and XhoI and the PCR generated EnR domain ligated in after excision of that fragment from pGEMT .

The introduction of a two amino acid linker to the final protein has been used previously in other EnR fusion dominant negative proteins. (E.g Tinman and Pannier in *Drosophila* Han and Olson 2002, Klinedinst and Bodmer 2003).

Constructs injected to generate transgenic lines as described above.

2.4.2 *Him* reporter constructs and Him Gal4.

Him 3.8Kb pStinger GFP

The Him EcoRI / XbaI 3.8Kb pStinger construct was generated from an EcoRI / XbaI 3.8Kb fragment in pBS ks II vector which was generated previously in the lab by D.Liotta. This fragment was used in the generation of the Him 3.8Kb GFP fusion mini gene that was used in a previous publication (Liotta et al, 2007). The EcoRI site in this fragment is endogenous to the Him non-coding sequence but the XbaI site was introduced artificially by PCR.

Briefly, this Him 3.8Kb GFP fusion mini gene fragment was made by D.Liotta in the following three-step process;

1. Generation of an EcoRI-BamHI 2.7Kb fragment from a simple restriction digest of a Him λ clone in pBluescript utilising internal restriction sites endogenous to the Him non-coding region and cloning of this fragment into pBSKSII+ vector.

2. Generation of a BamHI-XbaI 1.1Kb fragment by PCR using the following primers

Fwd (5'-3') : CCG ATT GGA TCC CAT CTT GCG GCA C *(BamHI underlined)*

Rev : (5'-3') : TGA CGC CCA TCT AGA TTG GTG GCT CTG *(XbaI underlined)*

(The BamHI site is endogenous to the Him region but the XbaI site is generated artificially by PCR at the end of the fragment).

3. Ligation of this 1.1Kb fragment into the EcoRI-BamHI 2.7Kb pBSKSII+ construct to generate an EcoRI-XbaI 3.8Kb pBSKS+ construct.

From this EcoRI / XbaI 3.8Kb pBSks II construct, I cut out the Him 3.8Kb EcoRI / XbaI fragment and cloned into the pStinger GFP vector (Barolo et al, 2000) as follows:

The 3.8Kb pBS ks II construct was first cut with EcoRI, the ends were blunted, and then a cut with XbaI was made. This fragment was then carefully separated from the 3.0Kb pBS

ks II vector by running on a gel, extracting the band and gel purification (Qiagen). In parallel, the pStinger vector was cut with BglII, blunted, and then cut again with XbaI. The opened vector was dephosphorylated by CIP and gel purified in preparation for ligation with the 3.8Kb fragment. This was subsequently transformed into bacteria and clones containing the insert taken, confirmed by restriction analysis and PCR to the Him region and prepared for injection.

Him 3.8Kb pTGAL

In addition, in parallel to this I made a Him 3.8Kb Gal4 construct using the same DNA fragment but this time cloning into pPTGAL (Brand and Perrimon, 1993) instead of pStinger. The pPTGAL vector was cut with StuI, blunted and then cut with XbaI and the construct generated in the same way as with pStinger above.

Him 1Kb T pStinger GFP

As the 1Kb T construct contains the *Him* TATAA box, this region was cloned into the pStinger GFP vector (a gift from J.Posakony, (from Barolo et al, 2000) which itself contains no TATAA box.

The template for this was a previously generated Him 1.1Kb T pGEM-T Easy construct generated in the lab by D.Liotta. This fragment (originally called 1C6 1Kb PCR3), was generated using the following primers :

Fwd (5'-3') : CCG ATT GGA TCC CAT CTT GCG GCA C *(BamHI underlined)*

Rev : (5'-3') : TGA CGC CCA TCT AGA TTG GTG GCT CTG *(XbaI underlined)*

The BamHI site is endogenous to the Him region but the XbaI site is generated artificially by PCR at the end of the fragment. There is also an endogenous XhoI site within this fragment approximately 100bp upstream of the BamHI site.

To clone the XhoI-XbaI fragment into pStinger to generate Him 1Kb T pStinger I did the following :

Digested Him 1.1Kb pGEMT with XhoI, blunted the ends and then cut with XbaI to generate a Him 1Kb XhoI-XbaI fragment and purified this fragment by gel extraction (Qiagen). I prepared the pStinger vector by digesting with BglII, blunting the ends and then digesting with XbaI. The cut vector was then dephoshorylated using CIP enzyme and purified by gel extraction ready for ligation with the XhoI-XbaI fragment. This was subsequently transformed into bacteria and clones containing the insert taken and prepared for injection (Qiagen spin mini/midi and DNA precipitation to concentrate DNA).

Him 1Kb NT pHStinger

This region contains no TATAA box and so was inserted into the pHStinger GFP vector (Barolo et al, 2000)), which does.

I designed the following primers for Dynazyme EXT PCR to generate the fragment.

Fwd: GAGATCTCTCGAGTAGTTTTTAGATGCAG

Rev: GAATTCTGTGCTCTCTGCGGGTTTG

These generate a fragment of 870bps which was originally cloned into pGEM-T and sequenced. BglII and EcoRI sites introduced in the Fwd and Rev primers respectively were used to generate the fragment from pGEM-T, which was purified and cloned into prepared pHStinger GFP vector and injected into *yw* flies.

2.4.3 *Him* site directed mutagenesis reporter constructs

Analysis of the Him 1Kb sequence identified a number of Twist sites and a Mef2 site within the sequence region (Him chapter section). As a result of this I designed a number of primers to delete the consensus Mef2 site and the proximal and overlapping Twist sites in the region according to the mutagenesis criteria outlined by Stratagene.

Him 1Kb NT ΔMef2 SDM pHStinger

Primers

Mef2-I SDM : TTATTTTTAA to TTCGGCGGTAA (SacII site introduced)

Him dMef2 1 fwd	cag taa cac atg ggc cca cga gtt atg ttt ccg cgg taa tcc cac aaa gag tcg atc tcc aaa ac
Him dMef2 1 rev	gtt ttg gag atc gac tct ttg tgg gat tac cgc gga aac ata act cgt ggg ccc atg tgt tac tg

Template Him 1Kb NT pGEMT (see section 2.4.2). Stratagene Quikchange protocol. BglII / EcoRI digest to confirm clone insert. SacII digest to check SDM site change. Sequencing of whole region to confirm SDM and check for other mutations. Subcloning of fragment into pH Stinger using BglII / EcoRI and prep of construct and injection in usual way.

Him 3.8Kb ΔTwist OL pStinger GFP

Primers

Twi OL SDM : CACATGTG to CGGCCGTG

Him Twi-OvLAP fw	gcg gcg ctg gtg ctg ccg gcc gtg ttc tgt gtt ggg ct
Him Twi-OvLAP rv	agc cca aca cag aac acg gcc ggc agc acc agc gcc gc

Template Him 1Kb T pGEMT (BamHI-XbaI fragment in pGEMT - see section 2.4.2; strictly the BamHI-XbaI fragment is 1.1Kb not 1Kb). Stratagene Quikchange protocol. BglII / EcoRI digest to confirm clone insert. Sequencing of whole region to confirm SDM and check for other mutations.

To generate the Him 3.8Kb ΔTwist OL pStinger GFP construct I removed a BamHI-XbaI 1.1Kb fragment from Him 3.8Kb pStinger GFP and replaced it with a BamHI-Xbal 1.1Kb fragment taken from this Him "1Kb" T ΔTwist OL pGEMT fragment containing the desired Twist mutation. Digests for both were simple double digests with subsequent vector dephosphorylation, gel purification, preparation and injection in the usual way.

I was unsuccessful in generating a Him 1Kb T ΔTwist OL pStinger GFP construct. For this the following preparation is necessary :

Digestion of Him 1Kb T ΔTwist OL pGEMT with (XhoI (Blunt) / XbaI) to generate fragment for insertion into pH Stinger (BglII (Blunt) / XbaI) prepared vector.

2.4.4 *meso18E* Reporter constructs

Primers: *Underlined shows restriction site.*

Construct A – 1848bp :

18E-A fwd:SphI GCATGCCAAGAATAAGAATCCACC Tm = 61.0°C

18E-A rev :BglII AGATCTTCGACTGGATAAAATCGGTC Tm = 61.6°C

Construct B - 1759bp :

18E-B fwd:BglII AGATCTGAAAGATTGAAAGATACAAGCAG

Tm = 61.0°C

18E-B rev:EcoRI GGAATTCGTATTAACAAAGTAATATCCAAGG

Tm = 61.0°C

Construct C – 1155bp :

Fwd (EcoRI) - GAATTCATTATACCCGCCTGTTGG Tm 61.1°C

Rev (BamHI) - GGATCCCGTTGCCGATACTAAC Tm = 62.1°C

Construct D – 771bp :

Fwd (BglII) – AGATCTCAGGACGGCGGACTAC Tm = 63.9°C

Rev (BamHI) - GGATCCTTTGTGACACTTAACGTCTAG Tm = 63.5°C

Constructs were amplified from 2057 genomic DNA with 20-30 cycles of PCR using the high fidelity DNA polymerase, Dynazyme EXT (Finnzymes). The fragment was extracted and purified using a Qiagen gel extraction kit, ligated into pGEM-T vector (Promega) and subsequent Spin-mini preps (Qiagen) containing the insert were sequenced (Lark Sequencing or Cardiff University sequencing service). The fragment was then extracted from pGEM-T and ligated into pHStingerGFP (construct D) or pStingerGFP (construct C) using the appropriate restriction enzymes. A Midi-prep of the construct was performed (Qiagen) and after DNA precipitation to obtain a DNA concentration of at least 100ng/ul was ready for injection into *yw* embryos.

(meso18E A and meso18E B were not made : PCR fragments were generated of the appropriate sizes but were not successfully ligated into pGEMT due to time restraints. Primers work well, give clean single products and are included here for future reference).

2.4.5 meso18E Site directed mutagenesis reporter constructs

Mef2 binding site consensus sequence YTAWWWWTAR (Andres et al, 1995)

Primers were designed to destroy the Mef2 site by site directed mutagenesis using the Stratagene Quikchange II kit guidelines.

One set used a 6bp change introducing a SacII site into the sequence

CTATTTTTAG Mef2 site

CCCGCGGTAG SacII site introduced by SDM

Fwd : 18E C Mef2-SDM SacII

5' 3'

CTGCACAACATACTCGTATCCCGCGGTAGGCTACGACTTTTCCCATTTGGC

Rev : 18E C Mef2-SDM SacII

5' 3'

GCCAAATGGGAAAAGTCGTAGCCTACCGCGGGATACGAGTATGTTGTGCAG

Tm = 78.2 n = 51

This strategy is similar to that used by Cripps et al in the Mef2 autoregulation paper (Cripps et al, 2004). The new sequence in the context of the full meso18E C region was checked for the potential of introducing new binding site to the region using Patch (gene-regulation.com) and none were found.

There is a potential hair pin in the oligo at 55deg (Generunner) but this appears unavoidable. In addition, primers were designed to completely destroy the mef2 site by introducing a NotI site (in a similar manner to the Kelly et al Act57B Mef2 paper – but without the introduction of an extra base! Kelly et al, 2002) This requires an 8bp change.

CTATTTTTAG

CGCGGCCGCG

Fwd : 18E C Mef2-SDM NotI

5' CCATACTGCACAACATACTCGTATCGCGGCCGCGGCTACGACTTTTCCCATTTGGCC

Rev : 18E C Mef2-SDM NotI

5' GGCCAAATGGGAAAAGTCGTAGCCGCGGCCGCGATACGAGTATGTTGTGCAGTATGG

Tm = 78.6

This oligo has the potential for forming hairpin loops at 55, dimers at 55 and bulge loops at 58 – hence the concern for designing the other primer.

The SacII site SDM primers were used to generate the construct.

Construct generation :

Genomic DNA prepped from 2057 sequencing strain embryos. SacII Mef2 SDM primers used to generate change in the 18E C fragment in pGEM-T (the intermediate construct from generation of the 18E C pStinger construct above) – pGEMT construct used as considerably smaller than pStinger (3Kb plasmid rather than 10Kb) thus more convenient for SDM PCR. Protocol as Stratagene Quikchange II manual (Stratagene). 3.5ml LB amp cultures from colonies grown O/N and plasmids extracted using Qiagen Spin Mini Prep kits according to protocol.

Clones were selected for using EcoRI / BamHI (NEB) restriction digest, to check that the correct 1155bp C reporter region, and if so a separate digest using SacII (NEB) was performed to check for introduction of the SDM at the Mef2 site. Positive clones were then sequenced to confirm appropriate SDM change (and no other mutations within the region) and cloned into pStinger using EcoRI / BamHI to make the final meso18E C ΔMef2 SacII SDM pStinger construct.

2.4.6 UAS 18E 1-125 and UAS 18E 1-197 truncations

UAS 18E 1-125 construct.

Amino acids 1-125. Contains the myb-like region (18-86), the putative NLS (86-102) and then continues to include some weak conservation homology on blasted sequence.

Fwd uses a conveniently situated native EcoRI site and rev introduces a Stop site and an XbaI site for cloning into pUAST.

Fwd : 18E 1-125 EcoRI

5' 3'

CACCACAGAATTCCCAA**ATG**GATACGAAG

Tm = 65.3 EcoRI site within meso18E underlined. ATG initiation codon in bold.

Rev : 18E 1-125 XbaI

5' 3'

TCTAGA**CTA**GCCATTCGATCCCCAGC

Tm = 66.4 Stop codon in bold. Introduced XbaI site for construct underlined.

Rev as read (GCTGGGGATCGAATGGC**TAG**TCTAGA

Primer Tm equation 18 ≥ = 69.3 + [(0.41 x % GC) – (650 / length)]

UAS 18E 1-125 construct generation.

Meso18E cDNA in pNB40 vector (Nick Brown library) from MVT [7F9.5A] (Taylor, 2000) used as template for the PCR. Phusion DNA pol (NEB) used for PCR fragment generation gave appropriately sized 375bp product. PCR fragment gel purified (Qiagen) and ligated into pGEM-T and appropriate colony screened by restriction digest (EcoRI /

XbaI) and sequenced in house (Cardiff University). Fragment subcloned into pUAST and prepped for injection in usual way.

UAS 18E 1-197 construct.

Meso18E truncation to include the myb-like domain, NLS and the Serine rich region (165-191).

Fwd : 18E 1-197 EcoRI

5' 3'

CACCACAGAATTCCCAAA**TG**GATACGAAG

Tm = 65.3

(This is just the same primer for the 1-125 construct)

RevA : 18E 1-197 XbaI

5' 3'

TGTAGA**TTA**CAGGAAGCGGTCCAGCTTG

Tm = 66.5

(But gives potential primer dimer at 58.5 degrees)

RevB : 18E 1-197 XbaI

TGTAGA**CTA**CAGGAAGCGGTCCAGC

Tm = 66.2

But has less matching residues to anneal to the region.

Meso18E 1-197 was not generated. Primers included for reference.

Meso18E 1-125 truncation amino acid sequence :

MDTKNPPPVTSSYHHQRAPRTPESYFNVPESVALLNIVKSERIQSAFQSN
RKNHASVWEMVAEVLNRFSARKRTAKQCCNRYENLKKIYTQLKKNPERHV
RRNWPYMFLFKEIEEQRGECWGSNG stop

Meso18E 1-197 truncation amino acid sequence :

MDTKNPPPVTSSYHHQRAPRTPESYFNVPESVALLNIVKSERIQSAFQSN
RKNHASVWEMVAEVLNRFSARKRTAKQCCNRYENLKKIYTQLKKNPERHV
RRNWPYMFLFKEIEEQRGECWGSNG**K**RLALITKNHNELSYYQRRRQAAEL
GVLLNKDNLTPHQHSLLQSLSQSQSQSHSHAHSTDSSQSGSKLDRFL stop

Meso18E 1-553 full length amino acid sequence :

MDTKNPPPVTSSYHHQRAPRTPESYFNVPESVALLNIVKSERIQSAFQSN
RKNHASVWEMVAEVLNRFSARKRTAKQCCNRYENLKKIYTQLKKNPERHV
RRNWPYMFLFKEIEEQRGECWGSNG**K**RLALITKNHNELSYYQRRRQAAEL
GVLLNKDNLTPHQHSLLQSLSQSQSQSHSHAHSTDSSQSGSKLDRFL**P**NH
FVEAQLSEVAGPVGGSASGVSGMSAGGFDENPLQMQMVQAAAAAAAVAAH
KRHELQMASVGGVQMTPEDDDEDEPQRPAFKNHLHVLGHGHGLGLGHAPM
DDSGEAPDFEKDCNGALNMHHQNNNHNENHISMKSEPLSEGEFNPDDIQL
MQTNYNGAQNYYSPGMDANILHPDVIVDTDILSDCSSSTTLKKKRKMSTS
TDGDSTNYELIEYLKRREKRDEELLKRMDAREDRLMNLLERTVVAIETLA
VKRALTFPVNPTKENAPATARPLSPPPPEAQFAAPPATQEQPTSPERNGI
ATGRSGTIPVANQDAAIEVPDDGDSGDDVQVKDKLAKLTPKAGGDERTDG
RQT

2.4.7 UAS 18E Δmyb-like SDM construct

Site directed mutagenesis to the myb-like region of meso18E, specifically targeting the conserved residues of the 3rd (DNA interacting) helix. Changing to prolines or glycines. Ideally with only a one base change to achieve this. Change 6 residues using 8bp changes.

RTAK**QC**CN**RY**E**NL**KKIYTQL to RTAKPGCNGPEGPKKIYTQL

RTAKQCCNRYENLKKIYTQL *MADF conserved residues in the 3rd helix*

RTAKQCCNRYENLKKIYTQL *Myb-like conserved residues in the 3rd helix*

RTAKQCCNRYENLKKIYTQL *BLAST identified residues in the 3rd helix*

Primers designed according to Stratagene SDM Quikchange kit specifications

(Tm = 81.5 + 0.41(%GC) - 675/ N - % mismatch)

N = 63 Tm = 79.3°C

Fwd : 18E myb SDM

5'CGGAAGCGAACGGCCAAGCCGGGCTGCAATGGGCCCGAGGGCCCCAAGAAG

ATCTACACGCAG

Rev : 18E myb SDM

5'CTGCGTGTAGATCTTCTTGGGGCCCTCGGGCCCATTGCAGCCCGGCTTGGCCG

TTCGCTTCCG

meso18E wild type sequence and translation :

```
R   K   R   T   A   K   Q   C   C   N   R   Y   E   N   L   K   K
CGG AAG CGA ACG GCC AAG CAG TGC TGC AAT CGG TAC GAG AAC CTC AAG AAG

 I   Y   T   Q
ATC TAC ACG CAG
```

meso18E Site Directed Mutagenesis sequence and translation :

```
R   K   R   T   A   K   P   G   C   N   G   P   E   G   P   K   K
CGG AAG CGA ACG GCC AAG CCG GGC TGC AAT GGG CCC GAG GGC CCC AAG AAG

 I   Y   T   Q
ATC TAC ACG CAG
```

Construct generation was attempted according to Stratagene Quikchange manual using UAS 18E full length 1-553 pUAST (MVT – [UAS 7F9.5A])as template for PCR. A small number of clones (two - after a previous unsuccessful SDM attempt with no colonies) were generated after plating out, but these were negative for the appropriate change on

sequencing. Would recommend subcloning the 1-553 fragment into pGEMT for a smaller template for SDM in order to generate the construct successfully.

2.5 Gene Deletions :

2.5.1 FRT element mediated deletion of the *Him* gene region

As outlined in the Him chapter, the deletion occurs between the f06349 pBacWH element and the f04435 pBacWH element.

A recombination event between these results in a deletion of approx 98Kb that removes *Him* and five other genes; *Frq1, Andorra, Frq2, Her* and *CG33639.* (FIG 6.4.1)

The crossing scheme for the recombination event is shown in FIG 2.5.1

2.5.2 FRT element mediated deletion of *meso18E*

As outlined in the meso18E chapter, the deletion occurs between the DrosDel RS3 element UM-8195-3 and the Exelixis element pRB e02398. The scheme required two steps; the initial conversion of the pRS3 w+ UM-8195-3 element into an element pRS3r w- so that it was ready for recombination and the second step required the trans-recombination between this pRS3 w- element and the pRB e02398 w+ element.

The crossing schemes are outlined in FIG 2.5.2A and 2.5.2B respectively.

FIG 2.5.2 *meso18E* transposable element Deletion.

2.5.2A) DrosDel element UM8195-3 pRS3 w+ converted to UM8195-3r pRS3r w-

1. ♂ w^{1118} / Y ; TM6B/ MKRS,**hsFLP 86E** x ♀v w^{1118} iso, **p{ FRT, w+ }RS3** ; 2iso; 3iso

Heat shock progeny ↓

*Collect ♂ w^{1118} iso, **p{FRT, w+ }RS3 / Y;MKRS,hsFLP 86E / 3iso***

2. ♂ w^{1118} iso, **p{FRT, w+ }RS3** / Y ;MKRS,**hsFLP 86E** / 3iso x ♀v FM7h iso ;2iso;3iso

↓

*Collect ♀v FM7h / w^{1118} iso **p{FRT, w-}RS3r***

3. ♀ FM7h / w^{1118} iso **p{FRT, w-}RS3r** x ♂ FM7h iso / Y ; 2iso ; 3iso

↓

*Collect ♂ w^{1118} iso **p{FRT, w-}RS3r** / Y*

*and ♀v FM7h / w^{1118} iso **p{ FRT, w-}RS3r***

4. ♂ w^{1118} iso **p{FRT, w-}RS3r** x ♀v FM7h / w^{1118} iso **p{ FRT, w-}RS3r**

↓

*Collect ♂ w^{1118} iso **p{FRT, w-}RS3r** / Y*

*and ♀v FM7h / w^{1118} iso **p{ FRT, w-}RS3r***

5. ♂ w^{1118} iso **p{FRT, w-}RS3r** / Y x ♀v FM7h / w^{1118} iso **p{ FRT, w-}RS3r**

↓

*Collect ♂ w^{1118} iso **p{FRT, w-}RS3r** / Y and ♀v w^{1118} iso **p{ FRT, w-}RS3r***

And cross for STOCK.

FIG 2.5.2cont. *meso18E* transposable element Deletion

FIG 2.5.2B)

Trans-recombination between UM8195-3r pRS3r w- element and Exelixis e02398 pRB w+ element

1. ♂ w^{1118} ; TM6B/ MKRS,**hsFLP 86E** x ♀v w^{1118} iso, **p{FRT, w+ }RB** ; 2iso ; 3iso

↓

*Collect ♂ w^{1118} iso, **p{FRT, w+ }RB / Y ; MKRS,hsFLP 86E***

2. ♂ w^{1118} iso, **p{FRT, w+ }RB** / Y; MKRS,**hsFLP 86E** x ♀v w^{1118} iso **p{FRT, w-}RS3r** (from 2.5.1A stock)

Heat shock progeny

↓

*Collect ♀v w^{1118} iso **p{FRT, w-}RS3r / w^{1118} iso, p{FRT, w+ }RB ; MKRS,hsFLP 86E***

3. ♀v w^{1118} iso **p{FRT, w-}RS3r** / w^{1118} iso, **p{FRT, w+ }RB** ; MKRS,**hsFLP 86E**

x ♂ FM7h iso ;2iso ;3iso

↓

Collect ♀v w^{1118} iso **p{FRT, w-}RS3r ---- p{FRT, w+ }RB** / FM7h iso

4. ♀v w^{1118} iso **p{FRT, w-}RS3r ---- p{FRT, w+ }RB** / FM7h iso

x ♂ FM7h iso ;2iso ;3iso

Screen progeny for emergence of w+ ♂'s.

Two possibilities…

If none, suggests recombination is lethal...

5.1 Stock : w^{1118} iso **p{FRT, w-}RS3r ---- p{FRT, w+ }RB** / FM7h iso

If w+ ♂ can occur, suggests recombination is viable

5.2 Stock : w^{1118} iso **p{FRT, w-}RS3r ---- p{FRT, w+ }RB**

2.5.3 Screen / Confirmation of transposable element mutant lines.

For the Him deletion, PCR had to be used to screen the lines. It was subsequently used to confirm the lines. For meso18E, eye colour suggested a deletion (*w*+) or a duplication (*w*-) event, but PCR was needed to distinguish these from un-recombined elements.

2.5.4 Genomic DNA Extraction from individual flies.

As large number of single flies needed to be prepped for genomic DNA for the screening I used an alternative quicker (and cruder) method for obtaining DNA than outlined in 2.1.8 for construct preparation. Emerging females from the progeny to be screened were allowed to mate (crossed with FM7h males) and once a number of eggs were seen to be laid to ensure genes were passed on she was prepped for DNA to test the line as follows.

Genomic DNA Extraction from individual flies.

Engels quick prep genomic DNA extraction.

1. 1 anaesthetised fly in 50ul Squishing Buffer pipetted up and down 10 times.
2. 30mins at 37deg C.
3. 5mins at 85deg C to inactivate Proteinase K.

Crude DNA prep stored at 4deg and used that day or next in PCR reaction.

Squishing Buffer :

10mM Tris-HCl pH 8.8
1mM EDTA
25mM NaCl
200ug/ul Proteinase K

PCR Reaction :

1.5ul ThermoPol Buffer NEB

0.5ul Fwd primer (25pmol/ul)

0.5ul Rev primer (25pmol/ul)

0.5ul 10mM dNTP's NEB

2.0ul quick prep DNA

10.1ul diH20 RNAse free SIGMA

0.2ul Taq DNA pol NEB

20ul Total Volume

PCR Program :

1. 5min @ 95°C
2. 30sec @ 95°C
3. 1min @ Annealing temp
4. 1min @ 72°C
5. Go to step 2. x35 times
6. 5min @ 72°C
7. Forever @ 4°C

Annealing temp was specified as 2°C lower than lowest Tm of primer pair used.

2.5.5 Primers used in screen

Him primers

Him P Element deletion confirmation primers (A,B,C,D pairs)

Primers specific to a P-element and adjacent genomic DNA

<u>For element pWH f06349</u>

A Fwd gen : GCGTGGCAAGAAGACGGAAATG 62.11

A Rev pWH : TCCAAGCGGCGACTGAGATG 61.4

Fragment size will be 448bps

B Fwd pWH : CCTCGATATACAGACCGATAAAAC 59.3

B Rev gen : ACTAGCAAATAATTCCCCAAAGCC 59.3

Fragment size will be 286bps

For element pWH f04435

C Fwd gen : GGGAAATTTCATCTAGGTGGCG 60.25

C Rev pWH : TCCAAGCGGCGACTGAGATG 61.4

Fragment size 506bps

D Fwd pWH : CCTCGATATACAGACCGATAAAAC 59.3

D Rev gen : ATTACAGTCATTGCGGCTTACG 58.39

Fragment size will be 386bps

Because of the number of flies involved with the Him screen, I just initially screened using the primer pairs A and D. A positive result for both of these for a line suggests a deletion, a result for just A suggests unrecombined pBacWH f06349 , a result for just D suggests unrecombined pBacWH f04435 and a result for neither suggests a duplication. If a A and D positive result was obtained for a line, the test was repeated using A,B,C and D pairs with controls using these primer pairs against P-element stocks. The line was further tested using primers specific to the region outside of the deletion area at either side and inside of the deletion area. These primers are described below.

Primers specific to genes upstream (Ari1), downstream (Upd2) and within (Him) the deleted region :

Ari1 primers

5' end of gene

FWD1 : GCCTGGAGCCACCTTCTAG TM = 60.95

REV1 : CAGTCACAAGGCTCAGAAGC TM = 59.35

Product size = 356 bp' s

3' end of gene

FWD2 : CACAAAGGCACAGTCGAAAAGC TM = 60.25

REV2 : GCACCCATCGATAAGCAGATG TM = 59.82

Product size = 387 bp's

Upd2 primers

5' end of gene

FWD1 : CTCGCTATAATACTGGAAGGGC TM = 60.25

REV1 : GAGCGTCTCAACTTTCACACG TM = 59.82

Product length

3' end of gene

FWD2 : GCTGAGACTCATATCACTGTCG TM = 60.25

REV2 : GCAGCAAGCGATTGTGATAGTTG TM = 60.64

Product length = 544 bp's

Him region primers

5' end

FWD1 : CGATCTCCAAAACAAACCCGC TM = 59.82

REV1a : CAGTATCTTGTAGATGACGCCC TM = 60.25

Product size = 190bps

REV1b : CTAGAAATCTGCACAGCTGCTG TM = 60.25

Product size = 428

3' end

FWD2 : GCTGCTCTTCCATTTTCCCAC TM = 59.82

REV2 : CCGGAAATCAGAACAGGCATC TM = 59.82

Product size = 356

Meso18E deletion primers

Dmeso18E P element deletion

Primers specific to a P-element and adjacent genomic DNA

For element pRB e02398

A Fwd gen : GATGTCGTCCGGATTGAACTCG 62.18

A Rev pRB : TCCAAGCGGCGACTGAGATG 61.4

Fragment size will be 434bps

B Fwd pRB : CCTCGATATACAGACCGATAAAAC 59.3

B Rev gen : ACCCGACTTCGAAAAGGACTG 59.82

Fragment size will be 444bps

For element pRS UM8195-3

C Fwd gen : ATCCCGTTGCCGATACTAAC 57.3

C Rev pRS : CACAACCTTTCCTCTCAACAA 56.98

Fragment size will be 308bps

D Fwd pRS : CAATCATATCGCTGTCTCACTC 58.39

D Rev gen : GTTGGAATCATGCTTGCTCTG 57.87

Fragment size will be 360bp

Mef2 Dominant Negative

3.1 Introduction

As outlined previously there are limitations to using the *Mef2* hypomorph or null alleles to investigate the roles of Mef2 in the orchestration of muscle differentiation (Section 1.5.9), and as a result of this I designed and generated two Mef2 Dominant Negative proteins that could be over-expressed using the Gal4 UAS system (Brand and Perrimon, 1993) and reduce Mef2 activity in a spatially and temporally controlled manner through the use of appropriate Gal4 lines and driving temperatures.

Normal Mef2 protein consists of three key domains that provide distinct aspects essential for its function. At the N terminus there is a MADS box domain, which is a 57 amino acid region that allows the Mef2 protein to bind to DNA at its specific binding sites (Yu et al, 1992; Andres et al, 1995; Molkentin et al, 1996). The MADS box is highly conserved and is named after a number of proteins from across the animal and plant kingdom that the domain was first identified in (MCM1, Agamous, Deficiens and SRF) (Shore and Sharrocks, 1995). The MADS box also enables Mef2 to homodimerise with other Mef2 molecules (Black and Olson, 1998). Adjacent to the MADS box is a Mef2 domain, a region of 29 amino acids which allows the Mef2 protein to dimerise with a different protein (heterodimerisation), such as a bHLH transcription factor (Molkentin et al, 1996; Black and Olson, 1998). At the C terminal end of the Mef2 protein is a transactivation domain that is essential for activation of Mef2 gene targets once the protein has bound to the DNA (Yu 1996; Black and Olson 1998). These three regions are highly conserved among all Mef2 proteins with respect to their relative position in the protein and with respect to sequence for the MADS and Mef2 domains – the transactivation domain varies between organisms and even Mef2 isoforms in the same

organism (Pothoff and Olson, 2007). However, all three domains are essential for the correct function of the Mef2 protein (Black and Olson, 1998; Nguyen et al, 2002).

The MADS domain of *Drosophila* Mef2 is situated at amino acids 1-57 and the Mef2 domain is at amino acids 58-86 (Taylor et al, 1995). I designed my dominant negative constructs so that the protein should retain DNA binding and protein dimerisation capability (the MADS and Mef2 domains), but due to a truncation of the C terminal end, lack the transcriptional activation capability of wild type Mef2 protein. This introduced protein should then compete with the wild type Mef2 protein present and reduce the transcriptional activation of Mef2 dependent genes. Such Mef2 dominant negative constructs have been successfully used previously for the different vertebrate Mef2 copies in cell culture, (Ornatsky et al, 1997; Krainc et al, 1998; Shin et al, 1999; Kolodziejczyk et al, 1999; Okamoto et al, 2000), and the rationale behind the design of these dominant negative constructs was based upon studies analysing the requirement of the different Mef2 regions through various degrees of truncation (Molkentin et al, 1996; Yu, 1996).

I have generated two different versions of the Mef2 dominant negative; one is just a truncation alone, the other is the truncation with the engrailed repressor domain fused to it (Han and Manley, 1993; Smith and Jaynes, 1996). Such engrailed repressor fusions have been used previously in a number of other successful dominant negative proteins, such as Tinman and Pannier in *Drosophila* and Nkx2.5 in *Xenopus* (Han et al, 2002; Klinedinst and Bodmer, 2003; Fu at al, 1998) and more recently for successful Mef2 dominant negative proteins in vertebrate systems; Mef2C in mice (Arnold et al, 2007) and Mef2C in mice and P19 cells (Karamboulas et al, 2006a; Karamboulas et al, 2006b). Fusion to the engrailed repressor domain has been shown in previous constructs in other systems to increase the

strength of phenotype achieved by the dominant negative when compared to the phenotype associated with the truncation alone (Karamboulas et al, 2006b).

The two Mef2 dominant negative constructs were designed as follows ;

The Mef2 dominant negative fused to the Engrailed repressor domain consists of the first 128 amino acids of the *Drosophila* Mef2 protein which is fused in frame to the repressor domain of engrailed (amino acids 2-298 of engrailed) (Han and Manley, 1993; Smith and Jaynes, 1996). The size of the Mef2 truncation was chosen to include the MADS and Mef2 domains (amino acids 1-86) but be of an appropriate length to abolish transactivation properties based upon previous analysis of Mef2 proteins (Taylor et al, 1995; Molkentin et al, 1996; Yu 1996). I also considered the lengths of previous successful Mef2 dominant negatives in vertebrate systems generated through truncation and used these as a guide for a suitable size for a *Drosophila* Mef2 dominant negative. The lengths of previous successful vertebrate Mef2 truncations are as follows :

Mef2A, amino acids 1-131: Ornatsky et al, 1997 (from a study by Yu, 1996)
Mef2C, amino acids 1-109: Krainc et al, 1998
Mef2C, amino acids 1-105 : Okamoto et al, 2000
Mef2D, amino acids 1-153: Shin et al, 1999 (from a study by Molkentin et al, 1996)

Considering the lengths of these previous proteins and the established location of the MADS and Mef2 domains a length of around 110-140 amino acids seemed suitable for a truncation of *Drosophila* Mef2. A length of 128 amino acids was chosen based on the criteria outlined and that it fell conveniently with primer design.

I called this Mef2 dominant negative truncation fused to the engrailed repressor, Mef2-En.

The second dominant negative is a Mef2 truncation alone. It consists of the first 128 amino acids of Mef2 followed by an introduced Stop codon. I called this Mef2 dominant negative

protein Mef2-Stop. Both of the Mef2 dominant negatives were made as UAS constructs for use with the Gal4 UAS system (Brand and Perrimon, 1993). A schematic of the Mef2-En, Mef2-Stop and Wild Type Mef2 is shown in FIG 3.1.1 See Materials and Methods 2.4.1 for Primer sequence and cloning protocol for generation of the constructs.

After generating the Mef2-En and Mef2-Stop constructs, I first confirmed them by sequencing and they were injected in-house (J.Han) to establish multiple transgenic lines. I chose to concentrate my investigations on homozygous viable insertion lines in order to try to minimise any potential phenotypes arising from effects caused by construct insertion and to make analysis more straight forward on crossing with Gal4 flies (avoiding the need to select against balancer chromosome markers of heterozygous insertion lines in the experimental progeny). After initial testing of a number of insertion lines (See Table 2.3.4 Materials and Methods), I chose to use the following homozygous lines for characterisation; Mef2-En L10-1 (X) and Mef2-En L2-1 (II) and Mef2-Stop L6-1 (II) ; Mef2-Stop L4-1 (III).

Initially I wanted to test if any muscle phenotype at all could be generated through the use of the constructs, and if so, to characterise this phenotype in detail and establish the nature of it; asking if it occurs through a reduction in Mef2 activity, as one would expect if the constructs were functioning correctly as dominant negative proteins.

3.2 Mef2 dominant negative lines disrupt somatic myogenesis

To test if the Mef2 dominant negative constructs gave any phenotype I over-expressed them in the embryo using Mef2 Gal4. I chose this driver because it would allow for the most direct competition with endogenous Mef2 protein (being expressed in all the same places) and because Mef2 Gal4 is a particularly strong mesodermal driver (Ranganayakulu et al, 1996).

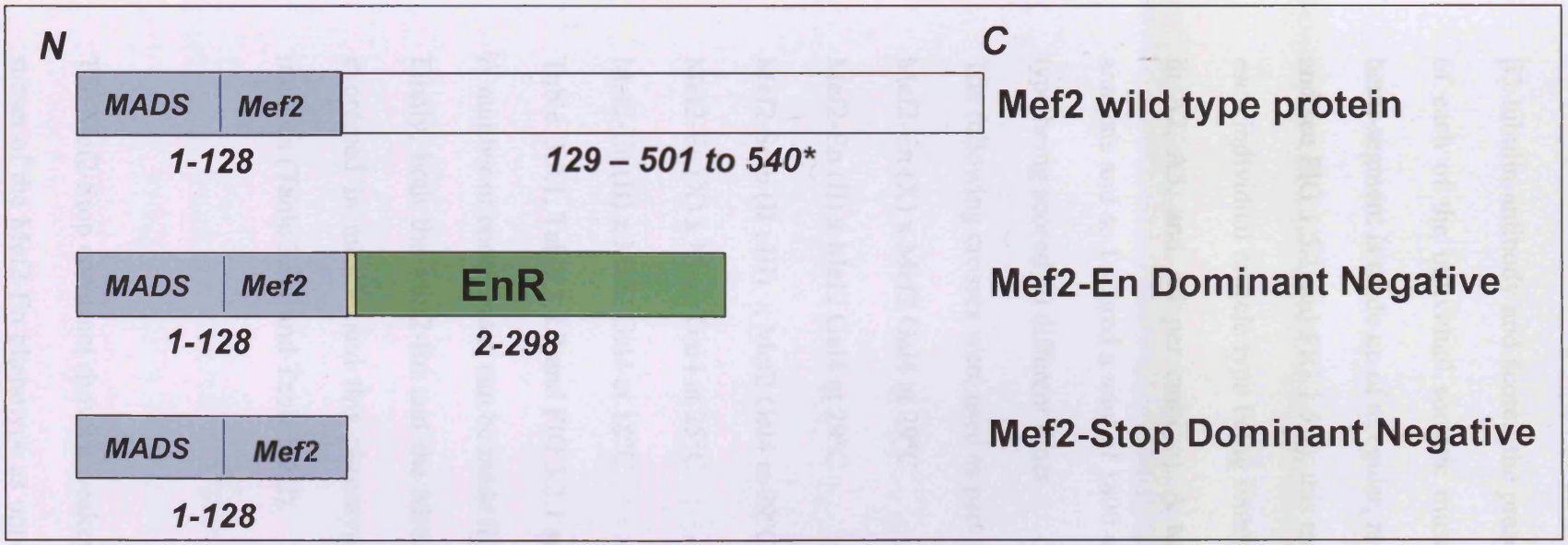

FIG 3.1.1 The structure of wild type Mef2 and the Mef2-En and Mef2-Stop Dominant Negative proteins.

Schematic showing the structure of normal Mef2 protein in *Drosophila* and the two types of Mef2 dominant negative designed for this study.; Mef2-En and Mef2-Stop.

Wild type Mef2 contains the MADS domain and the Mef2 domain at its N terminal end. The MADS domain confers DNA binding ability and Mef2 homodimerisation ability and the Mef2 domain provides heterodimerisation ability; allowing Mef2 to bind other proteins. The C terminus contains the transactivation domain which is responsible for Mef2 activating genes once bound to Mef2 binding sites within their regulatory DNA region.

*The size of the Mef2 protein is between 501 and 540 amino acids depending upon splice variant (A,B,C,D or F) of the gene; however the first splice event occurs at amino acid 186, so amino acids 1-128 are present within all *Drosophila* Mef2 isoforms (Taylor et al, 1995 and Gunthorpe et al, 1999, Flybase).

The Mef2-En dominant negative contains the MADS and Mef2 binding domains, but at amino acid 128, is fused in frame to the repressor domain of the engrailed protein. This domain is covered by amino acids 2-298 of the engrailed protein. The length of Mef2-En is 427 amino acids, including an introduction of 2 amino acids at the restriction site linker that joins the two sections and a stop codon at the end of the engrailed repressor domain.

Mef2-Stop consists of the N terminus of Mef2 alone, and is just amino acids 1-128 with an additional stop codon at the end.

For analysis of the terminal phenotype of somatic musculature I stained St17 embryos with β3-tubulin antibody and scored the presence, absence, shape defects and attachment defects of each of the individual somatic muscles in hemi-segments A2-A4. As each abdominal hemi-segment is made up of a regular, repeating pattern of 30 individual muscles (Bate, 1993) and see FIG 1.5.1 and FIG 1.5.2), this meant I scored a total of 90 muscles per embryo, with each individual muscle type being scored three times per embryo (e.g muscle DT1 is scored in A2, A3, and A4 per embryo). A total of 20 different embryos were scored for each analysis and so I scored a total of 1800 muscles per experiment, with each individual muscle type being scored 60 different times.

The following crosses were used as part of this analysis :

Mef2-En (X) x Mef2 Gal4 at 29°C

Mef2-En (II) x Mef2 Gal4 at 29°C

Mef2-Stop (II ; III) x Mef2 Gal4 at 29°C

Mef2-En (X) x Mef2 Gal4 at 25°C

Mef2-En (II) x Mef2 Gal4 at 18°C

Table 3.2.1, Table 3.2.2 and FIG 3.2.1 and FIG 3.2.2 show the results from this.

A number of conclusions can be made from this data and they are summarised as follows:

Firstly, both the Mef2-En and the Mef2-Stop constructs do give a phenotype when over-expressed in muscle and this phenotype is associated with a decrease in the number of muscles (Table 3.2.1 and Table 3.2.2).

The Mef2-Stop construct shows a weaker phenotype than the Mef2-En construct, but this is a subset of the Mef2-En phenotype as opposed to a completely distinct phenotype. This effect

of Mef2-En being stronger than the Mef2-Stop is perhaps not surprising from previous work which compares a Mef2 truncation with a Mef2 truncation fused to the Engrailed repressor (Karamboulas et al, 2006a).

The Mef2-En (X) line is stronger than the Mef2-En (II) line; more muscles are lost with Mef2-En (X) than with the Mef2-En (II) line when driven at the same temperature (Table 3.2.1, Table 3.2.2 and FIG 3.2.1 compare analysis when driven at 29°C for these two lines).

However, the phenotype of the Mef2-En (II) line driven at 29°C gives a subset of muscle missing that are lost in the Mef2-En (X) line driven at 29°C (Compare Table 3.2.2 row 1 with row 2) and lowering the driving temperature of the Mef2-En (X) line to 25°C makes the phenotype more similar to that produced by the Mef2-En (II) line at 29°C (Compare data for these lines in Table 2.3.1 and in Table 2.3.2); This suggests that the difference in phenotype is due to one line expressing more Mef2-En protein than the other, rather than the effects of an additional gene associated with the position of the Mef2-En (X) insertion in the genome.

The strength of the phenotype can be varied using either choice of line (Mef2-En (X), Mef2-En (II) or Mef2-Stop (II ; III) and choice of driving temperature and each of these phenotypes give a clear range of effects.

From this range of effects conclusions can be made about which individual muscles are more susceptible to effects from the constructs; i.e which muscles are more easily lost and which are more readily retained in the embryo (Table 3.2.2).

Muscle Phenotype	**Mef2-En (X)** x Mef2 Gal4 **(29°C)**	**Mef2-En (X)** x Mef2 Gal4 **(25°C)**	**Mef2-En (II)** x Mef2 Gal4 **(29°C)**	**Mef2-En (II)** x Mef2 Gal4 **(18°C)**	**Mef2-Stop (II ; III)** x Mef2 Gal4 **(29°C)**	**Wild Type** (Oregon R) **(29°C)**
% Embryos with Muscle missing	100 %	100 %	100 %	75 %	37.5 %	0 %
Average No. Muscles Missing per embryo	34.2	22.3	25.9	2.5	1.5	0
Range of Muscles Missing per embryo	26 – 45	9 - 46	20 - 34	0 - 6	0 - 3	0

Table 3.2.1 The Mef2 Dominant Negative lines cause a loss of muscle with a range of effects according to line and driving temperature.

The two different types of Mef2 Dominant Negative ; Mef2-En and Mef2-Stop, were tested by driving throughout the musculature with Mef2 Gal4 at various temperatures. Two homozygous lines for the Mef2-En construct were tested (Mef2-En (X) and Mef2-En (II)) and a single stock of the Mef2-Stop construct was tested. This stock, Mef2-Stop (II;III), has a homozygous insertion for the Mef2-Stop construct on the second and third chromosomes.

Fixed embryos were stained with β3-tubulin antibody to visualise the musculature and the individual somatic muscles of St17 embryos were scored. Scoring was performed for each of the 30 muscles in an abdominal hemi-segment for hemi-segments A2-A4 (a total of 90 muscles) and this was done for 20 separate embryos for each experimental condition tested. An individual embryo only needs to have one muscle missing (A2-A4) to be scored as having muscles missing. The average number of muscles missing per embryo corresponds to A2-A4 only, therefore the maximum number of muscles that can be missing in an embryo is 90 (30 x 3 hemisegments) for any one embryo. The range of muscles missing corresponds to the variation in the total number of muscles missing (A2-A4) for each of the embryos scored for that experiment.

Twenty wild type (Oregon R) embryos were scored for this experiment and found to have no muscles missing.

	Muscles Missing in > 50 % Embryos	Muscles Missing in 25 -49 % Embryos	Muscles Missing in 10 -24 % Embryos
Mef2-En (X) x *Mef2 Gal4* **(29°C)**	DA1, **DA2**, **DO3**, DO4 DA3, LT4, LO1, SBM, VL1, VL4, VA1, VA3, VO1, VO2, VO3, **VO4**, VO5, **VO6**	DO2, DO5, LL1 LT1, LT3, VT1 VL2, VL3	DO1, DT1, LT2 VA2
Mef2-En (II) x *Mef2 Gal4* **(29°C)**	**DA2, DO3**, DO4, DA3, DO5, VO1, VO2, **VO4 VO6**, VL4, VA1, VO5	DA1, LL1, VL1, VL2	DO2, LT3, SBM
Mef2-En (X) x *Mef2 Gal4* **(25°C)**	**DA2**, **DO3,** DO4, DA3, DO5, LL1, SBM, VA3, VO3, **VO4**, VO5, **VO6**	DO2, LT1, LT4, LO1, VT1, VL1, VL2, VL3, VL4, VA1, VO1, VO,	DO1, DA1, LT2, LT3
Mef2-En (II) x *Mef2 Gal4* **(18°C)**	-	**DA2**, **VO4**, **VO6**	**DO3**, VO5
Mef2-Stop (II) ; (III) x *Mef2 Gal4* **(29°C)**	-	-	**DA2, DO3, VO4**

TABLE 3.2.2 Phenotype analysis of muscles missing in Mef2 dominant negative experiments.

Individual somatic muscles missing in various experimental conditions using either the Mef2-En and Mef2-Stop Dominant Negative lines. Two lines were tested for the Mef2-En Dominant Negative; Mef2-En (X) and Mef2-En (II).

To be scored as missing in an embryo for this table, one or more copies of the individual muscle must be lost within hemi-segments A2-A4. The data presented then corresponds to the total percentage of embryos that show this muscle loss out of all the embryos scored in the analysis.

Highlighted in bold are the individual muscles that are more susceptible to the action of the constructs; they are lost at the highest frequency within each experimental condition.

Embryos were stained with β3-tubulin antibody to allow visualisation of the St17 muscles for analysis.

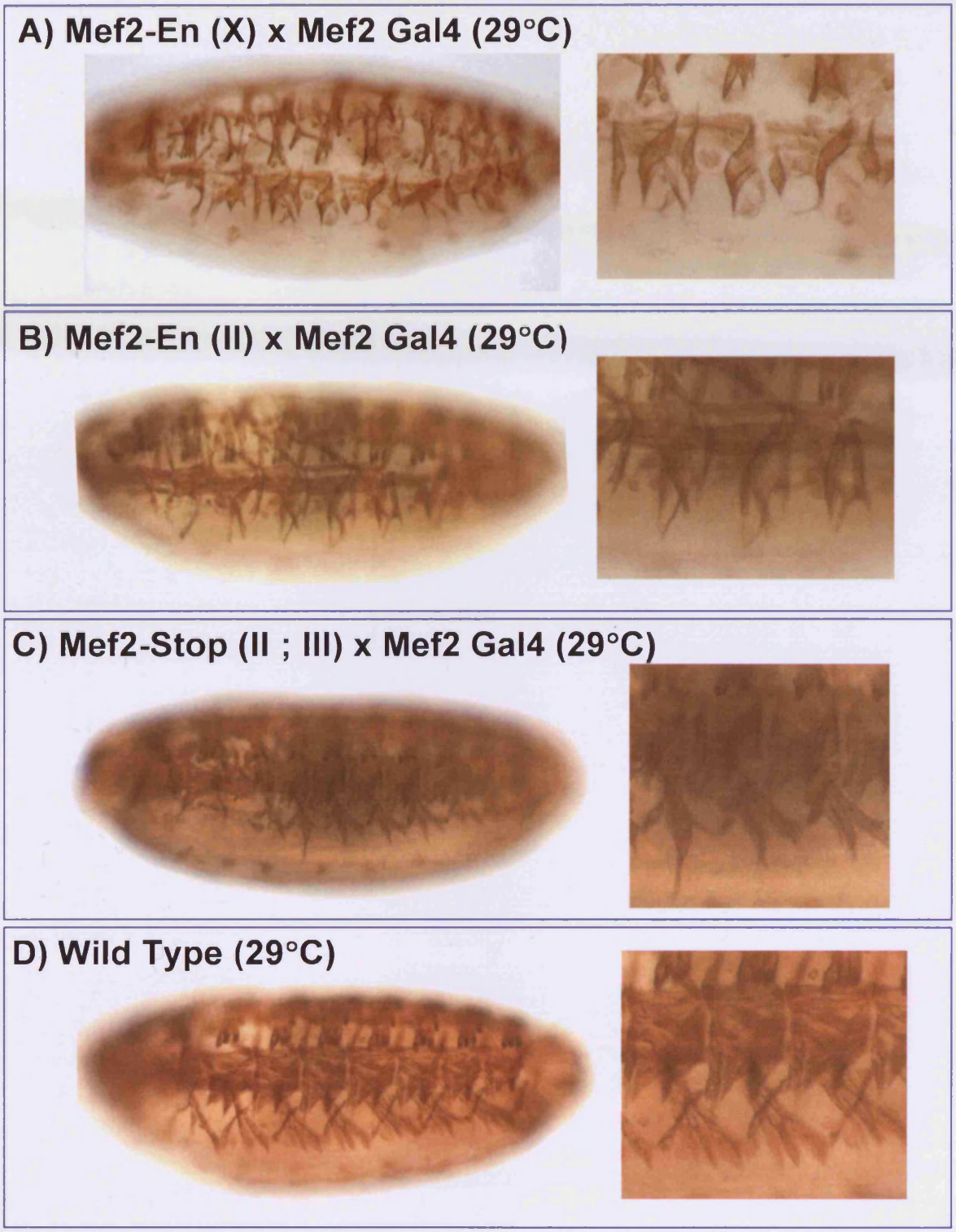

FIG 3.2.1 The Mef2-En and Mef2-Stop constructs give a somatic muscle phenotype

The Mef2-En (X), Mef2-En (II) and Mef2-Stop constructs were driven by Mef2 Gal4 at 29°C, stained with β3-tubulin to visualise musculature and representative St17 embryos shown (A, B, C). A comparison to wild type (D) can be made.

FIG 3.2.2 Graphs to show muscle phenotype for Mef2 Dominant Negative lines at different temperatures

Different Mef2-En and Mef2-Stop dominant negative lines were driven at various temperatures and the individual muscles of hemi-segments A2-A4 for 20 embryos of each experimental condition were scored. The percentage of embryos that show at least one individual muscles to be missing (Blue) or duplicated (Red) are shown in the graphs. Only one copy of a particular muscle type needs to be missing from A2-A4 for that embryo to be scored.

Muscles labelled in graph in following order left to right; DO1, DA1, DO1, DA2, DO3, DO4, DO5, DT1, LL1, LT1, LT2, LT3, LT4, SBM, LO1, VT1, VL1, VL2, VL3, VL4, VA1, VA2, VA3, VO1, VO2, VO3, VO4, VO5.

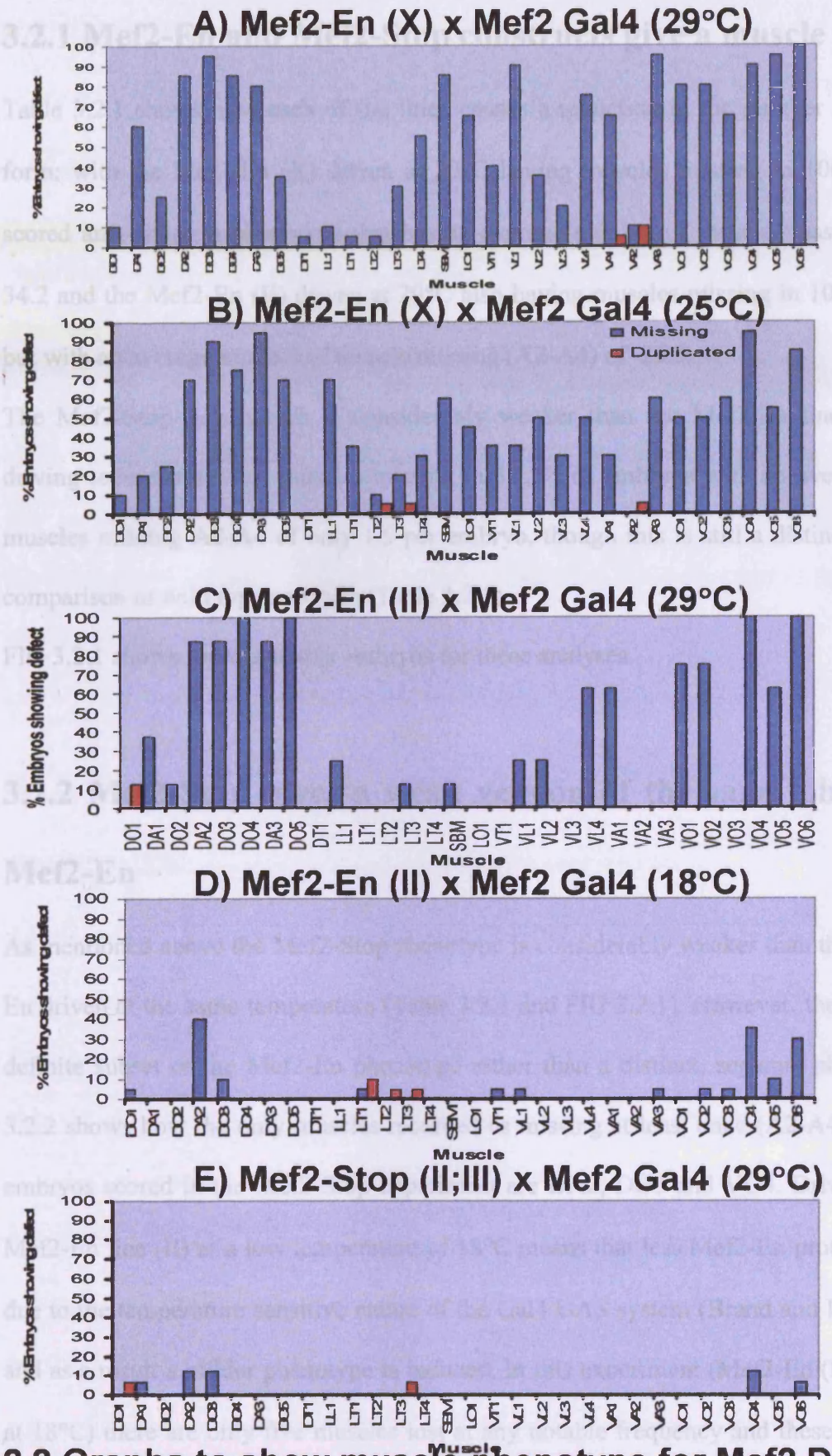

FIG 3.2.2 Graphs to show muscle phenotype for Mef2 Dominant Negative lines at different temperatures

3.2.1 Mef2-En and Mef2-Stop constructs give a muscle phenotype

Table 3.2.1 shows how each of the lines causes a reduction in the number of muscles that form; with the Mef2-En (X) driven at 29°C having muscles missing in 100% of embryos scored and giving a phenotype that has an average number of muscle missing (A2-A4) of 34.2 and the Mef2-En (II) driven at 29°C also having muscles missing in 100% of embryos but with an average number of muscle missing (A2-A4) of 25.9.

The Mef2-Stop line, which is considerably weaker than the Mef2-En lines at this same driving temperature, has muscles missing in 37.5% of embryos with an average number of muscles missing A2-A4 of only 1.5 per embryo, though this is still a distinct phenotype in comparison to wild type embryos (Table 3.2.1).

FIG 3.2.1 shows representative embryos for these analyses.

3.2.2 Mef2-Stop gives a weak version of the same phenotype as Mef2-En

As mentioned above the Mef2-Stop phenotype is considerably weaker than that of the Mef2-En driven at the same temperature (Table 3.2.1 and FIG 3.2.1). However, the phenotype is a definite subset of the Mef2-En phenotype rather than a distinct, separate phenotype. Table 3.2.2 shows how the only muscles recorded as missing at least once (A2-A4) in 10-24% of embryos scored in the Mef2-Stop experiment are DA2, DO3 and VO4. Driving the weaker Mef2-En line (II) at a low temperature of 18°C means that less Mef2-En protein is produced due to the temperature sensitive nature of the Gal4 UAS system (Brand and Perrimon, 1993) and as a result a milder phenotype is induced. In this experiment (Mef2-En (II) x Mef2 Gal4 at 18°C) there are only five muscles lost at any notable frequency and these are DA2, VO4

and VO6 missing at least once (A2-A4) in 25-50% of embryos scored and DO3 and VO5 missing at least once (A2-A4) in 10-24% of embryos scored (Table 3.2.2). This result is very encouraging in that it shows that the Mef2-Stop gives a subset effect of the Mef2-En phenotype but also gives indication as to which muscles are more easily lost or gained in an experiment using these constructs. In FIG 3.2.2 this comparison can be seen in a graph representing all muscles that were either missing or duplicated for each experiment. Comparing Mef2-En (II) x Mef2 Gal4 at 18°C here (FIG 3.2.2, D) with Mef2-Stop (II ; III) x Mef2 Gal4 at 29°C (FIG 3.2.2 , E), shows very clearly the similarity of phenotypes, and from this we can also see that the VO6 muscle is lost in 5% of embryos in the Mef2-Stop experiment (not included in Table 3.2.2 data) suggesting the importance of this muscle in the phenotype also.

3.2.3 Mef2-En (X) is stronger than Mef2-En (II), but both give similar phenotypes on temperature variation.

As discussed in section 3.2.1, Mef2-En (X) gives a stronger phenotype in terms of the average number of muscles missing than Mef2-En (II) when driven at 29°C. This is also true for the range of muscles missing (26-45 for Mef2-En (X) and 20-34 for Mef2-En (II) (Table 3.2.1). The analysis of the individual muscles missing (Table 3.2.2) also shows that Mef2-En (X) gives a stronger phenotype than Mef2-En (II); more muscles are missing at a greater frequency. In Table 3.2.2b, I have shown this data again but highlighted the similarities between the muscles affected; in red are muscles that are lost at the same frequency range in Mef2-En (II) as Mef2-En (X) at 29°C and in underlined are muscles that are missing in the adjacent frequency range. This shows very strikingly that the same subset of muscles are lost

	Muscles Missing in > 50 % Embryos	Muscles Missing in 25 -50 % Embryos	Muscles Missing in 10 -24 % Embryos
Mef2-En (X) x *Mef2 Gal4* **(29°C)**	DA1, DA2, DO3, DO4 DA3, LT4, LO1, SBM, VL1, VL4, VA1, VA3, VO1, VO2, VO3, VO4, VO5, VO6	DO2, DO5, LL1 LT1, LT3, VT1 VL2, VL3	DO1, DT1, LT2 VA2
Mef2-En (II) x *Mef2 Gal4* **(29°C)**	DA2, DO3, DO4, DA3, DO5, VL4, VA1, VO1, VO2, VO4, VO5, VO6	DA1, LL1, VL1, VL2	DO2, LT3, SBM

TABLE 3.2.2b Comparison of the muscle phenotypes of Mef2-En (X) and Mef2-En (II) driven by Mef2 Gal4 at 29°C.

for the two lines, with nearly all the muscles lost in Mef2-En (II) being lost at the same or similar frequencies in Mef2-En (X) at this temperature. FIG 3.2.2 shows this information in the form of a graph (compare A with C). Dropping the driving temperature of Mef2-En (X) to 25°C brings the muscle phenotype to one that is more similar to that of Mef2-En (II) at 29°C, as seen in FIG 3.2.2 B and C and the average number of muscles missing (A2-A4) and the range of muscles missing for these experiments (Table 3.2.1).

3.2.4 The strength of phenotype can be varied by changing the UAS line or the driving temperature.

As has been shown in this section (3.2.1-3.2.4) the different UAS lines (Mef2-En (X) or (II) and the different constructs (Mef2-En or Mef2-Stop) can be placed in order for the strength of phenotype associated with them; Mef2-En (X) > Mef2-En (II) > Mef2-Stop (II ; III) and as one would expect with the Gal4 UAS system, the driving temperature can also vary this phenotype due to increased or decreased amounts of protein production with higher or lower temperature respectively (Brand and Perrimon, 1993). Consequently this shows that the three lines can be used accordingly to give a range of phenotypes as desired.

3.2.5 There are subsets of muscles that appear more readily lost.

As alluded to in the Mef2-Stop section (section 3.2.2), there are muscles that seem to be most easily lost – DA2, DO3, VO4 and VO6 and these are missing in all experimental conditions; In mild phenotype associated with Mef2-Stop they are the only muscles missing and this loss is at a low frequency (at least once A2-A4 in 5-24% of embryos). When driving the weaker Mef2-En at a low temperature (Mef2-En (II) at 18°C) they represent the majority of the

muscles missing (4 out of 5, the other being VO5) with this loss occurring at a higher frequency (at least once (A2-A4) in 25-50% of embryos for DA2, VO4 and VO6 and at least once (A2-A4) in 10-24% of embryos for DO3) and when the Mef2-En lines (II) or (X) are driven at a higher temperatures they are the consistently the most frequently lost individual muscle types (FIG 3.2.2) of a subset of a large number of muscles missing (Table 3.2.2).

3.2.6 There are subsets of muscles that appear more readily retained.

Conversely, from this there are individual muscles that remain present in the embryo even in the conditions where there is substantial muscle loss with a severe phenotype (e.g Mef2-En (X) or Mef2-En (II) at higher driving temperatures of 29°C or 25°C. Here we can see that the individual muscles DO1, DT1, LT2 and VA2 appear to be frequently present in all conditions. This suggests that the development of these muscles is less susceptible to the Mef2-En and Stop constructs.

FIG 3.2.3 shows a summary of the muscles most frequently missing and present with the constructs.

3.2.7 Characterisation of the Mef2-En construct

After establishing that the Mef2-En can give a strong muscle phenotype and the severity of the phenotype is dependent upon the strength of the Gal4 driver used and the temperature the experiment is performed at, I wanted to further investigate the nature of this phenotype for both of the homozygous lines investigated. At this point, due to the weak nature of the Mef2-

Muscles most frequently missing

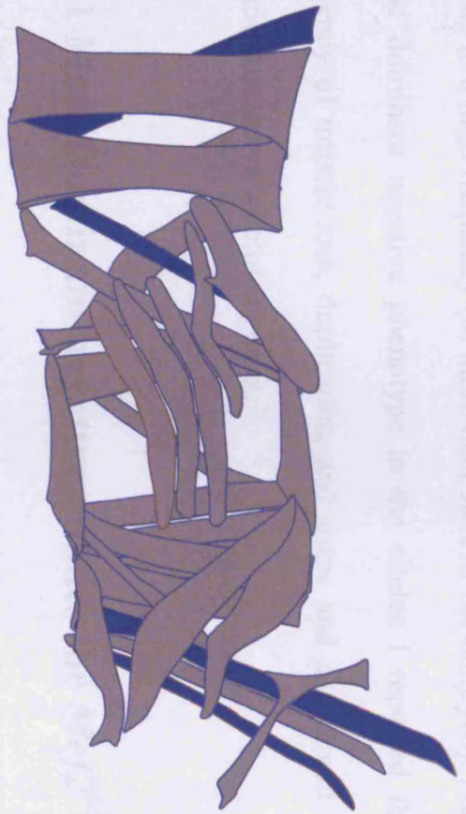

DA1, DO3, VO4, VO6

Muscles most frequently present

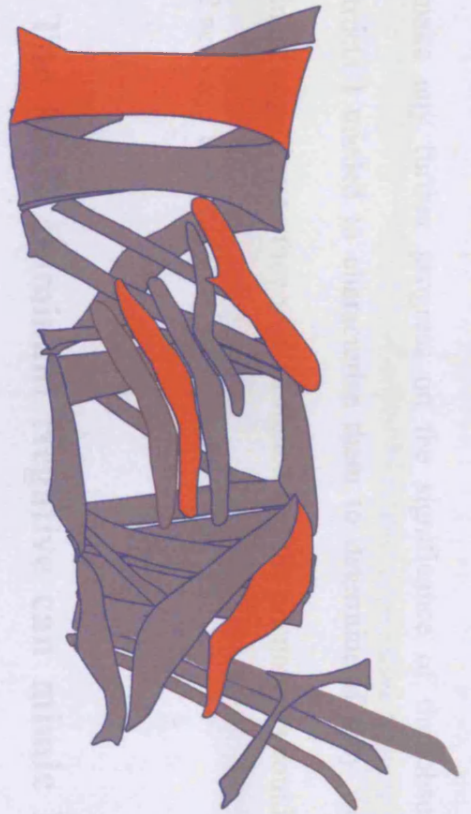

DO1, DT1, LT2, VA2

FIG 3.2.3 Muscles most frequently missing and present in the somatic muscle phenotypes associated with Mef2-En and Mef2-Stop constructs.

Stop phenotype (and that it appeared to be a weaker version of the Mef2-En dominant negative), I decided to predominantly concentrate on characterisation of the Mef2-En construct lines.

To make any further progress on the significance of the observations made with the constructs I needed to characterise them to determine if they were functioning as Mef2 dominant negatives as they were designed and the phenotypes could be attributed to a loss of Mef2 activity. This characterisation is described below.

3.3 The Mef2 Dominant Negative can mimic Mef2 hypomorph alleles.

The previous studies of *Mef2* hypomorphs (Ranganayakulu et al, 1995; Gunthorpe et al,1999) went into limited detail regarding somatic muscle defects, only reporting muscles that were missing at a high frequency (in more than 50% of the embryos). For an accurate comparison of the dominant negative phenotype to the alleles I repeated this analysis, scoring the frequency of muscle loss, duplication, and shape and attachment defects for all of the 30 somatic muscles in a hemi-segment.

3.3.1 Mef2 Dominant negative mimics the *Mef2*^{65} allele.

The *Mef2*^{65} mutant is a weak hypomorph, which has some muscle deletions and defects due to a decrease in Mef2 activity. In the Ranganayakulu study it is reported that the LO1 and SBM muscles are consistenty missing, and in the Gunthorpe study it is reported that LO1, VA3, VO3 and LT4 are missing in over 50% of embryos scored (10 embryos were scored for the Gunthorpe analysis and SBM was never observed as missing) (Ranganayakulu et al, 1995;

	Muscles Missing in > 50% Embryos	Muscles Missing in 25 -49% Embryos	Muscles Missing in 10 -24% Embryos	Shape Defects in > 75% of embryos
Mef2^{65}	VA3, **VO4**	LT4, LO1, **VO5**, **VO6**	**DA2**, **DO3**, SBM, VL2, VL3, VO3	DO3, DO4, DA3, LT1 VT1, VA1, VA2, **VA3** VO4, VO5, VO6
Mef2-En (II) x Mef2 Gal4 @ 18°C	-	**DA2**, **VO4**, **VO6**	**DO3**, **VO5**	**VA3**
Mef2^{65} (Ranganayakuku 1995)	LO1, SBM			
Mef2^{65} (Gunthorpe 1999)	LO1, VA3, VO3, LT4			

Table 3.3.1 The same subsets of muscles are missing and affected in the *Mef2*^{65} hypomorph as the Mef2 Dominant Negative.

The *Mef2*^{65} mutant is a weak *Mef2* hypomorph which has some muscle deletions and defects due to a decrease in Mef2 activity. (Ranganayakulu et al 1995, Gunthorpe et al 1999). When Mef2 activity is reduced mildly, by using the Mef2 Dominant Negative at a low temperature, the mild *Mef2*^{65} hypomorph can be mimicked. All of the individual somatic muscles missing when the Mef2 Dominant Negative is driven at 18°C are missing in the *Mef2*^{65} mutant (Highlighted as Bold in Table).

The data for the *Mef2*^{65} phenotype from the Ranganayakulu et al, 1995 and the Gunthorpe et al, 1999 studies are included in the table for comparison to the detailed data for the *Mef2*^{65} phenotype obtained for this study.

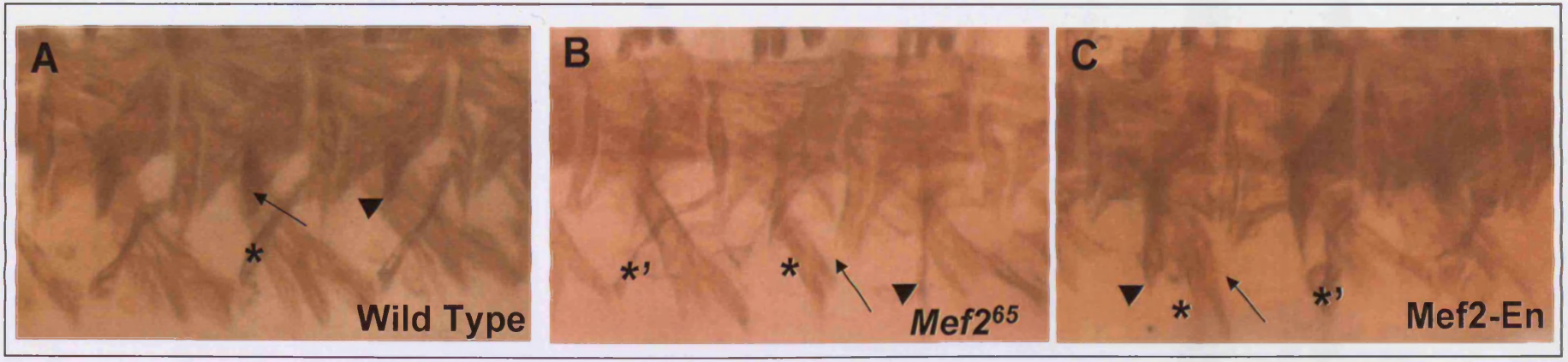

FIG 3.3.1 The Mef2 Dominant Negative can mimic the muscle phenotype of the *Mef2^{65}* mutant.

Driving the Mef2-En (II) Dominant Negative in the Mef2 pattern at 18°C can mimic the phenotype of the weak *Mef2^{65}* hypomorph mutant. For example in the ventral muscles VO6 is missing (arrow in B and C), VA3 is either missing (* in B and C) or misshapen (* ' in B and C) and VA2 is misshapen, projecting further ventrally than wild type (compare arrow head in B and C to wild type, A).

A schematic of these muscles affected muscles is shown in D.

Dominant negative line used is Mef2-En (II), crossed with Mef2 Gal4 at 18°c. The *Mef2^{65}* mutants were first selected against GFP to ensure embryos were homozygous mutants. All embryos were stained with anti β3-tubulin antibody and viewed laterally, with ventral muscles of hemi-segments A2-A4 shown in figure.

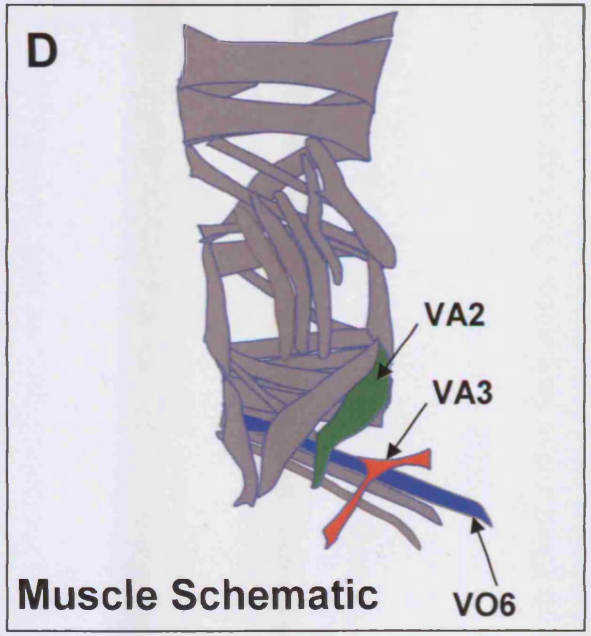

Gunthorpe et al, 1999). Here I present data showing muscle loss over a range of frequencies and shape defects seen in individual muscles in over 75 % of embryos scored (20 embryos scored for each experimental condition) (Table 3.3.1).

When the Mef2-En (II) dominant negative was driven by Mef2 Gal4 at a temperature of 18°C, a mild muscle phenotype was seen. This phenotype is similar to that seen with the $Mef2^{65}$ allele; all of the muscles that were missing in the Mef2 DN were missing at a similar frequency in the $Mef2^{65}$ mutant (Table 3.3.1 – muscles highlighted in bold). In addition, muscle defects that are seen in the $Mef2^{65}$ mutant, such as VA2 projecting further ventrally and VA3 being misshapen compared to wild type, are also seen in the Mef2 dominant negative (FIG 3.3.1).

The similarity of phenotype between the Mef2-En driven by Mef2 Gal4 at the relatively low temperature of 18°C and the phenotype of the weak $Mef2^{65}$ mutant allele suggests that the Mef2-En muscle phenotype may occur as a result of a mild reduction in Mef2 activity. In addition this similarity of phenotype from a reduction in Mef2 activity by two completely different ways may indicate the individual muscles that are more readily lost when Mef2 activity is reduced and that perhaps have a higher Mef2 requirement for their correct development than other individual somatic muscles.

3.3.2 Mef2 Dominant negative mimics the $Mef2^{424}$ allele.

As previously established in the Ranganyakulu and Gunthorpe studies the $Mef2^{424}$ hypomorph has a much more severe phenotype than $Mef2^{65}$; the weak $Mef2^{65}$ allele causes a phenotype where fewer muscles are missing than the stronger $Mef2^{424}$ intermediate hypomorph, though these muscles lost are a subset of those missing in the $Mef2^{424}$ phenotype (Ranganayakulu et al, 1995; Gunthorpe et al, 1999).

Experiment	Muscles Missing in > 50% Embryos	Muscles Missing in 25 -49% Embryos	Muscles Missing in 10 -24% Embryos
Mef2^{424}	DA1, **DA2**, DA3, **LT4, SBM, LO1, VL2, VO4, DO3,** DO4, DO5, VO2, **VO6**	DO1, DO2, LT3, **VL3,** VL4, **VA3,** VO1, **VO3, VO5**	DT1, VT1
Mef2^{65}	**VA3, VO4**	**LT4, LO1, VO5, VO6**	**DA2, DO3, SBM, VL2, VL3, VO3**
Mef2^{424} (Ranganayakulu 1995)	DO3, DA3, LO1, SBM, VL2, VL3, VL4, VO5		
Mef2^{65} (Ranganayakulu 1995)	LO1, SBM		
Mef2^{424} (Gunthorpe 1999)	DO3, DA3, *VO3, VA3, LO1,* ((VO4, VO5, VO6))		
Mef2^{65} (Gunthorpe 1999)	*LO1, VA3, VO3,* LT4		

Table 3.3.2 Comparison of muscles missing in *Mef2*^{424} and *Mef2*^{65} hypomorph mutants

Table to show how individual muscles are lost in *Mef2*^{424} and *Mef2*^{65} hypomorph mutants in the three studies carried out on them (this study, Ranganayakulu et al, 1995 and Gunthorpe et al, 1999). For each study, the muscles lost in the *Mef2*^{65} hypomorph are a subset of those lost in the *Mef2*^{424} hypomorph mutant (highlighted as bold for this study, underlined for Ranganyakulu study and italicised for Gunthorpe study).

Brackets surrounding VO4,VO5,and VO6 in *Mef2*^{424} analysis of Gunthorpe study mean that two out of these three muscles are lost in 50% of embryos scored.

Embryos were stained with β3-tubulin to visualise musculature and muscles were scored in hemi-segments A2-A4 for 20 embryos. Only one individual muscle out of the three scored (A2-A4) need be missing for an embryo to be scored as having that muscle type missing.

The analysis required for this study, went into greater depth, showing that not only are all the muscles missing in $Mef2^{65}$ mutants also missing in $Mef2^{424}$ mutants, but also that these muscles are often missing at a higher frequency in $Mef2^{424}$ mutants (Table 3.3.2) – for example LT4 and LO1 were missing in 25-49% of $Mef2^{65}$ embryos but over 50% of $Mef2^{424}$ embryos. Similarly, VL3 and VO3 were missing in 10-24% of $Mef2^{65}$embryos but in 25-49% of $Mef2^{424}$ embryos. Muscles, such as DT1 and VT1, that were only occasionally lost in $Mef2^{424}$ mutants were never observed as lost in any of the $Mef2^{65}$ mutants scored. All of this shows that not only does $Mef2^{65}$give muscles missing that are a subset of $Mef2^{424}$ but also that this phenotype is a milder version of the same effect – suggesting that each of the individual somatic muscles can be ordered into their requirement of Mef2 activity to correctly form. Muscles such as VO4 and LO1, are the most easily lost and so we can conclude that these require the most Mef2 activity to form, whereas muscles such as DT1 and VT1 often remain present even in conditions associated with a significant decrease in Mef2 activity and thus require only a low amount of Mef2 activity to correctly form (Table 3.3.2).

In addition I found that both the average number of muscles missing per embryo scored, and the range of muscles missing in an embryo are considerably higher in the $Mef2^{424}$ mutant compared to the $Mef2^{65}$ mutant (Table 3.2.3) This stronger muscle phenotype consequently results in a lower embryo survival rate, when hatching and survival experiments are performed (Table 3.3.3).

By driving the Mef2 Dominant Negative with Mef2 Gal4 at a higher temperature (29°C instead of 18°C) a more severe muscle phenotype was induced. This is because the Gal4 UAS system is temperature dependent; an increase in temperature causes a greater production of Gal4 protein which consequently leads to expression of more UAS protein (Brand and Perrimon, 1993). So, in theory this would mean that there is more Mef2 dominant negative protein available to compete with endogenous Mef2.

Muscle phenotype	***Mef2*** ^{424} (25°c)	***Mef2*** ^{65} (25°c)
% embryos with muscle missing	100 %	100 %
Average No. muscles missing per embryo	25.1	4.5
Range of muscles missing per embryo	14 - 34	1 - 9

Survival assay		
Hatching	7.8 %	79.9 %
Survival	0 %	0 %

Table 3.3.3 Comparison of severity of *Mef2* ^{424} and *Mef2* ^{65} hypomorphs.

Table showing how the severity of the *Mef2*^{424} mutant varies compared to the *Mef2*^{65} mutant.

Individual somatic muscles were visualised with anti β3 tubulin antibody and muscles in abdominal hemisegments A2-A4 of 20 St17 embryos were scored after homozygous mutant embryos were taken after selection against GFP. Stocks used *Mef2*^{424} / CyO *wg* GFP and *Mef2*^{65} / CyO *wg* GFP (Ranganayakulu et al, 1999)

For Hatching and Survival assay 200 homozygous fertilised embryos were selected by absence of GFP marker gene and gut auto-fluorescence respectively and then their progress through the life cycle (FIG 1.1) was charted from hatching of 1st instar larva at the end of embryogenesis to eclosion of adult flies after pupation. 20 Wild type embryos scored showed no muscles missing and gave a hatching rate of 99% and survival rate of 98%.

This severe muscle phenotype is strikingly similar to the muscle phenotype of *Mef2*^{424} mutants. Analysis of the somatic musculature (abdominal hemi-segments A2-A4) of St17 embryos revealed that the severity of the Mef2 dominant negative and *Mef2*^{424} phenotypes are the same; both in terms of the average number of muscles missing per embryo (25.1 / 90 missing in A2-A4 of *Mef2*^{424} embryos, compared to 25.9 / 90 missing in A2-A4 of embryos over-expressing the Mef2 dominant negative) and in terms of the range of muscles missing per embryo (between 14 and 34 muscles missing (A2-A4) in *Mef2*^{424} embryos compared to between 20 and 34 muscles missing (A2-A4) in Mef2 dominant negative embryos) (Table 3.3.4). More importantly, it is the same individual muscles that are missing in the two experimental conditions that are generating these phenotypes; the same muscles are lost at the same or similar frequencies in the *Mef2*^{424} mutant and the Mef2 dominant negative. For example, DA2, DO3, DO4, DA3, VO4 and VO6 are all missing in over 50% of embryos in both *Mef2*^{424} and the Mef2 dominant negative driven by Mef2 Gal4 at 29°C (underlined and bold, Table 3.2.5). In addition, not only are other muscles lost at similar frequencies, but the same muscles frequently remain present (e.g LT1, LT2 and VA2 were never scored as missing in either experimental condition) (Table 3.3.5).

The appearance of the phenotype can be seen to mimic *Mef2*^{424} in St17 embryos stained with anti β3-tubulin antibody (FIG 3.3.2).

In addition, although the stronger Mef2 dominant negative line (Mef2-En (X)) gave a phenotype when it was driven by Mef2 Gal4 at 29°C that was generally more severe in terms of number of muscles affected than the *Mef2*^{424} allele (an average number of muscles missing of 34.2 (A2-A4) with a range of 26-45 for Mef2-En (X) driven by Mef2 Gal4 at 29°C (Table 3.2.1) as opposed to an average of 25.1 muscles missing (A2-A4) and a range of 13-34 for the *Mef2*^{424} mutant (Table 3.3.3)) , it could still show individual embryos within

Muscle phenotype	***Mef2*** ^{424} (25°c)	**Mef2-En x *Mef2 Gal4*** (29°c)
% embryos with muscle missing	100 %	100 %
Average No. muscles missing per embryo	25.1	25.9
Range of muscles missing per embryo	14 - 34	20 - 34

Survival assay		
Hatching	7.8 %	52 %
Survival	0 %	0 %

Table 3.3.4 Mef2 Dominant Negative can mimic the *Mef2* ^{424} hypomorph.

When driven at a higher temperature the Mef2-En (II) Dominant negative can cause a greater reduction in Mef2 activity, mimicking the intermediate *Mef2* hypomorph mutant allele *Mef2*^{424}. Both the severity of the muscle phenotype (this table) and the individual muscles missing (Table 3.2.5) are comparable. Images of representative embryos show the similarity of the phenotype (FIG 1.2.1).

For the muscle phenotype experiment 90 muscles were scored (hemisegments A2-A4) per embryo, with a total of 20 embryos scored for each cross. Only 1/90 muscles need be missing for an embryo to be scored as having muscles missing. 20 Wild type embryos scored showed no muscles missing and gave a hatching rate of 99% and survival rate of 98%.

Lines used : Mef2-En (II) for Mef2 Dominant Negative and Mef2^{424} *(Ranganayakulu et al, 1999), Oregon R for wild type . Embryos stained with anti b3-tubulin (guinea pig).*

	Muscles Missing in > 50% Embryos	Muscles Missing in 25 -49% Embryos	Muscles Missing in 10 -24% Embryos
Mef2^{424}	**DA1, DA2, DA3,** LT4, SBM, LO1, **VL2, VO4, DO3, DO4, DO5, VO2, VO6**	DO1, **DO2, LT3,** VL3, **VL4,** VA3, **VO1,** VO3, **VO5**	DT1, LL1, VT1
Mef2-En (II) x Mef2 Gal4 (29°C)	**DA2, DO3, DO4, DA3, DO5, VO1, VO2, VO4, VO6, VL4,** VA1, **VO5**	**DA1,** LL1, VL1, **VL2**	**DO2, LT3,** SBM
Mef2^{424} (Ranganayakulu 1995)	DO3, DA3, LO1, SBM, VL2, VL3, VL4, VO5		
Mef2^{424} (Gunthorpe 1999)	DO3, DA3, VO3, VA3, LO1, ((VO4, VO5, VO6))*		

Table 3.3.5 - The same subsets of muscles are missing and affected in the *Mef2*^{424} hypomorph as the Mef2 Dominant Negative

The *Mef2*^{424} mutant is an intermediate Mef2 hypomorph which has many muscle deletions and defects due to a decrease in Mef2 activity. (Ranganayakulu et al,1995; Gunthorpe et al, 1999,this study). The UAS Gal4 system is temperature sensitive and can be driven harder, producing more protein, at higher temperatures, consequently inducing a stronger phenotype (Brand and Perrimon, 1993). By driving the Mef2-En (II) Dominant Negative at 29°C instead of 18°C a stronger muscle phenotype can be induced, altering the phenotype from one that mimics the weaker *Mef2*^{65} hypomorph to one that mimics the intermediate *Mef2*^{424} hypomorph.

*In the Gunthorpe study one or more of either VO4, VO5 or VO6 muscles are missing. They are not scored individually.

The vast majority of muscles missing when the Mef2 Dominant Negative is driven by Mef2 Gal4 at 29 °C are also missing in the *Mef2*^{424} hypomorph (bold in table).

FIG 3.3.2 Mef2-En dominant negative can mimic the *Mef2^{424}* hypomorph

A wild type embryo at 29 °c shows the regular muscle pattern (A) whereas an embryo over-expressing the Mef2-En (II) Dominant Negative at 29°c in the Mef2 Gal4 pattern (B) shows a phenotype that resembles that seen in the *Mef2^{424}* hypomorph mutant (C). Dorso-lateral muscles such as DO3, DO4 and DA3 are frequently missing or misshapen.

Embryos are St17, stained with anti β3-tubulin antibody to visualise musculature and orientated dorso-laterally. *Mef2 ^{424}* mutants were first selected against GFP with antibody staining to ensure homozygosity of the mutant.

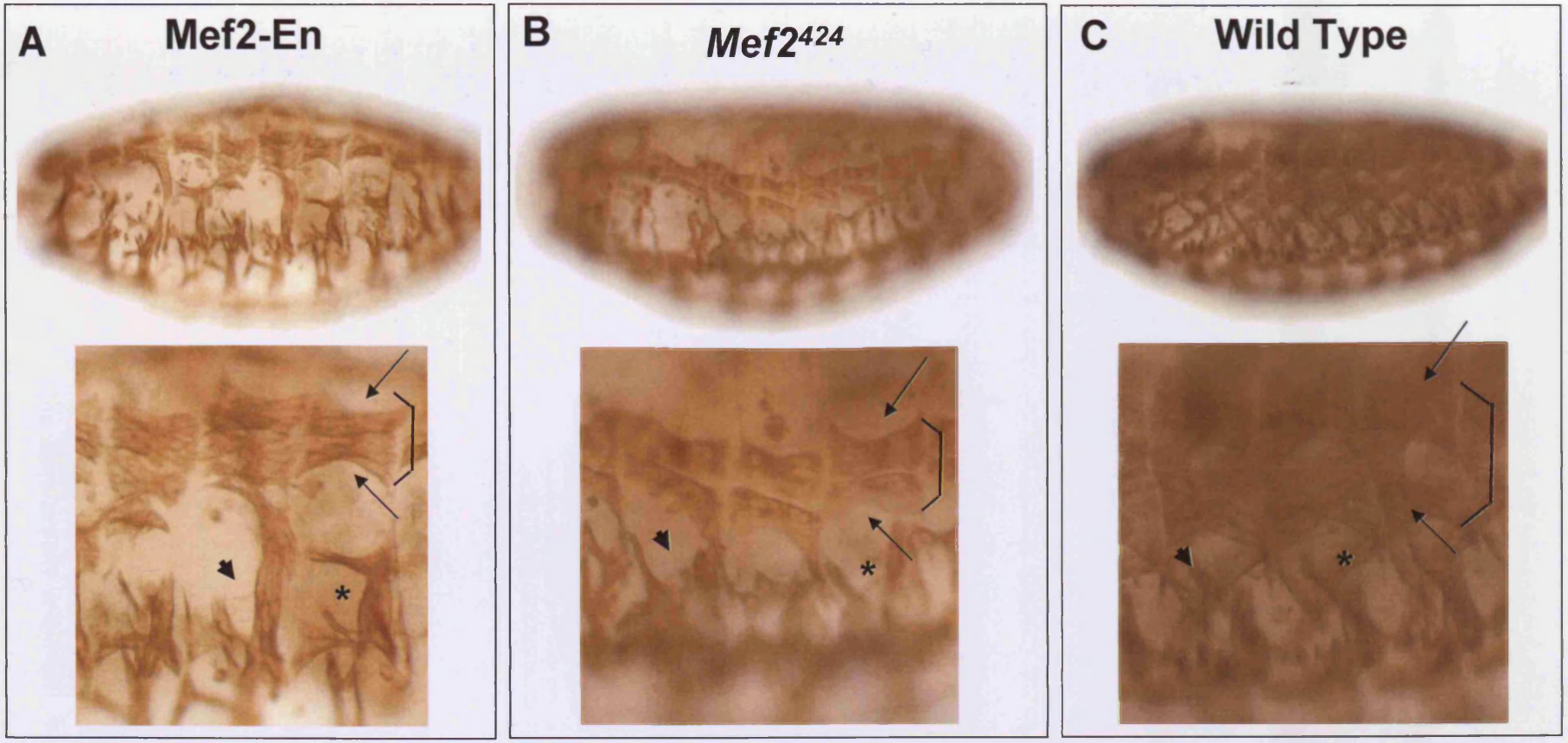

FIG 3.3.3- Mef2-En (X) Dominant Negative can also mimic the *Mef2*^{424} hypomorph allele

Representative St17 embryos stained with b3-tubulin show that the Mef2 Dominant Negative driven at 29°c with Mef2 Gal4 (A) is capable of mimicking the *Mef2* ^{424} hypomorph (B). DA1 and DA2 are missing (compare arrows in A and B to wild type C), DO3 is missing (compare arrowhead in A and B to wild type C), DA3 is missing or missattached (compare asterisk in A and B to wild type C) and DO1 and DO2 muscles are thinner than wild type (bracket in A and B versus C). In addition to the same individual somatic muscles being affected in the Mef2 DN at this temperature and the *Mef2* ^{424} mutant (this fig and Table 1.2.2), the embryos have the same severity of muscle phenotype, with the similar average numbers of muscles missing per embryo and the same range of muscles missing per embryo (Table 1.2.1).

the phenotype range that were close mimics of the *Mef2*^{424} muscle phenotype (FIG 3.3.3). This shows that the mimicry of the Mef2-En (II) dominant negative to the *Mef2*^{424} hypomorph does not occur as a result of a chance phenotype caused due to position effects upon insertion of the line, but is due to the genuine action of the Mef2-En dominant negative protein.

The fact that driving the Mef2 dominant negative at a higher temperature gives a mimic of the phenotype associated with the *Mef2*^{424} allele again suggests that the dominant negative phenotype occurs as a result of a reduction in Mef2 activity. However, importantly, it also suggests that through control of the driving temperature of the Mef2 dominant negative, the degree of Mef2 activity level reduction can be regulated. Driving the Mef2 dominant negative at a low temperature, results in a mild reduction in Mef2 activity, giving a phenotype similar to the *Mef2*^{65} allele, whereas driving the dominant negative at a high temperature results in a greater reduction of Mef2 activity, giving a phenotype that mimics the *Mef2*^{424} mutant. One significance of this in the embryo is that it means phenotypes intermediate to those produced by the alleles can be generated when driving with Mef2 Gal4 at various temperatures, but most importantly by using different Gal4 lines it means Mef2 activity level can be reduced by controlled amounts in more specific places and times in development.

3.4 The Mef2 Dominant negative gives a distinct phenotype to UAS Mef2.

Despite the fact that the Mef2 dominant negative can mimic the Mef2 alleles, it is important to show that over-expression of this truncated form of Mef2 protein is not functioning in any way as full-length Mef2. This is especially important as it is well established that over-

expression of full length Mef2 gives a muscle phenotype which shows a significant disruption to muscle pattern (Bour et al, 1995; Gunthorpe et al, 1999). To address this I analysed the phenotype of UAS Mef2 and compared it to the dominant negative phenotype.

3.4.1 Mef2 Dominant negative gives a distinct terminal somatic musculature phenotype when compared to UAS Mef2.

In her study D.Gunthorpe reports that in embryos over-expressing Mef2 "Aberrations in every muscle were seen at least once after scoring 15 hemi-segments for defects." and that "These included deletions and duplications of muscles, as well as muscles found in the wrong position and muscles with shapes that did not resemble wild-type", but that there "did not appear to be a reproducible pattern to this disruption as the precise defects varied from segment to segment and from embryo to embryo" (Gunthorpe et al, 1999).

In this study, I analysed the somatic muscles in abdominal hemi-segments A2-A4 of 20 embryos (60 hemi-segments) and found that although the muscle phenotype gives a range of affects, with muscles being missing, duplicated, missattached or misshapen there is a pattern to the phenotype, with certain muscles being more easily lost than others (e.g, DT1, LT4 and VA1 are missing in over 50% of embryos scored) and other individual muscles remain present more than others (e.g, DO3, DA4, VA3, VO1, VO2 which were either never missing or missing in only 5% of embryos) (FIG 3.4.1, A). What is most striking about this result is how this phenotype, which arises through an increase in Mef2 activity, differs from the phenotype associated with the Mef2 dominant negative. Although both over-expression of full length Mef2 and over-expression of the Mef2 dominant negative cause a disruption to the muscle pattern (See FIG 3.4.2), the way in which the pattern is disrupted is distinct under each condition, in fact in many respects the disruption to pattern is the inverse of the other;

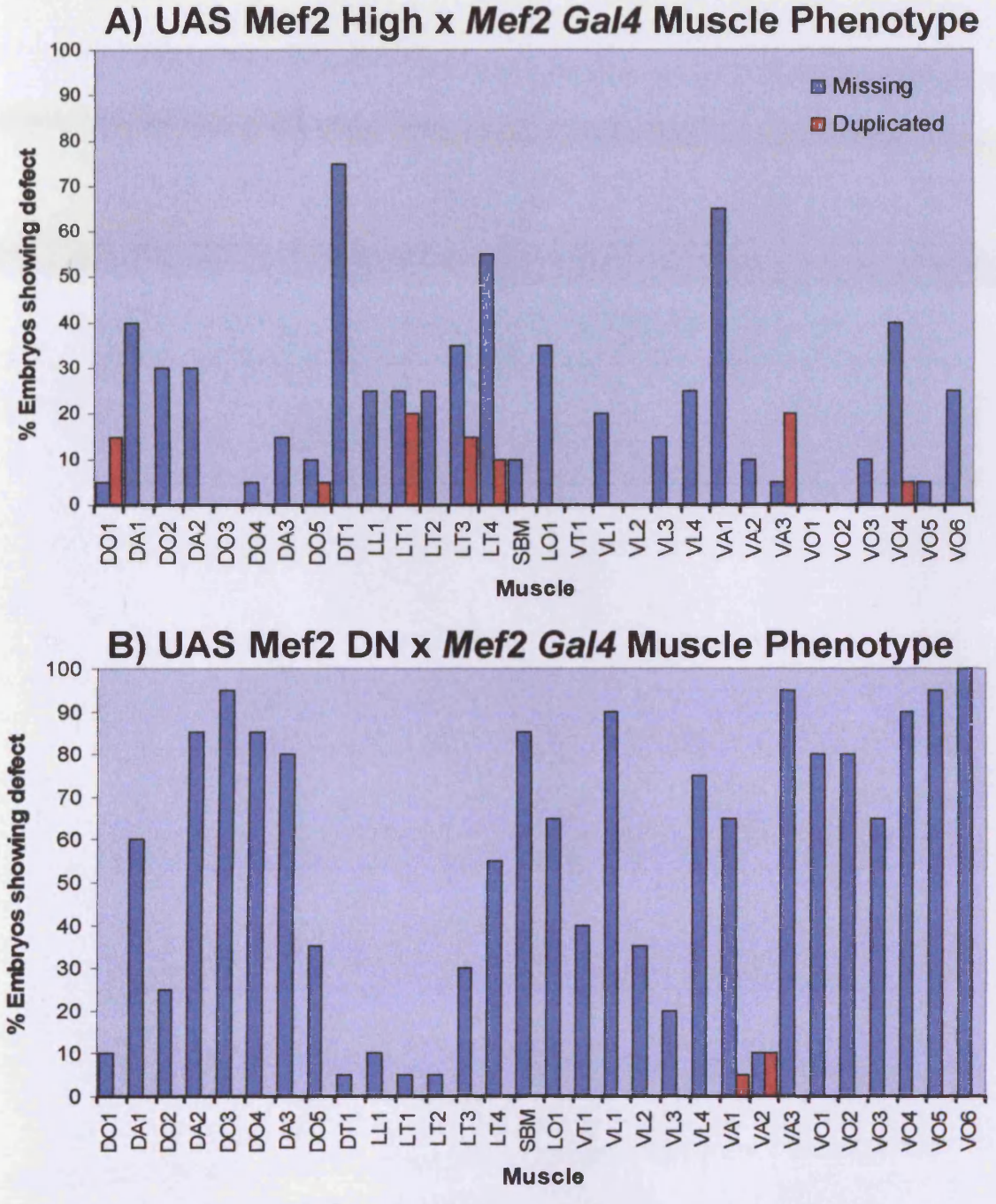

FIG 3.4.1 Graphs to show variation in muscle phenotype between over expression of full length Mef2 and the Mef2 dominant negative.

Full length Mef2 or Mef2-En dominant negative were driven with Mef2 Gal4 at 29°C and the individual muscles of hemi-segments A2-A4 for 20 embryos of each experimental condition were scored. The percentage of embryos that show at least one individual muscles to be missing (Blue) or duplicated (Red) are shown in the graphs. Only one copy of a particular muscle type needs to be missing from A2-A4 for that embryo to be scored. UAS Mef2 and Mef2-En show different individual muscles to be affected.

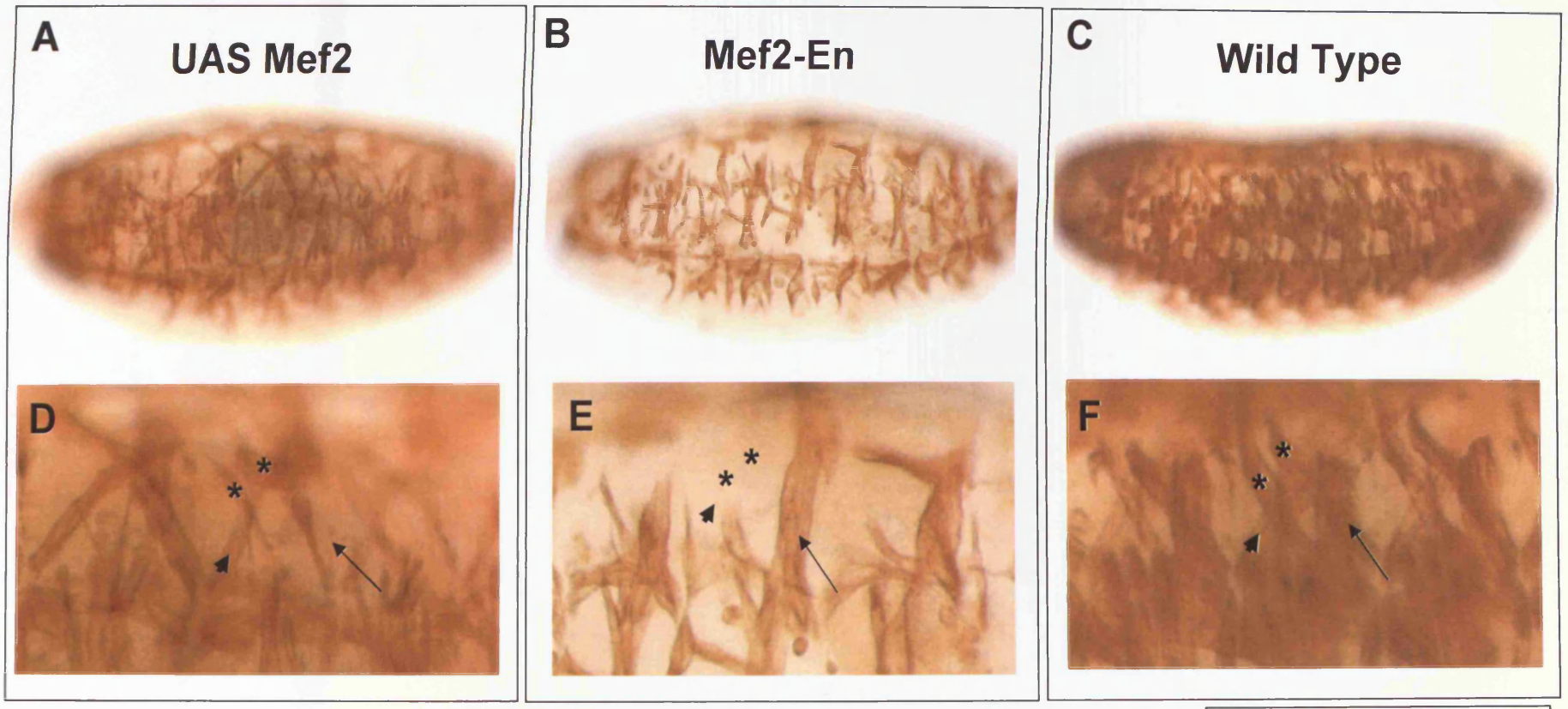

FIG 3.4.2 Over-expression of full length Mef2 gives a different phenotype to over-expression of the Mef2 Dominant Negative

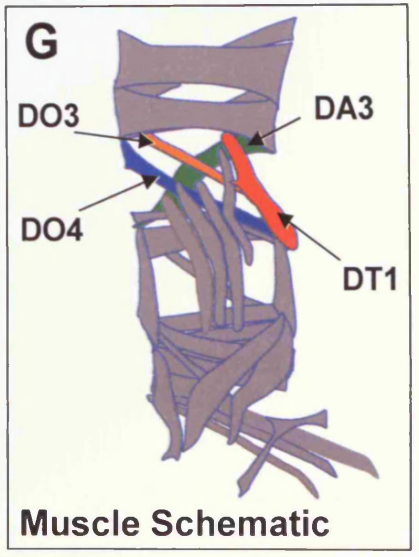

FIG 3.4.2 Over-expression of full length Mef2 gives a different phenotype to over-expression of the Mef2 Dominant Negative

Over-expression of full length Mef2 gives a muscle phenotype that is different to over-expression of the Mef2-En Dominant Negative. Although an increase in Mef2 activity (UAS Mef2) and a decrease in Mef2 activity (Mef2-En) both cause a disruption to the muscle pattern (compare A and B with wild type C), the way the pattern is disrupted and the individual muscles affected are very different. In UAS Mef2 embryos the DT1 muscle is often missing (arrow in A), whereas in Mef2 DN embryos (and in other situations with decreased Mef2 activity such as *Mef2* hypomorphs – see other tables) the DT1 muscle remains present (arrow in B). In fact in embryos with decreased Mef2 activity, DT1 is one of the few muscles that remains present and its shape relatively unaffected - even in embryos with a severe muscle phenotype affecting the majority of muscles. Conversely DA3 and the DO3 and DO4 muscles are frequently missing when Mef2 activity is reduced, seen here with the Mef2 DN (arrowhead (DA3) and asterisks in B), whereas in UAS Mef2 these muscles often remain present (arrowhead and asterisks in A).

G shows a schematic of the wild type muscles highlighted in this phenotype comparison.

Mef2-En line shown here is Mef2-En (X) and UAS Mef2 line is UAS Mef2 High (Bour et al, 1995). Both were driven at 29°C with the Mef2 Gal4 driver. Wild type embryos are Oregon R. Muscles stained using anti β3-tubulin antibody.

Cross	% Embryos with muscles MISSING	Average MISSING per embryo	Range	Muscles frequently MISSING		% Embryos with muscle DUPLICATED	Average DUPLICATED muscle per embryo	Range	Muscles DUPLICATED
UAS Mef2 (High) X *Mef2 Gal4 (25°C)*	100 %	8.95	3-18	DT1		60 %	1.5	0-2	DO1, DO5, LT1, LT3, LT4, VA3, VO4
Mef2-En (X) X *Mef2 Gal4 (29°C)*	100 %	34.2	26-45	DA2, DO3, DO4, DA3, DO5, VO1, VO2, VO4, VO6		15 %	1.33	0-2	VA1, VA2

Table 3.4.1 – UAS Mef2 gives a different muscle phenotype to Mef2 Dominant Negative

Increase of Mef2 activity through over-expression of full length Mef2 gives a distinct muscle phenotype which is different to the phenotype associated with over-expression of the Mef2 Dominant negative, which causes a decrease in Mef2 activity. With UAS Mef2, fewer muscles are missing, and the individual muscles missing are different to the Mef2 dominant negative. In addition a much greater frequency of muscles are duplicated in the UAS Mef2 embryos, and the individual muscles duplicated are different compared to those duplicated in the Mef2 Dominant negative embryos.

Lines used are Mef2-En (X) for the dominant negative and UAS Mef2 High (Bour et al, 1995).

	Muscles Missing in >75% Embryos	Muscles Missing in 50 - 74% Embryos	Muscles Missing in 25-49% Embryos	Muscles Missing in 15-24% Embryos
UAS Mef2 x *Mef2 Gal4* (25°c)	DT1	LT4, VA1	DA1, DO2, DA2, LL1, LT1, LT2, LT3, LO1, VL4, VO4, VO6	DA3, VL1, VL3
Mef2-En x *Mef2 Gal4* (29°c)	DA2, DO3, DO4 DA3, SBM, VL1 VL4, VA3, VO1 VO2, VO4, VO5 VO6	DA1, LT4, LO1, VA1, VO3	DO2, DO5, LL1 LT1, LT3, VT1 VL2, VL3	DO1, DT1, LT2 VA2

Table 3.4.2 - Mef2 over-expression affects individual muscles differently than Mef2 DN.

The muscles frequently missing in Mef2-En Dominant Negative embryos are frequently present in embryos where Mef2 is over-expressed (Blue in table). There are also muscles that are frequently present in Mef2 DN embryos which are often missing in UAS Mef2 embryos (Red in table). This data shows that although the muscle pattern is disrupted in response to either a decrease (Mef2 DN) or an increase in Mef2 activity (UAS Mef2) the way the pattern is disrupted is distinctly different and it highlights the way different individual somatic muscles respond to Mef2 levels, possibly due to their relative requirement for Mef2 during development. *Mef2-En (X) for Mef2 Dominant negative and, UAS Mef2 (High) (III).*

with individual muscles that are frequently missing in the Mef2 dominant negative, remaining frequently present in embryos over-expressing full length Mef2, and muscles that are often unaffected in Mef2 dominant negative frequently being missing or misshapen in UAS Mef2 embryos (FIG 3.4.1). For example, in embryos over-expressing the Mef2 dominant negative in the Mef2 pattern the dorsal muscles DO3, DO4 and DA3 are missing in 95%, 85% and 80% of embryos scored respectively, whereas in embryos over-expressing full length Mef2 protein in the Mef2 pattern DO3, DO4 and DA3 are *present* in 100%, 95% and 85% of embryos respectively. Other examples in this vein also occur; the lateral muscle, SBM, is missing in 85% of dominant negative embryos but missing in only 10% of UAS Mef2 embryos, and the ventral muscles VA3, VO1, and VO2 are missing in 95%, 80% and 80% of Mef2 dominant negative embryos respectively but remain present in 95%, 100% and 100% of UAS Mef2 embryos respectively (FIG 3.4.1). The opposite situation also occurs, with the DT1 muscle being the most severely affected in embryos which over-express full length Mef2 (missing in 75% of embryos), whereas this muscle is one of the few to remain unaffected in embryos which undergo a reduction in Mef2 activity, remaining present even in severe phenotypes where a large number of muscles are missing, such as in the $Mef2^{424}$ hypomorphic allele (Table 3.3.2) or, in this case, in the Mef2 dominant negative, where it remains present in 95% of embryos. (FIG 3.4.1, Table 3.4.1, Table 3.4.2).

The observation that particular muscles are missing, whereas other muscles remain present, in response to the same levels of Mef2 activity show that groups of muscles respond differently to Mef2. However, the fact that when the opposite Mef2 condition is imposed on the system (i.e there is a gain rather than a loss of Mef2 activity) these same muscles respond in the opposite manner to previously (under a loss of Mef2 activity) suggests a potential role for Mef2 in patterning. The observation is less easy to explain as a simple observation of

some muscles requiring highMef2 and others requiring low Mef2 and could suggest more of a role at the level of founder cell patterning for Mef2.

In addition, over-expression of full length Mef2 causes a number of muscle duplications, with at least one duplication occurring in 60% of the embryos scored (Table 3.4.1). These duplications predominantly occur in the dorsal muscle DO1, the lateral muscles LT1-LT4 and the ventral muscle VA3 (FIG 3.4.1 and FIG 3.4.3) and seem to be the individual somatic muscles that are repeatedly duplicated in conditions which involve an increase in Mef2 activity (see later chapters). In the Mef2 dominant negative there are rarely examples of a muscle being duplicated; only four cases of a muscle duplication occurs, (within 3 embryos – 15% of embryos scored) and these duplications are in muscles VA1 and VA2 (the total number of duplications in the UAS Mef2 experiment was 18) (FIG 3.4.1). So, not only are there significantly more duplications that occur in embryos that over-express full length Mef2 as opposed to the Mef2 dominant negative, but also these duplications are in a different subset of muscles, again highlighting a difference in the phenotypes of the two conditions.
These considerable differences in phenotype between UAS Mef2 and the Mef2 dominant negative strongly suggest that the two constructs are working in different ways, that the muscle phenotype associated with the Mef2 dominant negative does not occur as a result of an increase in Mef2 activity, and that the truncated version of the Mef2 protein does not retain any of the wild type function. Additionally this experiment also further highlights the response of different individual somatic muscles to Mef2 activity levels. It suggests that not only are particular muscles reliably/reproducibly lost with a reduction in Mef2 activity (in the Mef2 dominant negative and the Mef2 alleles) – suggesting a high requirement for Mef2 activity for these particular muscles, but also how muscles that have a low requirement for Mef2 activity to form correctly (frequently present in the Mef2 dominant negative and Mef2

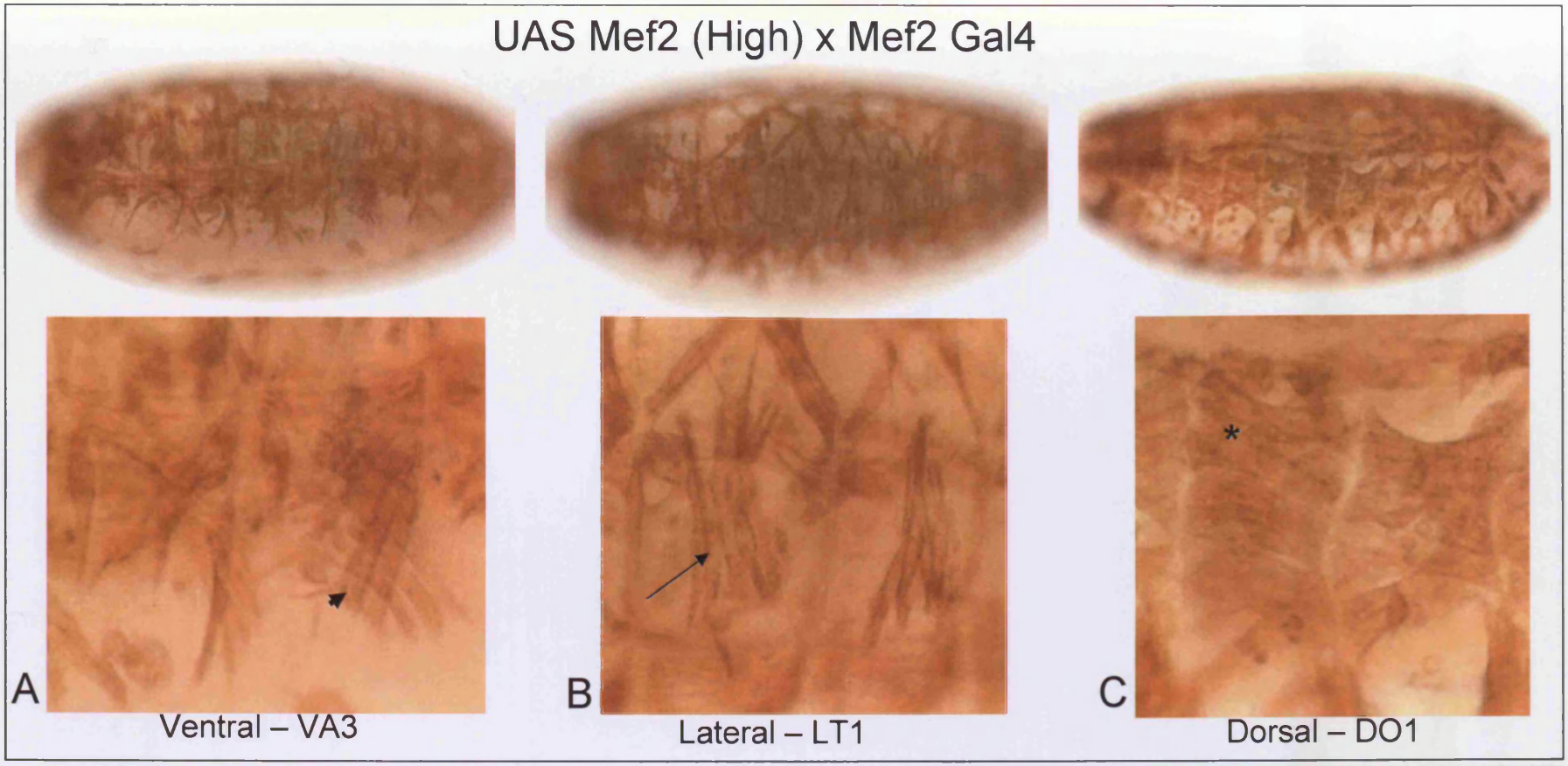

FIG 3.4.3 Examples of duplications seen in UAS Mef2 embryos

Unlike the Mef2-En lines over-expression of full length Mef2 causes a large number of muscle duplications. Duplications can occur ventrally (e.g in muscle VA3 - arrowhead in A), laterally (e.g in LT1 – arrow in B) and dorsally (e.g in DO1 – asterisk in C). A schematic showing these three muscles in the wild type musculature is shown in D.

However, duplications are not the only aspect of the phenotype, there is considerable disruption to the muscle pattern when Mef2 is over-expressed, with muscles missing, misshapen, missattached, heart defects and a considerable number of unfused myoblasts present throughout the body wall of the embryo (See FIG 3.4.2).

UAS Mef2 (High) used, driven by Mef2 Gal4 at 25°C. Muscles stained with β3-tubulin antibody.

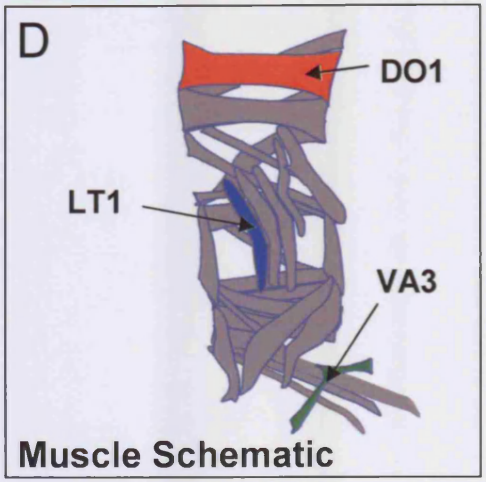

alleles) are also the most susceptible to large increases in Mef2 activity, being lost the most readily in UAS Mef2 embryos. This again suggests a possible role for Mef2 in patterning of the somatic musculature.

3.4.2 The Mef2 Dominant Negative reduces β3-tubulin expression in the early embryo whereas UAS Mef2 increases it.

In addition to comparing the muscle phenotype of the Mef2 dominant negative with full length Mef2 at St17, I also compared the effects of over-expression at earlier stages in development by looking at the protein levels of β3-tubulin. β3-tubulin is expressed in the somatic mesoderm, where it is a Mef2 target, and in the developing visceral mesoderm, where it is not (Damm et al, 1998). *Mef2* $^{22.21}$ embryos, which are null mutants for Mef2 (Bour et al, 1995), lose all somatic *β3-tubulin* expression, but the visceral muscle is unaffected (Damm et al, 1998). When the Mef2 dominant negative was over expressed in the Mef2 Gal4 pattern it caused a reduction in β3-tubulin levels in the somatic muscle compared to wild type (FIG 3.4.4, A). In contrast, over-expression of full length Mef2 caused an increase in β3-tubulin levels in the somatic muscle compared to wild type (FIG 3.4.4, B). In the visceral muscle levels of β3-tubulin were unaffected in both the Mef2 dominant negative and UAS Mef2 embryos. For this experiment, embryos were fixed and stained in parallel and fifteen individual embryos for each stage for each experimental condition were imaged and the representative one shown. This experiment shows that the Mef2 dominant negative definitely reduces Mef2 activity and that it works in an opposite manner to full length Mef2, giving a phenotype that sends β3-tubulin levels in the opposite direction.

FIG 3.4.4 Levels of β3-tubulin are reduced by the Mef2 DN compared to wild type and UAS Mef2

Over-expression of a dominant negative form of Mef2 reduces the amount of the muscle protein β3-tubulin in the developing somatic mesoderm (arrow, A) when compared to wild type (arrow, B) this is seen throughout the developmental stages.
When full-length Mef2 protein is over-expressed in the same way somatic β3-tubulin increases (arrow, C) compared to wild type at the corresponding stages (arrow, B).
In the visceral mesoderm, where β3-tubulin is not a Mef2 target, over-expression of the dominant negative does not reduce expression (arrowhead, A), and over-expression of full length Mef2 does not increase expression (arrowhead, C) in comparison to wild type (arrowhead, B).

Embryos shown are from St11–St12l, stained with anti-β3-tubulin antibody and viewed laterally. All experiments were performed at 29°c and fixed and stained under the same conditions. Mef2 DN line used was Mef2-En (II), UAS Mef2 line was Nguyen. UAS proteins were driven by Mef2 Gal4. Wild type are Oregon R. Each embryo shown is representative and one of fifteen others recorded of the same type at the same stage.

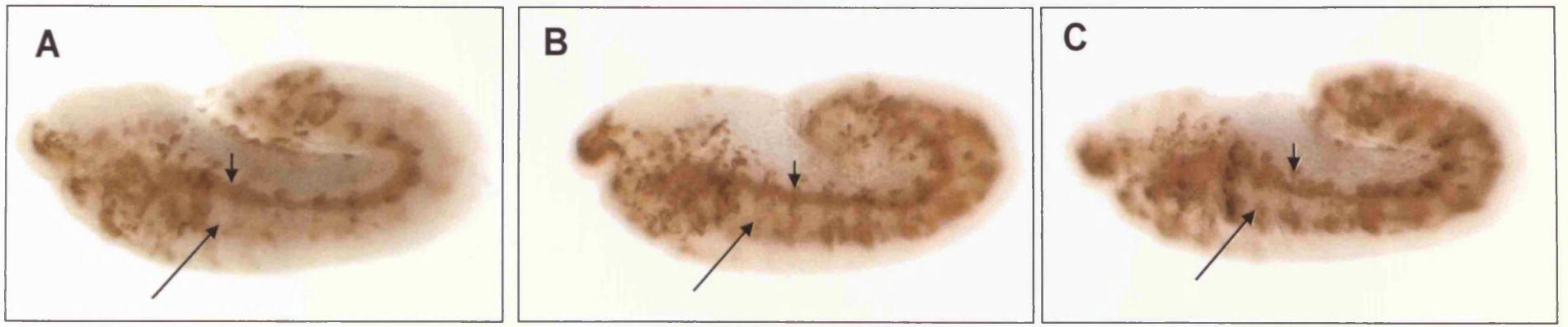

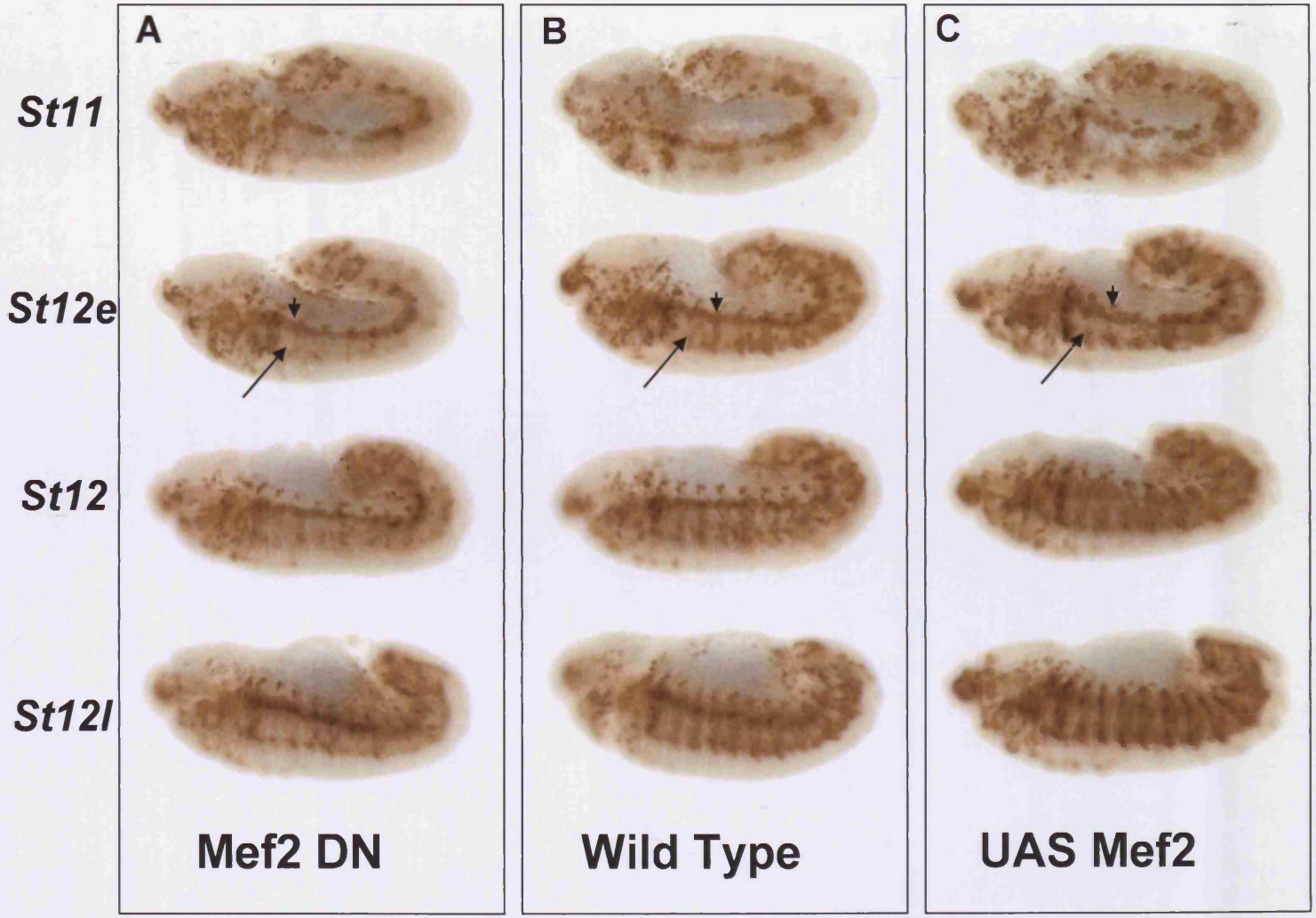

FIG 3.4.4 Levels of β3-tubulin are reduced by the Mef2 DN compared to wild type and UAS Mef2

3.5 The Mef2-En construct acts as a Dominant Negative protein; its phenotype can be rescued with co-expression of full length Mef2.

If the Mef2 dominant negative construct is acting upon Mef2 targets and reducing Mef2 activity through competition with endogenous Mef2 protein then co-expression of full length Mef2 should rescue the muscle phenotype that the dominant negative induces.

To test this, I generated stocks which contained a copy of the Mef2 dominant negative construct and a copy of the UAS Mef2 construct. For the experiment outlined below I used stocks containing Mef2-En (II) and UAS Mef2 low (III) (Gunthorpe et al ,1999), but I have generated stocks containing either Mef2-En (II) or Mef2-En (X) and UAS Mef2 High (III) or UAS Mef2 low (III) (See materials and methods).

3.5.1 Co-expression full length Mef2 rescues the St17 phenotype associated with the Mef2 Dominant Negative.

Over-expression of the Mef2 dominant negative (Mef2-En (II)) with the mesodermal driver 24B Gal4 (Brand and Perrimon, 1993) at 29°C gave a strong muscle phenotype; 95% of all embryos scored have muscles missing, with an average of 20.5 muscles missing (A2-A4) per embryo and the range of muscles missing in an embryo being between 0 and 45 (Table 3.5.1). When UAS Mef2 low is co-expressed with the Mef2 dominant negative under the same experimental conditions the severity of the muscle phenotype is considerably reduced. Only 66% of embryos scored have muscles missing, with an average of 2.2 muscles missing (A2-A4) per embryo, and the range of muscles missing in an embryo being between 0 and 9 (Table 3.5.1). Detailed analysis of the individual somatic muscles that are affected in these

Muscle phenotype	**Mef2-En x *24B Gal4*** (29°C)	**Mef-En ;UAS Mef2 x *24BGal4*** (29°C)
% embryos with muscle missing	95 %	66 %
Average missing per embryo	20.5	2.2
Range	0 - 45	0 - 9

Survival assay		
Hatching	52 %	62 %
Survival	0 %	0 %

Table 3.5.1 Over-expression of full length Mef2 can rescue the phenotype of the Mef2 Dominant Negative.

For the muscle phenotype experiment 90 muscles were scored (hemisegments A2-A4) per embryo, with a total of 20 embryos scored for each cross. Only 1/90 muscles need be missing for an embryo to be scored as having muscles missing. 20 Wild type embryos scored had no muscles missing.

For hatching and survival 200-300 fertilised embryos were aligned and allowed to hatch on apple juice plates at 29 degrees. Wild type embryos gave a hatching rate of 99% and a survival rate of 98%.

Lines used : Mef2-En (II) for Mef2 DN and UAS Mef2 low (III) . Embryos stained with anti b3-tubulin (guinea pig)

	Muscles Missing in 50- 75% Embryos	Muscles Missing In 25 -49% Embryos	Muscles Missing in 10 -25% Embryos
Mef2-En x *24B Gal4* (29°C)	DA2, **DO3**, **DO4**, DO5, LT4, VT1, VL4, VA1, VA3, VO1, VO2, VO3, **VO4**, **VO5**, VO6	DA1, DA3, LL1, LT3, SBM, **LO1**, VL1, VL2, VL3, VA2	DO2, DT1, LT1 LT2
Mef2-En ; UAS Mef2 x *24B Gal4* (29°C)	-	**VO4**	**DO3**, **DO4**, **LO1**, **VO5**

Table 3.5.2 Over-expression of full length Mef2 can rescue the individual muscle phenotype of the Mef2 Dominant Negative.

When UAS Mef2 is co-expressed with the Mef2 DN the severity of the muscle phenotype is reduced, with considerably fewer muscles in terms of both muscle type and frequency being lost. However all the muscles that are lost in the Mef2 dominant negative and UAS Mef2 co-expression embryos are also lost in the Mef2 dominant negative embryos (but at a higher frequency) (highlighted as bold in table), showing that the muscles lost in the rescue embryos are a subset of those lost in the Mef2 dominant negative embryos.

For the muscle phenotype experiment 90 muscles were scored (hemisegments A2-A4) per embryo, with a total of 20 embryos scored for each cross. Only 1/3 of each muscle type need be missing for an embryo to be scored as having that muscle missing.

Lines used : Mef2-En (II) for Mef2 DN and UAS Mef2 10T4A (low) (III) . Embryos stained with anti b3-tubulin (guinea pig)

two phenotypes reveals that the muscles missing in embryos co-expressing the Mef2 dominant negative and UAS Mef2 are a subset of the muscles missing in the embryos over-expressing the dominant negative alone, and that these muscles are lost at a reduced frequency (Table 3.5.2). For example, the VO4 muscle is the most frequently lost in the Mef2 dominant negative embryos, missing in 65% of embryos scored at an average rate of 2.2 muscles absent per A2-A4 hemisegment. (Table 3.5.2), whereas in the Mef2 dominant negative and UAS Mef2 co-expression embryos VO4 is still the most frequently lost muscle, but here it is missing in 30% of embryos scored at an average rate of 1.8 muscles absent per A2-A4 hemisegment (Table 3.5.2). A similar pattern exists for all of the muscles missing in the co-expression embryos (Table 3.5.2).

This change is similar to the reduction in phenotype seen in going from a *Mef2* ^{424} to a *Mef2*^{65} hypomorph mutant (Table 3.3.3), reflecting a similar change in Mef2 activity levels.

In fact, reassuringly the muscles lost in the Mef2 dominant negative and UAS Mef2 co-expression embryos are the same as those lost in a *Mef2* ^{65} mutant and so, from this one can gauge the level of Mef2 activity in each of the conditions; over-expression of the Mef2 dominant negative alone gives a phenotype with Mef2 activity levels similar to those of a *Mef2* ^{424} mutant (Table 3.5.3), whereas co-expression of UAS Mef2 with the Mef2 dominant negative reduces the Mef2 activity levels to give a phenotype that is similar to, but weaker than, a *Mef2* ^{65} mutant (the same muscles are missing in the co-expression embryos as those in the *Mef2* ^{65} mutant, but at a lower frequency) (Table 3.5.3).

This shows an additional level of control for varying Mef2 activity levels; one could use either the weaker or stronger Mef2-En dominant negative line, or one of these with UAS Mef2 being co-expressed, as well as varying the temperature. For example, if the Mef2 activity levels with the Mef2-En (II) weaker dominant negative line were too high in an

experiment at 18°C, the Mef2-En could be co-expressed with UAS Mef2 to achieve the desired level rather than lowering the temperature further.

3.5.2 Ectopic expression of a Mef2 target gene is lost when the Mef2 dominant negative is co-expressed with UAS Mef2.

Ectopic over-expression of Mef2 is sufficient to induce the expression of its target genes (Lin et al, 1997; Gunthorpe et al, 1999). However this is on the proviso that the levels of ectopic Mef2 are sufficiently high as to meet the threshold of Mef2 activity required for that particular gene (Elgar et al, 2008). For example, a Mef2 target gene that has a low requirement for Mef2 activity, such as *Act57B* can be induced by low levels of Mef2 over-expression whereas a gene with a high requirement for Mef2 activity, such as *Myosin Heavy Chain*, cannot (Elgar et al, 2008 and observations from this study). (But *MHC* can be induced with sufficiently high levels of Mef2 over-expression). With this in mind, I wanted to see if a gene that could be ectopically expressed in response to low levels of *Mef2* over-expression could no longer be expressed if the Mef2 levels were sufficiently reduced when UAS Mef2 had the Mef2 dominant negative co-expressed with it. *Mind Bomb 2 (CG17492)* is a gene that requires low levels of Mef2 activity for its expression (Elgar et al, 2008), and its expression can be induced ectopically in the ectoderm by both UAS Mef2 High (Elgar et al, 2008) and UAS Mef2 low (this study) when driven by the ectodermal driver 69B Gal4 (Brand and Perrimon, 1993). As revealed by in-situ hybridisation, ectopic expression of *Mind Bomb 2* is seen in the ventral midline of embryos which over-express UAS Mef2 low ectopically in the 69B Gal4 pattern (FIG 3.5.4, A). However, when the Mef2 dominant negative (Mef2-En (X)) is co-expressed with UAS Mef2 low under the same experimental conditions the ectopic expression of *Mind Bomb 2* is reduced to barely detectable levels

	Muscles Missing in 50- 75% Embryos	Muscles Missing In 25 -49% Embryos	Muscles Missing in 10 -24% Embryos
Mef2-En x ***24B Gal4*** (29°C)	DA2, **DO3**, **DO4**, DO5, LT4, VT1, VL4, VA1, VA3, VO1, VO2, VO3, **VO4**, **VO5**, VO6	DA1, DA3, LL1, LT3, SBM, **LO1**, VL1, VL2, VL3, VA2	DO2, DT1, LT1 LT2
Mef2 En; UAS Mef2 x ***24B Gal4*** (29°C)	-	**VO4**	**DO3**, **DO4**, **LO1**, **VO5**
Mef2^{424}	DA1, DA2, DA3, DO3, DO4, DO5, LT4, SBM, LO1, VL2, VO2, VO4, VO6	DO1, DO2, LT3, VL3, VL4, VA3, VO1, VO3, VO5	DT1, VT1
Mef2^{65}	VA3, VO4	LT4, LO1, VO5, VO6	DA2, DO3, SBM, VL2, VL3, VO3

Table 3.5.3 The rescue of the dominant negative phenotype by co-expression of UAS Mef2 causes a similar reduction in muscle phenotype as going from a *Mef2^{424}* to a *Mef2^{65}* hypomorph mutant.

Table 3.5.3 The rescue of the dominant negative phenotype by co-expression of UAS Mef2 causes a similar reduction in muscle phenotype as going from a *Mef2^{424}* to a *Mef2^{65}* hypomorph mutant.

The muscles that are missing in the Mef2 dominant negative over-expression embryos are similar to those that are lost in the *Mef2^{424}* hypomorph mutant (underlined in table). In addition the muscles that are missing in embryos that co-express the Mef2 dominant negative and UAS Mef2 are similar to those lost in *Mef2^{65}* embryos (underlined in table). From this we can gauge that the rescue of the Mef2 dominant negative muscle phenotype by UAS Mef2 is similar in going from a Mef2 activity level of the *Mef2^{424}* hypomorph to a level associated with the *Mef2^{65}* hypomorph.

Lines used : Mef2-En (II) for Mef2 DN and UAS Mef2 10T4A (low) (III) . 24B Gal4 for driving line. Embryos stained with anti b3-tubulin (guinea pig)

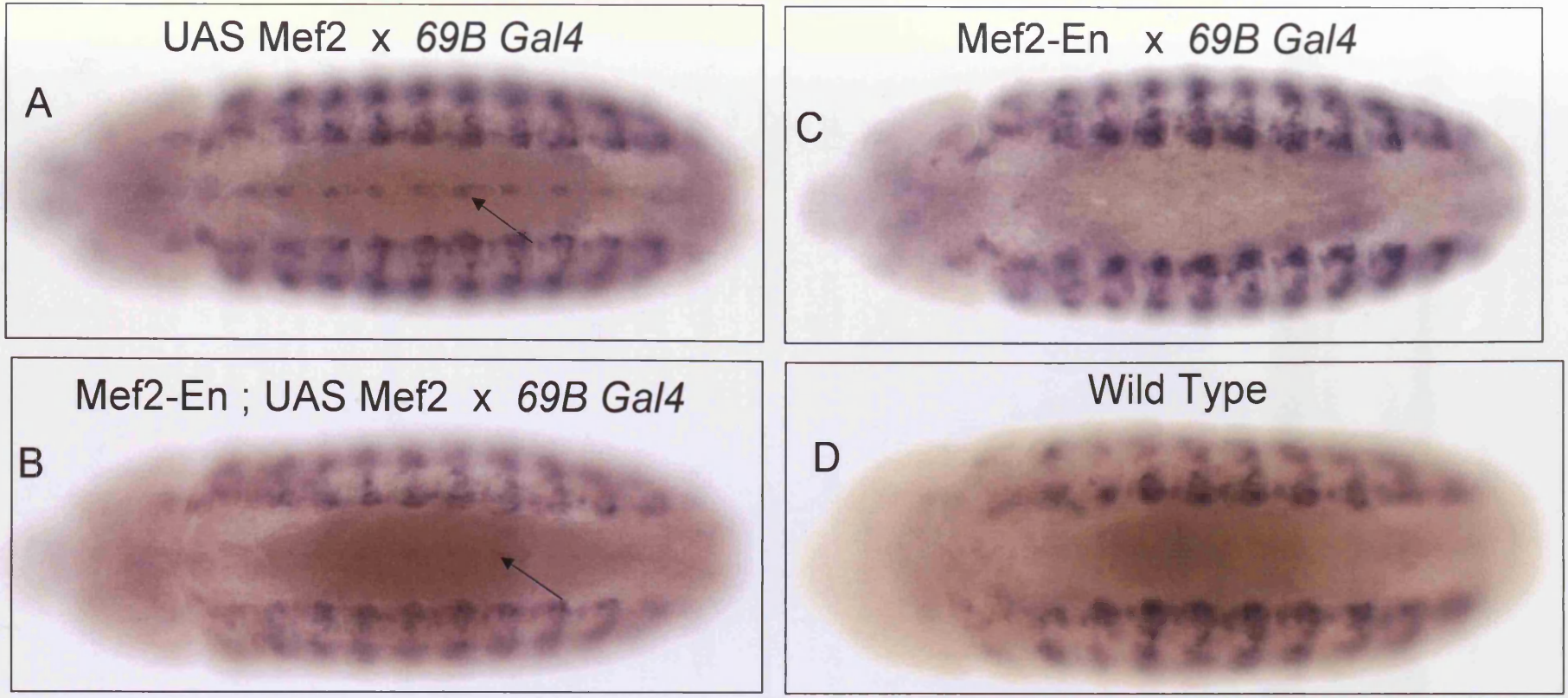

FIG 3.5.4 Mef2 DN can compete with full length Mef2 to rescue ectopic expression of a Mef2 target gene

UAS Mef2 driven by 69B Gal4 at 25°C is capable of inducing ectopic expression of the Mef2 target gene CG17492 (arrow in A). Co-expression of Mef2 DN rescues this expression with considerably reduced expression of the Mef2 target gene (arrow in B). The Mef2 DN alone does not induce any expression of CG17492 (C), giving an expression pattern identical to wild type (D). Embryos are St 13 shown ventrally. Experiments were incubated, fixed and stained in parallel. Images of 15 St13 embryos for each experiment were captured and representative ones are shown. Mef2 Dominant Negative line is Mef2-En L10-1 (X). UAS Mef2 is 10T4A (III). 69B Gal4 (II). Wild type is Oregon R.

(FIG 3.5.4, B). When the Mef2 dominant negative alone is driven by 69B Gal4 it produces no ectopic *Mind Bomb 2* transcript as one would expect, with the *Mind Bomb 2* expression pattern in these experimental embryos looking like wild type. (FIG 3.5.4, C and D). This experiment again shows how the Mef2 dominant negative and full length Mef2 can compete with each other and that more of one (the dominant negative) causes a reduction in Mef2 activity, whereas more of the other (UAS Mef2) causes an increase in Mef2 activity.

3.6 Using the Mef2 dominant negative to investigate the role of Mef2

After characterising the Mef2 dominant negative and establishing it as a useful tool for reducing Mef2 activity, the next step is to begin investigating its use with specific Gal4 lines in order to reduce Mef2 activity level with temporal and spatial control. With variation in experimental temperature driving the Gal4 line, the strength of the Mef2 dominant negative insertion line and (as outlined in 3.5.1) the possibility of combining the Mef2 dominant negative line with UAS Mef2, there exists a number of ways of controlling the generated level of Mef2 activity reduction in time and space in the fly. Consequently the Mef2-En dominant negative is a useful tool for investigation into the many roles of Mef2 in the orchestration of differentiation.

3.6.1 Reducing Mef2 activity specifically in the founder cells.

By driving the Mef2 dominant negative with rP298 Gal4 (Menon and Chia, 2001) Mef2 activity can be reduced specifically in the founder cells of the developing embryo.

rP298 was initially identified as an enhancer trap line which drove expression specifically in the founder cells (Nose et al, 1992; Nose et al, 1998). Subsequent analysis revealed this expression to correspond to that of *Dumbfounded (Duf),* the founder cell specific FCM (fusion competent myoblast) attractant (Ruiz-Gomez at al, 2000).

As outlined in my introduction (section 1.5.7 and 1.5.9) *Mef2* is expressed in both the founder cells and the surrounding FCMs (Taylor, 2003) and though both of these cells express a different set of proteins essential for the fusion process, Mef2 may play a role in activating both sets (Sandmann et al, 2006).

Over-expression of the Mef2 dominant negative specifically in the founder cells results in a complex disruption to muscle pattern, with loss, duplication and shape and attachment defects in individual muscles (Table 3.6.1 and FIG 1.6.1).

The predominant phenotype was shape defects (100% of embryos) and muscle loss (66.6% of embryos), though a large percentage of muscles are also duplicated (41.7%) (Table 3.6.1).

The individual muscles most frequently missing when Mef2-En is over-expressed in the founders are the same as those most often missing when the Mef2 dominant negative is driven throughout the developing muscle by Mef2 Gal4 (Table 3.6.2). Interestingly though, the individual muscles that are duplicated when the Mef2 dominant negative is over-expressed using rP298 Gal4 are more like the set of individual muscles duplicated when an increase in Mef2 activity occurs, for example in the UAS Mef2 embryos seen in Table 3.4.1/ FIG 3.4.1. This could again suggest a role for Mef2 in patterning at the level of the founder cells as previously alluded to in section 3.4.1. If this was the case one might expect to see an opposite phenotype to the one described here with over-expression of full length Mef2 driven in these cells.

	% Embryos with muscles MISSING	Average MISSING per embryo	Range	% Embryos with muscle DUPLICATED	Average DUPLICATED Muscle per embryo	Range	% Embryos with SHAPE DEFECTS	Average SHAPE DEFECTS per embryo	Range
Mef2-En (X) x *rp298 Gal4* (29°c)	66.6 %	5.1	2- 9	41.7 %	2.4	1- 3	100 %	18.7	4-41

Table 3.6.1 – Muscle phenotype when Mef2 activity is reduced in founder cells by Mef2 DN

A reduction of Mef2 activity specifically in the founder cells was achieved using the Mef2 DN and the Gal4 UAS system. This gives a complex disruption to muscle pattern, with muscle loss, duplication and shape defects highlighted here.

Somatic muscles were visualised by staining against β3-tubulin antibody. Muscles in abdominal hemi-segments A2-A4 were scored in 10 individual embryos for this analysis.

Mef2 dominant negative line used is Mef2-En (X), and driven by rP298 Gal4 at 29°C.

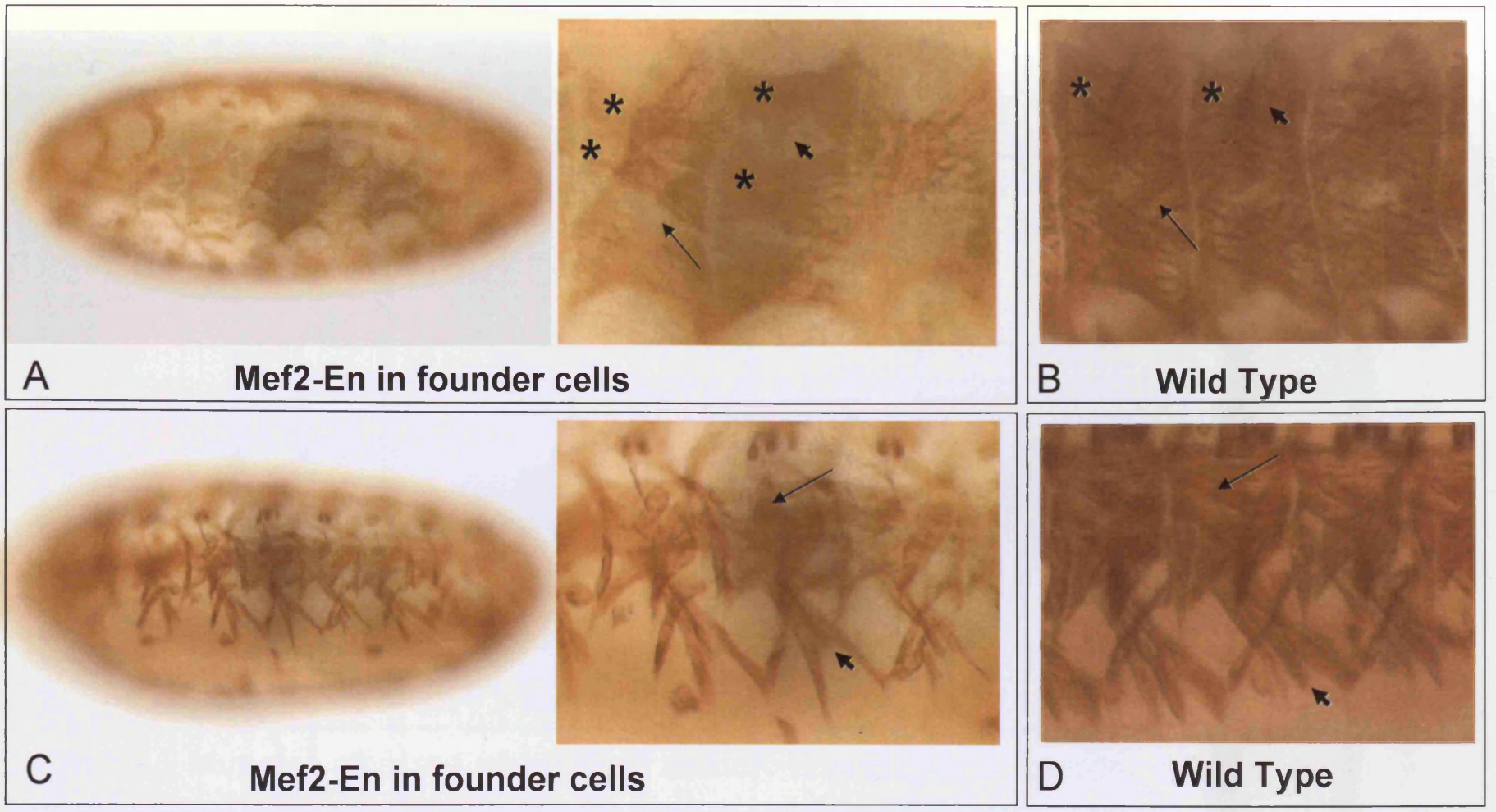

FIG 3.6.1 – Reducing Mef2 activity in founder cells disrupts muscle pattern

Over-expression of the Mef2 DN specifically in the founder cells at 29 °C results in a complex disruption to muscle pattern with loss, duplication and shape and attachment defects in individual muscles. In some embryos both loss and gain of muscles were observed – in the example shown in hemi-segment A2, DO1 is duplicated (asterisks, A) and DA2 is missing (arrow) and in hemisegment A3, DO1 is duplicated and DA1 is missing (arrowhead). Compare with wild type, B. In others, individual muscles did not find their attachment points and balled up (e.g VO1, compare arrow in C to wild type, D), or had other shape defects, such as being narrower and shorter than wild type (e.g VO5, compare arrowhead in C to wild type D).

Mef2 Dominant negative line used is Mef2-En (X) and driving Gal4 for founder cells is rP298 Gal4 (Menon and Chia, 2002). Wild type is Oregon R. Embryos St17 and muscles stained with ß3-tubulin antibody.

	Muscles MISSING in > 50 % Embryos	**Muscles MISSING in 25 – 49 % Embryos**	**Muscles MISSING in 8 -24% Embryos**	**Muscle DUPLICATED in 8 – 24% Embryos**
Mef2-En (X) x *rp298 Gal4* (29°c)	**DA2**	**DA1, DO3, DA3**	**DO5, LO1, VL2, VO1, VO4, VO5**	DO1, DO3, LT1, LT2, VO4
Mef2-En (X) x *Mef2 Gal4* (29°c)	**DA2 DO3** DO4 **DA3** SBM VL1 VL4 VA3 **VO1** VO2 **VO4 VO5** VO6 **DA1** LT4 **LO1** VA1 VO3	DO2, **DO5**, LL1, LT1, LT3, VT1 **VL2**, VL3	DO1, DT1, LT2 VA2,	VA1, VA2

Table 3.6.2 Muscles affected when Mef2 activity is reduced in founder cells by Mef2-En

A reduction of Mef2 activity specifically in the founder cells was achieved using the Mef2 DN and the Gal4 UAS system. The same individual muscles are most readily lost when driven in founder cells as when driven in the Mef2 Ga4 pattern (highlighted as bold in the table).

Somatic muscles were visualised by staining against β3-tubulin antibody. Muscles in abdominal hemi-segments A2-A4 were scored in 10 individual embryos for the rP298 Gal4 analysis and 20 for the Mef2 Gal4 analysis.

Mef2 dominant negative line used is Mef2-En (X), and driven by rP298 Gal4 or Mef2 Gal4 at 29°C.

3.6.2 Reducing Mef2 activity in the adult muscles

As well as providing a means for investigating the role of Mef2 in muscle development in the embryo, this Mef2-En dominant negative can also be used to study Mef2 in the adult musculature. The adult muscles in *Drosophila*, are an interesting model for studying muscle differentiation, as their physiology, attachment and interaction with neurones, closely resembles vertebrate musculature (Bernstein et al, 1993; Vigoreaux, 2001). Unlike the muscles of the embryo or larvae they are made up of muscle fibres (Miller, 1950), which means they have a closer resemblance to the skeletal muscle in vertebrates. The *Mef2* null and hypomorphic mutants, that have provided insight into the importance of Mef2 in muscle differentiation in the embryo, cannot be used in the conventional way to study Mef2 in the adult musculature because they are embryonic lethal. (Lilly et al, 1995; Bour et al, 1995; Ranganyakulu et al, 1995).

Because of this, a study of the role of Mef2 in these muscles using Mef2 mutants has had to be previously performed using heteroallelic combinations of Mef2 alleles that are weak enough to pass through embryogenesis and larval life (Ranganyakulu et al, 1995) or through use of a temperature sensitive Mef2 hypomorph (Goldstein et al, 2001 and Baker et al, 2005). However, the use of both of these techniques is quite limited for an investigation of Mef2's role at this stage because they still retain a relatively high level of Mef2 activity.

As I have shown, my Mef2 dominant negative protein is capable of achieving a reduction in Mef2 activity that is comparable to the $Mef2^{424}$ hypomorphic allele. Consequently this means that a reduction of Mef2 activity levels in the adult musculature can now be achieved that is of comparable strength to the strong Mef2 hypomorphic alleles.

By using the Mef2 dominant negative with adult muscle Gal4 driver lines, such as 1151 Gal4 (Anant et al, 1998), a considerable reduction in Mef2 activity could be achieved for the first

time to investigate the role of Mef2 in adult muscle development without any reduction of Mef2 activity in embryogenesis.

I drove the Mef2 dominant negative lines in the developing adult musculature using 1151 Gal4 and investigated the effect of reducing Mef2 activity on the formation of the Dorsal Longitudinal Muscles (DLMs). The DLMs are large multifibre muscles involved in powering the wings for flight in the adult fly. They exist as two sets of six muscles, one set of six each side of the thorax of the fly (Vigoreaux, 2001) (See FIG 3.7.1, A for wild type DLM pattern). Reduction of Mef2 activity using either of the Mef2-En dominant negative lines results in the formation of these muscles being inhibited (FIG 3.7.1) Analysis of DLM's after dissection of black pupae revealed that frequently 0 DLM's form instead of the wild type number of six when the Mef2 dominant negative is over-expressed using 1151 Gal4. And also, that the Mef2-En (X) line gives a stronger muscle phenotype than the Mef2-En (II) line, as was previously observed in embryonic muscle analysis when driving the dominant negative lines with Mef2 Gal4. With Mef2-En (X) 82% of hemi-thoraces scored had lost all of the DLMs (18 / 24), whereas with Mef2-En (II) 55% of hemi-thoraces scored had lost all of the DLMs (12 / 22) (Table 3.7.1). Other thoraces in both lines that did not have all DLMs missing, had between one and two DLM muscles present (Mef2-En (X)) or between one and four DLMs present (Mef2-En (II)) (Table 3.7.1). There was one fly which over-expressed the Mef2-En (II) dominant negative and showed a phenotype of four DLMs in one hemithorax and three DLMs in the other hemithorax. The formation of three DLMs is associated with a failure of the developing DLMs to split and form the final six muscles (Baker et al, 2005), however in this example the muscle are also very strangely positioned, being aligned laterally as opposed to along a dorso-ventral axis as seen in the splitting phenotype. More flies need to be dissected and examples observed to further investigate this aspect of the Mef2 dominant negative phenotype before any conclusions can be drawn from it. In using the adult system I

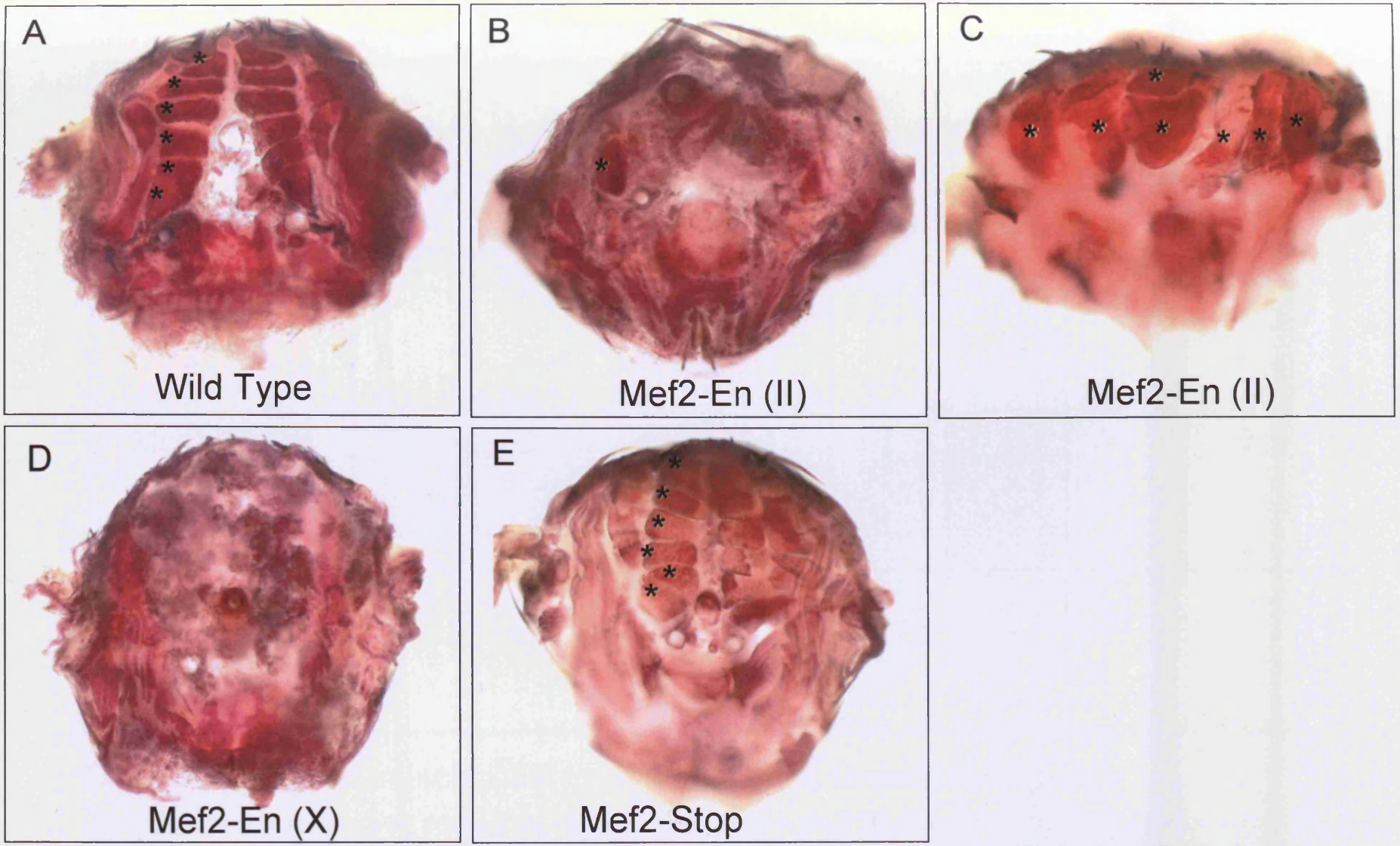

FIG 3.7.1 : A reduction in Mef2 activity in the adult causes a decrease in DLM fibre number

When Mef2 activity is reduced in the adult by either the Mef2-En DN (B,C,D) there is a severe disruption to DLM fibre formation. Wild type flies develop 6 DLMs per hemi-thorax (A), whereas the stronger Mef2-En DN line (D) tend to develop 0 DLMs. The less strong Mef2-En DN often shows 0 DLMs developing (see Table 3.7.1) but also frequently 1 DLM (B). There was one example with this line which showed the formation of 4 DLMs (C - left side) and 3 DLM's (C - right side), suggesting a phenotype more like the ts Mef2 alleles. The weak Mef2-Stop line showed wild type like numbers of DLM formation (E). *(All experiments at 25°C, adult muscle expression driven with 1151 Gal4, wild type flies were 1151 Gal4 alone.)*

	Number DLM's per hemi-thorax							
Cross	0	1	2	3	4	5	6	Total
Wild Type (*M1151 Gal4)*	-	-	-	-	-	2	22	24
Mef2-Stop (II ; III) x *M1151 Gal4*	-	-	-	-	-	2	22	24
Mef2-En DN (II) x *M1151 Gal4*	12	7	1	1	1	-	-	22
Mef2-En DN (X) x *M1151 Gal4*	18	4	2	-	-	-	-	24

Table 3.7.1 – Adult muscle DLM analysis for Mef2 Dominant Negative

DLM fibre number was scored in dissected 96hr APF black pupae. Mef2 DN driven by 1151 Gal4. All experiments performed at 25°C. Wild type controls were 1151 Gal4 alone.

decided to again test the use of the Mef2 Stop truncation dominant negative construct. This gave a phenotype at a driving temperature of 25°C that was identical to wild type in terms of number of DLM missing and so, as with the work done in the embryo, shows that the Mef2 Stop dominant negative is very weak.

3.6.3 Reducing Mef2 activity in other systems.

Mef2 is also a key regulator in other aspects of biology (Pothoff and Olson, 2004), including the differentiation of neurons (for review see Shalizi and Bonni, 2002). Recent work from the lab of Justin Blau at New York University has explored a role for Mef2 in the adult *Drosophila* brain. For this study, we sent the group lines of the Mef2-En dominant negative, which they used in their system to reduce the activity of Mef2. The Mef2-En dominant negative gave an opposite phenotype to Mef2 gain-of-function (Blanchard et al, 2010 in press). Their work highlights that the use of the Mef2-En construct is transferrable to other developmental systems and makes an important contribution to the tools available for investigating the role of Mef2 in various aspects of *Drosophila* development, not just Mef2's role in the differentiation of muscles.

3.7 The Mef2 Dominant Negative can also mimic a Mef2 RNAi line

Recently efforts have been made to provide a means of being able to reduce every gene in the genome through the generation of large scale RNAi stocks (Dietzl et al, 2005). An RNAi line for Mef2 was generated in this effort and consequently I ordered it to analyse in comparison to the Mef2 Dominant Negative protein.

Initially I confirmed that the Mef2 RNAi stock was acting upon Mef2 by showing that over-expression of the RNAi line resulted in a reduction of Mef2 transcript. FIG 3.7.1 shows the result from this. Mef2 RNAi x Mef2 Gal4 causes a reduction in Mef2 expression relative to Mef2 Gal4 controls (C and D). Also, it has been shown that overexpression of Dicer2, a component of the cells RNA processing machinery can enhance this phenotype. Consequently, UAS Dicer ; Mef2 Gal4 stocks were made in the lab (J.Han) and I also tested this line at driving over-expression of Mef2 RNAi in comparison to UAS Dicer ; Mef2 Gal4 controls. These embryos show an even greater reduction of Mef2 transcript levels, suggesting that co-expression of Dicer would give a stronger phenotype in this case.

I analysed the terminal somatic musculature of embryos driving Mef2 RNAi with UAS Dicer ; Mef2 Gal4 at 29°C in the usual way (20 embryos, A2-A4). They show a strong muscle phenotype with striking similarity to Mef2-En (X) x Mef2 Gal4 at 29°C. Table 3.7.1 shows how the two conditions give very similar severities of muscle phenotype in terms of average number of muscles missing and range of muscles missing (34.2 and 26-45 for Mef2-En, 36.2 and 24-58 for Mef2 RNAi). The conditions are lethal at the embryonic stage as shown by hatching and survival tests .Table 3.7.2 shows this similarity in terms of individual muscles missing, there is striking similarity between the type of individual muscle lost and the frequency the loss occurs at. Representative embryos show this very clearly in FIG 3.7.2.

In addition, analysis also revealed that like the Mef2 Dominant Negative, Mef2 RNAi was able to mimic the $Mef2^{65}$ hypomorph (Mef2 RNAi x Mef2 Gal4 at 29°C.) and the $Mef2^{424}$ hypomorph (Mef2 RNAi x UAS Dicer ; Mef2 Gal4 at 29°C.).

This further highlights another proof that the Mef2 Dominant Negative is acting to reduce Mef2 activity and by use in side by side comparison adds strength to any observation attained using the Gal4 UAS system to reduce Mef2 activity; if a phenotype is the same from over-

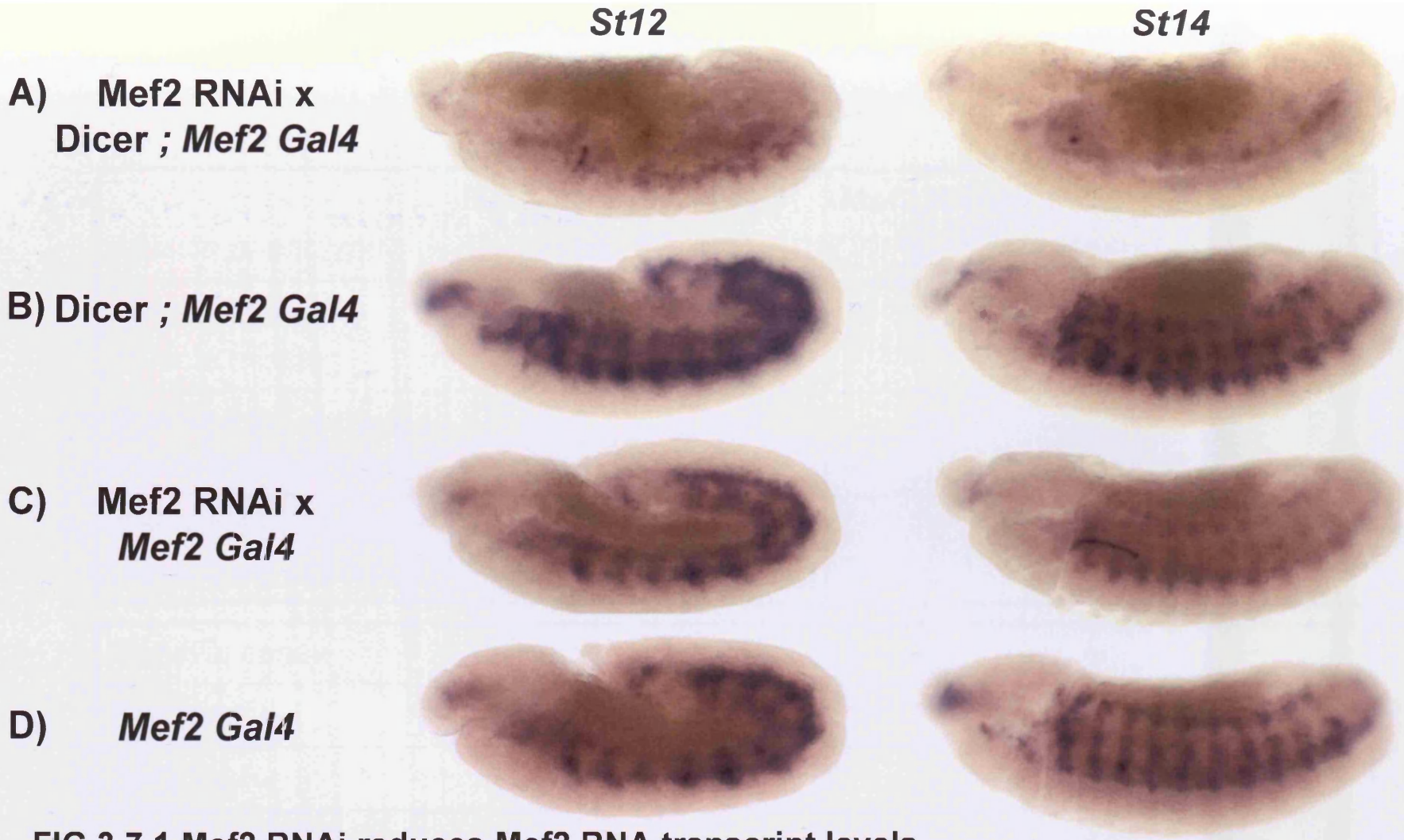

FIG 3.7.1 Mef2 RNAi reduces Mef2 RNA transcript levels

Mef2 RNAi targets Mef2. *In-situ* hybridisation to detect Mef2 RNA transcript shows almost complete loss of Mef2 RNA when Mef2 RNAi is driven by Mef2 Gal4 in the presence of additional Dicer (A).

Whereas Dicer; Mef2 Gal4 control embryos without Mef2 RNAi show wild type levels of Mef2 transcript (B).

When Mef2 RNAi is driven by Mef2 Gal4 without additional Dicer in the cross, Mef2 RNA levels are still reduced (compare C to wild type D) but to a lesser extent (compare C to A). This milder reduction in Mef2 transcript levels correlates with the weaker muscle phenotype observed when Mef2 RNAi is expressed without Dicer.

Mef2 RNAi line used #15550 (III) (VDRC), UAS Dicer (II) (VDRC).Experiments performed at 29°C.

Mef2-En and Mef2 RNAi give similar muscle phenotypes

Muscle phenotype	**Mef2-En x *Mef2 Gal4*** (29°c)	**Mef2 RNAi x *Dicer ; Mef2 Gal4*** (29°c)
% embryos with muscle missing	100 %	100 %
Average No. muscles missing per embryo	34.2	36.2
Range of muscles missing per embryo	26 - 45	24 - 58

Survival assay		
Hatching	0 %	0 %
Survival	0 %	0 %

Table 3.7.1. Mef2 Dominant Negative and Mef2 RNAi give similar muscle phenotypes.

For the muscle phenotype experiment 90 muscles were scored (hemisegments A2-A4) per embryo, with a total of 20 embryos scored for each cross. Only 1/90 muscles need be missing for an embryo to be scored as having muscles missing. Wild type embryos have no muscles missing over 20 embryos scored and gave a hatching rate of 99% and a survival rate of 98%.

Lines used : Mef2-En (X) for Mef2 DN and Mef2 RNAi #15550 (VDRC) (III) . Embryos stained with anti b3-tubulin (guinea pig).

	Muscles Missing in >75% Embryos	Muscles Missing in 50 - 75% Embryos	Muscles Missing in 15-50% Embryos	Muscles Missing in 0-15% Embryos
Mef2 DN x *Mef2 Gal4* (29°C)	**DA2 DO3** DO4 **DA3 SBM** VL1 **VL4 VA3 VO1 VO2** VO4 VO5 VO6	DA1 LT4 LO1 **VA1** VO3	**DO2** DO5 LL1 **LT1** LT3 VT1 **VL2** VL3	**DO1 DT1** LT2 **VA2**
Mef2 RNAi x *Dicer ; Mef2 Gal4* (29°C)	DA1 **DA2 DO3 DA3** LT3 LT4 **SBM** LO1 **VL4 VA3 VO1 VO2** VO3	DO4 DO5 LT2 VL3 **VA1** VO4 VO6	**DO2 LT1 VL2** VO5 VL1	**DO1** LL1 VT1 **DT1 VA2**

Table 3.7.2 Mef2 Dominant Negative and Mef2 RNAi give similar muscle phenotypes.

Analysis of muscle type missing in Mef2 Dominant Negative and Mef2 RNAi lines driven by Mef2 Gal4 at 29 °C.

For two very different ways of reducing Mef2 activity the phenotypes are strikingly similar, with the same muscles generally being affected in the same way. For example, DA2, DO3, DA3, SBM, VL4, VA3, VO1 and VO2 are missing in over 75% of embryos in both experiments and DO1, DT1 and VA2 are frequently present (in 85-100% of embryos). A similar subset of muscles are affected in the *Mef2*^{424} hypomorph (see Table 3.3.5) indicating a reproducible requirement of Mef2 activity for different muscle types. Bold black indicates muscle type missing with similar frequency in both lines. Blue indicates muscles missing in over 50% of Mef2 RNAi embryos and 75% of Mef2 DN, suggesting a similar but stronger effect in the DN. Red indicates muscles missing in over 50% of Mef2 DN embryos and 75% of Mef2 RNAi, suggesting a similar but stronger effect in the RNAi for these muscles. *Lines used : Mef2-En (X) for Mef2 DN and Mef2 RNAi #15550 (VDRC) (III) . Embryos stained with anti b3-tubulin (guinea pig)*

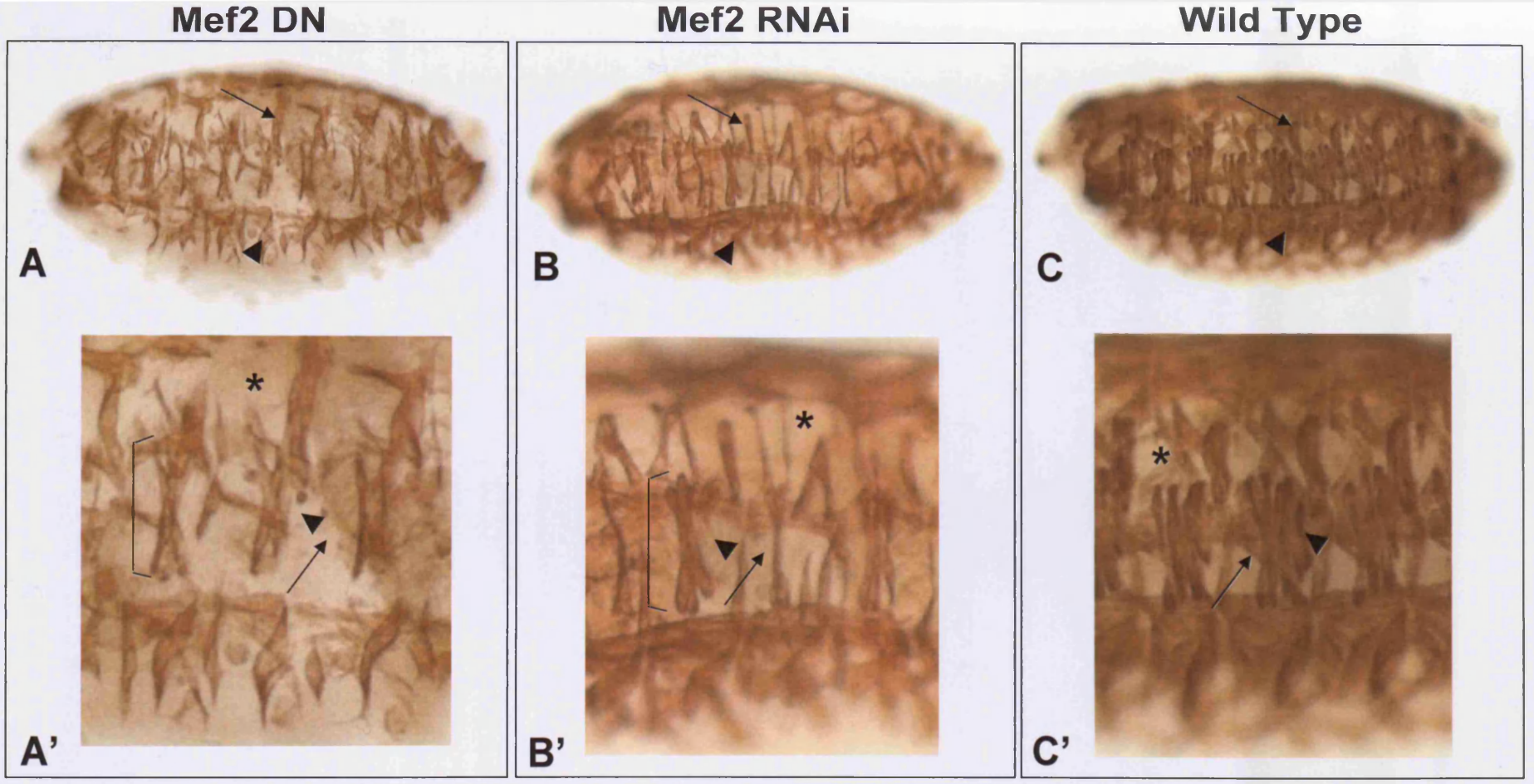

FIG 3.7.2 Mef2 Dominant Negative and Mef2 RNAi give similar muscle phenotypes.

Representative St17 embryos for Mef2 DN (A) and Mef2 RNAi (B) driven by Mef2 Gal4 at 29°C, with wild type for comparison (C). Both Mef2 embryos show striking similarity, with similar muscles being missing (e.g DA3/DO4/DO3, LO1 and LT4 – shown by asterisk, arrow and arrowhead in A' and B', with wild type muscles in C') and similar muscles remaining present (DT1 arrow in A and B, VA2 arrowhead in A and B). Those that are present but show defects are affected in similar ways, e.g LT1 and LT2 being thinner in the middle and mishapen at the ends (Bracket in A' and B').

Lines used : Mef2-En (X) for Mef2 DN, Mef2 RNAi #15550 VDRC. Mef2 RNAi also had UAS Dicer in the cross

expression of Mef2 Dominant Negative and from over-expression of RNAi then that phenotype would be very reliable as it would have been achieved through two very distinct mechanisms.

3.8 Discussion

The Mef2 Dominant negative proteins can reduce Mef2 activity in a spatial and temporal manner. Though the Mef2-En dominant negative proteins give a stronger phenotype than the Mef2-Stop truncation, both affect the same subset of individual somatic muscles, suggesting that they decrease Mef2 activity in a similar way. Detailed characterisation of two Mef2-En lines reveal that the dominant negative protein functions by competition with wild type Mef2 protein; co-expression of full length Mef2 reduces the severity of the Mef2-En phenotype and similarly the ectopic expression of a known Mef2 target gene seen on over-expression of wild type Mef2 protein is lost when Mef2-En is co-expressed.

Once it was established that the Mef2 dominant negative could reduce Mef2 activity, detailed analysis of the terminal somatic musculature after over-expression of the dominant negative in the Mef2 pattern revealed that the Mef2-En lines could reliably reproduce the phenotype of the *Mef2* hypomorphic alleles. In addition, by varying the type of dominant negative used (Mef2-En fusion or Mef2-Stop), the line used (Mef2-En (II) or the stronger Mef2-En (II)) or the driving temperature, phenotypes that were milder, intermediate or stronger than the $Mef2^{65}$ and $Mef2^{424}$ alleles could be achieved. This means that a convenient method of reducing Mef2 activity to specific levels can be achieved in a spatial and temporal manner.

Following the characterisation of the Mef2 dominant negative lines and the $Mef2^{65}$ and $Mef2^{424}$ mutant alleles a distinct pattern emerged regarding which muscles were affected

under different conditions of decreased Mef2 activity. A subset of muscles were more easily lost than others; DA2, DO3, VO4, VO6 were either the only muscles missing in conditions associated with a mild reduction of Mef2 activity or the most frequently missing muscles in conditions associated with a severe reduction in Mef2 activity. Conversely, there was a different subset of muscles that frequently remained present, even under conditions of severe reduced Mef2 activity that cause the majority of somatic muscles to be missing. The DO1, DT1, LT2, VA2 muscles belong in this category. Consequently, one can conclude that the individual somatic muscles have different requirements for Mef2 activity, with muscles that are lost most easily having a high requirement for Mef2 and the muscles that frequently remain present having a low requirement for Mef2. Observations that the levels of Mef2 activity are essential for correct muscle differentiation have been previously well established (Gunthorpe et al, 1999) and a whole genome analysis of Mef2 mutants by Elgar et al revealed specific high Mef2 requirement and low Mef2 requirement genes in development (Elgar et al, 2008). One could imagine that such high and low Mef2 requirement genes would be a means of instigating the formation of a high or low Mef2 requirement muscle.

Over-expression of the Dominant Negative in specific patterns using various Gal4 lines highlights the real strength of the constructs as a tool for investigating Mef2 function

Him Expression Regulation

4.1 Introduction

As previously established through over expression and RNAi studies (Liotta et al, 2007), Him is a repressor of muscle differentiation which acts to inhibit the activity of Mef2 protein.

In my thesis I further characterised the role of Him in muscle development. I did this in a number of ways as outlined below ;

- Investigation of *Hims'* expression regulation using GFP reporter constructs.
- Detailed analysis of the muscle phenotype associated with over-expression phenotype of Him in the mesoderm.
- Generation and characterisation of Him loss of function alleles.

Together these different means of investigation allowed for further insight into the function of Him.

4.2 *Him* expression.

The *Him* expression pattern is tightly regulated and goes through a number of specific changes throughout embryogenesis. *Him* is initially expressed in a broad mesodermal pattern during development, but prior to the onset of muscle differentiation expression rapidly declines, only remaining on in the undifferentiated cells of mesodermal origin; the adult muscle precursors (A.M.Ps) and the pericardial cells of the heart. It is expressed in undifferentiated cells of the developing mesoderm. Such strict maintenance of expression in undifferentiated cells, but rapid decline of expression in cells at the point of differentiation is characteristic of a repressor and the tight regulation of Him in this manner

is essential for correct muscle development; as seen when *Him* expression is maintained ectopically in the developing somatic musculature in over-expression studies (See Chapter 5).

The expression pattern of *Him* in wild type Oregon R embryos is shown in FIG 4.2.1 by *in-situ* hybridisation. Expression begins around St9 in the developing mesoderm, and around St11 follows the pattern of mesodermal segmentation. It is around this stage that expression in the somatic muscle precursors, heart precursors and pharyngeal muscle precursors begins. At late St12, around the time of onset of somatic muscle differentiation, *Him* rapidly declines in the somatic muscle cells, but is maintained strongly in the A.M.Ps, heart pericardial cells and also the pharyngeal muscle. By late St13, by the time the somatic muscle has completed differentiation, all somatic muscle *Him* expression has been completely lost, and from this point, remains solely in the A.M.Ps, pericardial cells and pharyngeal muscle until the end of embryogenesis at St17. From around St15 the level of expression decreases in these cells until it is barely detectable at St17.

This distinctive expression pattern of *Him* poses a number of questions which could provide insight into the role of *Him* and to gene regulation in general. Specifically these are :- "Which factors are responsible for Hims' expression?", "How is Hims' expression rapidly down-regulated?" and "What makes Him persist in the A.M.Ps?"

4.3 *Him* Reporter construct analysis

A previous study looking for potential Suppressor of Hairless Su(H) target genes (Rebeiz et al, 2002) identified the region upstream of Him playing a part in the expression of *Him*. They identified in this region a cluster of four Su(H) binding sites and seven Twist sites. Subsequently analysis by myself identified two Mef2 sites, according to the consensus YTAWWWWTAR (Andres et al, 1995) (FIG 4.3.1). This region was divided up and GFP

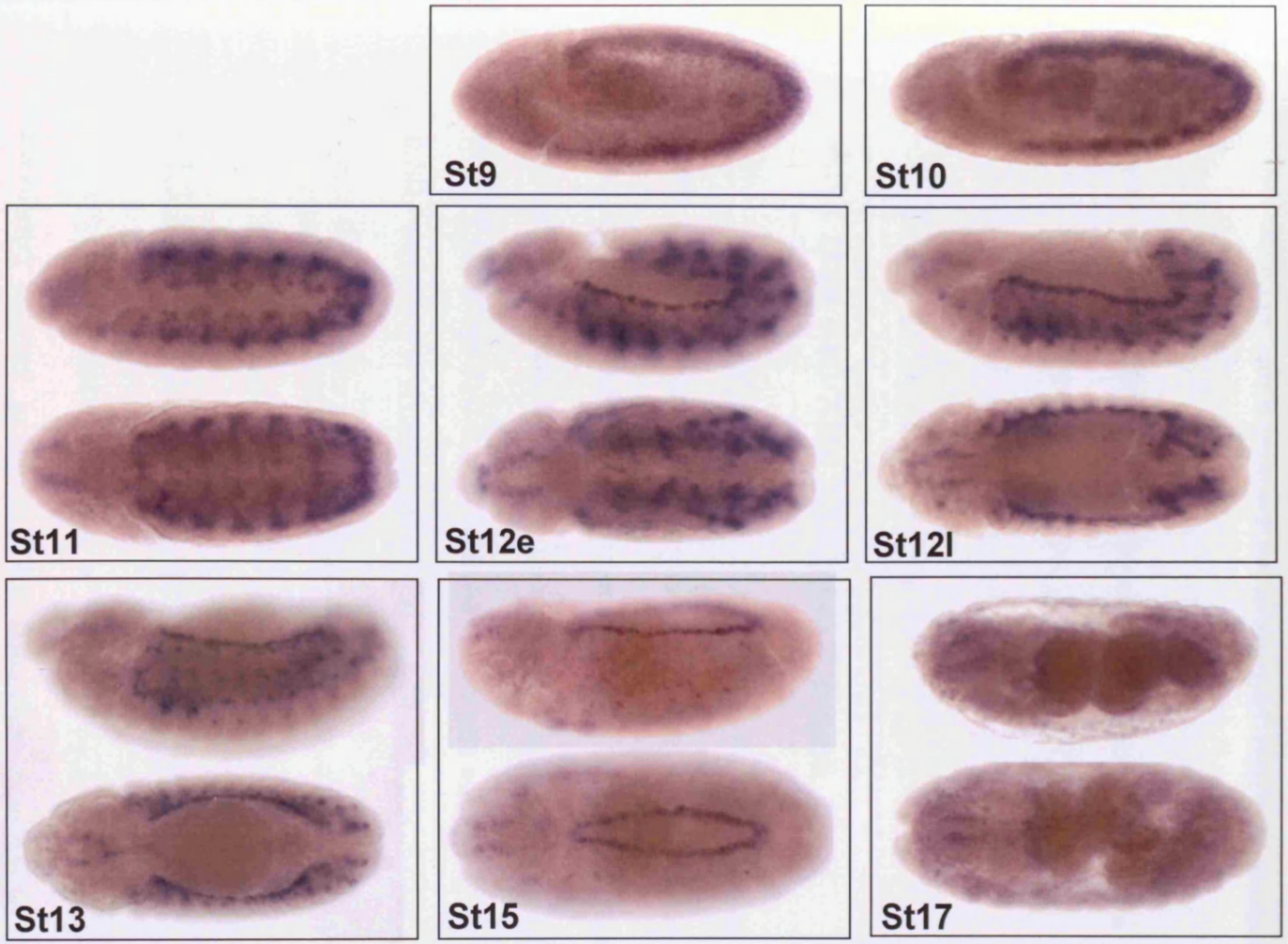

FIG 4.2.1 Him expression pattern - RNA in-situ hybridisation

Him expression declines as muscle differentiates. Expression begins at St9 where it is expressed in the developing mesoderm. At St12 it is also expressed in the somatic muscle precursors and heart precursors. Around the onset of somatic muscle differentiation, at late St12, Him expression begins to rapidly decline in the developing somatic muscle, whilst remaining in the adult muscle precursors and heart pericardial cells. By St13, when the somatic muscle has differentiated, Him expression is lost completely in the somatic muscle, but still expressed strongly in the AMP's and heart. By the end of embryogenesis, at St17, Him expression in the AMP's and pericardial cells weakens considerably, until it is barely detectable.

St9 and St10 embryos are shown laterally only. St11, St12e, St12l, St13, St15 and St17 embryos are shown laterally (upper image) and dorsally (lower image). Embryos were wild-type, Oregon R.

reporter constructs to analyse the area (FIG 4.3.1). The Him Xho/Xba 1Kb T pStinger and the Him 1Kb NT pHStinger constructs were designed and generated by me (See FIG 4.3.8 and Materials and Methods), the Him Posakony pStinger constructs are from the Rebeiz et al study, the Him 3.8Kb GFP fusion construct is from Liotta et al, 2007 Him study and the Him Xho/Xba 2.8Kb pStinger constructs and Him Set1-3 constructs were generated by Stuart McConnell, a previous post-doc in the lab. Binding sites for Su(H), Twist and Mef2 were searched using the following established consensus sequences; Su(H) – YGTGDGAA (Rebeiz et al, 2002), Twist – CACATG (Cripps et al, 1998), Mef2 YTAWWWWTAR (Andres et al, 1995).

4.3.2 Him Eco/Xba 3.8Kb GFP fusion

This covers the region upstream of the Him gene. The expression of the Him Eco/Xba 3.8Kb GFP fusion construct comes on early, at St9, in the same way as Him expression and follows the same basic expression pattern as *Him* up to the end of embryogenesis at St17. There are differences in how the somatic muscle expression persists, for example compare the GFP fusion embryo at St13 with the Him in-situ embryo at St13 in FIG 4.3.2b and also at St17 especially it is noticeable how the pericardial and ring gland expression is stronger than in the *Him* in-situ at the corresponding stage.

4.3.3 Him Eco/Xho 2.8Kb GFP reporter

This covers the region upstream of Him, without the inclusion of the 1Kb region immediately adjacent to the start site. The early mesodermal expression of the Him Eco/Xho 2.8Kb reporter is weaker than the Him in-situ at stages 10 and 11 and lacks the initial anterior expression in the head region at these stages. At the later stages, St16 and

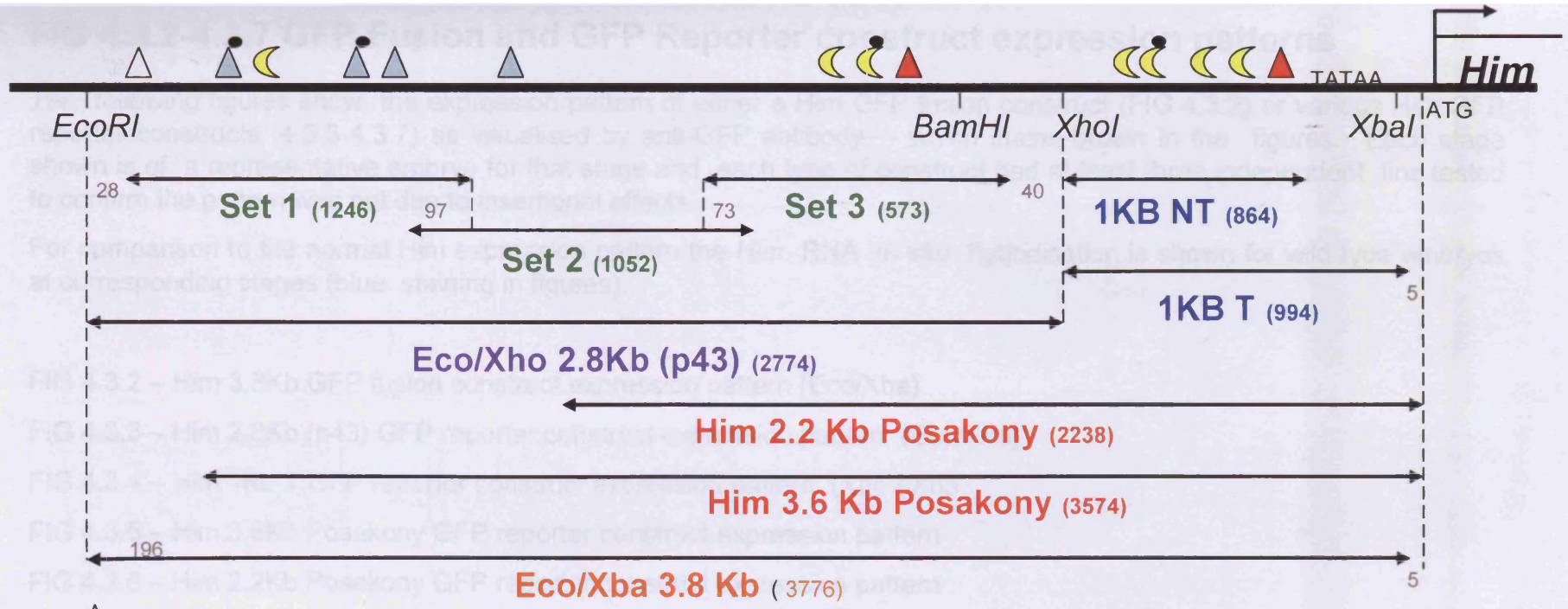

FIG 4.3.1 GFP Reporter construct map of the Him regulatory region

The region between the *Her* and *Him* genes was previously shown to be the potential regulatory region for *Him* (Rebeiz et al 2002). Two GFP reporter constructs were generated from this Rebeiz et al study; one named "Posakony 3.6Kb", which covers a large region upstream of the *Him* transcription start site up to and including the cluster of Su(H) sites and another named "Posakony 2.2Kb" which does not include the Su(H) sites.

To investigate the Him regulatory region in detail, me and previous members of the lab made GFP reporter constructs to cover the whole region, in order to establish the key regions and transcription factor binding sites for the correct expression of the *Him* gene.

FIG 4.3.2-4.3.7 GFP Fusion and GFP Reporter construct expression patterns

The following figures show the expression pattern of either a Him GFP fusion construct (FIG 4.3.2) or various Him GFP reporter constructs (4.3.3-4.3.7) as visualised by anti-GFP antibody - which stains brown in the figures. Each stage shown is of a representative embryo for that stage and each type of construct had at least three independent lins tested to confirm the pattern was not due to insertional effects.

For comparison to the normal Him expression pattern the *Him* RNA in-situ hybridisation is shown for wild type embryos at corresponding stages (blue staining in figures).

FIG 4.3.2 – Him 3.8Kb GFP fusion construct expression pattern (Eco/Xba)

FIG 4.3.3 – Him 2.8Kb (p43) GFP reporter construct expression pattern (Eco/Xho)

FIG 4.3.4 – Him 1Kb T GFP reporter construct expression pattern (Xho / Xba)

FIG 4.3.5 – Him 3.6Kb Posakony GFP reporter construct expression pattern

FIG 4.3.6 – Him 2.2Kb Posakony GFP reporter construct expression pattern

FIG 4.3.7 – Him 1Kb NT GFP reporter construct expression pattern

Him Eco/Xba 3.8 Kb GFP fusion(3776)

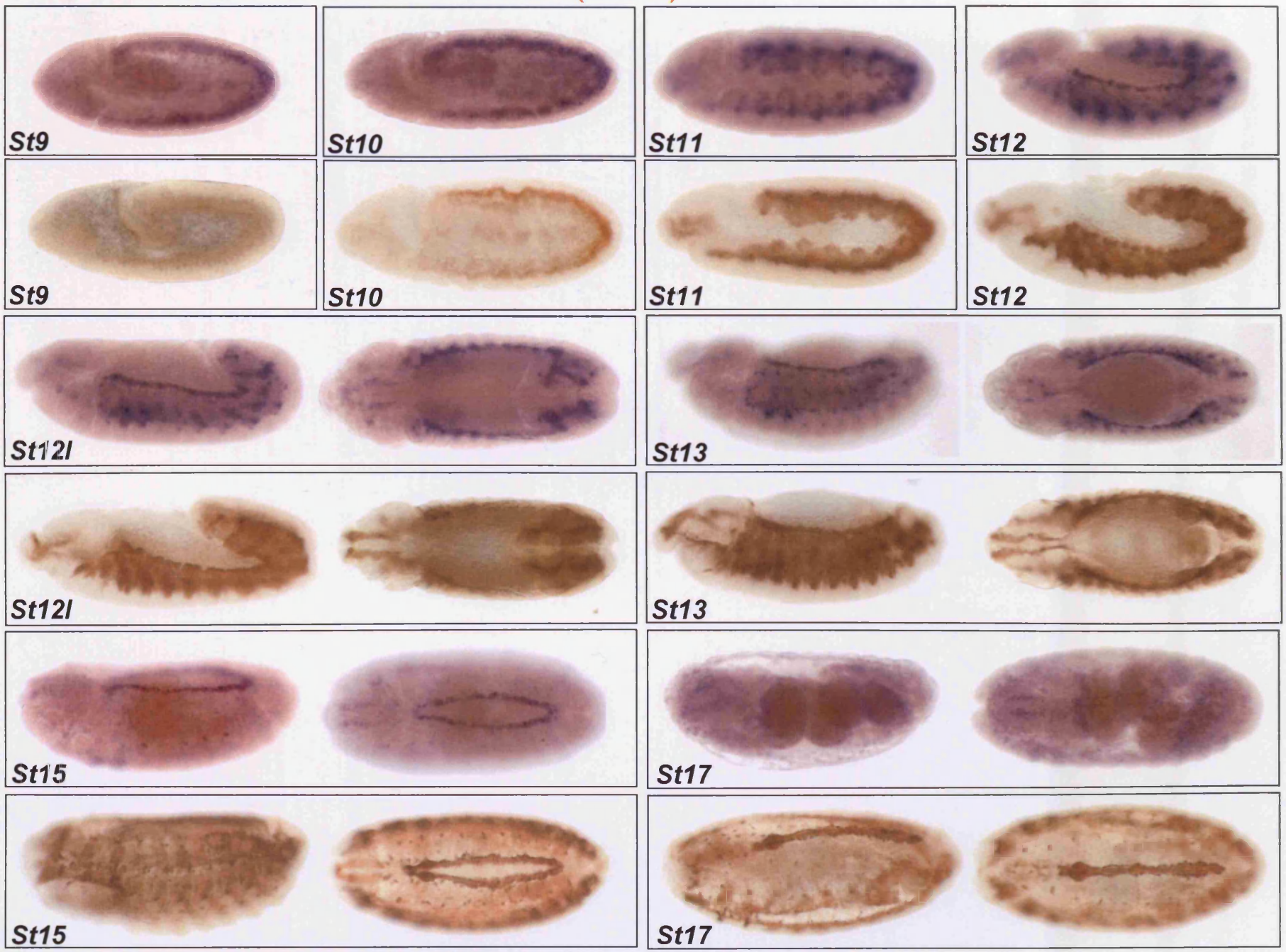

FIG 4.3.2 Him Eco/Xba 3.8Kb GFP fusion construct expression

Him Eco/Xho 2.8Kb (p43) pH Stinger (2774)

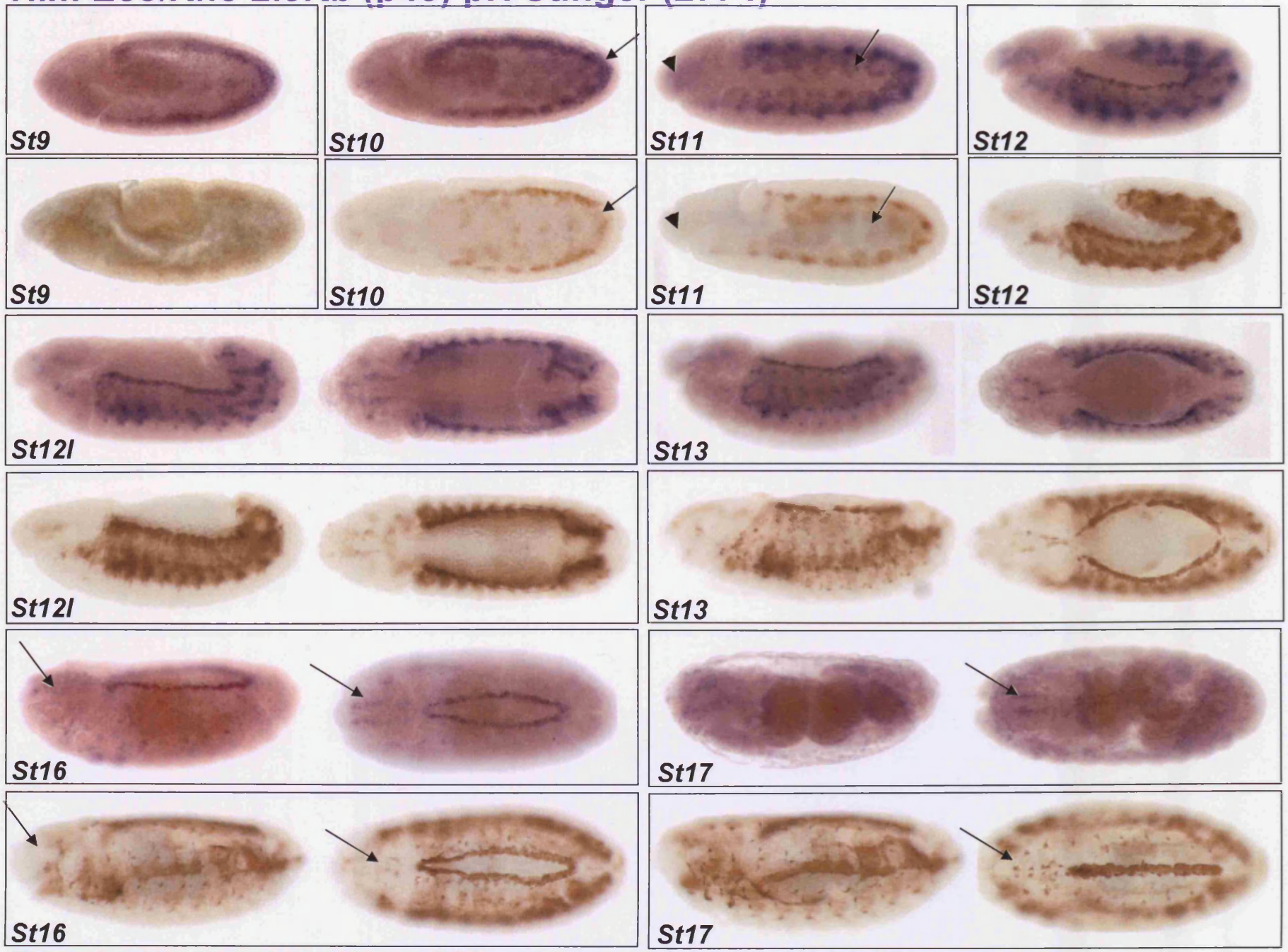

FIG 4.3.3 Him Eco/Xho 2.8Kb GFP reporter construct expression

Him Xho / Xba 1KB T GFP pStinger (994)

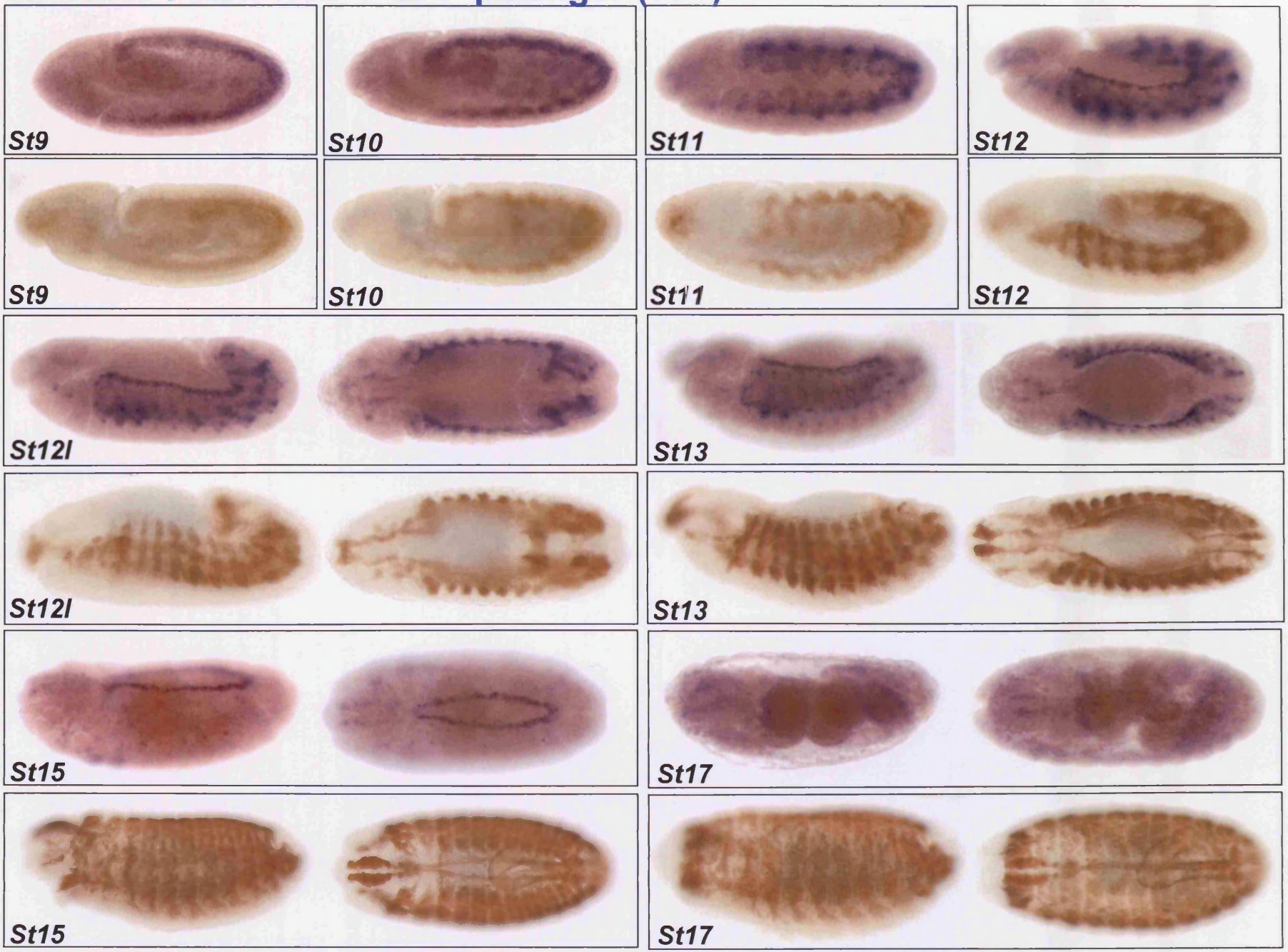

FIG 4.3.4 Him Xho / Xba 1Kb T GFP reporter construct expression

Him 3.6 Kb Posakony pStinger (3574)

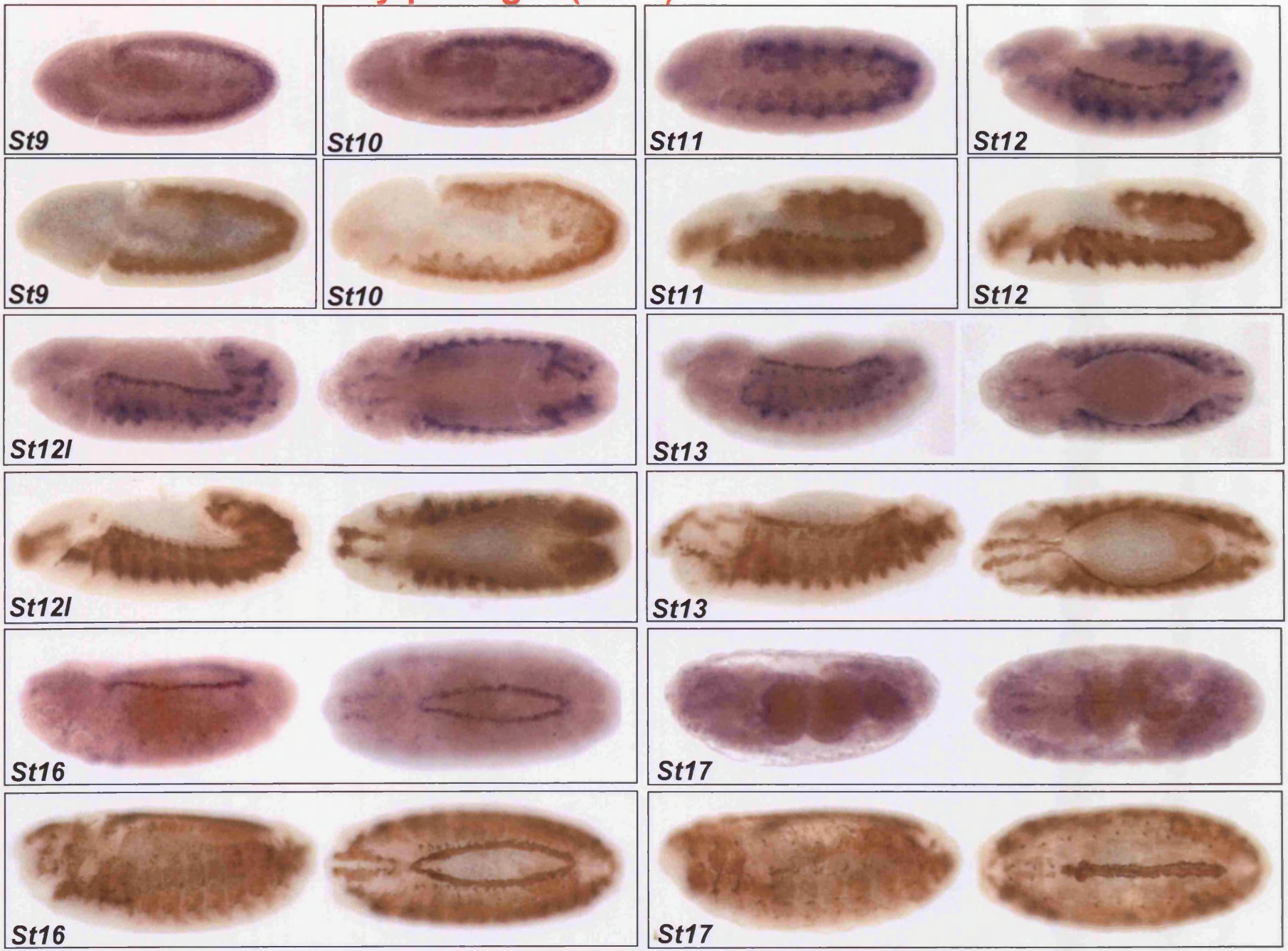

FIG 4.3.5 Him Posakony 3.6Kb GFP reporter construct expression

Him 2.2 Kb Posakony pStinger (2238)

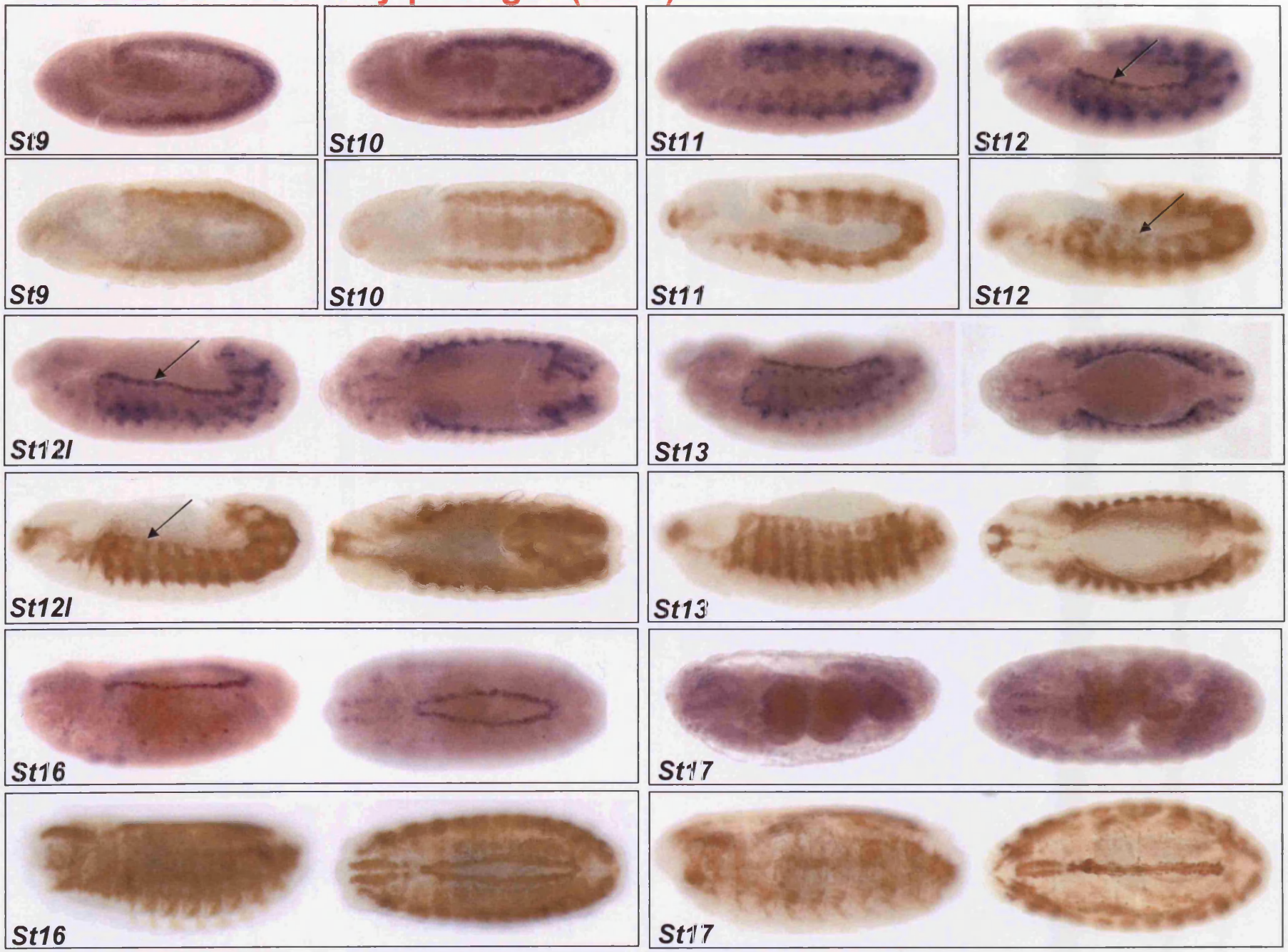

FIG 4.3.6 Him Posakony 2.2Kb GFP reporter construct expression

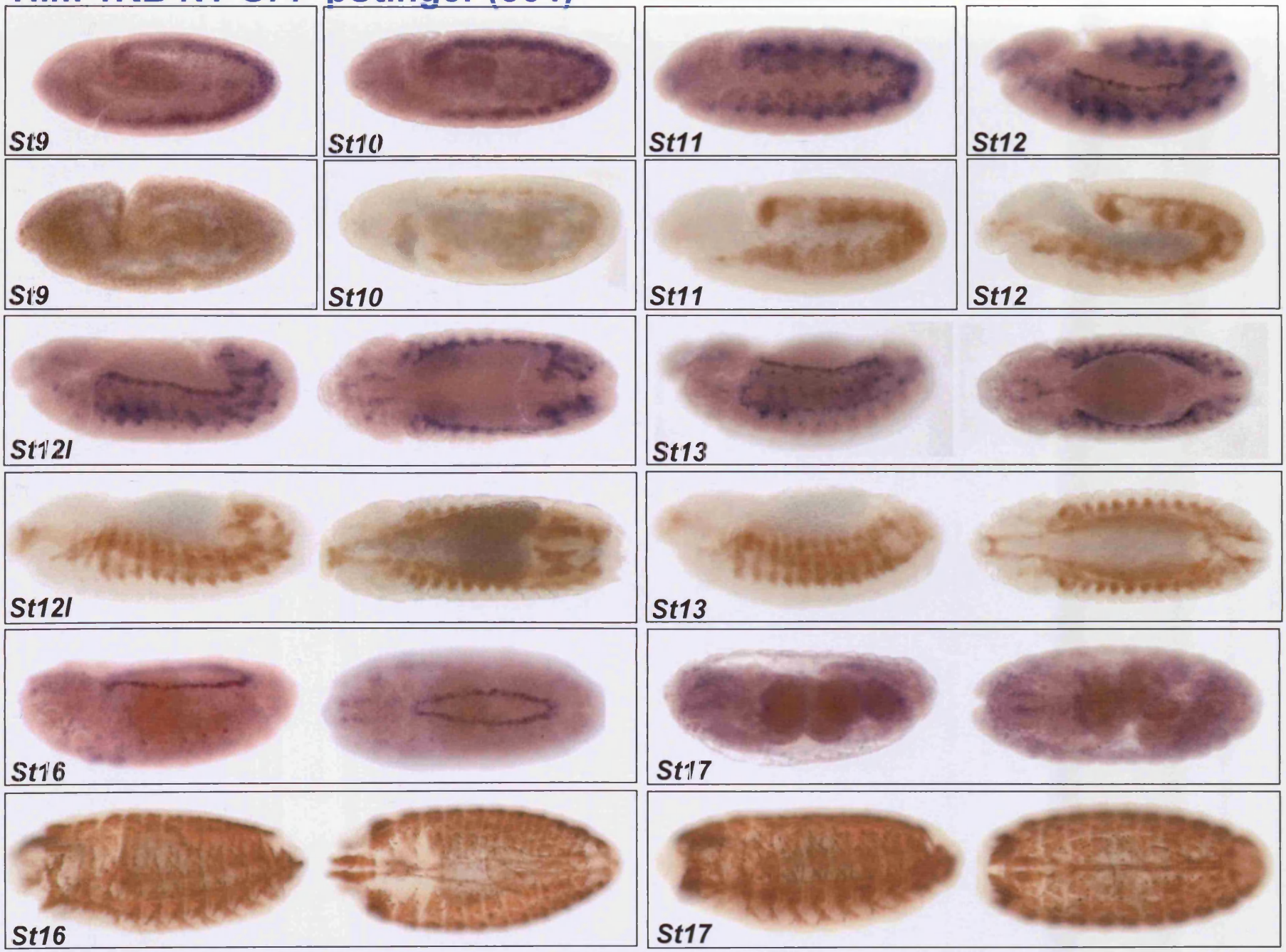

FIG 4.3.7 Him 1KB NT GFP reporter construct expression

St17, expression in the pharyngeal muscle is not detectable in the Him Eco/Xho 2.8Kb reporter, whereas it is still detectable in the Him in-situ at the corresponding stages. By comparison the pericardial expression of the heart is just as strong at St16, and stronger at St17 in the reporter compared to the Him in-situ. (See FIG 4.3.3b). Other than this the expression closely resembles that of the Him in-situ, with loss of the somatic expression occurring in the same way as the Him in-situ at St13 and appropriate A.M.P, pericardial cell and early pharyngeal expression.

4.3.4 Him Xho/ Xba 1Kb GFP reporter

The 1Kb region immediately upstream of the Him start site, containing the TATA box. The early expression pattern is similar to Him expression in the Him in-situ, with the appropriate onset and level of expression in the developing mesoderm. The expression in the anterior region is also induced appropriately. However as the mesoderm begins to specialise at St12 it is apparent that this reporter shows striking differences, there is no expression in the cardiac precursors, but there is expression in the visceral precursors. Somatic muscle expression does not get turned off at all and instead persists until the end of St17, being expressed in the fully differentiated musculature. Visceral muscle expression and head muscle expression also occurs from St12 through to the end of St17 and the cardiac expression, which begins around St14 is weak and occurs in the cardioblasts. Pharyngeal muscle expression remains strong until St17.

4.3.5 Him Posakony 3.6Kb GFP reporter

This covers the same region as the Him Eco/Xho 3.8Kb GFP fusion construct short of 200bp farthest upstream from the Him gene. The expression pattern is similar to the Him Eco/Xho 3.8Kb GFP fusion construct although, perhaps the somatic muscle expression persists for longer

4.3.6 Him Posakony 2.2Kb GFP reporter

This construct covers the 2.2Kb immediately upstream of the Him gene. It is the same region as the Him Posakony 3.6Kb construct but with the region containing the cluster of Su(H) sites and one Twist site removed.

The expression pattern is the same as the Him Posakony 3.6Kb construct, but the expression is weaker in intensity in the developing mesoderm and especially so in the heart precursors around St12.

4.2.7 Him 1Kb NT GFP reporter

This construct is shorter than the Him 1Kb Xho/XbaI construct. It contains the same Mef2 and Twist binding sites, but has the TATA box excluded. The expression pattern is the same as the Him 1Kb Xho/XbaI construct.

4.2.8 Him 1Kb NT delMef2 SDM (SacII) GFP reporter

I analysed the 1kb region in detail (FIG 4.2.8) and I designed primers to delete the Mef2 site within this region and also to Twist sites in the region to investigate their function. I generated a deletion construct to the 1Kb NT region (FIG 4.3.8 and Materials and

FIG 4.3.8 Analysis of the Him 1Kb region

CTCGAGTAGTTTTTAGATGCAGTATTATTAAGTAGAAAATTGTAACCG
TATAATATTCCATTATATTAAATATTTTTATAGCACTAAAGAAATAAAAGC
CCATTTTATAATTTATATTACAAAAATACTTAACCATAGAAACTTATGATA
TGATACCAATATTTAAGTTCCAAAAAATGTAGAACATTTTTAAGTATATAC
TCGAAAATATTAATTTTCAAAATTGATATTCAAGAGATATTATAAAAAGA
TCCCCATTCTAAATATCTAACATCATGCCATGCTTTCTAATGAGTATAGTA
TACCCCTGCTACCCTGTCAATCCGCAAAACAGGCGCCGAAACATGCGGTT
TCTCGCAGCAGACTGCCACGGGAAAAATTCGGTTCGAGATTTGGGAATGG
ATGTATGACGGAGCAGAAGGAGCAGGACCCGGATTTCGGATTTCGGAATG
GATATGGAAATGAAGATGGAAATGGGACTTTGACTGCGCGACGGCCACAT
GCGCCGCTGGCGATGCCGCTGGATGTTGCATGTGGCAGCGGTCGGTGCAG
CAGCGAAAGTGTTGCAGCTGTATGAGAGGGTCTATTTTTGGGGCGATTGT
GCGGCGCTGGTGCTGCCACATGTGTTCTGTGTTGGGCTGCTAAAAGGCA
TTGTAATGAGAGCAGAAAATAGAATTGACTCTACTTGAGCAATGTCCC
ATAAAGCGGGAGTTTCGAGTTTGGCGCGCAATGTGCCGCACCAGCAA
ACGAACAAAAGAAAAAAAAAAAAAAAAAACACAGCCAGTAACACATGG
GCCCACGAGTTATGTTTTATTTTTAATCCCACAAAGAGTCGATCTCCAAA
ACAAACCCGCAGAGAGCACATATAAAGAGACTCGGTGGACGAGTGGT
TCGAAACAGTCTTCCGCCGCAGCTCGACGCGCTCGCATATCGGGAATATA
TAGATCGGAGATATCGCAGGACCCACAGCAGAGCAGAGCCGCAGAGCC
ACCAACCTCGATG

CANNTG = General E Box motif *(Murre et al, 1989)*

CACATG = Twist E Box *(Cripps et al, 1998)*

YTAWWWWTAR = Mef2 site motif *(Andres et al, 1995)*

TTATTTTTAA = Mef2 site to consensus (Mef2-I)

CTATTTTTGG = Mef2 site one away from consensus (Mef2-0)

CAGAAAATAG = Mef2 site 2 away from consensus – not bothering with.

GGGCCC = ApaI site – can be used to split construct into two.

TTATTTTTAA Mef2 site is similar to the Mef2 site shown to be functional in *microRNA-1 (DmiR-1) TTAATTTTAG (Sokol and Ambros, 2005)*

CACATGTG is the exact same overlapping Twist Ebox shown to be functional in Mef2 regulation (Cripps et al, 1998)

CTCGAGTAGTTTTTAGATGCAG Marks the fwd primer of the 1Kb T and 1KB NT constructs. Note the Endogenous XhoI site.

CAAACCCGCAGAGAGCACA Marks the rev primer of the 1Kb NT construct.

CAGAGCCACCAA Marks the rev primer of the 1Kb NT construct. An ectopic Xba I site is introduced at the end.

FIG 4.3.8 Analysis of the Him 1Kb region cont.

From this Site Directed Mutagenesis primers aiming to mutate the following sites were designed

Mef2 site to consensus (Called "Mef2-I") : TTATTTTTAA

Mef2 site one away from consensus (Called "Mef2-0") : CTATTTTTGG

Twist site most proximal to the Him gene start site (Called "Twi Prox") : CACATG

Over-lapping Twist sites (Called "Twi OL") : CACATGTG

Primers:

Primers designed according to Stratagene requirements

Mef2-I SDM : TTATTTTTAA to TTCGGCGGTAA (SacII site introduced)

Him dMef2 1 fwd	cag taa cac atg ggc cca cga gtt atg ttt ccg cgg taa tcc cac aaa gag tcg atc tcc aaa ac
Him dMef2 1 rev	gtt ttg gag atc gac tct ttg tgg gat tac cgc gga aac ata act cgt ggg ccc atg tgt tac tg

Mef2-0 SDM : CTATTTTTGG to CCCGCGGTGG

Him dMef2 0 fwd	gtt gca gct gta tga gag ggt ccc gcg gtg ggg cga ttg tgc ggc gct gg
Him dMef2 0 rev	cca gcg ccg cac aat cgc ccc acc gcg gga ccc tct cat aca gct gca ac

Twi Prx SDM : CACATG to TGCATA

Him Twi-Prox fwd	gaa caa aag aaa aaa aaa aaa aaa aaa cac agc cag taa tgc ata ggc cca cga gtt atg ttt ta
Him Twi-Prox rev	taa aac ata act cgt ggg cct atg cat tac tgg ctg tgt ttt ttt ttt ttt ttt ttc ttt tgt tc

Twi OL SDM : CACATGTG to CGGCCGTG

Him Twi-OvLAP fw	gcg gcg ctg gtg ctg ccg gcc gtg ttc tgt gtt ggg ct
Him Twi-OvLAP rv	agc cca aca cag aac acg gcc ggc agc acc agc gcc gc

The Twist OL site is exactly the same as that shown to be functional as the Key Twist E Box in Mef2 regulation. I mutated the sequence in exactly the same way as they did which lost expression of a reporter construct (Cripps et al, 1998).

I successfully generated the following SDM constructs which were sequenced and found to be correct (Strategy using Stratagene Quikchange II SDM Kit).

: Him 1Kb NT ΔMef2-I SDM pGEMT
: Him 1Kb T ΔTwi OL SDM pGEMT
: Him 1Kb T ΔTwi Prox SDM pGEMT

From these constructs I subcloned the fragments to get the following reporter constructs

: Him 1Kb NT ΔMef2-I SDM pH Stinger
: Him 3.8Kb T ΔTwi OL SDM pStinger

Methods) and the subsequent injection, generation of multiple transgenic lines and their analysis was done by J.Han in the lab. She found that in all of the lines there was no expression of GFP (J.Han pers.comm), showing that the Mef2 site is responsible for the expression of the 1Kb region and therefore that there is a functional Mef2 site that contributes to the expression of Him.

The contribution of this Mef2 site to Him expression may occur early in the development; comparison of the Him 3.8Kb GFP fusion construct with the Him 2.8Kb (p43) GFP construct, shows a distinct difference early on; compare the St11 embryos, where expression of the Him 3.8Kb construct is more like wild type Him expression (FIG 4.2.1) than the Him 2.8Kb expression (FIG 4.2.2). However, there are also distinct differences in the late expression of the two constructs that suggest Him 2.8Kb is more like the wild type Him pattern than Him 3.8Kb.

Further analysis of this and site directed mutagenesis to the 1Kb region in the context of the 3.8Kb GFP reporter would be most informative for the specific action of Mef2 upon Him regulation.

4.4 Discussion

The identification of Mef2 as a direct activator of *Him* is a particularly interesting result in that, not only does it identify a mechanism for the regulation of *Him* that has not been established previously, but also, as Him is a repressor of Mef2 protein, it means that Mef2 is indirectly instigating its own regulation. This action of "activating its repressor", is a novel role for Mef2.

It is well known that the regulation of Mef2 must be tightly controlled throughout differentiation, but especially so early on in muscle development where the positive action

of Mef2 must be restrained until the appropriate time for differentiation to occur. Liotta et al provide a model for this whereby the repressive action of Him upon Mef2 means that the Mef2 protein is present in the cell and poised ready for activation at the appropriate time until the restraining mechanisms can be removed.

This observation would then sit nicely alongside the previous result that Mef2 is capable of auto-regulation; increasing its activity later in development by acting upon its own enhancer (Cripps and Olson, 2004). If, as suggested above, the Mef2 site in the 1Kb region has a contribution to Him expression early in development (before St13 and the onset of differentiation) this allows for a model of Mef2 auto regulation (indirect – then direct) which reinforces its repression early on (mediated by Him) when it must be restrained and then at the point of muscle differentiation a switch would occur enabling the reinforcement of Mef2 activation (mediated by Mef2 directly upon itself). Though an equally likely mechanism is that early on, both the indirect and direct Mef2 auto-regulation occurs and this ensures a tuning of Mef2 levels in the context of other factors laying down the central expression of Mef2 and of Him. This would fit with the rapid down-regulation of Him.

Him Gain-of-Function

5.1 Introduction

As outlined in Chapter 4, *Him* expression rapidly declines in the somatic mesoderm and has disappeared completely from this lineage by the time the somatic muscle has fully differentiated at St13. If Him expression is maintained ectopically in the somatic muscle past this stage through the use of the Gal4 UAS system, muscle differentiation is severely inhibited. This inhibition is through the repressive action of Him on Mef2 (Liotta et al, 2007).

For the Liotta et al study, the phenotype of Him over-expression was shown to mimic the phenotype associated with Mef2 loss of function; over-expression of Him throughout the mesoderm with 24B Gal4 at 25°C could give a phenotype like the $Mef2^{113}$ hypomorph in terms of general severity and muscle morphology (Liotta et al, 2007). As part of my thesis, I wanted to investigate the Him gain-of-function in greater detail; specifically I wanted to look at which individual somatic muscles were affected when Him was over-expressed and whether certain muscles were more easily affected than others. Not only does this information provide a more comprehensive analysis of the Him over-expression somatic muscle phenotype and provide greater insight into the action of Him in muscle differentiation, it also allows a direct comparison with the somatic muscle phenotypes associated with other experimental conditions.

5.2 Over-expression of *Him* inhibits somatic muscle differentiation

For my analysis of Him gain-of-function, I over-expressed *Him* in the Mef2 pattern, using Mef2 Gal4 (Ranganayakulu et al, 1996). Mef2 Gal4 is a strong mesodermal driver, and by driving in the Mef2 pattern, it meant that the expression of Him would continue in the somatic musculature until St17 rather than decline at St12. In addition the mesodermal expression levels of Him would be increased at St9-12 due to this over-expression.

I drove UAS Him with Mef2 Gal4 at 29°C and 21°C and visualised muscles with β3-tubulin antibody. The phenotype gave a dramatic reduction in muscle formation at both temperatures, with a similar degree of muscle loss at both 29°C and 21°C (Table 5.2.1) The average number of muscles missing per hemi-segment was 67 for Him driven at 29°C and 68 for Him driven at 21°C – meaning that around three quarters of the somatic muscles completely fail to form under both conditions. For this analysis I scored the presence or absence of the 30 individual muscles for the abdominal hemi-segments A2, A3 and A4. Those muscles that were present were scored for shape or attachment defects.

Despite the severity of the phenotype the identity of the muscles could still be determined as they generally still retained their position attachments and though the shape was often disrupted to some extent, the way it was disrupted was characteristic of that muscle type observed in milder examples of the phenotype observed in the range of results for that experiment.

As one would expect the individual muscles that are lost at both temperatures are generally the same (Underlined in Table 5.2.2).There are certain muscles which are lost almost all of the time in each of the hemi-segments scored in all embryos under both experimental conditions; for example, DO5, LO1, VA3, VO3, VO4, VO5 and VO6 are missing at an

Muscle phenotype	**UAS Him x *Mef2 Gal4*** (29°C)	**UAS Him x *Mef2 Gal4*** (21°C)
% embryos with muscle missing	100 %	100 %
Average No. muscles missing per embryo	67.1	68.0
Range of muscles missing per embryo	59 - 72	65 - 77

Survival assay		
Hatching	0 %	0 %
Survival	0 %	0 %

Table 5.2.1 – Muscle phenotypes in embryos over-expressing Him at different temperatures.

Over expression of Him gives a severe muscle phenotype, with the majority of somatic muscles being lost. The severity of the phenotype is similar when driven by Mef2 Gal4 at 29°C and 21°C.

Muscles scored A2-A4 for 20 embryos.

average of at least 2.8 / 3 times in hemi-segments A2-A4 in 100% of embryos scored (Table 5.2.2) This shows that these individual muscles are more readily lost than others under Him over-expression conditions. Conversely there are muscles that appear to be more resistant to a decrease in Mef2 activity due to Him over-expression; for example DT1 is more frequently present than it is missing – it is missing only in one hemi-segment of the three scored in 50% of embryos at 21°C (Table 5.2.2) and was always present in the experiment driving Him at 29°C. Similarly VT1 and VA2 are lost less frequently in both the experiments (Table 5.2.2).

The severity of the Him over-expression phenotype can be seen in the representative embryo in FIG 5.2.1. This embryo, which had UAS Him driven at 29°C, shows a severe disruption to the muscle pattern, with large gaps and holes in the somatic musculature due to the large number of muscles missing. The few muscles that are present in the embryo have either severe shape defects or attachment defects or both. There are no muscles that are wild type in appearance. For example in this embryo, DA2 is considerably thinner than wild type, DA1 stretches from a dorsal to ventral position instead of an anterior to posterior one, and DT1 is misshapen, being of varying degrees of thickness as opposed to a uniform thickness as in the wild type condition. Other muscles, such as the VL muscles frequently form but fail to find both their anterior and posterior attachment points and consequently ball up. The identity of specific muscles that have lost their attachment (for example DA1 in this embryo) can be determined based upon their other characteristics that are retained such as position within the embryo and general shape, and also, more importantly the observation that the same muscle may often be affected in a similar way with less severity elsewhere, and from this is indicative of the same effect but caused slightly more severely.

A comparison of embryos showing the over-expression of Him at either 29°C or 21°C is shown in FIG 5.2.2. Though the phenotypes look very similar, the number of muscles

Cross	Muscles **Missing** in 100 % Embryos	Muscles **Missing** in 90-99 % Embryos	Muscles **Missing** in 80-89% Embryos	Muscles **Missing** in 60 - 79% Embryos	Muscles **Missing** in 50 – 59% Embryos	Muscles **Present** in 70 – 89 % Embryos	Muscles **Present** in 90 – 100% Embryos
UAS Him x *Mef2 Gal4* (29°C)	**DO2, DO3, DO5, LL1, LT1, LT2, LT3, LT4, LO1, VL4, VA3, VO2, VO3, VO4, VO5, VO6**	**DA2, DA3, SBM, VL3, VA1, VO1,**	**DO4, VL2,**	**DA1, VT1 VA2, DO1**	**VL1**	-	**DT1**
UAS Him x *Mef2 Gal4* (21°C)	**DA1, DA2, DO3, DO5, LT2, LT3, LT4, LO1, VL2, VA1, VA3, VO1, VO2, VO3, VO4, VO5, VO6**	**DO4, DA3, SBM, VL3, VL4**	**DO1, LT1, VL1**	**DO2, LL1**	**DT1, VA2**	**VT1**	

Table 5.2.2 – Muscles missing in embryos over-expressing Him at different temperatures.

Muscle scoring analysis for UAS Him driven by Mef2 Gal4 at 29°C and 21 °C. The 30 individual somatic muscles of abdominal hemi-segments A2, A3 and A4 (a total of 90 muscles) were scored per embryo. 20 embryos were scored for UAS Him at 29 and 10 embryos were scored for UAS Him at 21 °C.

Only one individual muscle from any of the three hemi-segments scored needs to be missing for an embryo to be scored as having that individual muscle type missing. A muscle that is coloured blue is missing in that percentage of embryos at an average frequency of 2.8 or greater per embryo scored – i.e that individual muscle was missing almost every time in each of the three hemi-segments scored per embryo. Muscles that are underlined are lost in a similar percentage of embryos at both temperatures.

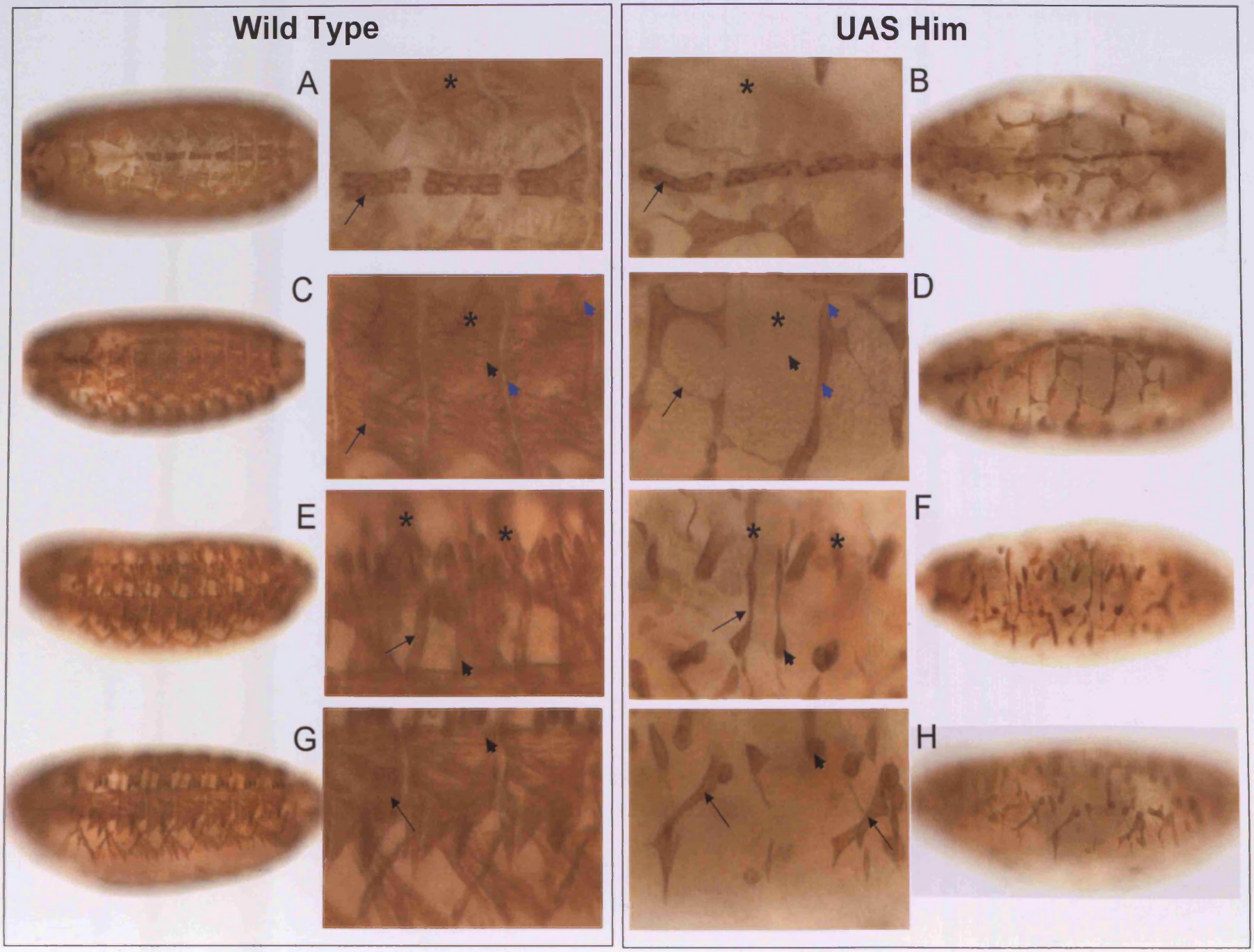

FIG 5.2.1 Over-expression of Him inhibits formation of somatic muscle in the embryo

FIG 5.2.1 Over-expression of Him inhibits formation of somatic muscle in the embryo

Over-expression of Him in the somatic muscle causes a severe disruption to muscle pattern due to inhibition Mef2 activity. The majority of somatic muscles are missing (see Table 5.2.2 for details), however the heart appears relatively unaffected in comparison to wild type (compare B to wild type A – this figure, and FIG 5.2.3)

In the dorso-laterally aligned embryo (D) the dorsal muscles DO1 and DA1 are missing (arrowhead and asterisk), and the few muscles that are present have either severe shape defects, such as DA2 being considerably thinner than wild type (compare arrow in D to arrow in C), or have attachment defects, such as in DA1 stretching from dorsal to ventral instead of anterior to posterior (compare attachment points marked by blue arrowheads in D to those of wild type in C).

In the laterally aligned embryo (F) the majority of lateral muscles are missing, with only one misshapen SBM muscle (arrow) and one misshapen LT muscle (arrowhead) forming out of the three hemi-segments shown. DT1 is present more frequently (asterisks), although still has shape defects.

The majority of ventral muscles are also missing or severely misshapen. VA2 is often distinguishable (arrow) and frequently one or two, but not all, of the VL muscles form in a hemi-segment, but do not attach properly and ball up (arrowhead)

Experimental embryos are UAS Him J7 driven at 29°C by Mef2 Gal4. Wild type are Oregon R. All embryos are St17 and stained with anti β3-tubulin antibody.

missing is similar (Table 5.2.1) and the types of individual somatic muscles missing is similar (Table 5.2.2) there is some difference in the frequency that an individual muscle is lost in an embryo. For example the LT muscles are missing at a greater frequency per embryo A2-A4 when Him is driven at 29°C than when driven at 21°C (Table 5.2.3), though the percentage of embryos that have at least one of the individual LT muscles missing is the same at both temperatures (Table 5.2.2) .

These data can be seen in FIG 5.2.2, where there are a greater number of LT muscles present in the embryo over-expressing Him at 21°C than compared to the embryo over-expressing Him at 29°C. In addition, the shape defects in the LT muscles that remain present in the embryos over-expressing Him at 29°C, appear to be more pronounced than the shape defects affecting those present in the embryos over-expressing Him at 21°C; the dorsal attachment points do not seem to be reached in the LT muscles as often in the embryos over-expressing Him at 29°C and they can show a greater degree of balling up.

Though the majority of somatic muscles are missing in Him gain-of-function embryos, β3-tubulin expression in the heart appears relatively unaffected in comparison to wild type. In wild type embryos, β3-tubulin is expressed in four of the six cardioblasts that make a hemi-segment of the linear heart tube (Damm et al, 1998; FIG 5.2.3). Mef2 is expressed in all six of the cardioblasts (Bour et al, 1994; Lilly et al, 1994; Taylor et al, 1995), and consequently the Mef2 Gal4 driver would cause ectopic Him expression in these cells. With Him over-expression here there is little effect upon the heart; it generally appears wild type apart from the occasional loss or gain of β3-tubulin positive cardioblasts or kinking in the heart tube (FIG 5.2.3).

Previous work in the lab found that this to be in contrast to Myosin Heavy Chain (MHC) expression in the heart of embryos that used Mef2 Gal4 to drive over-expression of Him in

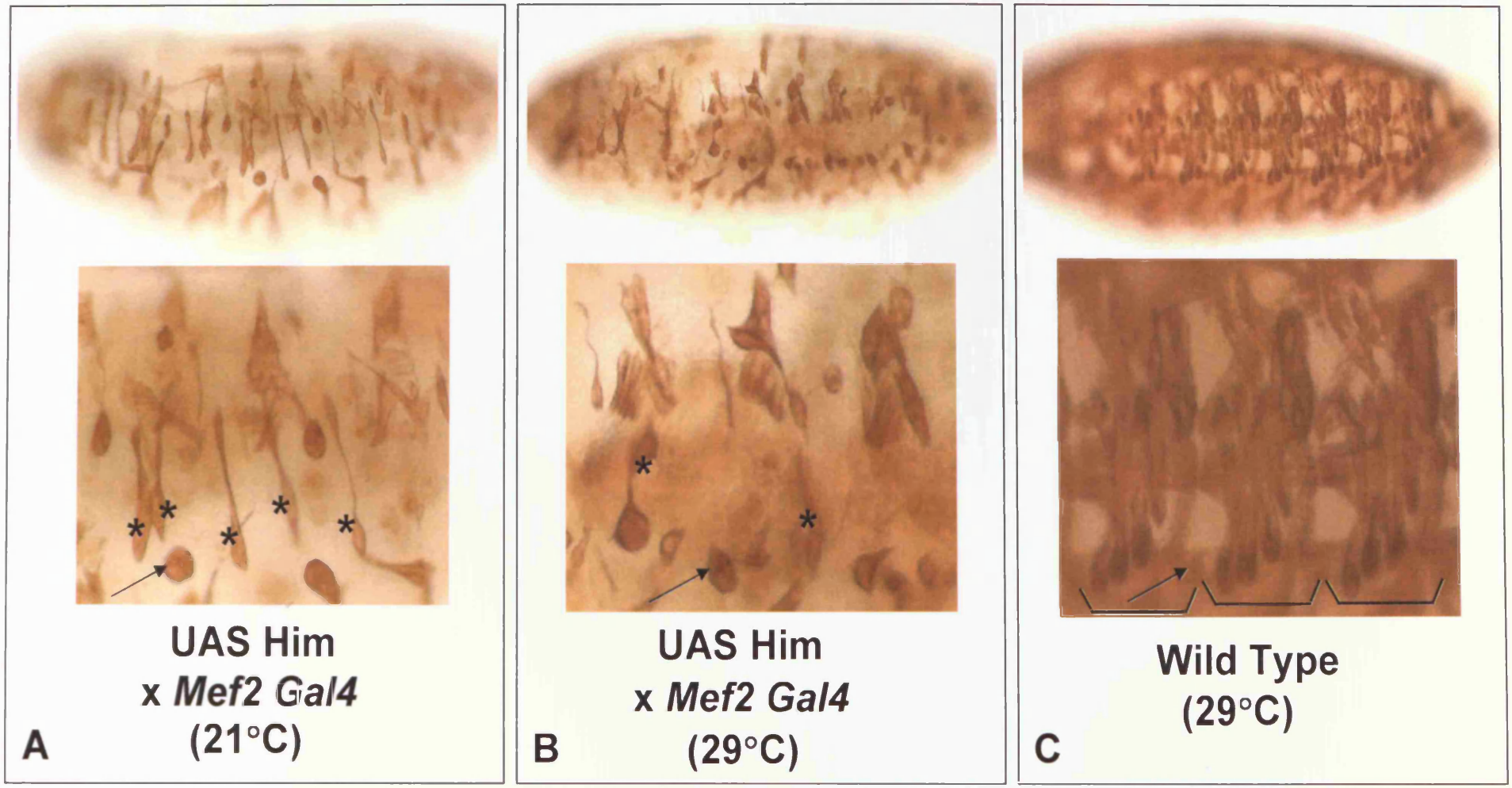

FIG 5.2.2 Over-expression of Him at a higher temperature shows an increased frequency of individual muscle loss.

FIG 5.2.2 Over-expression of Him at a higher temperature shows an increased frequency of individual muscle loss.

Over-expression of Him driven by Mef2 Gal4 at 21°C and 29°C both give severe muscle phenotypes with the majority of individual somatic muscles being missing at least once in each embryo of the three hemi-segments (A2-A4) scored (Table 2.3.2) . The main difference between the two phenotypes is that the frequency of certain muscles being missing can be higher in an embryo when Him is driven at the higher temperature. For example with the lateral muscles LT1,LT2, LT3 and LT4 the average number of muscles present is higher at 21°C than at 29°C and those that are present at the higher temperature show a more severe degree of shape defects (5 LT muscles present here at 21°C, A. 2 LT muscles present at 29°C, B and the full set of 12 LT muscles for the three hemi-segments in a wild type embryo, C – all shown by asterisks). Other muscles, such as the VL's show similar phenotypes at both temperatures – being missing or balled up with incorrect attachment when the muscle is present (arrow).

Embryos are St17, shown laterally and stained with anti β3-tubulin antibody. Representative embryos are shown. Wild type embryo is Oregon R and was at 29°C.

The average number of LT muscles missing per hemi-segment in each embryo scored is as follows

: UAS Him @ 21 : LT1 = 1.63, LT2 = 2.2, LT3 = 2.5, LT4 = 2.8

: UAS Him @ 29 : LT1 = 2.95, LT2 = 2.82, LT3 = 2.95, LT4 = 3

	Average Number of LT muscles lost (A2-A4) per embryo			
Cross	**LT1**	**LT2**	**LT3**	**LT4**
UAS Him x *Mef2 Gal4* (29°C)	2.95	2.82	2.95	3
UAS Him x *Mef2 Gal4* (21°C)	1.63	2.2	2.5	2.8

Table 5.2.3 Average number of LT muscles missing A2-A4 per embryo for UAS Him at 29°C and 21°C.

Table to show the variation in the average number of LT muscles missing in abdominal hemi-segments A2, A3 and A4 for embryos over-expressing Him when driven by Mef2 Gal4 at either 29°C or 21 °C. In the cases of all of these individual LT muscles they are missing at least once in every embryo scored (Table 5.2.2). As each individual muscle occurs once in an hemi-segment in wild type embryos the maximum number of muscles that can be missing in hemi-segments A2-A4 is 3. So, for example, LT4 in UAS Him at 29°C is missing in every hemi-segment scored in every embryo scored.

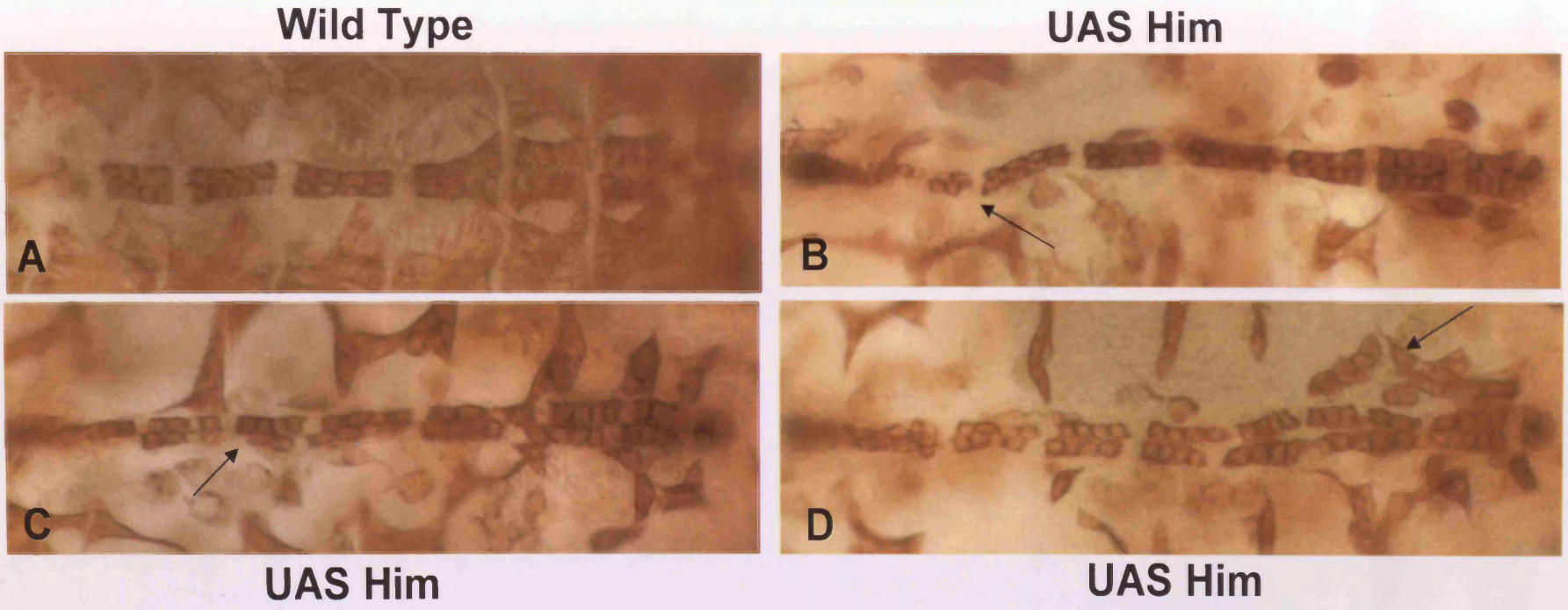

FIG 5.2.3 Over expression of Him has mild effects on β3-tubulin expression in the heart.

In wild type embryos, the St17 heart is a linear tube of two rows of cardioblasts surrounded by pericardial cells. β3-tubulin is expressed in a repeating pattern of four out of six cardioblasts per heart hemi-segment (wild type A). When Him is over-expressed in the embryo using Mef2 Gal4, only mild defects are seen in the heart when visualised using anti-β3-tubulin antibody. Generally the heart appears wild type, though occasionally the heart tube may show a kink in its structure (arrow, B), a β3-tubulin positive cardioblast may not form (arrow, C) or a number of additional cardioblast-like cells form outside of the vessel (arrow, D).

Heart images are from St17 embryos viewed dorsally and stained with anti β3-tubulin antibody. Wild type is Oregon R and UAS Him J7 was driven by Mef2 Gal4. All embryos were at 29°C.

the cardioblasts. These embryos show a severe disruption to MHC expression in the cardioblasts although the cells themselves were present (Liotta, PhD thesis 2006). These results are consistent with the phenotype associated with Mef2 mutants, where the cardioblasts of the heart are able to form and can express β3-tubulin, but do not express MHC (Ranganayakulu et al, 1995; Damm et al, 1998).

There are a number of points of interest from these results; it should be remembered that wild type expression of Him occurs in the pericardial cells not the cardioblasts of the heart, and so any over-expression of Him in the cardioblasts is ectopic. Mef2 however is expressed in the cardioblasts (and not the pericardial cells) so with respect to β3-tubulin expression in the cardioblasts either Him has no effect upon Mef2 when driven in these cells or more likely, Mef2 itself has no effect upon β3-tubulin expression in the cardioblasts. The fact that β3-tubulin expression occurs in the cardioblasts of Mef2 mutants makes this first scenario unlikely.

5.3 Discussion

My analysis of UAS Him over-expression with Mef2 Gal4 involved a thorough investigation of the formation of the somatic muscles and from this I was able to reveal a distinct subset of muscles more readily affected than others; again showing that certain muscles have specific requirements for Mef2 and that, as described in the dominant negative chapter, these can be High or Low Mef2 requirement muscles. As this is the same subset as those seen with the Mef2 Dominant negative and the Mef2 alleles it suggests that the phenotype associated with UAS Him is due to the action of Him solely upon Mef2 and as such means that the UAS Him line can be can be considered another component of the Drosophilist's tool kit for reducing Mef2 activity in a spatial and temporal manner.

Him Loss of Function

6. 1 Introduction

The classical way of understanding a process in developmental genetics is through the generation and characterisation of mutants. This can either be through isolation of a gene through a random mutagenic screen of the genome searching for the generation of a particular affect, or more recently, though the targeted deletion of a known gene of interest. As part of my thesis I wanted to generate mutants which were null for *Him* as a means of investigating its role in muscle differentiation. There are two main approaches available for achieving the generation of a mutant through this targeted deletion; either FRT-containing transposable element mediated trans-recombination or Homologous recombination. Both of these techniques involve the directed removal of a region of DNA that the gene of interest occupies.

For this study, I generated a null mutation of *Him* using FRT mediated trans-recombination using transposable elements.

6.2 Generation of a *Him* mutant by transposable element mediated recombination.

FIG 6.2.1 shows a transposable element insertion map for the *Him* and *Her* gene region. The shortest region between two compatible FRT containing transposable elements that could fully delete the *Him* gene was that between two Exelxis pWH elements; pBacWH f06349, upstream of *Aril* and pBacWH f04435, downstream of *Upd2.* The result of recombination between these two elements is the generation of either a deletion or a duplication of DNA approximately 98Kb long in the 17A position on the X chromosome. This region contains *Him* and five other genes, *Frq1, Andorra, Frq2, Her,* and *CG33639.*

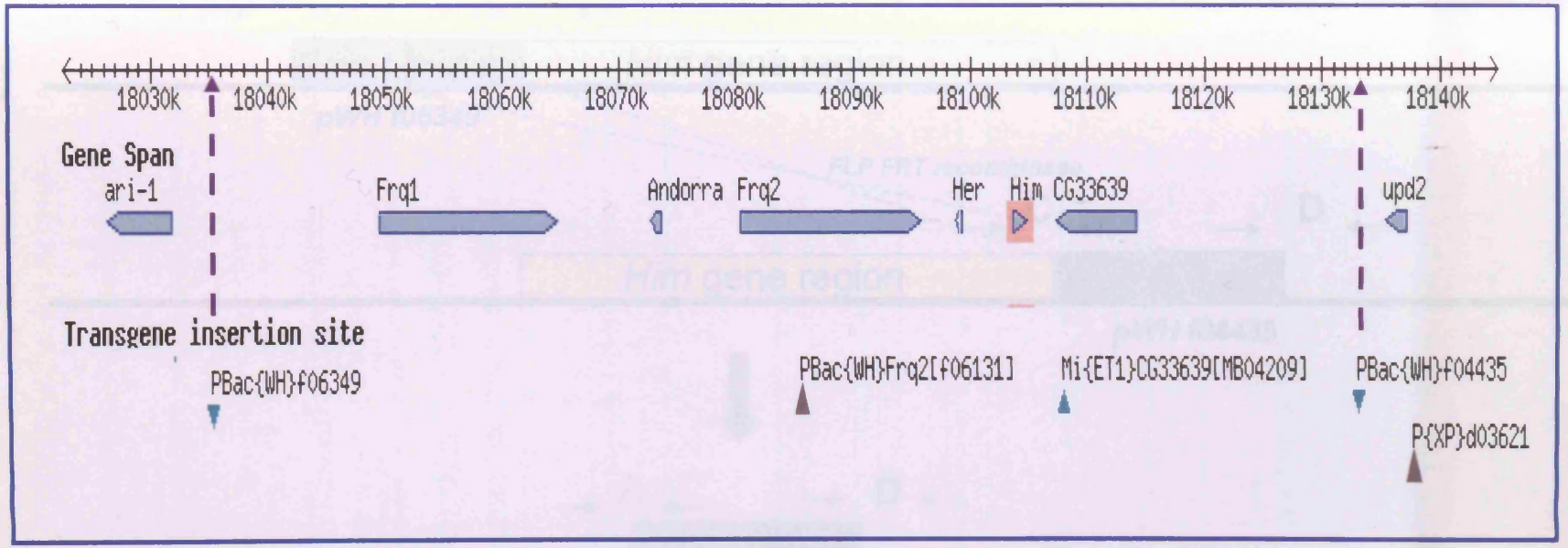

FIG 6.2.1 Transposable element mediated deficiency to *Him* gene region

GBrowse map (Flybase) of the *Him* gene region, showing the transposable element stocks available in the region. The area is a relatively "cold" spot transposable element insertion and consequently the smallest genomic fragment that can be deleted that results in a complete loss of the *Him* gene and its regulatory sequence is shown between the two purple arrows on the diagram. This corresponds to the region between the pBac WHf06349 and pBac WHf04435 elements and results in the loss of a region of DNA approximately 98Kb long which contains *Him* and five other genes; *Frq1, Andorra, Frq2, Her* and *CG33639*.

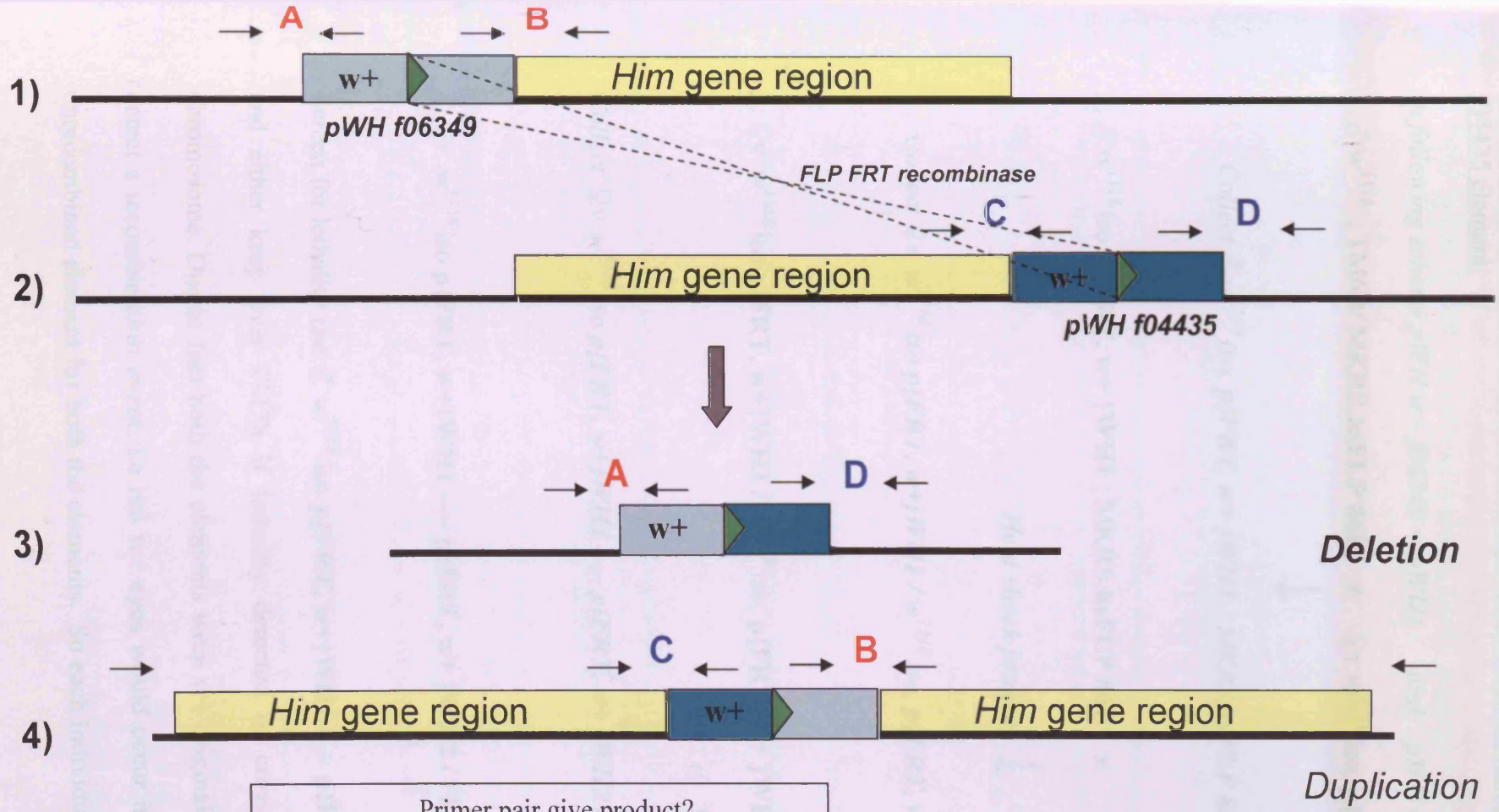

	Primer pair give product?			
Event	A	B	C	D
1) pWH 1 no rec	yes	yes	no	no
2) pWH 2 no rec	no	no	yes	yes
3) DELETION	yes	no	no	yes
4) Duplication	no*	yes	yes	no*

The DNA sequence for the two P elements is identical – they are both WH type. Different colour is to show recombination event.

**The primers for both A pair and D pair can bind but would each produce a product of >100Kb*

FIG 6.2.2 Transposable element mediated deficiency to *Him* gene region

6.2.3 *Him* region transposable element deletion

Trans-recombination between Exelixis pWH w+ f06349 element and Exelixis pWH w+ f04435 element.

In following scheme pWH w+ f06349 = pWH1 and pWH w+ f04435 = pWH2

1. ♂ w^{1118} ; TM6B/ MKRS,**hsFLP 86E** x ♀v w^{1118} iso, **p{FRT, w+ }WH1** ; 2iso ; 3iso

↓

*Collect ♂ w^{1118} iso, **p{FRT, w+ }WH1** ; MKRS,**hsFLP 86E***

2. ♂ w^{1118} iso, **p{FRT, w+ }WH1** ; MKRS,**hsFLP 86E** x ♀v w^{1118} iso **p{FRT, w+}WH2**

Heat shock progeny ↓

*Collect ♀v w^{1118} iso **p{FRT, w+}WH1** / w^{1118} iso, **p{FRT, w+ }WH2** ; MKRS,**hsFLP 86E***

3. ♀v w^{1118} iso **p{FRT, w+}WH1** / w^{1118} iso, **p{FRT, w+ }WH2** ; MKRS,**hsFLP 86E**

x ♂ FM7h iso ;2iso ;3iso

↓

*Collect ♀v w^{1118} iso **p{FRT, w+}WH1 ---- p{FRT, w+ }WH2** / FM7h iso*

4. ♀v w^{1118} iso **p{FRT, w+}WH1 ---- p{FRT, w+ }WH2** / FM7h iso

x ♂ FM7h iso ;2iso ;3iso

Screen for lethality (no ♂ w^{1118} iso **p{FRT, w+}WH1 ---- p{FRT, w+ }WH2** red eyed males) and either keep over FM7h if lethality detected or cross to homoygosity of the pWH chromosome. Due to fact both the elements were w+ originally, eye colour cannot be used to detect a recombination event. i.e red w+ eyes would occur in a duplication, a deletion or an unrecombined element for both the elements. So each individual fly must be screened by PCR.

The compatibility of the two elements for recombination is dictated by the presence and orientation of FRT sites within them. These sites are what the Flipase enzyme acts upon to mediate a trans-recombination event between the two elements (Thibault et al, 2004).

FIG 6.2.2 shows a schematic of the two possible outcomes of a successful recombination event, with either a deletion or a duplication of the region between the two elements being possible. Both of the elements are identical (pWH) and were w+ originally and because of this, eye colour cannot be used to detect a recombination event. As red w+ eyes would occur in a duplication, a deletion or an unrecombined element for both the elements (see FIG 6.2.2).

The crossing scheme to perform this recombination event is shown in FIG 6.3.2, and is taken from the original scheme as described in Parks et al, 2004. I performed the appropriate crossing scheme to induce the recombination event under heat shocked control as outlined. Because there is no associated change in eye colour with this particular recombination event, I screened for successful recombination solely by PCR; different PCR products are obtained with the same sets of primer pairs depending upon the genomic condition as shown in FIG 6.2.2. The primer sequence for these pairs is shown in the materials and methods, they consist of a primer specific to the p-element that has already been established (Thibault et al, 2004) and a genomic primer specific to the region around the element I designed to pair with this. Primers are shown in materials and methods as are primers specific to the Him region and the regions outside of the deletion area.

One line, *Him 52*, gave products for A and D but not B and C, showing that a successful recombination event had occurred. PCR product was obtained for the regions outside of the deletion area, specific to Ari1 and Upd2 but not for the Him region and an in-situ against *Him* was negative showing that the gene had been deleted FIG 6.2.4

Him mutant alleles by Homologous recombination (Zhe Han)

At the same time as this the lab of Prof.Zhe Han at the University of Michigan were generating null mutants targeting *Him* specifically using ends-out Homologous recombination, and these unpublished lines were sent to us as part of an ongoing collaboration. These lines were designed to target the Him gene specifically. Two lines were successfully generated that were mutants for Him; *Him 74* and *Him 195.*

I confirmed that these stocks were indeed mutant for Him by performing an in-situ against *Him*; if the gene region was deleted there will be no Him DNA to transcribe and hence no RNA present in the organism. This indeed was the case, as shown for the two homologous recombination lines and the transposable element mediated recombination line, where the in-situ is negative for Him in each of these stocks as shown in FIG 6.2.4.

6.3 *Him* mutant phenotype analysis

The first thing I tested with the three *Him* mutant lines was the hatching and survival rates to check for any lethality. Each of the lines were homozygous viable and fertile and on general observation the adult flies appeared healthy, normally sized and active. I aligned 200 fertilised embryos for each line on apple juice agar plates and charted their progress through development from embryo to adult as outlined in the Materials and Methods. Each of the lines show partial lethality, giving a reduced survival rate to adult flies. The lethality appears to occur mainly at the pupal stage, where the flies either die as black pupae or fail to get completely out of their pupal case, although there is some reduction in the hatching and survival rates compared to wild type for the mutant lines passing through embryogenesis and the larval stages. For example, with the *Him 52* line the hatching rate is reduced from 99% to

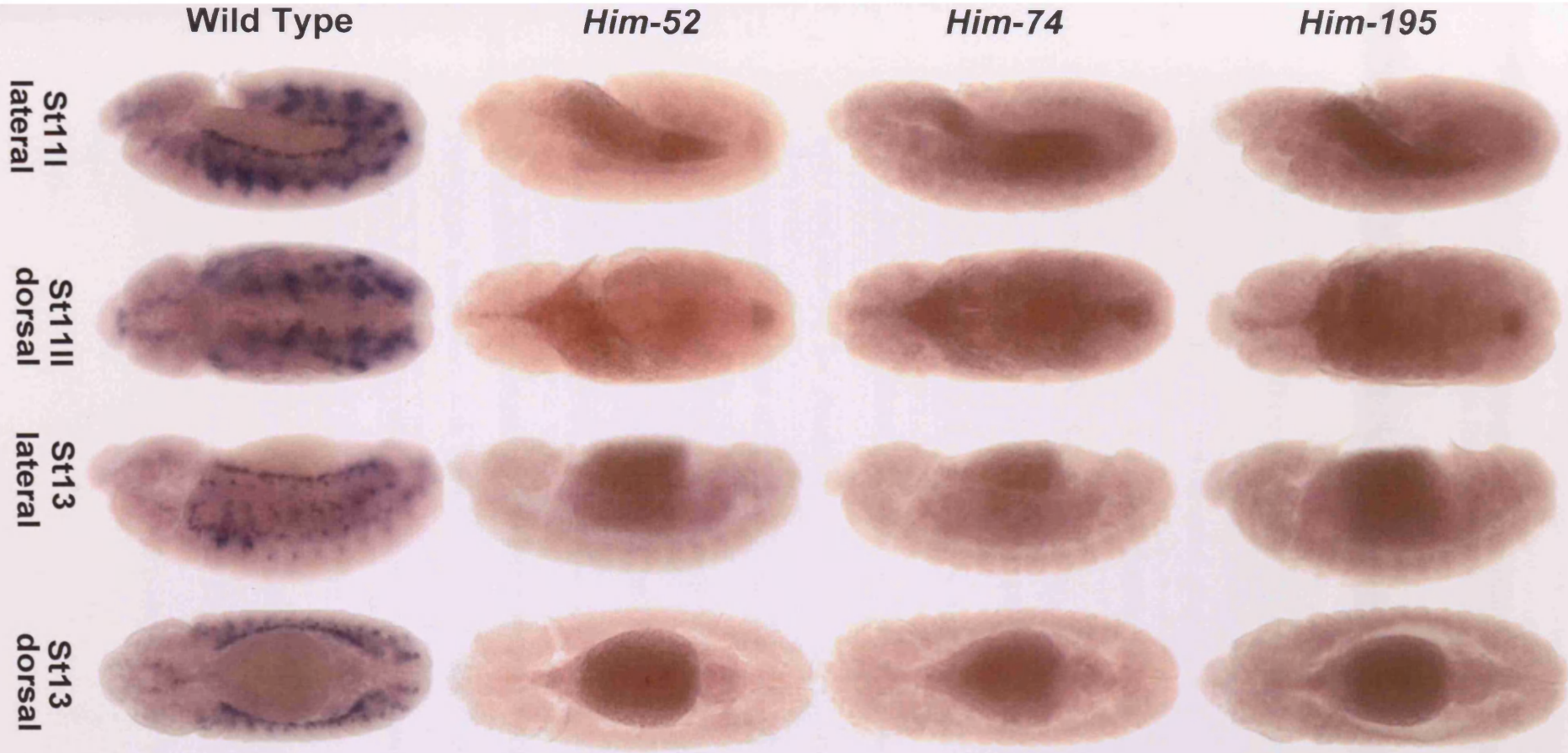

FIG 6.2.4 *Him* mutant embryos do not produce *Him* RNA transcript

In the *Him* mutant line generated by transposable element mediated recombination (*Him-52*) and the mutant lines generated by homologous recombination (*Him-74* and *Him-195*) the *Him* gene was removed. The lines show no detectable *Him* RNA transcript, confirming successful deletion of the gene. Wild Type and mutant embryos were fixed and RNA in-situ hybridisation against *Him* performed in parallel. Representative St13 and St11l embryos shown. *Him* RNA not detected in mutant lines at any stage.

95% in comparison to wild type and survival to the 3rd instar larval stage is reduced by a further 4% to 91%, whereas for wild type there is no reduction in survival to this stage (Table 6.3.5).

6.4 The embryonic phenotype of *Him* mutants.

Although the hatching and survival rates of the three *Him* mutant lines suggested that there may not be a severe phenotype in embryogenesis I still wanted to test the effect of Him loss of function on muscle differentiation.

I wanted to investigate any embryonic muscle phenotype through analysis of the final embryonic somatic musculature at St17, and as with the Him gain of function experiments described previously (Chapter 4), I did this by staining the muscles with anti β3-tubulin antibody and scoring for presence, absence, shape or attachment defects in each of the 30 individual somatic muscles of hemi-segments A2, A3 and A4 of 20 embryos. This means that a total of 1800 muscles were scored for each line and that for each individual somatic muscle 60 different examples of it were scored as part of the analysis.

On initial observation of the general somatic musculature, the Him mutants appear quite similar to Wild Type embryos, there is no massive disruption to the muscle pattern, unlike the phenotype associated with Him gain-of-function when the majority of somatic muscles are missing when Him is over-expressed in the Mef2 pattern (Compare the St17 musculature of the UAS Him and *Him 52* mutants with Wild Type in FIG 6.4.1). However, detailed investigation of the St17 musculature reveals a distinct phenotype associated with *Him* loss of function. Table 6.4.2 shows the data for the somatic muscle phenotype of the *Him* mutants; *Him 52*, *Him 74* and *Him 195* in comparison to Wild type (Oregon R) embryos.

Experiment	Embryo Hatching	Survival to 3rd Instar Larvae	Survival to black pupae	Survival to adult fly
Wild Type	99 %	99 %	98 %	98 %
Him 52	95 %	91 %	85 %	65 %
Him 74	95 %	93 %	88 %	81 %
Him 195	98 %	95 %	87 %	75 %

Table 6.3.5 *Him* mutants show partial lethality

Hatching and Survival analysis for Wild Type and *Him* mutant lines. 200 fertilised embryos were selected by gut auto-florescence, aligned on apple juice agar plates and allowed to develop at 25°C. Hatching rates were recorded and any larvae that reached the 2nd instar stage were transferred to vials at 25 °C and allowed to develop until adulthood.

The Him mutants show a reduced survival rate compared to wild type, and the lethality occurs to the greatest extent at the pupal stage. A large proportion of these, especially in the *Him 52* line fail to escape the pupal case as black pupae.

The stages of the flies life cycle are shown here in the inset FIG 2.4.5

FIG 2.4.5 Life cycle of *Drosophila melanogaster*

There are a number of defects in the final somatic muscle pattern of *Him* mutants; with embryos showing individual muscle gain or loss and shape and attachment defects in particular individual muscles. In *Him 52* mutant embryos the predominant aspect to the phenotype is the apparent duplication of muscles; at least one muscle duplication occurs in nearly all of the embryos scored in this line (19 / 20 - 95%)(Table 6.4.2). The nature and potential means of occurrence of these extra muscles is addressed later in this chapter, but initially I am describing these as duplications based solely on their appearance. They present as a second copy of an individual somatic muscle, which generally appears to have the wild type characteristics of that individual muscle type in terms of shape, position within the hemi-segment and general attachment (The attachment can only be generally wild type as there are two copies of the same muscle type in the same region and they do not attach to the exact same points). In the vast majority of cases there is no loss of other individual muscles in the region. FIG 6.4.3 shows examples of such duplications in *Him 52* mutant embryos. Embryo B in this figure shows a duplication in the dorsal muscle, DO1, the two copies appear very similar in terms of shape and position and a distinct division between them can be seen, suggesting they are two separate muscles rather than one large DO1 muscle. Embryo D shows two distinct duplications in the dorsal muscle DA1, one in hemi-segment A2 and another in hemi-segment A4. Embryo F shows distinct duplications in the lateral LT muscles, there is an additional LT1 and LT2 muscle in hemi-segment A2, meaning that there are five LT muscles in this hemi-segment instead of the usual three (LT1,2,3) that would be found in a wild type embryo. Focussing up and down with the microscope at the time of capturing this image revealed these extra LT muscles to be complete individual muscles that are separate from one another, rather than single muscles with split ends at the point of attachment that could also give the appearance of additional muscles in an image.

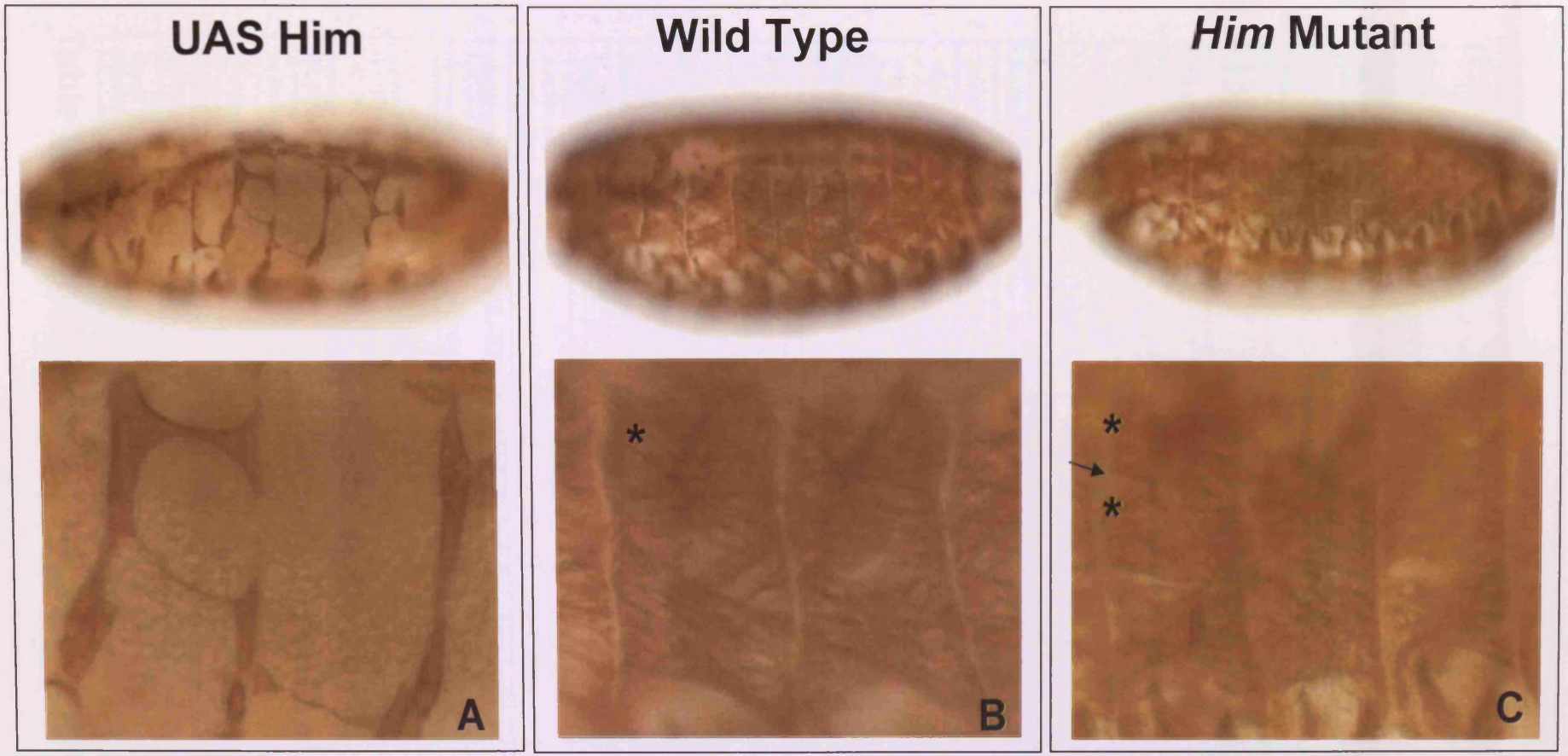

FIG 6.4.1 Him gain-of-function and Him loss-of-function give different phenotypes

Overexpression of Him causes a severe reduction in muscle formation (compare A to wild type, B), whereas *Him* mutant embryos show an opposite phenotype with a gain of muscle. In the *Him* mutant, (C) a duplication has occurred resulting in two copies of the DO1 muscle (asterisks) . There are two distinct DO1 muscles rather than one thick muscle as gap between the two can clearly be seen (arrow in C). Compare this to Wild type (B).

The Wild Type embryos in this experiment were Oregon R and the *Him* mutant was *Him52*. UAS Him was driven by Mef Gal4 at 29°C

Him 52	No. Embryo with muscles MISSING	No. Embryo with muscles DUPLICATED	No. Embryo with muscle mis-ATTACHMENT	No. Embryo with muscle SHAPE DEFECTS
No. Embryo Affected	11	19	5	20
% Embryo	55 %	95 %	25 %	100 %
Muscle total	14	44	6	228
Avg No. Muscle / Embryo Affected	1.3	2.3	1.2	11.4
Range of muscles affected	1 - 3	1 - 7	1 - 2	3 - 22

Him 74	No. Embryo with muscles MISSING	No. Embryo with muscles DUPLICATED	No. Embryo with muscle mis-ATTACHMENT	No. Embryo with muscle SHAPE DEFECTS
No. Embryo Affected	6	6	0	19
% Embryo	30 %	30 %	0 %	95 %
Muscle total	33	6	-	99
Avg No. Muscle / Embryo Affected	5.5	1	-	5.2
Range of muscles affected	1 – 14	1 - 2	-	1 - 11

Him 195	No. Embryo with muscles MISSING	No. Embryo with muscles DUPLICATED	No. Embryo with muscle mis-ATTACHMENT	No. Embryo with muscle SHAPE DEFECTS
No. Embryo Affected	8	6	4	20
% Embryo	40 %	30 %	20 %	100 %
Muscle total	16	8	18	305
Avg No. Muscle / Embryo Affected	2	1.33	4.5	15.25
Range of muscles affected	1 – 8	1 – 2	1 - 15	6 - 44

Wild Type	No. Embryo with muscles MISSING	No. Embryo with muscles DUPLICATED	No. Embryo with muscle mis-ATTACHMENT	No. Embryo with muscle SHAPE DEFECTS
No. Embryo Affected	0	1	0	15
% Embryo	0%	5 %	0 %	75%
Muscle total	0	1	0	41
Avg No. Muscle / Embryo Affected	-	1	-	2.7
Range of muscles affected	-	1	-	1 - 7

Table 6.4.2 Somatic muscle phenotype in *Him* mutants

FIG 6.4.3 Examples of somatic muscle duplication in *Him 52* mutants

St17 embryos stained with anti β3-tubulin antibody to visualise the muscles reveals frequent duplication in certain individual somatic muscles.

The dorsal muscles DO1 and DA1 and the lateral LT muscles are frequently duplicated (FIG 6.4.4), representative examples of which are shown in this FIG.

The *Him 52* embryo in image B shows a duplication in the DO1 muscle (indiciated by asterisks) in the A2 hemi-segment. Note how there is a definite division between the two DO1 muscles (arrow) and how the thickness of the two DO1 muscles is similar to each other and also the single DO1 muscles in A3 and A4 of this mutant embryo. Compare the embryo with a representative Wild Type embryo (A) which only has one DO1 muscle per hemi-segment.

In D the *Him 52* embryo shows a duplication in the DA1 muscle in hemi-segment A2 and hemi-segment A4 (arrows). Each of the duplicated DA1 muscles is distinctly

FIG 6.4.4 gives a breakdown in the form of a graph of which individual somatic muscles are duplicated or missing in the *Him* mutant embryos and the frequency of occurrence of these defects in the embryos scored. The raw data for this table is shown in Tables 6.4.3-6.4.6. There is a distinct trend as to which muscles are duplicated, this is most noticeable in the *Him 52* mutant line where the DO1, DA1, LT1 and LT2 muscles are duplicated in between 20 and 45% of the embryos. DO1 is the most frequently duplicated muscle and FIG 6.4.5 shows a breakdown of the most frequently duplicated muscles in the *Him 52* mutant. The same muscles are also duplicated in the *Him 74* and *Him 195* lines as shown in FIG 2.4.8, with DO1 again being the most frequently duplicated. Examples of some of the duplications seen in *Him 74* and *Him 195* embryos are shown in FIG 6.4.6.

The muscles that are missing in Him mutants seem to be quite varied and show less of an obvious trend than the duplicated muscles. However as can be seen in FIG 6.4.4, DA1, LT4, VO5 and VO6 are missing in all of the *Him* mutant lines. And VO6 is the most frequently lost muscle in the phenotypes associated with *Him 52, Him 195* and also *Him 74* (LT4 is lost at the same frequency as VO6 in the *Him 74* line). Of the 20 embryos scored for *Him 52,* 19 contain at least one muscle duplication and there is a range of duplications within an embryo (A2-A4) of 1-7 (Tables 6.4.3 and Table 6.4.6.). 55% of the embryos contain a duplication and also have muscles missing. However, in these embryos most of the time there are more muscles duplicated than there are missing and there seems to be no pattern between type of muscle duplicated and type of muscle missing. For example, though DO1 is the most frequently missing, there is no pattern with loss of other muscles when a duplication occurs.

This is a recurring observation for duplication of the DO1, DA1 and LT muscles; their duplication is not at the expense of the formation of another muscle. This can be seen in the

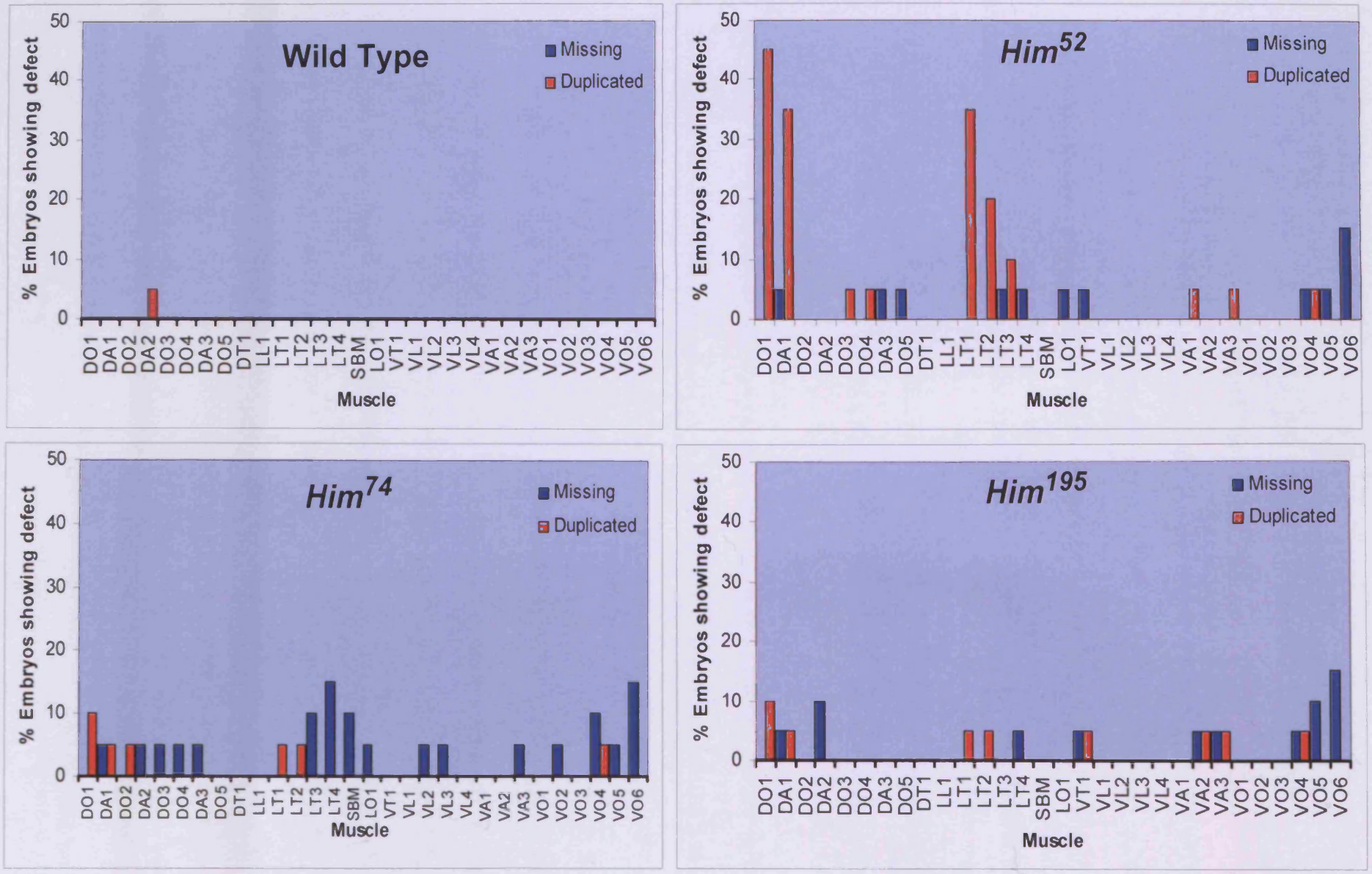

FIG 6.4.4 Somatic muscle phenotype of *Him* mutants – Muscle duplication and Muscle Loss

FIG 6.4.4 Somatic muscle phenotype of *Him* mutants – Muscle duplication and Muscle Loss

The thirty somatic muscles of abdominal hemi-segments A2, A3 and A4 were scored for 20 St17 embryos for each *Him* mutant line and Wild Type embryos at 25°C and the percentage of embryos that show either a duplication (red) or absence (blue) of an individual muscle is shown here. Only one individual muscle in an embryo (i.e one in hemi-segments A2, A3 or A4) need to be duplicated or missing for that embryo to be scored as having that defect in an individual muscle.

The Wild Type embryos in this experiment were Oregon R. In the 20 wild type embryos scored, only one embryo showed a muscle duplication and there were no examples of muscles being missing.

TABLE 6.4.3 : Muscles Duplicated and Missing : *Him 52* at 25°C

	1	2	3	4	5	6	7	8	9	10	11	12	13	14	15	16	17	18	19	20	Total	In X Embryo	Average(A2-4) In embryos affected
DO1			1		1			1		1				1	1	1	1		1		9	9	1
DA1		2		11	2	2	1	2									2				12 1	7 1	1.71 1
DO2																							
DA2																							
DO3		1																			1	1	1
DO4																				1	1		
DA3														1							1	1	1
DO5																	1				1	1	1
DT1																							
LL1																							
LT1	1				1				1			1	1					1	2		8	7	1.14
LT2												1	1					1	2		5	4	1.25
LT3					1												2		2		3 2	2 1	1.5 2
LT4					1																1	1	1
SBM																							
LO1		1																			1	1	1
VT1							1														1	1	1
VL1																							
VL2																							
VL3																							
VL4																							
VA1															1						1	1	1
VA2																							
VA3							2														2	1	2
VO1																							
VO2																							
VO3																							
VO4			2					1													2 1	1 1	2 1
VO5																		1			1	1	1
VO6			1									2	1								4	3	1.33
DUP	1	3	3	1	5	2	3	3	1	1	-	2	2	1	2	1	3	2	7	1	44	19	2.32
MISS	-	1	1	1	1	-	1	1	-	-	-	2	1	1	-	-	3	1	-	-	14	11	1.27

TABLE 6.4.4 : Muscles Duplicated and Missing : *Him 74* at 25°C

	1a	1b	1c	1d	1e	1f	2a	2b	2c	3a	3b	3c	3d	4a	4b	4c	4d	5a	5b	5c	Total	In X Embryo	Average(A2-4) In embryos affected
DO1				1													1				2	2	
DA1												1						1			1 1	1 1	
DO2	1																				1	1	
DA2																		2			2	1	
DO3																		2			2	1	
DO4													1								1	1	
DA3																		1			1	1	
DO5																					-	-	
DT1																					-	-	
LL1																					-	-	
LT1								1													1	1	
LT2								1													1	1	
LT3													1					1			2	2	
LT4													2	1				3			6	3	
SBM													3					2			5	2	
LO1																		1			1	1	
VT1																					-	-	
VL1																					-	-	
VL2													1								1	1	
VL3													1								1	1	
VL4																					-	-	
VA1																					-	-	
VA2																					-	-	
VA3													2								2	1	
VO1																					-	-	
VO2													1								1	1	
VO3																					-	-	
VO4		1											1					2			3	2	
VO5		1																			1	1	
VO6							1					1	1								3	3	
DUP	1	1	-	1	-	-	-	2	-	-	-	1	-	-	-	-	1	-	-	-	7	6	1.2
MISS	-	1	-	-	-	-	1	-	-	-	-	1	14	1	-	-	-	15	-	-	33	6	5.5

TABLE 6.4.5 : Muscles Duplicated and Missing : *Him 195* at 25°C

	1	2	3	4	5	6	7	8	9	10	11	12	13	14	15	16	17	18	19	20	Total	In X Embryo	Average(A2-4) In embryos affected
DO1				1								1									2	2	1
DA1						1														2	2 1	1 1	2 1
DO2																							
DA2	2						1														3	2	1.5
DO3																							
DO4																							
DA3																							
DO5																							
DT1																							
LL1																							
LT1																		1			1	1	1
LT2																		1			1	1	1
LT3																							
LT4																			1		1	1	1
SBM																							
LO1																							
VT1						2													1		1 2	1 1	1 2
VL1																							
VL2																							
VL3																							
VL4																							
VA1																							
VA2						1															1	1	1
VA3						1															1	1	1
VO1																							
VO2																							
VO3																							
VO4						1							1								1 1	1 1	1 1
VO5			1			2															3	2	2
VO6		1		1										1							2	2	1
DUP	-	-	-	1	-	-	-	-	-	-	-	1	1	-	-	-	-	2	1	2	8	6	1.33
MISS	2	1	1	1	-	7	1	-	-	-	-	-	-	1	-	-	-	-	1	-	16	8	2

TABLE 6.4.6

Him 52	No. Emb with Missing	No.Embryo with Dup	No. Emb Miss ONLY	No. Emb Dup ONLY	No. Emb Miss AND Dup	No. Emb Shape only	Total No. Embryo
No.Emb	11	19	0	8	11	1	20
% Emb	55 %	95 %	0 %	40 %	55 %	5 %	
Muscle total	14	44					
Avg No. Muscle / Emb	1.27	2.32					
Range	1-3	1-7					

Him 74	No. Emb with Missing	No.Embryo with Dup	No. Emb Miss ONLY	No. Emb Dup ONLY	No. Emb Miss AND Dup	No. Emb Shape only	Total No. Embryo
No.Emb	6	6	4	4	2	10	20
% Emb	30%	30%	20%	20%	10 %	50 %	
Muscle total	33	7					
Avg No. Muscle / Emb	5.5	1.2					
Range	1 - 15	1 -2					

Him 195	No. Emb with Missing	No.Embryo with Dup	No. Emb Miss ONLY	No. Emb Dup ONLY	No. Emb Miss AND Dup	No. Emb Shape only	Total No. Embryo
No.Emb	8	6	6	4	2	8	20
% Emb	40 %	30 %	30 %	20 %	10%	40%	
Muscle total	16	8					
Avg No. Muscle / Emb	2	1.33					
Range	1-8	1-2					

ONLY means that there isn't a duplication AND a missing muscle in the same embryo, there could be other defects such as shape, attachment etc.
Embryos described as Shape only have no muscles duplicated or missing but may have attachment and shape defects in individual muscles.
All scoring refers to abdominal hemi-segments A2-A4, so the maximum number of muscles missing for an individual muscle type in a single embryo is 3.

FIG 6.4.6 Examples of muscle duplications in *Him 74* and *Him 195* mutants

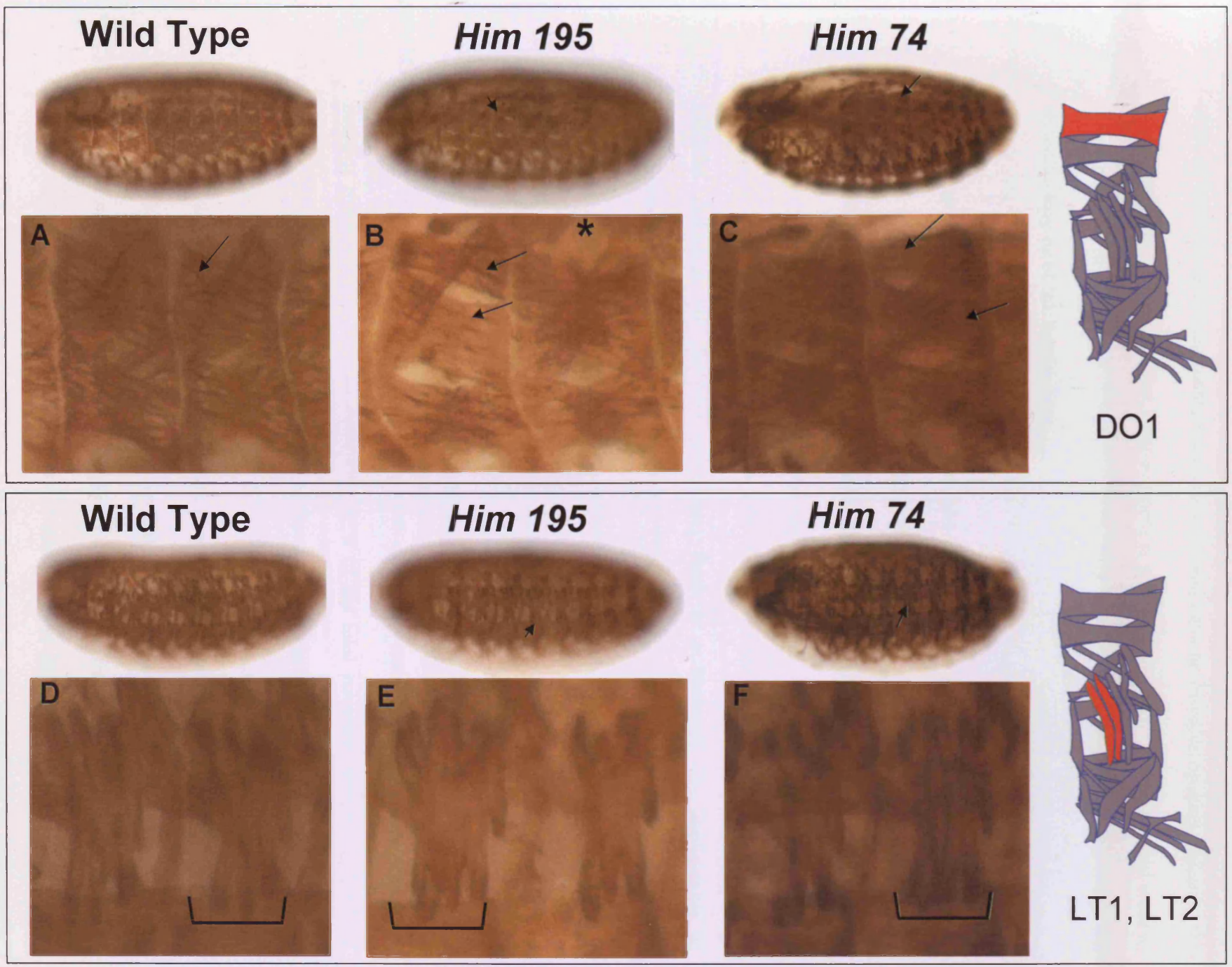

FIG 6.4.6 Examples of muscle duplications in *Him 74* and *Him 195* mutants

40% of embryos (8/20) that contain a duplication and have no muscles missing, meaning the total number of muscles for that hemi-segment is greater than 30 (with one recorded embryo containing 37 muscles in a hemi-segment!). This result is significant in considering the potential origins of the duplications.

Though similar, the phenotype for *Him 195* and *Him 74* appears less severe than that associated with *Him 52* (FIG 6.4.4 and Table 6.4.6). For *Him 195*, in 20 scored embryos 30% contained duplication and 30% had muscles missing. Only one third of each of these (i.e 2 embryos) contained both duplications and muscles missing. 20% of embryos had muscles missing without duplications and another 20% of embryos had duplications without muscles missing. Although the numbers are lower, there is a tendency for duplications to predominantly occur in DO1 DA1 and the LT's for *Him 195*. VO4-6 muscles are also missing in *Him 195* and various others including, unlike *Him 52*, DA2. (Table 6.4.5 and 6.4.6)

With *Him 74,* in the 20 embryos scored 30% contained duplications and 40% had muscles missing. As with Him 195, one third of the embryos containing duplications also have muscles missing (10% of total embryos). 20% of the total embryos contain duplications without muscles being missing and 30% of the total embryos have muscles missing without duplications also occurring (Table 6.4.6). Like *Him 195*, though the frequency of duplication is lower than *Him 52*, the main duplication occurs in the Dorsal (DO1) and lateral (LT1,2) muscles (FIG 6.4.4). The individual muscles that are missing are also similar to *Him 195* (e.g VO4-6), though there does tend to be generally a higher frequency of cases of muscles missing in *Him 74* than in the other Him mutants, this is especially so around the lateral region; LT3, LT4, SBM and LO1 (FIG 6.4.4). Inspection of the breakdown of the muscles

Duplicated Muscle	***Him-52* Mutant** (% of total duplicated muscles)
DO1	**20.5 %**
DA1	**27.3 %**
LT1	**18.2 %**
LT2	**11.4 %**
LT3	**6.8%**
Other muscles	DO3, DA3, VA1, VA3, VO4
Total No. Duplications	*44*

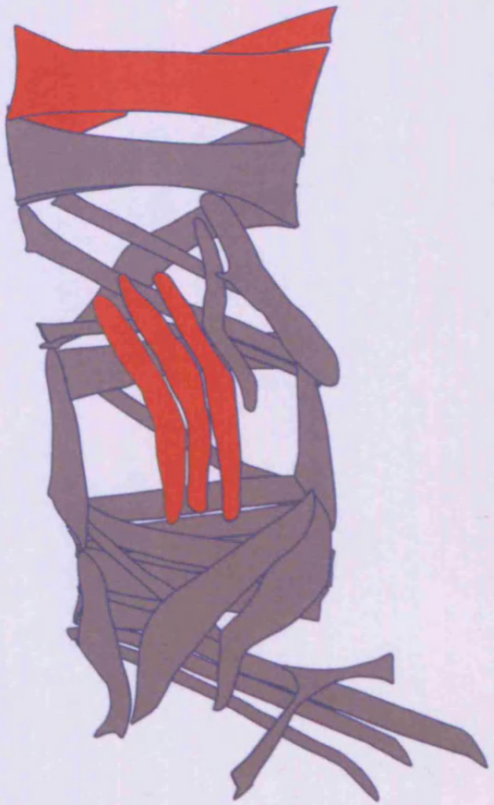

DO1, DA1, LT1/2/3

FIG 6.4.5 Frequent somatic muscle duplications in the *Him 52* mutant

FIG 6.4.6 Examples of muscle duplications in *Him 74* and *Him 195* mutants

Distinct duplications can be seen in individual somatic muscles of *Him* mutants. Shown here are representative examples of duplications in the dorsal DO1 muscle and the lateral LT1 and LT2 muscles for *Him 195* and *Him 74.*

The asterisks in B and C show duplications in the DO1 muscle of *Him195* and *Him74* respectively. Compare these to wild type (A) and the schematic highlighting the muscle in this figure.

Similarly the brackets in E and F show duplications in the LT muscles for *Him195* and *Him74* respectively compared to Wild type (F) and schematic.

The Wild Type embryos in this experiment were Oregon R. Muscles were stained with anti β3-tubulin antibody.

	No. of Embryos showing SHAPE defects (and % of Total scored)	Avg. No. of Muscles with SHAPE defects per Embryo (A2-A4)	Muscles with SHAPE defects in **75 - 100%** of Embryos	Muscles with SHAPE defects in **55 – 75 %** of Embryos	Muscles with SHAPE defects in **30 – 50 %** of Embryos	Muscles with SHAPE defects in **20- 25 %** of Embryos
Wild Type	15 (75 %)	2.7	-	-	VA3, VO4	LT1, LT2, VT1
Him 52	20 (100 %)	11.4	VA3	DO1, LT1, VA1, VA2, VO4, VO5	DO3, DO4, VT1, VO6	-
Him 74	19 (95 %)	5.5	-	LT1	LT4, VA3, VO4, VO6	DO4, VT1,VO5
Him 195	20 (100 %)	15.5	VA1, VA2, VA3, VO4	DO1, LT1, VT1, VO6	DA1, LT4, VO5	DO3, LT2, LT3

Table 6.4.7 Analysis of shape defects in the somatic muscles of *Him* mutant embryos

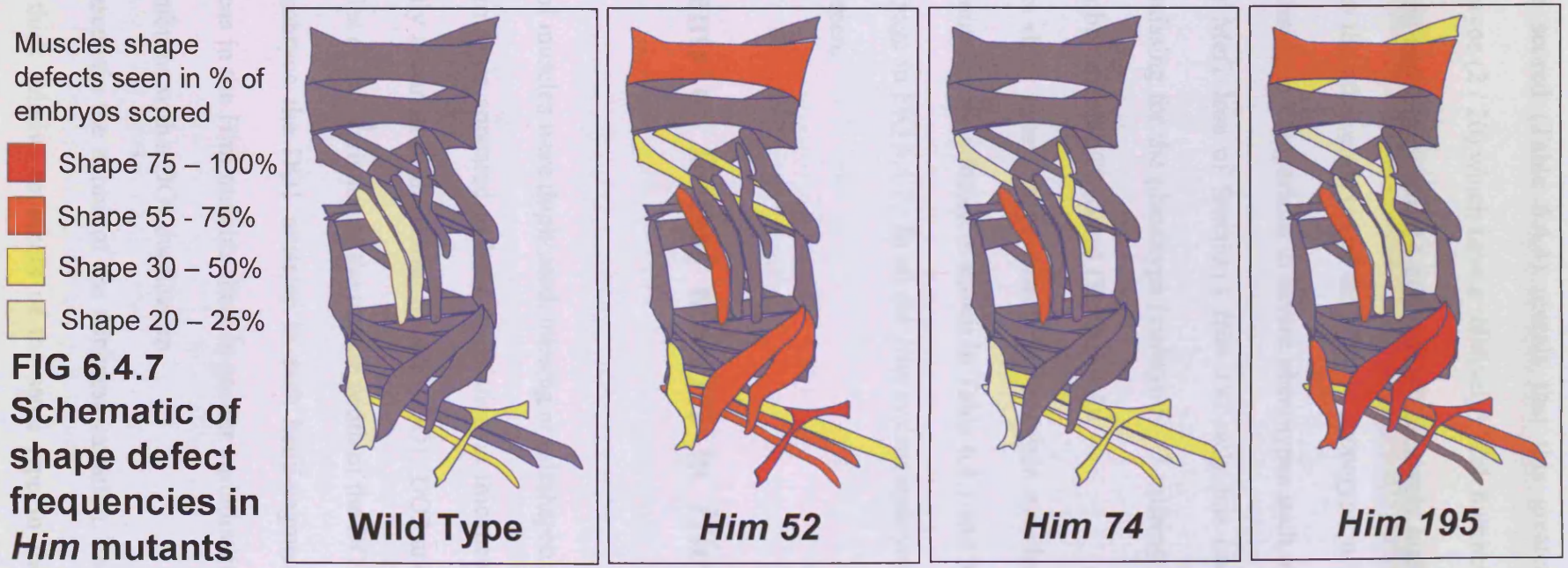

FIG 6.4.7 Schematic of shape defect frequencies in *Him* mutants

missing and in each individual embryo scored (Table 6.4.4) reveals that this greater frequency is due to a small number of embryos (2 / 20) which have a relatively* high number of muscles missing (embryo 3d, 15 missing and embryo 5a, 14 missing). (* relatively high number of muscles missing with respect to the other embryos of the *Him 74* phenotype, not for example a high number of muscles missing in comparison to severe phenotypes such as those seen with Him over-expression or Mef2 loss of function.) *Him 195* only has one embryo with a large number of muscles missing for the phenotype (embryo 6 - 7 missing ; Table 6.4.5) and *Him 52* shows no such embryos in the 20 scored (Table 6.4.4).

The majority of embryos in *Him* mutants show minor shape defects in multiple muscles (Table 6.4.2) and a breakdown of which muscles are affected is shown in Table 6.4.7 and in the corresponding schematic on the same page in FIG 6.4.7. In all the *Him* mutant embryos, the VO(4-6) muscles are frequently misshapen.

6.5 Thickness Measurements of Dorsal muscles in *Him* mutants

As well as the observation that a number of muscles were duplicated, missing or misshapen a large proportion of muscles in the Him mutants appeared to have a variation in thickness compared to wild type. This was especially apparent in the dorsal muscles, DO1, DO2 and DA1, DA2. FIG 6.5.1 shows some examples of this variation in the muscle width of the DO1 muscle in *Him* mutants. In wild type embryos the DO1 muscles in each hemi-segment appears to have a similar thickness, whereas in the Him mutants there is greater variation in width; this can be especially apparent in embryos with a DO1 duplication.

By observation alone it was difficult to ascertain the nature of the thickness variation. For example, whether a dorsal muscle was thick relative to others of the same type in the

adjacent hemi-segments, or if that muscle was normally sized but the others that are in the adjacent hemi-segments are thinner than wild type.

This difficulty is because there is a tendency to judge any variation in thickness of the muscles within an embryo rather than between embryos when scoring. Because of this I decided to measure the width of the dorsal DO1 and DO2 muscles in the Him mutants (and also in embryos over-expressing Mef2) and compare them to wild type. Measurements were taken of the thickness of the muscle at the midline of the hemi-segment at an angle parallel to the dorsal ventral axis regardless of the shape or angle of the muscle (described in FIG 6.5.2).

I measured the thickness of the DO1 and DO2 muscles in hemi-segments A2, A3, and A4 for both sides of 20 embryos for each of the Him mutant lines, Wild Type (Oregon R) and Mef2 over-expression embryos (UAS Mef2 10T4A x Mef2 Gal4 at 29°C), which meant that for each muscle type (DO1 or DO2) there were 120 separate muscle size measurements per line.

I measured each muscle and kept them scored separately for each hemisegment rather than taking an average over the three hemisegments because there is some slight variation between the sizes of the wild type muscle in a hemisegment due to variation along the A-P axis (Beckett and Baylies, 2009).

Table 6.5.1 shows the average muscle thickness and the range of muscle thicknesses for each DO1 and DO2 muscle in hemi-segments A2, A3 and A4 for wild type, the *Him* mutants and UAS Mef2 (10T4A) driven by Mef2 Gal4 at 29°C.

From this dataset it can be seen that in general *Him* mutants and UAS Mef2 show a relative decrease in average dorsal muscle thickness in comparison to wild type.

This is most noticeable when taking the average muscle thickness per muscle scored (counting the muscles in a duplication as two individual muscles). For example, with *Him 52*,

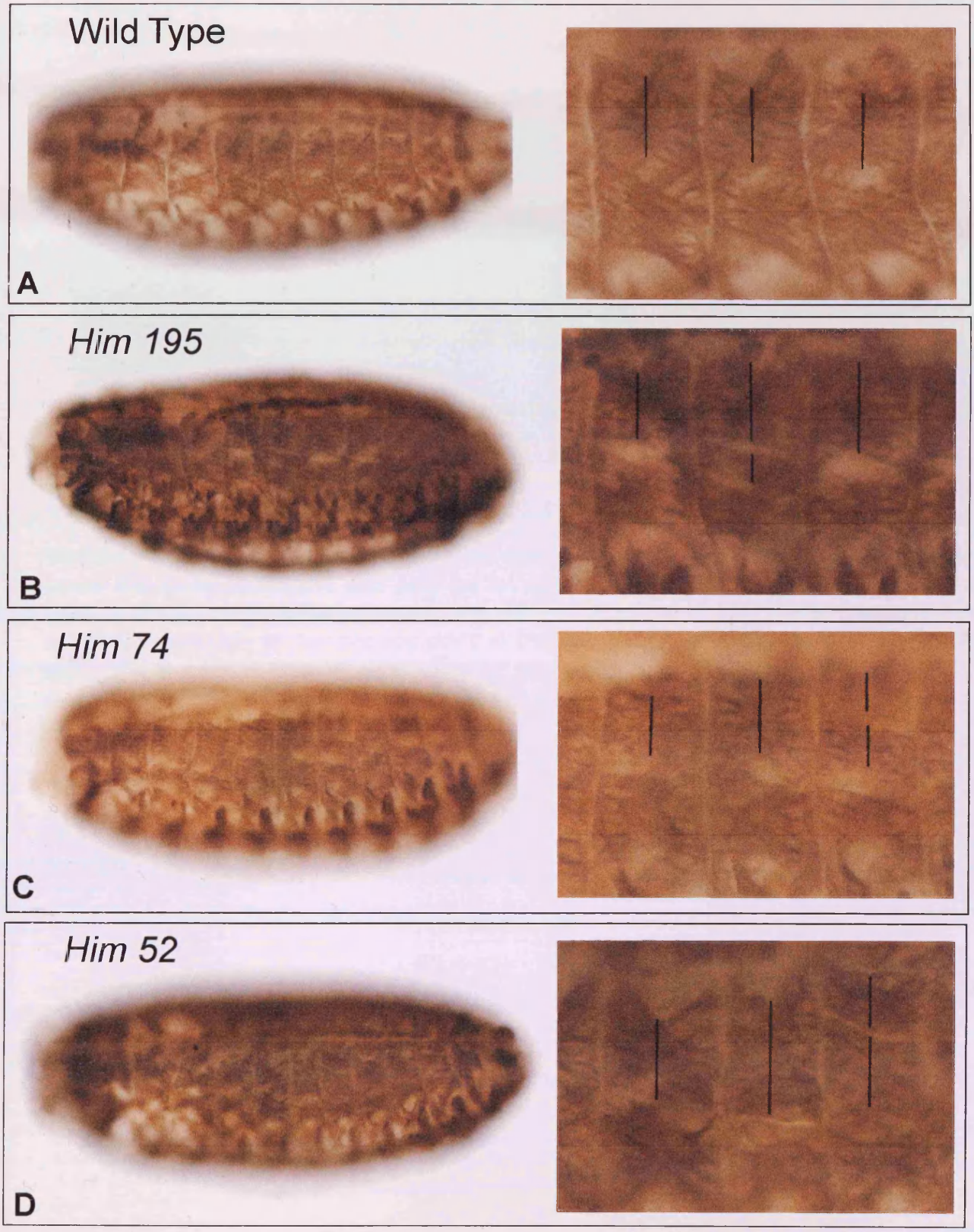

FIG 6.5.1 Dorsal muscle thickness varies in *Him* mutant embryos

the average measurement size of the DO1 muscle in A4 is 20.6μm, whereas the Wild Type average for this muscle is 25.5 μm, and in fact for each muscle scored in this line the average is lower than the wild type average. All measurements were made on screen and converted from mm to μm using a known standard graticule slide where 14mm = 10 μm.

When you instead consider the average muscle thickness per hemi-segment scored (effectively adding together the thickness of a duplicated/split muscle and treating it as one) the average size is brought closer to the wild type size for the DO1 muscles, though still lower than the wild type average in nearly all cases (in *Him 52* DO1 A2 the average comes above wt 24.3μm vs 23.6μm when considering the duplications as one).

This decrease in thickness is more pronounced for the DO2 muscles of the Him mutants and UAS Mef2 in comparison to wild type. However to some extent this observation may be related to the fact that more duplications occur in the DO1 muscles than the DO2 muscles (*Him 52* DO1 = 21 vs DO2 =3, *Him 195* DO1 = 6 vs DO2 =1 (or 2 if you don't allow the missing DO2 to cancel one out), Him 74 DO1 = 3 vs DO2 =1 and Mef2 10T4A DO1 = 6 vs DO2 =1) and that there seems to be a trend between occurrence of a DO1 duplication and reduction in DO2 size in the same segment (see below for more details).

From the measurements of the wild type muscles I got a range of thickness for each muscle (DO1 or DO2) in each hemi-segment (A2-A4) and used this range to decide whether an experimental muscle could be described as thick or thin. For example, for wild type DO1 in A2 the range of muscle thickness measured was 20.7-28.6μm. Consequently, I would define a DO1 muscle in the A2 hemi-segment as being thin if it had an onscreen measurement of 28mm (20 μm) or less and as being thick if it has an onscreen measurement of 41mm (29.3 μm) or more. I treated each muscle separately and only made comparisons between the same muscle types taken from the same hemi-segment type. For example a wild type DO1 in A3

would only be compared to a DO1 muscle in A3 in experimental embryos, not a DO1 muscle in A2 or A4. Therefore, each wild type muscle had a separate range to compare against to determine if individual muscles in the experimental embryos could be described as thick or thin.

Table 6.5.1 contains the muscle size ranges for each of the wild type DO1 and DO2 muscles and from this I was able to go through the complete collected experimental line data and assess whether an embryo contained at least one thick or thin dorsal muscle. For this I assessed the DO1 and DO2 size for A2, A3 and A4 of both sides of the embryo and compared the recorded size to the wild type range for that muscle as described above. If at least one of the muscles was below the wild type range the embryo was scored as Dorsal THIN. If at least one of the muscles was above the wild type range the embryo was scored as Dorsal THICK. If the embryo had one or more below the range and one or more above the range it was scored as Dorsal THICK and THIN and if all the muscles in the embryo fell within the wild type range then the embryo was scored as Wild Type. For this dataset only non-duplicated muscles were included in the scoring. Table 6.5.2 shows the results of this analysis. It was determined that 85% of *Him 52* embryos contained at least one thin DO muscle compared to wild type and 40% of embryos contained a thick DO compared to wild type (Table 6.5.2).

For *Him 195* 94.7% of embryos contained a thin DO muscle whereas 10.5% contained a thick muscle and for UAS Mef2 it was 65% of embryos containing a thin muscle, 25% containing a thick muscle. With *Him 74* the variation in muscle thickness is greater and less marked towards embryos having thinner muscles; 45% of embryos contain a thin muscle and 65% of embryos contain a muscle that is thicker than wild type (Table 6.5.2).

To summarise this data so far it can be said that for *Him 52, Him 195* and UAS Mef2 there is a reduction in dorsal muscle thickness, as seen by a lower average muscle thickness for DO1 and to an even greater extent, DO2 and also a high proportion of embryos that contain a thin muscle as it falls below the wild type size range. *Him 74* appears to be more similar to Wild Type in terms of muscle thickness for DO1, but not so for DO2 which, as with the other experimental conditions, has a lower muscle thickness average than wild type. Also *Him 74* is the only experimental condition that has a larger proportion of embryos with a thick muscle than a thin muscle.

In addition to simply addressing the thickness of the dorsal muscles relative to wild type for the different experimental lines, I was also able to gather data on the sizes of the two muscles within a duplication event and the effect on dorsal muscle thickness on nearby muscles when a duplication occurs. Also, as I made measurements from both sides of 20 embryos, I was able to record the frequency of dorsal duplication over 120 hemi-segments rather than 60 hemi-segments as with the standard muscle scoring dataset.

For *Him 52*, there were a total of 42 dorsal duplications (21 DO1, 3 DO2, 17 DA1 and 1 DA2), for *Him 195* a total of 11 (6 DO1, 2 DO2 and 3 DA1), for *Him 74* a total of 6 (3 DO1, 1 DO1, 2 DA1) and for UAS Mef2 a total of 8 (6 DO1, 1 DO2 and 1 DA1). Duplications in DA1 and DA2 muscles were noted at the time of recording but no measurements were made for these muscles. No dorsal duplications occurred in any of the wild type hemi-segments scored. (Table 6.5.3)

Table 6.5.4 gives a breakdown of the muscle sizes in every duplication recorded. It shows the thicknesses of the two muscles in a duplication event and their sum thickness and relates this to the average muscle size for that muscle and the muscle size range for both that

experimental line and the wild type condition. In addition it also shows the size data for the non-duplicated DO muscle in that segment to assess any affect on the size of that muscle when a duplication occurs.

The following data interpretation is based upon the *Him 52* line as this contains the largest number of duplications.

The majority of dorsal duplications are in the DO1 (and DA1) muscles and when a duplication occurs, 65% of the time one muscle is larger than the other and 35% of the time they are of a similar size. (Where similar in this case is defined as less than 5mm (3.6 μm) difference between the two).

In 74% (17/23) of cases the sum thickness of the two duplicated muscles is more than the average thickness of a single wild type muscle of the corresponding type. In nearly half of these cases (8/17) the sum is greater than the highest measurement in the wild type range for that muscle type – suggesting that if the muscles formed as a result of splitting then the original muscle that split was much larger than wild type in the first place.

There may be a correlation between occurrence of a DO1 muscle being duplicated and size of corresponding DO2 muscle in that segment. In more than half the cases (11/20) when a DO1 duplication occurs the corresponding DO2 muscle is smaller than the average for the line. In 20% they are the same size as average for the line and the remaining quarter are larger than average.

In addition, in such cases where the DO2 is smaller than average for the line, the sum muscle thickness of the two muscles in a DO1 duplications is larger than average. And it correlates that the larger the DO1 duplication muscle thickness total, the smaller the corresponding DO2 muscle (In 75% of cases when the DO1 total is larger than the maximum of the wild type range the corresponding DO2 is smaller than the average measurement for the line.) The

TABLE 6.5.1 : Dorsal muscle measurement table for Him mutants and UAS Mef2 embryos.

	DO1 Av.Size (µm) *Size Range (µm)*	DO1 # Dup *Size Range (µm)*	DO1 Av.Size (µm) *Size Range (µm)*	DO1 # Dup *Size Range (µm)*	DO1 Av.Size (µm) *Size Range (µm)*	DO1 # Dup *Size Range (µm)*	DO2 Av.Size (µm) *Size Range (µm)*	DO2 # Dup *Size Range (µm)*	DO2 Av.Size (µm) *Size Range (µm)*	DO2 # Dup *Size Range (µm)*	DO2 Av.Size (µm) *Size Range (µm)*	DO2 # Dup *Size Range (µm)*	Total # DO Dup
Line	**A2**	**A2**	**A3**	**A3**	**A4**	**A4**	**A2**	**A2**	**A3**	**A3**	**A4**	**A4**	
Wild Type	23.5 *21-29*	0	25.4 *19-31*	0	25.5 *21-31*	0	20.5 16-25	0	19.5 *14-21*	0	18.0 *11-22*	0	0
Him 52	19.1 *7-31*	10 (23.9)	21.7 *11-32*	5 (24.4)	20.6 *7-36*	6 (23.7)	16.2 *7-2.5*	0	14.2 *7-21*	1 (14.6)	13.6 *7-32*	2 (14.3)	24
Him 195	22.4 *11-32*	1 (22.9)	21.9 *7-29*	3 (23.7)	21.9 *9-32*	2 (23.1)	14.3 *7-20*	1 (14.0)	14.4 *7-19*	-1 (14.0)	13.1 *7-21*	1 (13.4)	8
Him 74	24.0 *18-32*	1 (24.6)	25.4 *(12-33)*	1 (26.0)	24.9 *(9-33)*	1 (25.5)	18.7 *(14-26)*	1 (19.2)	18.3 *(14-22)*	-2 (17.4)	16.8 *(13-23)*	0	4
Mef2 10T4A x Mef2 Gal4 (29°c)	21.4 *4-36*	1 (21.9)	20.9 *15-28*	1 (21.4)	21.0 *9-37*	4 (23.1)	16.0 *7-20*	0	16.1 *10-21*	1 (16.5)	15.8 *10-24*	0	7

Key :

	Muscle scored (e.g DO1 or DO2)	Duplications recorded for this muscle type
Line	Segment scored (e.g A2, A3 or A4)	In this segment
	Avg muscle size (µm) – taken from all muscles scored (i.e more than 40 if duplications occurred) *Muscle size range (µm)*	No. of muscles duplicated Avg muscle size (µm) per hemi-segment (divide by number hemi-segments not number muscles i.e a duplication is effectively added together and counted as one muscle)

Measurements made from screen in mm. Embryos viewed at x 20 objective. Frame size set at 512 x 512 pixels. Frame viewed as "Fit into window" – size of window expanded to full screen except for start bar.
Using known standard graticule with this measurement method 14mm screen measurement = 0.01mm real size (10µm)

Table 6.5.2 Dorsal muscle thickness measurements – percentage of embryos showing thick or thin muscles relative to wild type.

Line	Dorsal THIN	Dorsal THICK	Dorsal THICK + THIN	Dorsal WT
Him 52	50% (10 / 20)	5 % (1/20)	35 % (7/20)	10% (2/20)
Him 195	84.2% (16/19)	-	10.5% (2/19)	5.3% (1/19)
Him 74	20% (4 / 20)	40% (8 / 20)	25% (5 / 20)	15% (3 /20)
UAS Mef2 10T4A	50% (10/20)	10% (2/20)	15% (3/20)	25% (5/20)

For this table the Wild Type (WT) range for each muscle DO1 and DO2 in A2 A3 and A4 was used as standard (see Wild Type ranges in table 2.4.12). If a measured muscle in the line is less than the corresponding range for that type and segment it is defined as THIN, greater than the Wild type range and defined as THICK.
An embryo only needs to contain one muscle out of range in any segment on either side to be described as containing a DO thick or thin muscle. If it contains a thin and a thick muscle it is described as dorsal THICK + THIN. If it contains all muscles in range it is described as dorsal wt.
Duplications are disregarded for measurements – eg. only single muscles are included, so if a duplication occurred which consists of a narrow and a broad muscle this is not counted as a THIN and THICK muscle for this table.

Table 6.5.3 – Number of Dorsal Duplications in Him mutant and UAS Mef2 embryos

Line	DO1 Duplications	DO2 Duplications	DA1 Duplications	DA2 Duplications	Total Dorsal Duplications
Him 52	21	3	17	1	42
Him 195	6	2	3	-	11
Him 74	3	1	2	-	6
UAS Mef2	6	1	1	-	8
Wild Type	-	-	-	-	0

For each experiment the number of recorded muscle duplications for the dorsal muscles DO1, DO2, DA1 and DA2 are presented here. Measurements were only made for the DO muscles (see other Tables), no measurements were made for the DA muscles but any duplications in these muscles were noted at the time of recording.

Table 6.5.4 Muscle Duplications data – Muscle sizes when duplication occurs (sizes in mm from original on-screen measurements).

Line	Dup'd Muscle Type / Segmt	Muscle 1	Muscle 2	Total	Line Avg	Line Range	Wild Type Avg	Wild Type Range		Other muscle	Size	Line Avg	Line Range	Wild Type Avg	Wild Type Range
Him 52	DO1 A2	15	25	40	27	10-43	33	29-40		DO2 A2	23	23	10-35	29	22-35
Him 52	DO1 A2	28	16	44	27	10-43	33	29-40		DO2 A2	15	23	10-35	29	22-35
Him 52	DO1 A2	20	22 + 10	52	27	10-43	33	29-40		DO2 A2	15	23	10-35	29	22-35
Him 52	DO1 A2	25	10	35	27	10-43	33	29-40		DO2 A2	23	23	10-35	29	22-35
Him 52	DO1 A2	21	25	36	27	10-43	33	29-40		DO2 A2	22	23	10-35	29	22-35
Him 52	DO1 A2	30	10	40	27	10-43	33	29-40		DO2 A2	25	23	10-35	29	22-35
Him 52	DO1 A2	20	20	40	27	10-43	33	29-40		DO2 A2	20	23	10-35	29	22-35
Him 52	DO1 A2	17	20	37	27	10-43	33	29-40		DO2 A2	24	23	10-35	29	22-35
Him 52	DO1 A2	26	15	41	27	10-43	33	29-40		DO2 A2	22	23	10-35	29	22-35
Him 52	DO1 A3	20	17	37	30	16-45	36	26-43		DO2 A3	24	20	10-30	27	20-30
Him 52	DO1 A3	17	16	33	30	16-45	36	26-43		DO2 A3	20	20	10-30	27	20-30
Him 52	DO1 A3	30	13	43	30	16-45	36	26-43		DO2 A3	23	20	10-30	27	20-30
Him 52	DO1 A3	24	24	48	30	16-45	36	26-43		DO2 A3	20	20	10-30	27	20-30
Him 52	DO1 A3	22	33	55	30	16-45	36	26-43		DO2 A3	14	20	10-30	27	20-30
Him 52	DO1 A4	12	21	33	29	10-50	36	29-43		DO2 A4	20	19	10-45	25	16-31
Him 52	DO1 A4	10	20	30	29	10-50	36	29-43		DO2 A4	12 +11	19	10-45	25	16-31
Him 52	DO1 A4	23	20	43	29	10-50	36	29-43		DO2 A4	18	19	10-45	25	16-31
Him 52	DO1 A4	30	25	55	29	10-50	36	29-43		DO2 A4	15	19	10-45	25	16-31
Him 52	DO1 A4	25	20	45	29	10-50	36	29-43		DO2 A4	17	19	10-45	25	16-31
Him 52	DO1 A4	15	20	35	29	10-50	36	29-43		DO2 A4	17	19	10-45	25	16-31
Him 52	DO2 A3	15	10	25	20	10-30	27	20-30		DO1 A3	35	30	16-45	36	26-43
Him 52	DO2 A4	12	11	23	19	10-45	25	16-31		DO1 A4	10 +20	29	10-50	36	29-43
Him 52	DO2 A4	15	10	35	19	10-45	25	16-31		DO1 A4	30	29	10-50	36	29-43

Table 6.5.4 CONTINUED Muscle Duplications data – Muscle sizes when duplication occurs (sizes in mm from on screen measurements).

Line	Dup'd Muscle Type / Segmt	Muscle 1 Size (mm)	Muscle 2 Size (mm)	Total mm	Line Avg mm	Line Range mm	Wild Type Avg mm	Wild Type Range mm		Other muscle	Size mm	Line Avg mm	Line Range mm	Wild Type Avg mm	Wild Type Range mm
Him 195	DO1 A2	30	15	45	31	15-45	33	29-40		DO2 A2	20	20	10-28	29	22-35
Him 195	DO1 A3	25	10	35	31	10-41	36	26-43		DO2 A3	25	20	10-26	27	20-30
Him 195	DO1 A3	28	12	40	31	10-41	36	26-43		DO2 A3	21	20	10-26	27	20-30
Him 195	DO1 A3	30	11	41	31	10-41	36	26-43		DO2 A3	21	20	10-26	27	20-30
Him 195	DO1 A4	24	12	36	31	12-45	36	29-43		DO2 A4	15	18	10-30	25	16-31
Him 195	DO1 A4	25	20	45	31	12-45	36	29-43		DO2 A4	12	18	10-30	25	16-31
Him 195	DO2 A2	10	12	22	20	10-28	29	22-35		DO1 A2	26	31	15-45	33	29-40
Him 195	DO2 A4	13	10	23	18	10-30	25	16-31		DO1 A4	34	31	12-45	36	29-43
Him 74	DO1 A2	28	29	57	34	25-45	33	29-40		DO2 A2	21	26	19-36	29	22-35
Him 74	DO1 A3	32	17	49	36	17-46	36	26-43		DO2 A3	26	26	19-31	27	20-30
Him 74	DO1 A4	13	20	33	35	13-46	36	29-43		DO2 A4	21	24	18-32	25	16-31
Him 74	DO2 A2	27	22	49	26	19-36	29	22-35		DO1 A2	25	34	25-45	33	29-40
10T4A	DO1 A2	23	5	28	30	5-50	33	29-40		DO2 A2	10	22	10-28	29	22-35
10T4A	DO1 A3	21	21	42	29	21-39	36	26-43		DO2 A3	18	23	14-30	27	20-30
10T4A	DO1 A4	26	21	47	29	13-52	36	29-43		DO2 A4	21	22	14-33	25	16-31
10T4A	DO1 A4	22	24	46	29	13-52	36	29-43		DO2 A4	18	22	14-33	25	16-31
10T4A	DO1 A4	32	13	45	29	13-52	36	29-43		DO2 A4	25	22	14-33	25	16-31
10T4A	DO1 A4	23	15	38	29	13-52	36	29-43		DO2 A4	14	22	14-33	25	16-31
10T4A	DO2 A3	15	25	40	23	14-30	27	20-30		DO1 A3	22	29	21-39	36	26-43

Table 6.5.5 Muscle Duplications data – Muscle sizes when duplication occurs.

The complete dataset for muscle measurement sizes when a duplication occurs. The first data column refers to the muscle type that got duplicated (e.g DO1 or DO2) and which hemi-segment the duplication occurred in (A2-A4). The next two columns show the size of the two muscles in the duplication event. Muscle 1 is always the most dorsal of the two muscles. The Total is the combined thickness of Muscle 1 and 2 in the duplication event. The Line Average and Line Range are the average muscle thickness and range of muscle thicknesses for this muscle type in this hemi-segment position in the experimental line in question. Wild Type Average and Wild Type Range are the average muscle thickness and range of muscle thicknesses for this muscle type in this hemi-segment position in Wild Type embryos.
The Other Muscle section refers to the muscle within the hemi-segment that did not undergo the duplication*. For example, with a duplication of DO1 in A2 the other muscle that the comparison is made against is DO2 in A2. If the duplication is in DO2 in A2 the other muscle would be DO1 in A2 etc. The size of the other muscle is in the next column and then data on the average size and size range for that experimental line and the wild type condition follows from that.

* If a duplication occurs in the DO1 and DO2 within the same hemi-segment of an embryo – (i.e there are 4 DO muscles in the region) then the duplication data is included with respect to both duplication and Size of the other muscle is recorded as two numbers.

	DO1 Size (µm)	DO1 # Dup	DO1 Size (µm)	DO1 # Dup	DO1 Size (µm)	DO1 # Dup	DO2 Size (µm)	DO2 # Dup	DO2 Size (µm)	DO2 # Dup	DO2 Size (µm)	DO2 # Dup	Total DO Dup
Line	**A2**	**A2**	**A3**	**A3**	**A4**	**A4**	**A2**	**A2**	**A3**	**A3**	**A4**	**A4**	
Wild Type	23.5 *21-29*	0	25.4 *19-31*	0	25.5 *21-31*	0	20.5 16-25	0	19.5 *14-21*	0	18.0 *11-22*	0	0
Him 52	19.1 *7-31*	10 (23.9)	21.7 *11-32*	5 (24.4)	20.6 *7-36*	6 (23.7)	16.2 *7-2.5*	0	14.2 *7-21*	1 (14.6)	13.6 *7-32*	2 (14.3)	24
Him 195	22.4 *11-32*	1 (22.9)	21.9 *7-29*	3 (23.7)	21.9 *9-32*	2 (23.1)	14.3 *7-20*	1 (14.0)	14.4 *7-19*	-1 (14.0)	13.1 *7-21*	1 (13.4)	8
Him 74	24.0 *18-32*	1 (24.6)	25.4 *(12-33)*	1 (26.0)	24.9 *(9-33)*	1 (25.5)	18.7 *(14-26)*	1 (19.2)	18.3 *(14-22)*	-2 (17.4)	16.8 *(13-23)*	0	4
Mef2 10T4A x Mef2 Gal4 (29°c)	21.4 *4-36*	1 (21.9)	20.9 *15-28*	1 (21.4)	21.0 *9-37*	4 (23.1)	16.0 *7-20*	0	16.1 *10-21*	1 (16.5)	15.8 *10-24*	0	7

effect of a DO1 duplication causing the corresponding DO2 thickness to be decreased may be part of the explanation for the greater decrease in average muscle thickness for the DO2's when compared to Wild Type than the DO1's compared to Wild Type (Table 2.4.12). However though this effect may be true for lines such as *Him 52* which has a large number of DO1 duplications it would not provide such a significant contribution in conditions that have only a relatively small number of DO1 duplications such as in *Him 74.*

The observation that a DO1 duplication may cause a reduction in DO2 thickness could suggest that there are a smaller number of myoblasts available for DO2 formation (due to the greater demand from the extra DO1 muscle / larger DO1 muscle that subsequently splits. However this hypothesis suggests either a preference for myoblasts to attract to the DO1 over the DO2 or the formation of the DO1 before the DO2 (also assuming a limited supply of fusion competent myoblasts which may unlikely be the case).

6.6 Mef2 over-expression mimics the *Him* mutant phenotype.

Because Him is an established repressor of Mef2 activity, one would expect a *Him* mutant to cause an increase in Mef2 activity (Assuming that any other potential mechanisms of Mef2 regulation are not able to compensate for the loss of Him – which because of the mildness of the phenotype may be the case). If Mef2 activity is increased in Him mutants, then over-expression of Mef2 in the embryo may be able to mimic the *Him* phenotype.

By over-expressing the weaker UAS Mef2 line, UAS Mef2 low (Gunthorpe et al, 1999 – also called UAS Mef2 10T4A) with Mef2 Gal4 I was able to show that this is the case. Somatic muscle analysis of the A2-A4 hemisegments in the usual way shows how the same muscle are affected in the same way. As with the Him 52 mutant line the phenotype predominantly

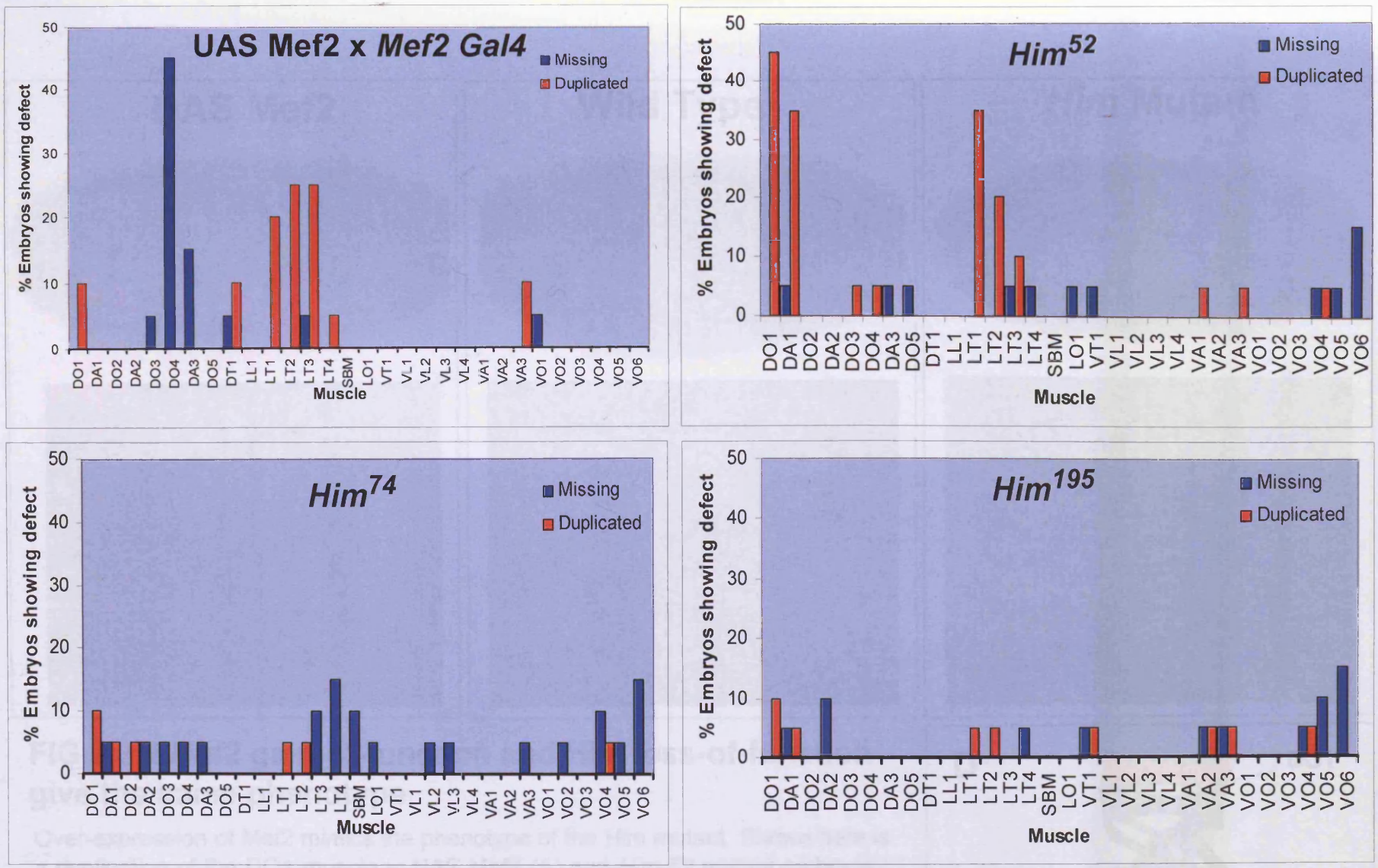

FIG 6.6.1 Somatic muscle phenotype of *Him* mutants – Muscle duplication and Muscle Loss

Graphs to show the percentage of embryos that contain at least one duplicated (red) or missing (blue) muscle in hemisegments A2-A4 for Him mutant and Mef2 overexpression lines. The thirty somatic muscles of abdominal hemi-segments A2, A3 and A4 were scored for 20 St17 embryos for each experimental condition. Only one individual muscle in an embryo (i.e one in hemi-segments A2, A3 or A4) need to be duplicated or missing for that embryo to be scored as having that defect in an individual muscle.UAS Mef2 10T4A line used x Mef2 Gal4 at 29°C.

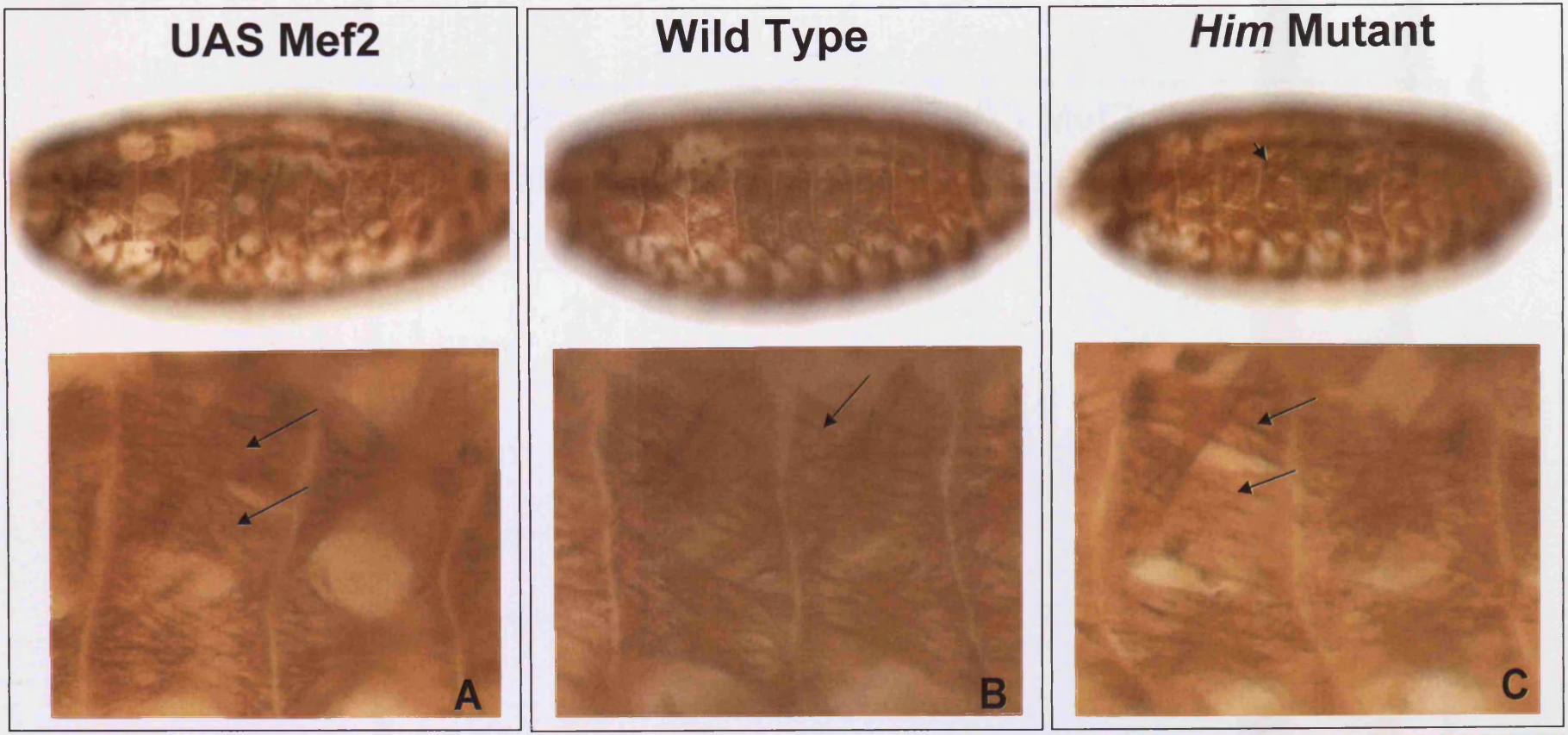

FIG 6.6.2 Mef2 gain-of-function and Him loss-of-function give the same phenotype

Over-expression of Mef2 mimics the phenotype of the Him mutant. Shown here is a duplication of the DO1 muscle in UAS Mef2 (A) and *Him 52* mutant embryos (C). With the wild type shown for comparison (B).

A schematic in D shows the position of the DO1 muscle in the wild type muscle pattern.

UAS Mef2 10T4A x Mef2 Gal4 at 29°C, *Him 52*, and Wild Type (Oregon R) embryos stained with anti β3-tubulin to visualise muscles.

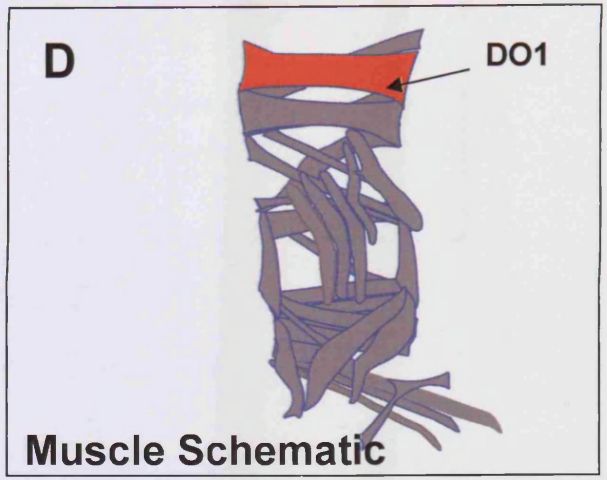

Duplicated Muscle	***Him-52* Mutant** (% of total duplicated muscles)	**UAS Mef2 x *Mef2 Gal4*** (% of total duplicated muscles)
DO1	**20.5 %**	**8.3 %**
DA1	**27.3 %**	**-**
LT1	**18.2 %**	**20.8 %**
LT2	**11.4 %**	**29.2 %**
LT3	**6.8%**	**20.8 %**
Other muscles	DO3, DA3, VA1, VA3, VO4	DT1, LT4, VA3
Total No. Duplications	*44*	*24*

Table 6.6.1 Muscles Duplicated in Him mutant and UAS Mef2

Muscle scored A2-A4 for 20 embryos. UAS Mef2 low driven by Mef2 Gal4 at 29°C.

involves a duplication of muscles and these muscles are the same subset ; DO1, LT1, LT2 and LT3. With VA3 also being duplicated as well – the significance of which is discussed in the next chapter.

FIG 6.6.2 shows an example of UAS Mef2 mimicking the *Him52* mutant with dorsal DO1 duplication and Table 6.6.1 shows a break down of the duplicated muscles.

6.7 Muscle duplication or muscle splitting?

When an additional muscle is observed its occurrence might be down to one of two possible events; the specification of an additional founder cell for this muscle type early in development or the normal formation of a muscle from one founder cell with subsequent splitting of the muscle late in development.

It has been well established that the duplication of an individual muscle can occur at the cost of the development of another muscle. This stems from a change in fate of one cell within a founder cell pair. For example, VA1 and VA2 arise from the same sibling founder cells, with one founder specifying VA1 and the other specifying VA2. In an embryo that is mutant for the transcription factor *Kruppel*, two copies of the VA1 muscle form at the expense of the VA2 muscle and alternatively embryos over-expressing Kruppel can show a duplication of the VA2 muscle with loss of the VA1 (Ruiz-Gomez et al, 1997).

Such examples of muscle fate change seem less likely in the Him mutants studied as there does not seem to be any correlation between a muscle that is duplicated and a muscle that is lost, and in fact multiple duplications can occur without any muscle loss in that embryo (Table 6.5.1-.6.5.5).

The first thing I needed to do was to determine whether the formation of an extra muscle could be described as a genuine duplication and the most obvious way to determine this was to look earlier in development before a developed (or developing) muscle would have had chance to split and give the impression of a duplication.

By considering the individual muscles that were most frequently duplicated, I was able to establish an idea of which founder cell markers would be best to investigate this.

6.8 Kruppel as a marker of the founders

In the *Him* mutants the most frequently duplicated muscles were DO1, DA1 and the LT muscles and from the established transcription factors specific to the individual somatic muscles (Baylies et al, 1998), I considered Kruppel to be the most appropriate to investigate duplication. Kruppel is expressed persistently in DO1, DA1, LT2, LT4, LL1, VL3, VO2, VA2 and VO5 (Ruiz-Gomez et al, 1997) and a comparison of its expression pattern with the most frequently duplicated muscles in the *Him* mutants is shown in FIG 6.7.1.

For founder cell analysis I decided to concentrate on *Him 52* as this line has by far the most frequent occurrence of muscle duplication (FIG 6.4.4, Table 6.5.3), and consequently any founder cell effects early in development are most likely to be seen with this line. In this line DO1 and DA1 are the most frequently duplicated and so I decided to concentrate on the founder cells associated with these muscles rather than those associated with the LT muscles. This is actually advantageous for a number of reasons; the DO1 and DA1 muscles are the easiest to follow in a Kruppel staining due to their isolated position within the embryo (consider how the other Kruppel positive muscles are grouped more closely together (FIG 6.7.1), which makes scoring the founders more difficult) and also through the combined use of an Kruppel ; Eve double staining the DO1 and DA1 founders can be determined with

Muscles most duplicated in *Him* mutants

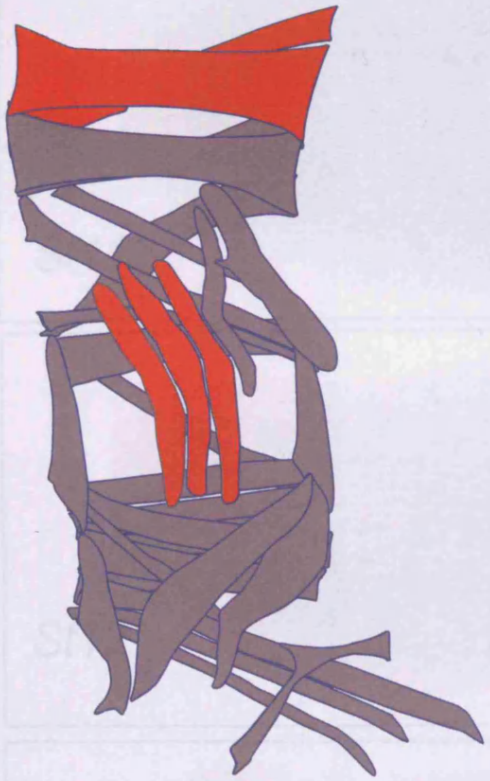

DO1, DA1, LT1/2/3

Muscles most duplicated in Mef2 over-expression

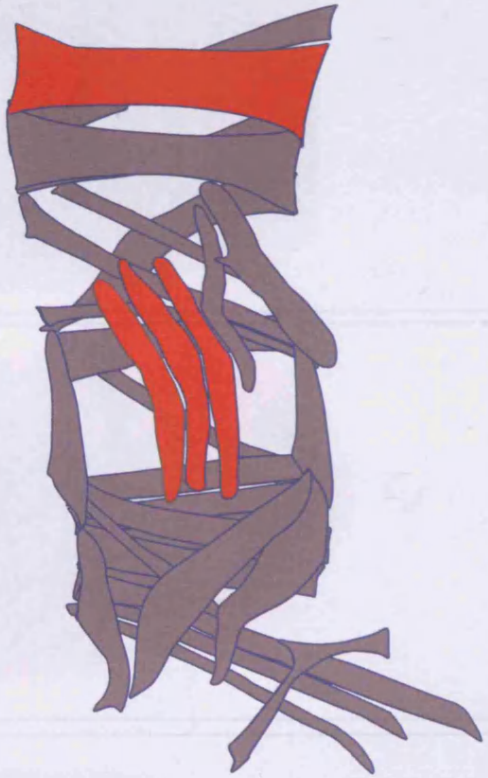

DO1, LT1/2/3

Kruppel positive founder cell derived muscles

DO1, DA1, LT2, LT4, LL1, VO2, VO5, VA2

FIG 6.7.1 Kruppel may be an indicator of duplication origin

The most frequently duplicated muscles in *Him* mutants are DO1, DA1 and the LT muscles LT1,2,3. and in UAS Mef2 embryos they are DO1 and the LT muscles .Kruppel is persistently expressed in DO1, DA1, LT2, LT4, LL1, VL3, VO2, VA2 and VO5 (Ruiz-Gomez et al, 1997) and consequently an antibody raised against this transcription factor may be a good means of investigating the number of founder cells in the muscles frequently duplicated in *Him* mutants.

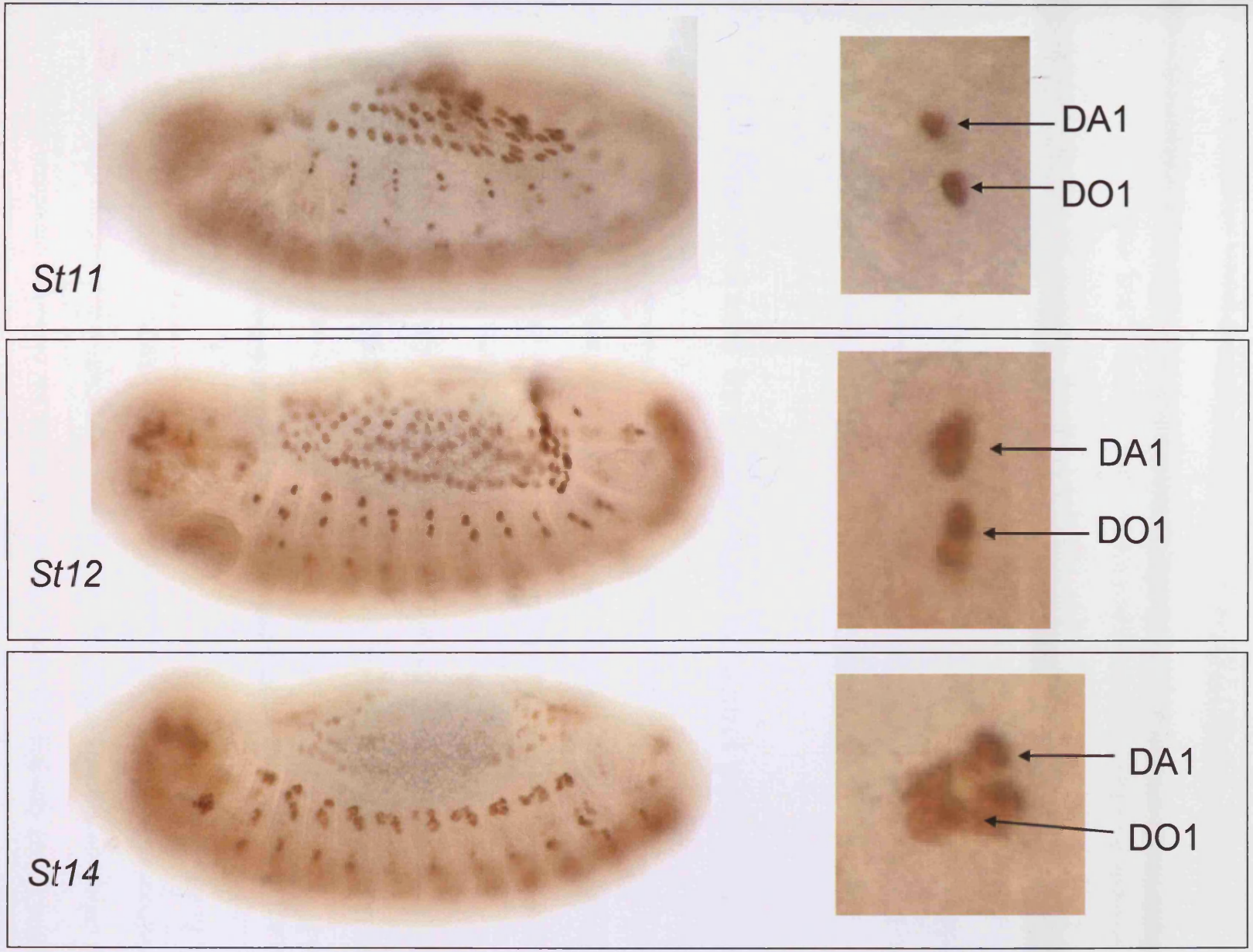

FIG 6.6.2 Wild Type DA1 and DO1 development can be traced with Kruppel antibody

certainty (Baylies et al, 1998), as has been established in multiple other studies on these muscles (Ruiz Gomez and Bate, 1997; Carmena et al, 1997; Park et al, 1998).

FIG 6.7.2 shows how a staining using anti-Kruppel antibody in wild type embryos can be used to trace the lineage of the DO1 and DA1 muscles from the time their founder cells are first specified at around St11. Originally a single founder cell expresses Kruppel and as fusion competent myoblasts fuse to this founder they too adopt expression of Kruppel, such that the number of Kruppel positive nuclei increase as the muscle develops. At St11 there are two Kruppel positive nuclei, one founder cell for DA1 and another for DO1.

6.9 *Him* Mutants have increased Kruppel positive founder cells

To investigate the occurrence of duplication in *Him 52* mutants I performed a Kruppel staining in embryos that were fixed and stained in parallel with wild type embryos. Additionally at this point I also performed this staining in parallel with embryos that were over-expressing Him in the Mef2 pattern (UAS Him x Mef2 Gal4 @ 29°C) to investigate any effect on over-expressing Him on founder cell formation as it was already established that these embryos have a reduction in muscle number, I wanted to see if this could be explained by a reduction in founder cell number in a potentially opposite way to the *Him 52* mutant phenotype. FIG 6.7.3 shows embryos from these experiments.

Though the number of Kruppel positive nuclei in a hemisegment is never completely uniform at a single timepoint throughout development (after the single founder cells stage) due to fusion competent myoblasts not fusing in synchrony, there is a distinctly greater number of Kr positive nuclei in the highlighted hemi-segment of the *Him 52* embryo shown here than in

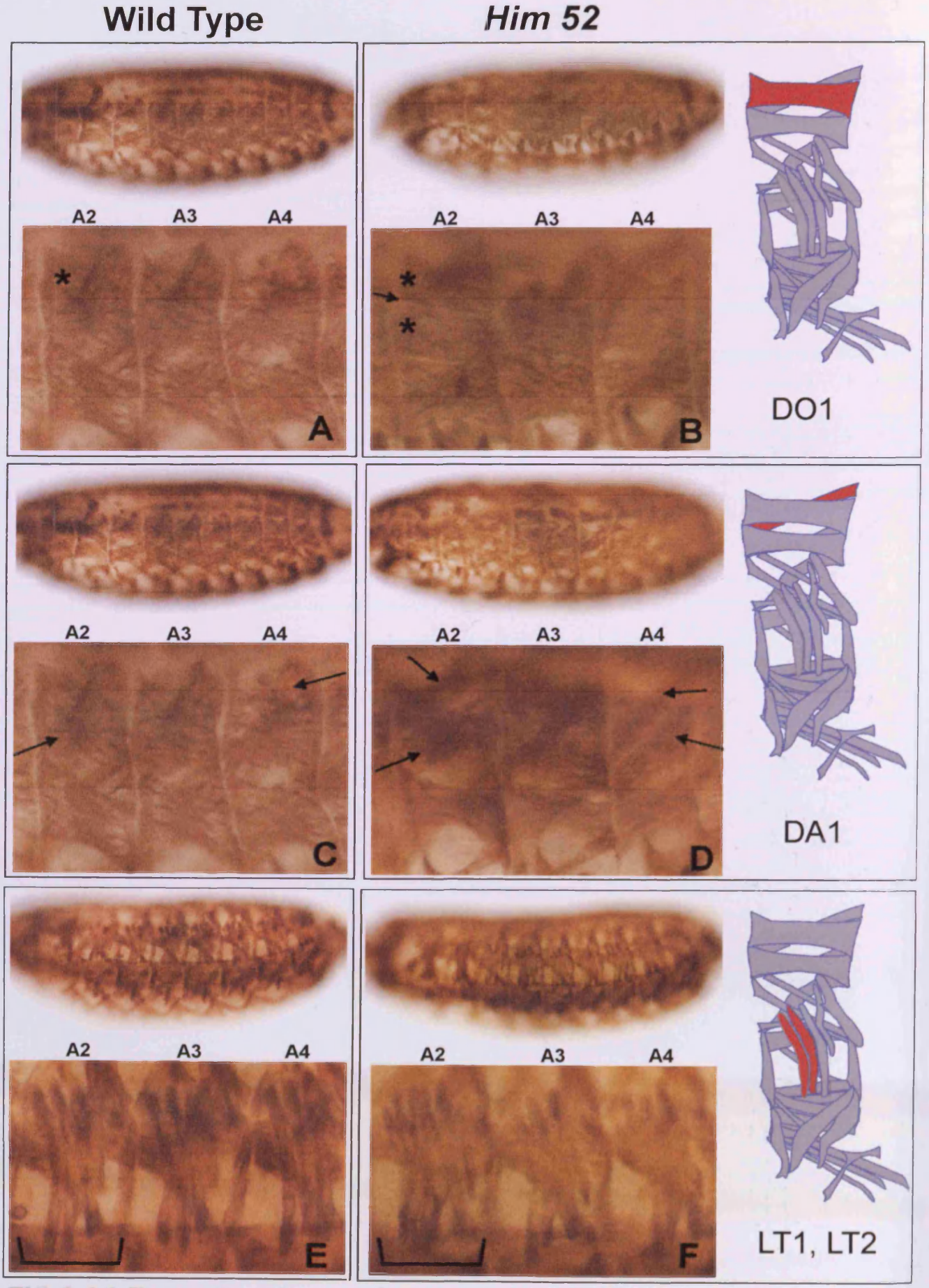

FIG 6.4.3 Examples of somatic muscle duplication in *Him 52* mutants

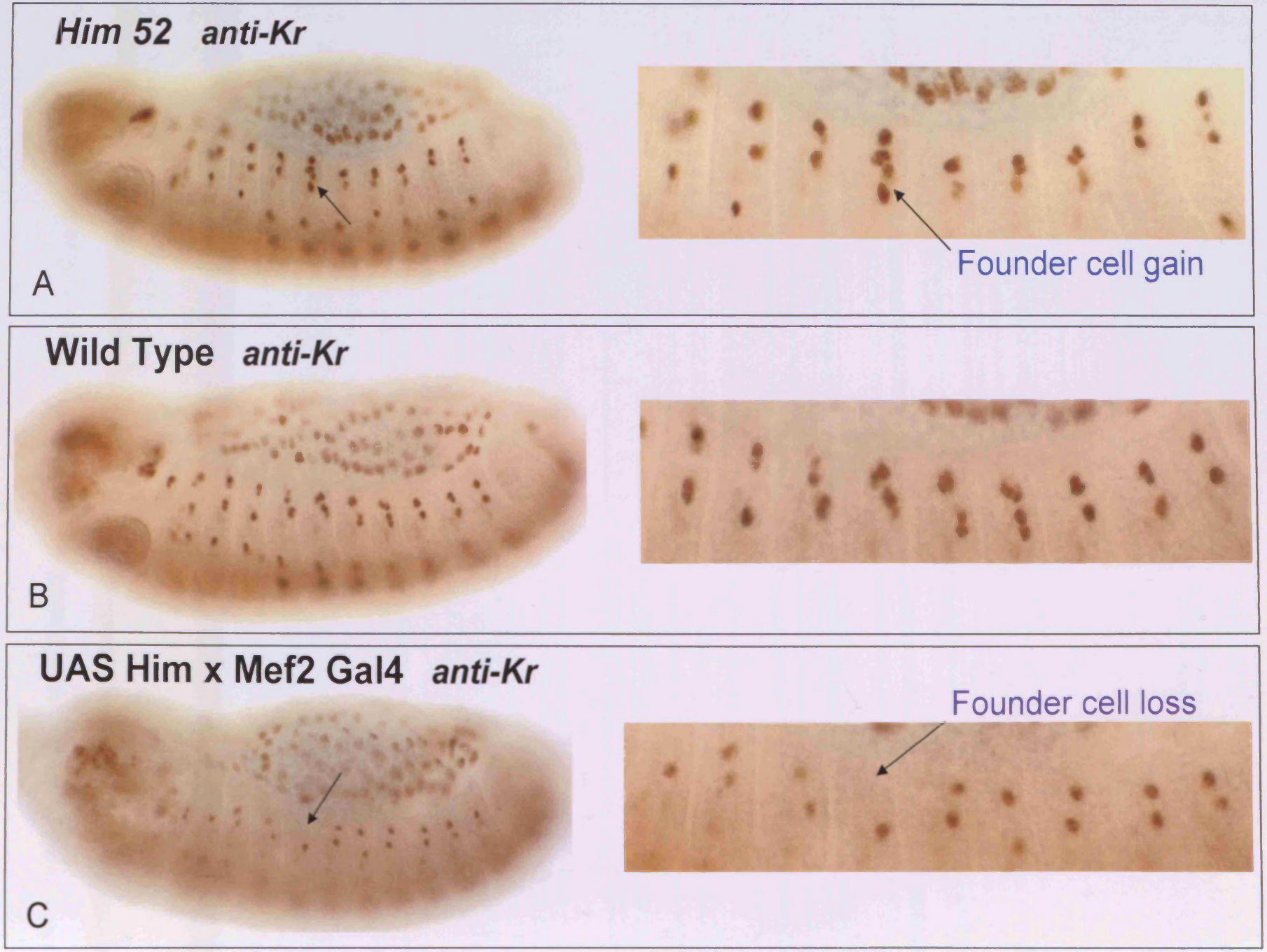

FIG 6.6.3 Him affects Kruppel positive founder cell number

FIG 6.6.3 Him affects Kruppel positive founder cell number

Him 52 mutant (A), Wild type (B) and Him over-expression (C) embryos were stained in parallel with Kruppel antibody to highlight Kruppel positive founder cells .

It reveals that Him loss of function conditions (A) cause an increase in founder cell number at St12 when compared to Wild type (B), whereas Him gain of function conditions (C) cause a decrease in founder cell number.

At least 15 embryos of the same stage for each line were found and imaged with representative images being shown here.

the other hemi-segments of the embryo; the majority of hemi-segments contain two Kr positive nuclei in the *Him 52* embryo, whereas in the hemi-segment indicated there are at least 5 Kr positive nuclei suggesting a duplication having occurred rather than just fusion occurring earlier in this hemi-segment. Compare this to the Wild Type embryo where the number of Kr positive nuclei appears fairly uniform across the hemi-segments.

In the Him over-expression embryo there is a clear reduction in founder cell number. There is only one Kr positive founder cell in some hemi-segments when there should be two or more at this stage. In addition, though the three stainings were performed in parallel the Kr staining in the UAS Him embryos appears weaker, which may suggest a general reduction in all Kr expression.

These results are significant on a number of levels; it shows that the duplications are genuine duplications that occur at the stage of founder cell specification, it gives further insight into the action of Him over-expression, and it suggests a role for Him and Mef2 early in development.

6.10 Discussion

The role of Him has previously been characterised mainly through its gain of function phenotype and is established as a repressor of Mef2 activity (Liotta et al and this study). Generation of a mutant deficient for *Him* through P-element mediated recombination as part of my study and the generation of two other targeted mutant lines by homologous recombination by the Zhe Han lab enabled the effect of complete loss of *Him* activity on somatic muscle differentiation to be investigated. Detailed analysis of the terminal somatic musculature of these mutants reveal that, though in general the musculature forms correctly, there were subtle changes to the muscle pattern; a particular subset of muscles are reliably

duplicated in *Him* mutant embryos. These were the DO1, DA1, LT1, and LT2 muscles and they were seen to be duplicated in all three of the *Him* mutant lines at various frequencies.

Whilst the loss of muscles in the terminal somatic musculature may occur for many different possible reasons, a duplication of muscle is a phenotype that is seen less frequently and often is associated with a role in patterning for a gene that caused the phenotype (Ruiz-Gomez et al, 1997). For Him then, any role in patterning would also imply a role for Mef2 on patterning and over-expression of Mef2 reveals this is likely to be the case; the Mef2 gain of function causes a duplication in these muscles too (and also VA3, see later chapter 7). The transcription factor Kruppel seemed a good candidate to investigate these duplications in the founder cells for these muscles and an initial analysis of the DO1 duplications showed that the Him mutant contained additional founder cells that would be associated with a duplication for these muscles and alternatively that over-expression of Him resulted in loss of these cells and this suggests a role for Mef2 in founder cell patterning that has not been established.

The dogma is that Mef2 is not required for initial specification of the founder cells and this comes from the observation that certain markers of the founders are still expressed and appropriately positioned in *Mef2* null mutants. Bour et al, showed this for *Eve* and *Nautilus* expression (Bour et al, 1995) and Lilly et al showed this for *Nautilus*, *Apterous* and *S59 / Slouch* (Lilly et al, 1995). However, neither paper show that all the founders are reliably formed and a number of observations have suggested that there may in fact be some role for Mef2 in this specification process. For example, a study of neuromuscular junctions that involved a detailed analysis of *Vestigial* and *Connectin* positive founders revealed that numbers of Vestigial positive nuclei are reduced in *Mef2* mutant embryos compared to Wild Type (Prokop et al, 1996).

This result with Kruppel expression in Him UAS and mutant embryos suggests that Mef2 may play some role in the patterning process, though not as the only factor otherwise there would be no Kruppel founders at all in Mef2 mutants and this is not the case. In other examples of patterning, such as that seen with Numb segregation (Ruiz Gomez et al, 1997) only a percentage of founder cells undergo a fate change suggesting other the involvement of multiple factors in a pathway.

Him and Zfh1

7.1 Introduction

Zfh1 (Zinc Finger Homeodomain 1) is a transcriptional repressor that is conserved in vertebrates and invertebrates. As its name suggests it contains a Zinc Finger domain and a homeodomain (Fortini et al, 1991). A number of key papers have identified a role for Zfh1 in somatic muscle differentiation (Lai et al, 1993; Postigo and Dean, 1997; Postigo et al, 1999). Mutants for Zfh1 are embryonic lethal and show defects in somatic muscle pattern formation (Lai et al, 1993) and over-expression of Zfh1 through a heat shock construct causes inhibition of somatic muscle differentiation (Postigo et al, 1999). Associated with this there may be a possible reduction in Mef2 expression in these embryos (Postigo et al, 1999). However, since this time research involving Zfh1 has been directed towards other aspects of its function, for example in the pericardial cells of the heart (Liu et al, 2006; Su et al, 1999, Johnson et al, 2007; Sellin et al, 2009), the gonadal mesoderm and testes (Moore et al, 1998; Broihier et al, 1998; Leatherman and Dinardo, 2008) and the nervous system (Layden et al, 2006; Lee and Lundell 2007; Volger and Urban, 2008). Though some of these papers do consider the fate of somatic dorsal muscles in conjunction with heart pericardial cells (Su et al, 1999; Johnson et al, 2007; Sellin et al, 2009) a general role for Zfh1 in somatic muscle myogenesis is not addressed.

As outlined, there is an opening in the field to investigate a role for Zfh1 in somatic muscle differentiation and in addition to this there are a number of parallels between Zfh1 and Him which make it worthy of investigation in the light of functional overlap between the two genes. Currently it is known in the literature that :

- Both Him and Zfh1 have repressor activity and have been shown previously to either clearly act upon Mef2 (Him - Liotta et al, 2007) or act upon Mef2 with some experimental uncertainty (Zfh1- Postigo et al, 1999).

- They have very similar expression patterns in the embryonic mesoderm, from the early stages of mesoderm formation through to the end of myogenesis at St17 (Fortini et al, 1991 ; Liotta et al, 2007 and Flyexpress).

- Over-expression of either gene causes a severe inhibition to muscle development (Liotta et al, 2007; Postigo et al, 1999).

With this in mind, I wanted to make a thorough comparison of the somatic muscle phenotypes associated with Him or Zfh1 gain of function and loss of function and determine if Zfh1 was capable of acting as a repressor of Mef2 function and if so, ask if there may be any functional redundancy between Him and Zfh1.

7.2 *Him* and *Zfh1* have similar expression patterns.

Him and *Zfh1* are expressed in similar patterns in developing muscle, heart and adult precursors (FIG 7.1). Earlier in embryogenesis they both show expression in the subdivided mesoderm, the precursors of the somatic muscle, precursors of the pharyngeal and the precursors of the heart, but at the point of muscle differentiation, around late St12, both transcripts show rapid down-regulation in the cells differentiating into muscle (somatic and pharyngeal), whilst remaining expressed in the undifferentiated adult muscle precursors (AMPs) and the pericardial cells of the developing heart. In addition to this co-expression

FIG 7.1 Him and Zfh1 have similar expression patterns in developing muscle.

Him and Zfh1 are both expressed in similar patterns in developing muscle. Earlier in embryogenesis they both show strong expression in the mesoderm (arrow), the precursors of the somatic muscle and the precursors of the heart, but at the point of muscle differentiation, around St12l, both transcripts show rapid down-regulation in the somatic muscle, whilst remaining expressed in the undifferentiated adult muscle precursors (A.M.P's) (arrow) and the pericardial cells of the developing heart (arrowhead). In addition to this co-expression though, Zfh1 is expressed in the nerve cord (blue arrow, out of focus), the embryonic brain, the gonads and the pharyngeal muscle, whereas Him is only expressed in the pharyngeal.

This co-expression may suggest both genes are expressed in (the same) a muscle cell to doubly ensure the appropriate regulation of Mef2; holding back its activity as a transcriptional activator until the appropriate time. As Him acts upon the Mef2 protein and Zfh1 acts upon the Mef2 RNA transcript this may suggest a "belts and braces" mechanism of Mef2 repression – whereby two different convergently evolved mechanisms exist to ensure the same result is achieved.

Embryos are wild type Oregon R. In-situ hybridisation performed using Him and Zfh1 RNA probes.

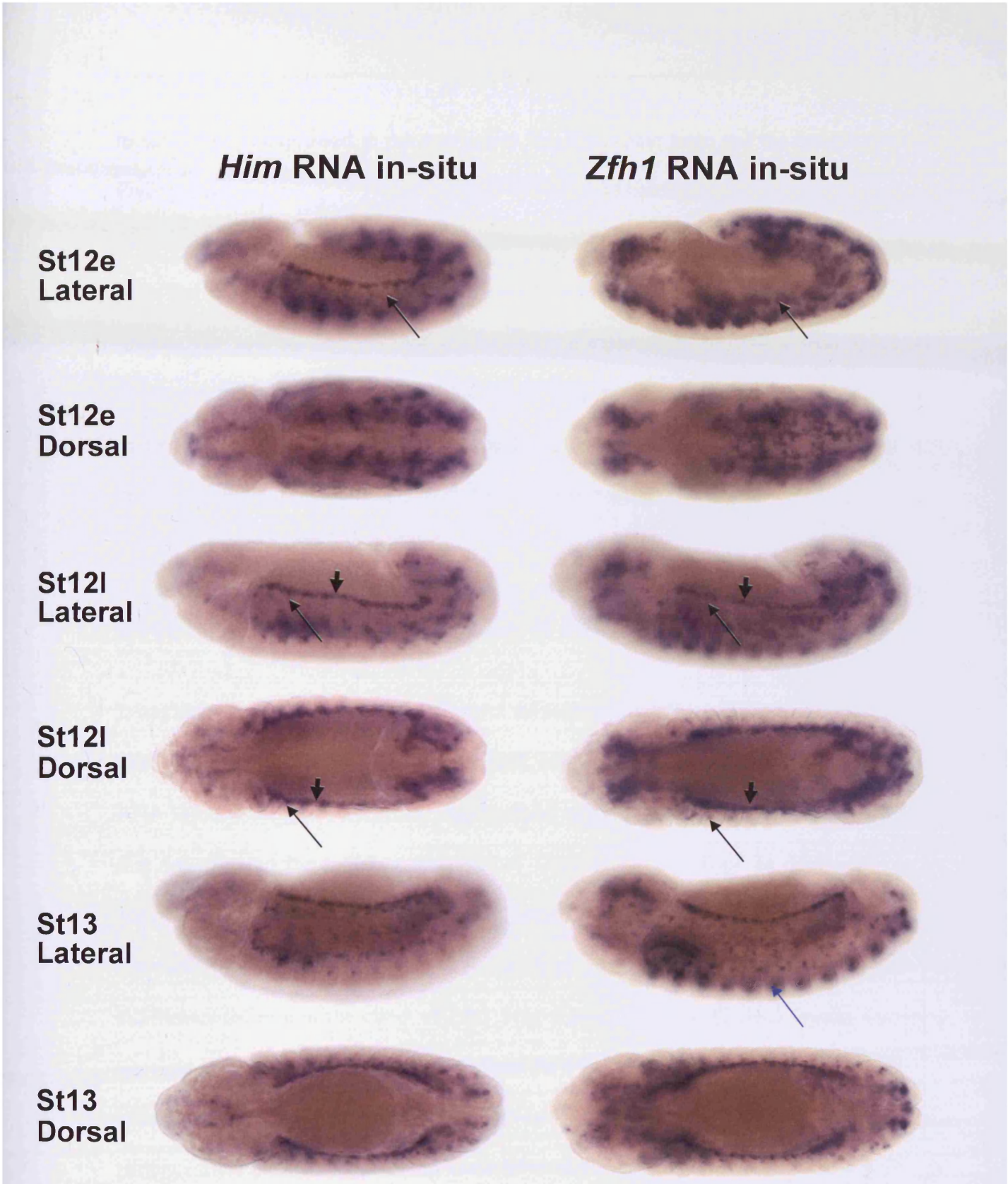

FIG 7.1 Him and Zfh1 have similar expression patterns in developing muscle.

though, Zfh1 is expressed in the nerve cord, the embryonic brain and the gonads (Flybase, FlyExpress).

This expression pattern in the developing muscle, whereby the gene is initially expressed in cells that are not yet differentiated, is rapidly lost in cells that begin to differentiate in muscle, but persists in cells that remain undifferentiated, is consistent with a potential repressor of muscle differentiation. Though, Twist, which is considered to be an activator in *Drosophila* development (Baylies and Bate, 1996) also has a pattern similar to this, being a marker of the undifferentiated AMPs (Bate et al, 1991).

7.2 Over-expression of Zfh1 reduces Mef2 RNA transcript levels, whereas over-expression of Him does not.

It was shown previously that Zfh1 binds to the regulatory regions of the Mef2 gene and that over-expression of Zfh1 through a heat shock construct causes a possible reduction in Mef2 RNA levels (Postigo et al, 1999). This method of gene over-expression is quite crude, in that not only can the inducing temperature required for the shock be detrimental to the normal development of the embryo, but also there is little control over where the over-expression occurs and at what level it occurs at. Because of this I wanted to repeat the experiment (of testing the effect of Zfh1 over-expression on Mef2 RNA levels), but using the Gal4 UAS system and at the same time do a direct comparison of over-expression of Him on Mef2 RNA levels. FIG 7.2a shows how over-expression of Zfh1 in the Mef2 pattern causes a severe reduction to Mef2 RNA transcript levels in comparison to wild type embryos of the same stage. At the driving temperature of 29°C the majority of Mef2 transcript is lost. The embryos shown are representative of the phenotype and there were some Zfh1 over-expression embryos where no Mef2 RNA was detected at all (FIG 7.2b).

FIG 7.2b UAS Zfh1 can have complete absence of Mef2 RNA transcript

An example of a UAS Zfh1 embryo, which causes a loss of all Mef2 RNA transcript. UAS Zfh1 driven with Mef2 Gal4 at 29°C.

The staining seen in the UAS Zfh1 embryo is an artefact of the in-situ hybridisation and does not represent Mef2 expression.

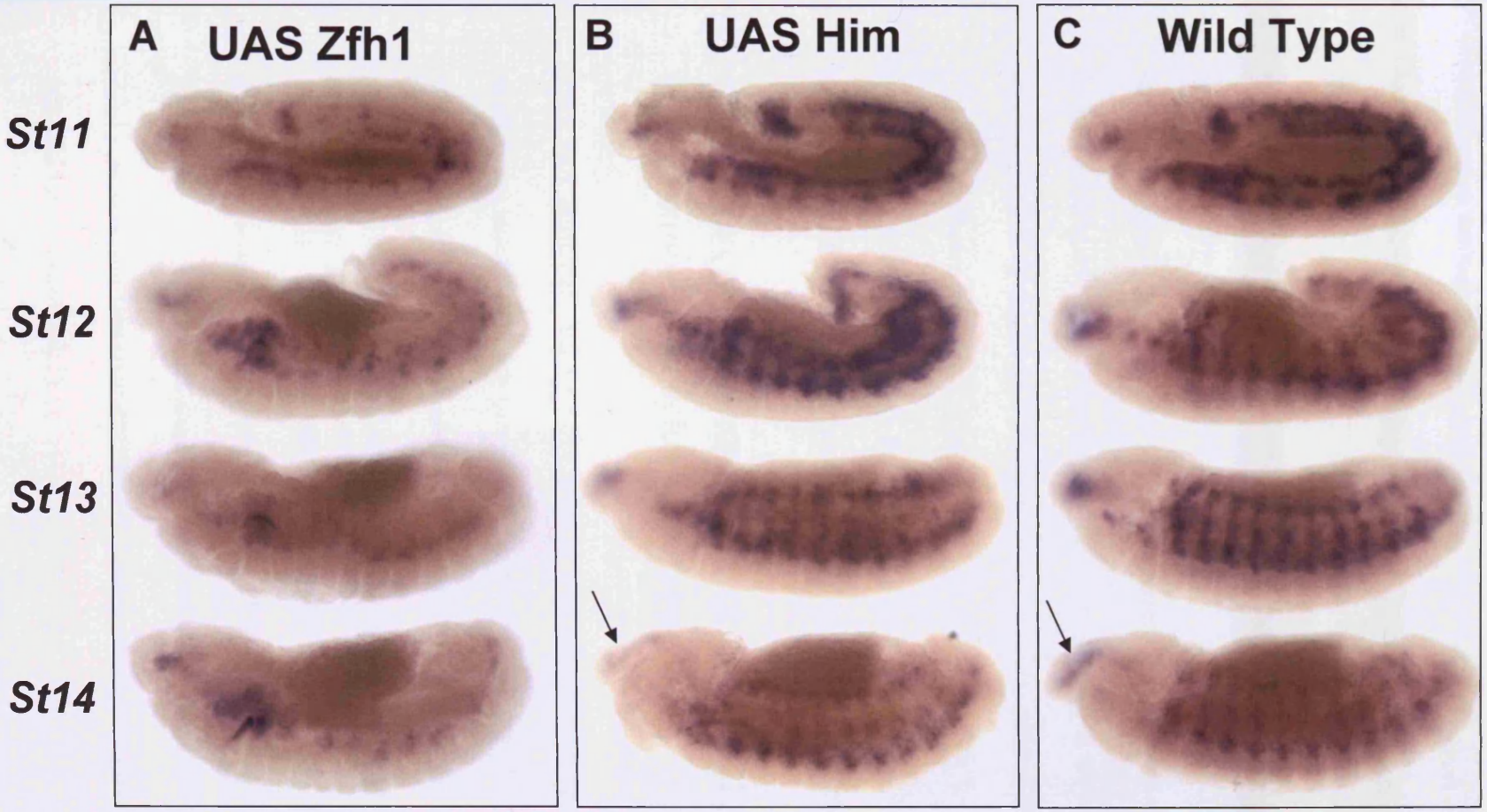

FIG 7.2a Zfh1 represses Mef2 at the RNA level, whereas Him does not.

Both Zfh1 and Him are repressors of Mef2. Zfh1 inhibits Mef2 activity at the RNA level. When over-expressed, Zfh1 causes a severe reduction in Mef2 transcript level across all stages of embryogenesis compared to wild type. This inhibition can be so severe that no Mef2 transcript is detected (FIG 7.2b) Him inhibits Mef2 activity by acting on the Mef2 protein, not the RNA, and consequently the levels of Mef2 transcript in embryos over-expressing Him are similar to those seen in wild type embryos. Later stage Him over-expression embryos do show a slight reduction in Mef2 transcript levels compared to wild type embryos of the same stage. This may be due to the effects of reducing Mef2 protein activity at the stages when Mef2 auto-regulation begins.

UAS Zfh1 and UAS Him driven by Mef2 Gal4 at 29c. Wild type is Mef2 Gal4 control at 29c. Embryos fixed and in-situ's performed in parallel. Representative embryos of 15 for each stage shown.

It was established previously that Him represses Mef2 through action upon the Mef2 protein, not through regulation of the Mef2 transcription or translation (Liotta et al, 2007). Consequently, one would expect over-expression of Him to not affect Mef2 RNA levels and this is the case (Compare B and C in FIG 7.2a). However, in some embryos it appears that Mef2 RNA levels in the later stages are reduced slightly in comparison to wild type levels (Compare St14 UAS Him embryo with St14 Wild Type FIG7.2a, arrow indicates developing pharyngeal muscle which is reduced compared to wild type). This may be due to the action of Mef2 auto-regulation (Cripps et al, 2004), whereby Mef2 protein acts upon its own regulatory region to increase expression of the gene at these stages.

This result shows that Zfh1 does indeed reduce Mef2 RNA levels, whereas Him does not, and through knowledge from previous publications, shows that Zfh1 and Him are both capable of inhibiting Mef2 activity but achieve this through alternative mechanisms.

7.3 Over-expression of Him and over-expression of Zfh1 gives similar somatic muscle phenotypes.

Zfh1 and Him can induce very similar somatic muscle defects on comparison of the phenotypes associated with their over-expression in the mesoderm.

When driven by Mef2 Gal4 at 29°C both over-expression of UAS Him or over-expression of UAS Zfh1 causes muscle loss in all embryos tested and they give a similar range and average number of muscles missing (A range of 59-72 muscles missing in UAS Him embryos (A2-A4) and a range of 47-72 muscles missing in UAS Zfh1 embryos. The average number of muscles missing is 67.1 and 59.9 for Him and Zfh1 respectively) (Table 7.3.1). In addition this over-expression causes embryonic lethality as seen in hatching and survival tests (Table 7.3.1).

Analysis of the individual somatic muscles missing also shows how similar the Him and Zfh1 over-expression phenotypes are (Table 7.3.2a).

For this analysis at 29°C, all the muscles (A2-A4) of 20 embryos were scored and the table shows the percentage of embryos that have an individual muscle type missing. Only one individual muscle from the three hemi-segments scored needs to be missing for an embryo to be scored as lacking that individual muscle type. As can be seen the majority of muscles are missing in the over-expression embryos; 24 out of the 30 muscles are missing in at least 80% of embryos for UAS Him at 29°C and 27 of the 30 muscles are missing in at least 80% of the embryos for UAS Zfh1 at 29°C (Table 7.3.2a).

Because of the severity of the phenotypes I broke down the data further to elucidate which individual muscles were the most severely affected and which, though still significantly affected, were less so in comparison. I did this in two ways, the first was to further categorise the percentage of embryos that show muscle loss; either lost in all embryos (100%), in 90-99% of embryos or 80-89% of embryos. And the second was to distinguish the individual muscles that were missing almost every time in *all three* of the hemi-segments scored per embryo. For this, I calculated the average number of muscles missing (A2-A4) in all the embryos that lacked that muscle type and defined having a muscle missing almost every time in every hemi-segment as those that were lost on average 2.8 times (A2-A4) in an embryo. For example, if a muscle type was lost in every hemi-segment in every embryo it would have an average loss of 3 (i.e missing 60 times over the 20 embryos scored), whereas if it was lost in almost every hemi-segment it would have a slightly lower average, e.g for an average of 2.8 then 56 out of a possible 60 muscles would be lost over 20 embryos scored. I highlighted the muscles that fell into this category on the Table in blue for UAS Him and red for UAS Zfh1.

Muscle phenotype	**UAS Him x *Mef2 Gal4*** (29°c)	**UAS Zfh1 x *Mef2 Gal4*** (29°c)
% embryos with muscle missing	100 %	100 %
Average No. muscles missing per embryo	67.1	59.9
Range of muscles missing per embryo	59 - 72	47 - 72

Survival assay		
Hatching	0 %	0 %
Survival	0 %	0 %

Table 7.3.1 – Muscle phenotypes in embryos over-expressing Him or Zfh1.

Over expression of Him and Zfh1 both gives a severe muscle phenotype, with the majority of somatic muscles being lost. The severity of the phenotype is similar with both genes, when driven by Mef2 Gal4 at 29°c.

Cross	Muscles Missing in 100 % Embryos	Muscles Missing in 90-99 % Embryos	Muscles Missing in 80-89% Embryos	Muscles Missing in 50 - 79% Embryos	Muscles Present in 90 – 100% Embryos
UAS Him x *Mef2 Gal4* **(29°C)**	DO2, **DO3**, **DO5**, **LL1**, **LT1**, **LT2**, **LT3**, **LT4**, **LO1**, **VL4**, **VA3**, **VO2**, **VO3**, **VO4**, **VO5**, **VO6**	**DA2**, **DA3**, SBM, **VL3**, **VA1**, **VO1**,	**DO4**, **VL2**,	DA1, **VT1**, VA2, **DO1**, **VL1**	**DT1**
UAS Zfh1 x *Mef2 Gal4* **(29°C)**	**DO3**, **DO5**, **LT1**, **LT2**, **LT3**, **LT4**, **LO1**, **VL4**, **VA1**, **VA3**, **VO1**, **VO5**, **VO6**	DA1, **DO4**, **LL1**, **VL2**, **VL3**, VA2, **VO2**, **VO3**, **VO4**	**DO1**, DO2, **DA2**, **DA3**, **VL1**	SBM, **VT1**	**DT1**

Table 7.3.2a A similar subset of muscles are missing with over-expression of Him or over-expression of Zfh1 at different temperatures.

Cross	Muscles Missing in 100 % Embryos	Muscles Missing in 90-99 % Embryos	Muscles Missing in 80-89% Embryos	Muscles Missing in 50 - 79% Embryos	Muscles Present in 90 – 100% Embryos
UAS Him x *Mef2 Gal4* **(21°C)**	DA1, DA2, **DO3**, **DO5**, **LT2**, **LT3**, **LT4**, **LO1**, VL2, **VA1**, **VA3**, VO1, **VO2**, **VO3**, **VO4**, **VO5**, **VO6**	**DO4**, DA3, SBM, **VL3**, **VL4**	**DO1**, **LT1**, VL1,	DO2, DT1, LL1, **VA2**	
UAS Zfh1 x *Mef2 Gal4* **(21°C)**	**DO3**, **DO4**, **DO5**, LL1, **LT2**, **LT3**, **LO1**, **VL3**, **VL4**, **VO3**, **VO4**, **VO5**, **VO6**	**LT4**, **VA1**, **VA3**, **VO2**	DA2,	**DO1**, DA1, DA3, **LT1**, VT1, VL2, **VA2**, VO1	DT1

Table 7.3.2b A similar subset of muscles are missing with over-expression of Him or over-expression of Zfh1 at different temperatures.

Table 7.3.2 A similar subset of muscles are missing with over-expression of Him or over-expression of Zfh1 at different temperatures.

The 30 individual somatic muscles of hemi-segments A2,A3 and A4 (a total of 90 muscles) were scored per embryo. Only one individual muscle from the three hemi-segments scored needs to be missing for an embryo to be scored as having that individual muscle type missing. Comparisons in the table are made between UAS Him and UAS Zfh1 at the same temperatures. 20 embryos for each experimental condition were scored at 29°C and 10 embryos for each experimental condition were scored at 21°C. Where a muscle is highlighted as bold and underlined in the table it is missing in the same category for both UAS Him and UAS Zfh1 at that temperature. A muscle highlighted as just bold is in the adjacent category. A muscle that is coloured (blue for UAS Him and red for UAS Zfh1) is missing in that percentage of embryos at an average frequency of 2.8 or greater per embryo scored – i.e that individual muscle was missing almost every time in each of the three hemi-segments scored per embryo.

Over-expression of Him or Zfh1 in the Mef2 pattern at either 29°C or 21°C shows a strikingly similar subset of individual somatic muscles being missing as shown by the number of muscles missing that fall into the same category for both phenotypes. In addition at 29°C and 21°C, although the phenotype of Him over expression is stronger than that of Zfh1 over-expression (as shown by the greater number of individual muscles that have an average missing frequency of 2.8 or greater in hemi-segments A2-A4 and Table 3.3.1) all of the muscles missing at this high frequency in UAS Zfh1 at 29°C (DO3, LT1, LO1, VO5, VO6) and 21°C (VO5, VO6) are missing at the same high frequency in UAS Him at that temperature, suggesting that they are a muscle type more susceptible to a decrease in Mef2 activity for both UAS Him and UAS Zfh1.

Data not shown in table : Him @ 21°C : VT1 missing 30%. Zfh1 @21°C : DO2, VL1 missing 30% . SBM missing 20%

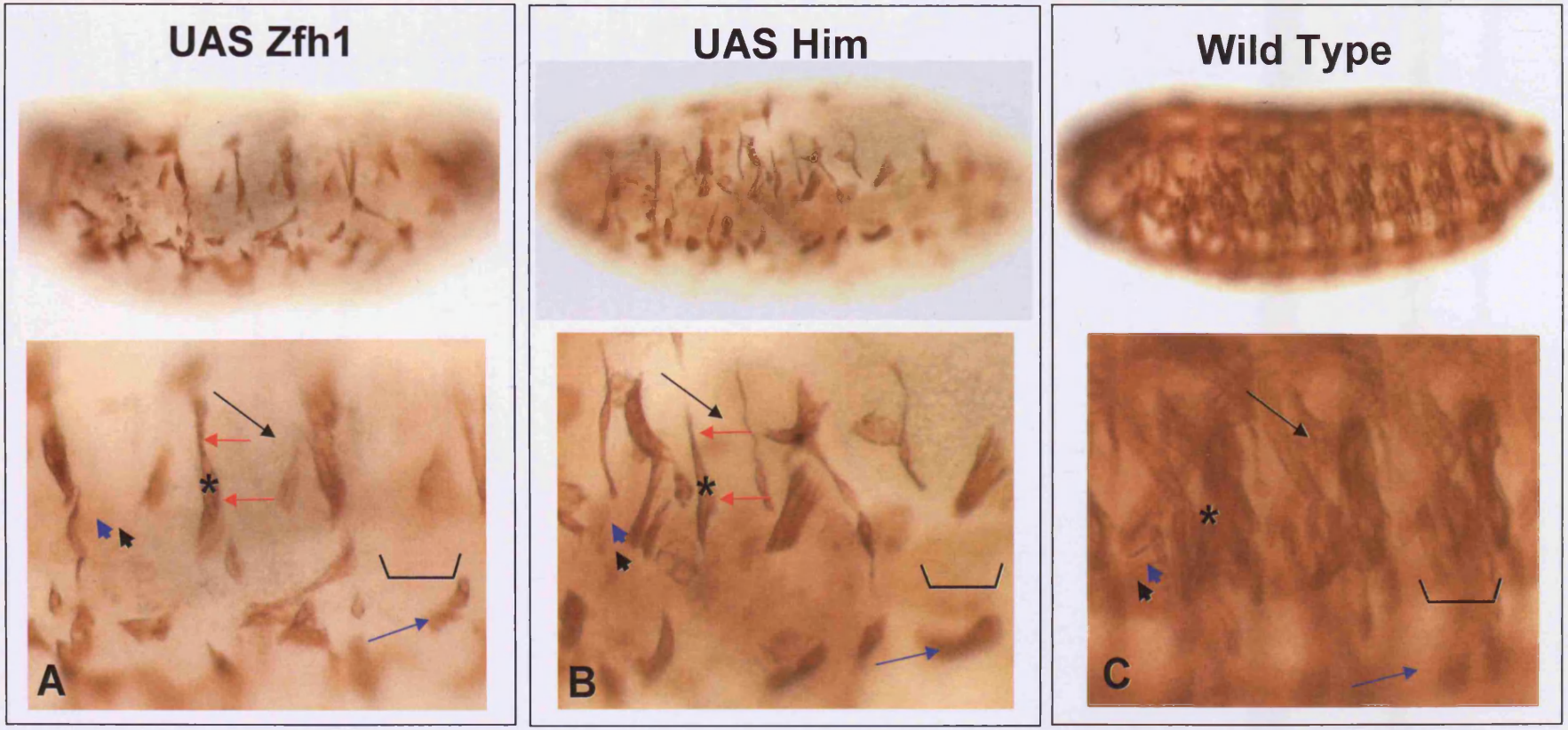

FIG 7.3.1a Over-expression of Him and Zfh1 gives similar somatic muscle phenotypes

UAS Him and UAS Zfh1 both give a similar phenotype of somatic muscle loss and disruption. A large number of muscles are absent in both UAS Him (B) and UAS Zfh1 (A) embryos compared to Wild Type, C. For example, DO3 (arrow), DO5 and LL1 (blue arrowhead and arrowhead), LT1-4 and LO1 (bracket). Similar muscles also remain present with similar defects, such as DT1 (asterisk), which is misshapen, having parts of the muscle that are thinner than others (compare red arrows in a single muscle for both A and B) whereas by comparison, wild type DT1 is a of a consistent thickness (asterisk in C). Also VL1 is similarly misattached in both UAS Zfh1 and UAS Him embryos (blue arrow in A – out of focus in B and C). A schematic of the muscles missing or affected is shown in D.*UAS constructs driven by Mef2 Gal4 at 29℃. All embryos St17 and viewed dorsally. Embryos stained with β3-tubulin. Wild type embryo is Oregon R at 29℃.*

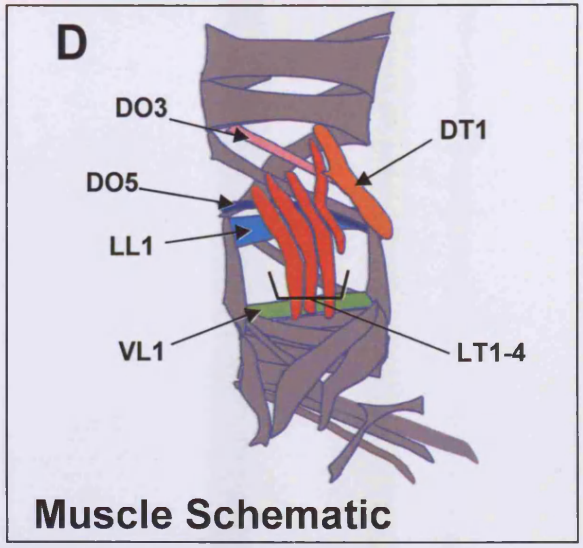

FIG 7.3.1b Over-expression of Him and Zfh1 gives similar somatic muscle phenotypes

As shown in Table 7.3.2a and FIG 7.3.1a the phenotypes of UAS Him and UAS Zfh1 in the somatic muscle are very similar. This FIG is an extension of 7.3.1b, showing that the somatic muscle phenotype is similar when viewed dorsally (A,B), dorso-laterally (D,E), laterally (G,H) and ventro-laterally (J,K). However, notice the striking difference in heart formation between the UAS Zfh1 and UAS Him embryos (A,B); the heart is severely disrupted with Zfh1 over-expression (A), whereas it is similar to wild type in Him over-expression (compare B with C) This is addressed further in FIG 7.3.3.

UAS constructs driven by Mef2 Gal4 at 29°C. All embryos St17. Embryos stained with β3-tubulin. Wild type embryo is Oregon R at 29°C.

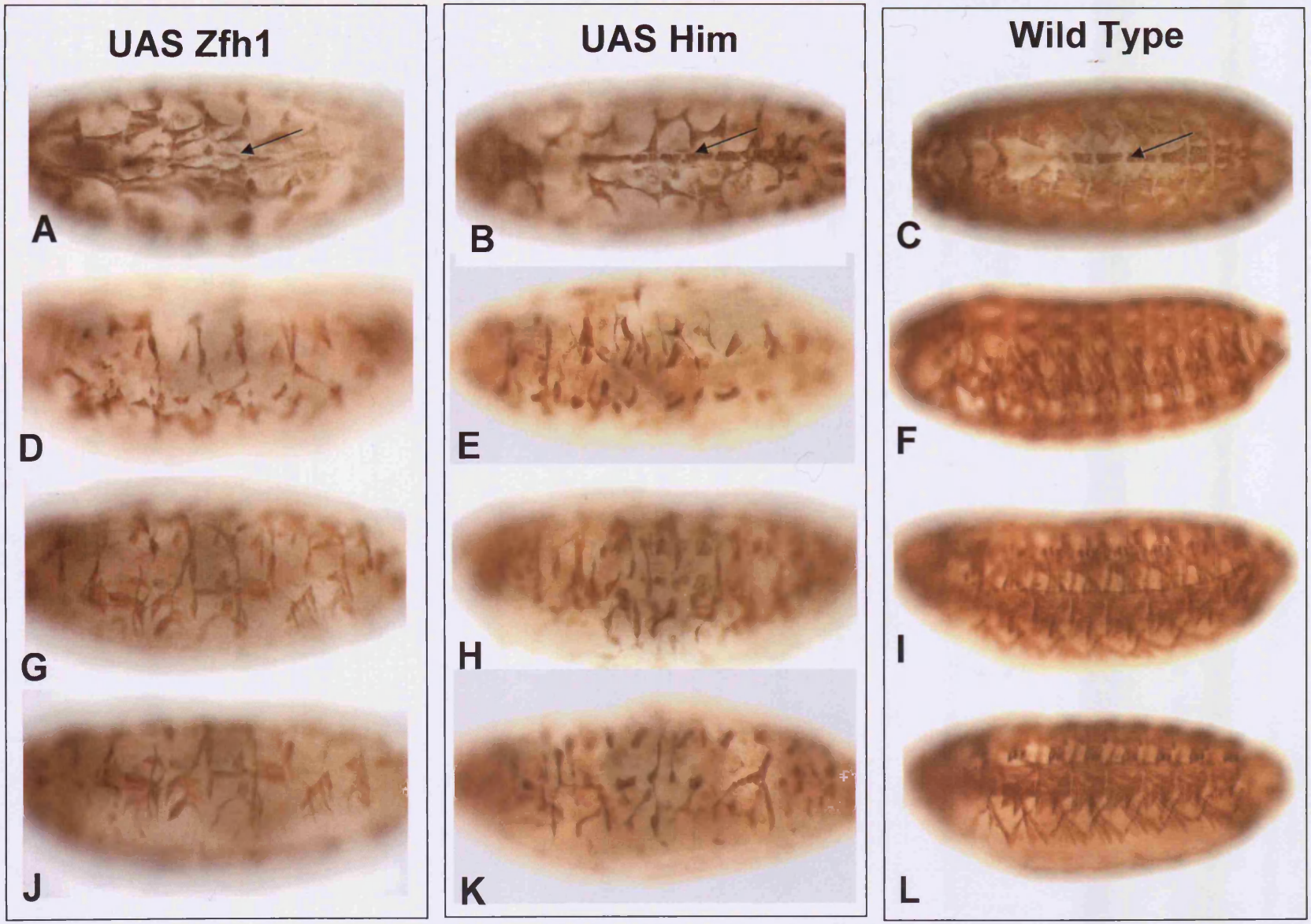

FIG 7.3.1b Over-expression of Him and Zfh1 gives similar somatic muscle phenotypes

With this in mind we can see that the individual somatic muscles that are lost on over-expression of Him or Zfh1 at 29°C are strikingly similar, with the same muscles being most readily lost and the same muscles being most easily retained. For example; DO3, DO5 dorsally, LT1, LT2, LT3, LT4 and LO1, laterally and VL4, VA3, VO5 and VO6 ventrally are all lost at least once in the three hemi-segments scored (A2-A4) in 100% of embryos (Table 7.3.2a), and of these DO3, LT1, LO1, VA3,VO5 and VO6 are missing in nearly every hemi-segment scored for both conditions.

On the other hand muscles such as DT1 and VT1 are ones that most frequently remain present in both UAS Him and UAS Zfh1 embryos (Table 7.3.2a).

These similarities can be seen visually in St17 embryos stained with β3-tubulin (FIG 7.3.1a and 7.3.1b). Both the UAS Him and the UAS Zfh1 embryos show a phenotype with large gaps in the muscle pattern; where particular muscles are consistently lost, such as DO3, DO5, LL1, LT1-4, LO1 as shown in the figure and the same muscles being consistently present such as DT1 and VL1. Those muscles that are present often are not wild type in appearance and show the same defects in both Him and Zfh1 embryos, for example the misattachment of VL1 or the way that DT1 is misshapen; being thinner in some parts of the muscle than others, whereas a wild type DT1 muscle is of a consistent thickness (FIG 7.3.1).

When the genes are over-expressed at a lower temperature, a milder phenotype is induced for both UAS Him and UAS Zfh1 but the similarity of muscles affected still holds true. With over-expression of Him or Zfh1 in the Mef2 pattern at the lower driving temperature of 21°C a number of observations and comparisons can be made. Firstly, the same muscles are most readily affected, but at a lower frequency, as you drop the temperature from 29°C to 21°C for UAS Him embryos – showing that although the phenotype associated with driving Him at a lower temperature is weaker, and muscles are less frequently lost, the

individual muscles affected are the same subset of muscles as those lost when Him is driven at the higher temperature. For example, over-expression of Him at 29°C gives 13 individual muscles (DO3, DO5, LL1, LT1, LT2, LT3, LT4, LO1, VA3, VO3, VO4, VO5, VO6) that are lost in nearly all hemi-segments of every embryo tested (7.3.2a, column1), whereas over-expression of Him at 21°C gives 9 individual muscles (DA2, DO5, LO1, VA1, VA3, VO1, VO2, VO3, VO4, VO5, VO6) that are lost in nearly all hemi-segments of every embryo tested (7.3.2b column 1). The same occurs for over-expression of Zfh1 at the lower temperature, the muscles lost here are the same subset as those lost when Zfh1 is over-expressed at 29°C, but the loss occurs at a lower frequency. For example, at 29°C DO3, LT1, LO1, VO5 and VO6 are lost in nearly all hemi-segment of every embryo scored (7.3.2a column1), whereas at 21°C only VO5 and VO6 are lost at this high frequency (7.3.2b column 1). Importantly from this, it follows that the same subset of muscles are missing in UAS Him embryos and UAS Zfh1 embryos at 21°C, for example all (with the exception of LL1) of the individual muscles that are missing in 90-100% of UAS Zfh1 embryos at this lower temperature (Table 7.3.2b column 1 and 2) are also missing in 90-100% of UAS Him embryos at the same temperature (Table 7.3.2b column 1 and 2). The fact that the muscle phenotype is still similar at a lower temperature is reassuring, in that not only is it good that the observation still holds true on being repeated but also it stems any concerns that the phenotypes may only seem similar at the higher temperature of 29°C because the genes were driven so hard, and the phenotype so strong that the majority of muscles were lost, and if the majority of muscles are lost it may be harder to accurately compare phenotypes.

Despite the definite similarities of somatic muscle phenotypes with Him and Zfh1 over-expression, it should be noted that the UAS Him line tested generally gives a slightly

stronger phenotype than the UAS Zfh1 line driven at the same temperature. For example, despite the LT muscles LT1-4 being missing in 100% of embryos for both UAS Him and UAS Zfh1 driven at 29°C, it is only LT1 in UAS Zfh1 embryos that is lost in an average of 2.8 / 3 hemi-segments, whereas LT1, LT2, LT3 and LT4 are lost in an average of 2.8 / 3 hemi-segments with UAS Him (Table 7.3.2a column1). This greater frequency of loss in UAS Him embryos is reflected in Table 7.3.1, where the range and average of muscles lost, though similar to UAS Zfh1 is slightly higher in the UAS Him experiments (for example, an average number of 67.13 muscles missing in the three hemi-segments scored per embryo for UAS Him embryos whereas UAS Zfh1 have an average of 59.85 muscles missing).

This slight difference in phenotype severity could be due to some variation in the strength of the line due to transgene insertion site or it may occur due to a difference in mechanism between Him and Zfh1; as Zfh1 likely acts upon Mef2 at the level of transcription any Mef2 RNA that does manage to become translated would be able to function as normal.

7.4 Differences in the UAS Zfh1 and UAS Him muscle phenotypes

7.4.1 UAS Zfh1 gives unfused myoblasts

Although the same individual muscles are missing in Him and Zfh1 over-expression embryos, there are two distinct differences in their associated phenotypes. The first is that UAS Zfh1 embryos have a considerable number of unfused myoblasts present in the abdominal wall region. This is especially so in the later, but not final, stages of muscle formation (i.e St16-early 17, but not late St17) – whereas UAS Him only has a few unfused myoblasts present in the abdominal wall at these stages even in both of the over-expression

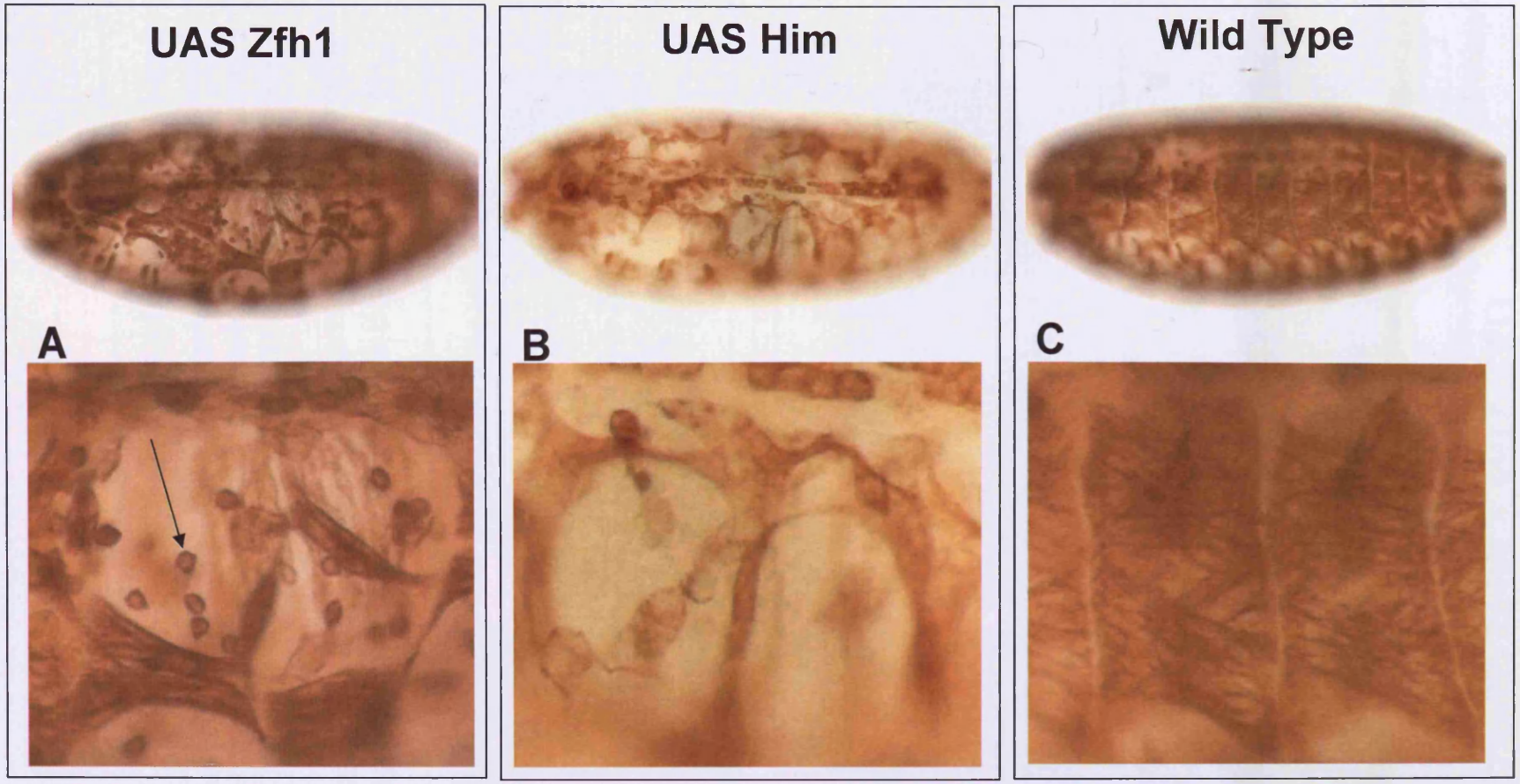

FIG 7.4.1 Over-expression of Zfh1 gives unfused myoblasts whereas Him does not

Despite having the same muscles missing, a distinct difference between Zfh1 and Him overexpression experiments is that there are a large number of unfused myoblasts present in the abdominal wall of UAS Zfh1 embryos in early St17 embryos whereas there are none in UAS Him embryos. Arrow in A, shows an example of a single unfused myoblast for clarity in UAS Zfh1 embryo.

Embryos here are driven by Mef2 Gal4 at 29°C, viewed dorso-laterally and stained with anti β3 tubulin.

UAS Zfh1 x Mef2 Gal4 (29°C)

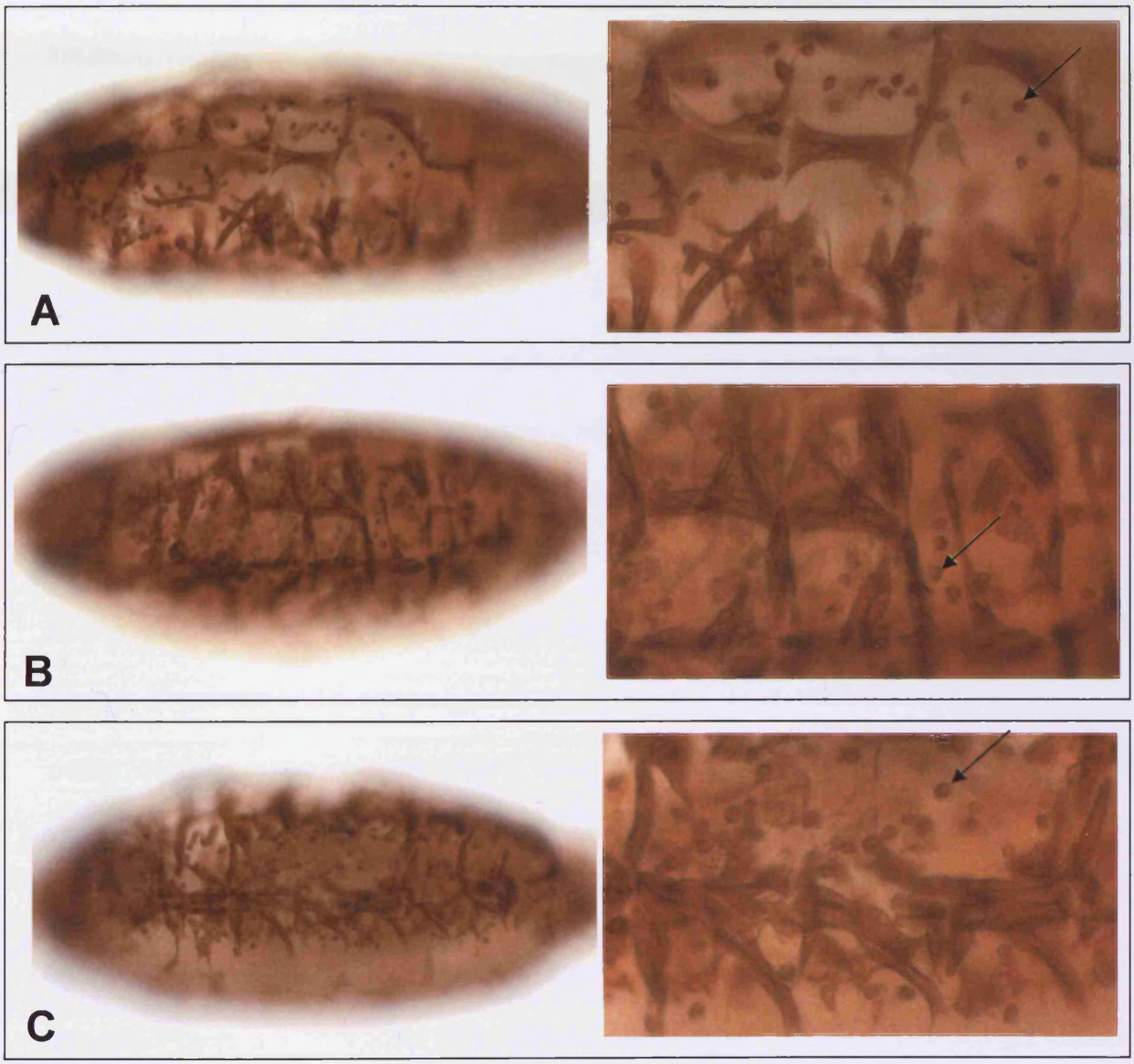

FIG 7.4.2 Examples of unfused myoblasts in UAS Zfh1 embryos.

Numerous unfused myoblasts can clearly be seen in the dorsal (A) , lateral (B) and ventral (C) regions of embryos over-expressing Zfh1 in the Mef2 Gal4 pattern at 29°C. Arrows only point to a single example of an unfused myoblast in each view.

Embryos are stained with anti β-tubulin.

temperatures tested (FIG.7.4.1). Examples of unfused myoblasts in Zfh1 over-expression embryos can be seen dorsally, laterally and ventrally within the abdominal wall (FIG 7.4.2).

7.4.2 UAS Zfh1 affects heart formation

The second difference is perhaps the most striking one, and this is that UAS Zfh1 embryos have a severe disruption to the development of the heart, inhibiting the expression of β3-tubulin and causing loss of the cardioblasts, whereas by comparison, the heart in UAS Him embryos appears generally unaffected even when UAS Him is driven strongly at 29°C with Mef2 Gal4.

In wild type embryos, four out of the six cardioblasts in each hemi-segment of the heart express β3-tubulin (7.4.3 image C). However, when Zfh1 is over-expressed in the Mef2 pattern only the occasional, mis-shapen, apparent β3-tubulin positive cardioblast is present (FIG 7.4.3 image A). In contrast to this, over-expression of Him in the Mef2 pattern has little effect on heart formation, with, in general, the full four β3-tubulin positive cardioblasts being present and correctly shaped and positioned within the linear heart tube structure. There are occasional mild defects, such as the loss of one or two β3-tubulin cardioblasts, (as seen in this embryo(B) in FIG 7.4.3), a kink in the shape of the heart, or extra β3-tubulin cardioblast-like cells outside of the dorsal tube (See FIG 5.2.3).

This observation for Him is consistent with results obtained previously on the role of Mef2 and of Him on cardioblast differentiation.

In *Mef2* null mutants the heart tube forms and the cardioblasts are specified, as shown by β3 tubulin expression, but the cells fail to differentiate as markers such as Myosin Heavy Chain (Mhc) are not expressed (Lilly et al, 1995; Damm et al, 1999).

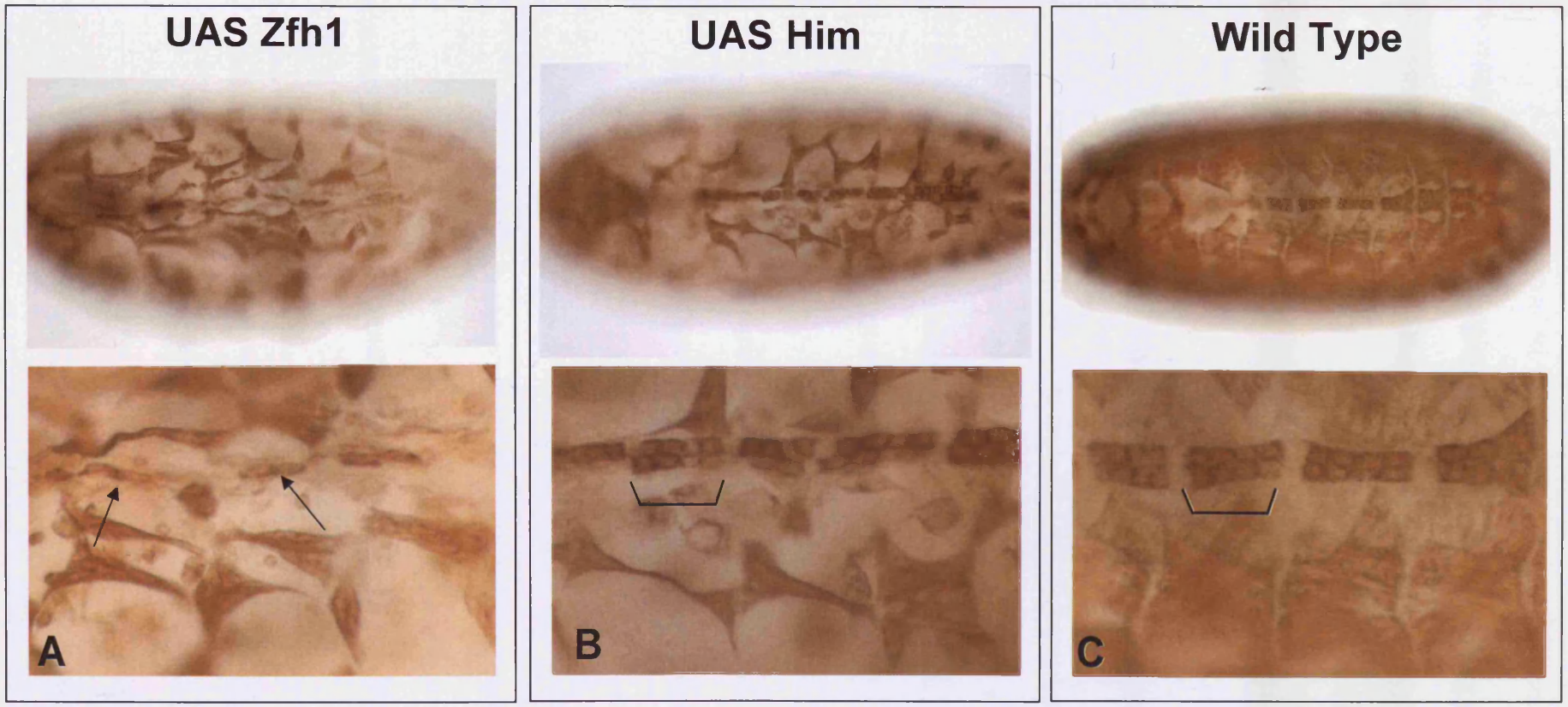

FIG 7.4.3 Over-expression of Him and Zfh1 give different phenotypes in the heart

Although UAS Him and UAS Zfh1 both give a similar phenotype of somatic muscle loss and disruption their phenotypes are very different in the heart. β3-tubulin expression in the cardioblasts of the heart in an embryo over-expressing Him is similar to wild type, with, in general, 4 out of 6 cardioblasts expressing β3-tubulin in a linear heart as expected (compare bracket in B with wild type, C and also Fig 2.3.2). However in Zfh1 over-expressing embryos β3-tubulin expression is severely disrupted, with only the occasional misshapen apparent β3-tubulin positive cardioblast forming (arrows in A).

UAS constructs driven by Mef2 Gal4 at 29℃. All embryos St17 and viewed dorsally. Embryos stained with β3-tubulin. Wild type embryo is Oregon R at 29℃.

A similar observation was seen with Him over-expression; β3 tubulin expression in the cardioblasts is unaffected, whereas there is a severe disruption to Mhc expression (Liotta, PhD thesis 2006). These results suggest that the expression of β3-tubulin in the heart is independent of Mef2 and that Zfh1 is capable of inhibiting whichever factor is responsible for this expression.

7.5 The St17 somatic muscle phenotype of *Zfh1*^{2} mutants.

After establishing that *Him* and *Zfh1* are expressed in the same pattern in the developing mesoderm and that their over-expression gives a similar terminal somatic phenotype I wanted to make a comparison of the *Zfh1* and *Him* mutant phenotypes.

The *Zfh1*^{2} mutants were originally established and their phenotype described by Lai et al in 1993 (Lai et al, 1993). However, the description of the somatic muscle phenotype in this paper was quite limited; their analysis of the somatic muscle described how loss of *Zfh1* function results in "various degrees of local errors in cell fate or positioning" and "a wide variety of errors in the pattern and a range of severities", but only mentioned a few specific effects on patterning. For this study, I wanted to go into the somatic muscle phenotype of *Zfh1*^{2} mutants in greater detail in order to further understand the role of Zfh1 in somatic muscle development, and also enable comparison to other experimental situations where Mef2 activity is increased; such as in *Him* mutants, and Mef2 over-expression embryos.

Analysis of the somatic musculature of hemi-segments A2-A4 of twenty individual embryos enabled a more detailed characterisation of which muscles are affected in *Zfh1*^{2} mutant embryos. As seen in the Lai et al study, the phenotype of *Zfh1*^{2} mutant embryos is variable. Embryos can show a predominant gain in muscles, a predominant loss of muscles

or both gain and loss of muscles. FIG 7.5.1 shows examples of this; where there are duplications in the LT muscles in an embryo that shows few other defects (Embryo B - an example of an embryo with a predominant gain of muscles). There are also embryos which show a predominant loss of muscles (Embryo D), where there are a number of the dorsal muscles missing. Embryos F and H are both show gain and loss of individual somatic muscles. In embryo H we see reproduction of the main specific phenotype described in the Lai et al study; where there is loss of the ventral muscles VO4, VO5 and VO6 to just a single VO muscle in this position.

LT muscles were observed to be genuine duplications on the basis that there was no end splitting of the muscles, they were distinct, single muscles that could be seen spanning fully between attachment points. In addition, all the LT muscles were of a similar size, with a height and width that corresponded to both the other LT muscles in a mutant embryo and more importantly to wild type LT muscles. This suggests that if each distinct muscle arose as a result of splitting during development, then the muscle that split would have been twice the thickness of a normal muscle. No such thicker LT muscles or intermediates in a splitting process were observed.

Of all of the embryos scored, the majority (75%) have at least one duplication and one muscle missing, 15% have muscles missing but no duplications and 10% have duplications but no muscles missing (Table 7.5.1); from this scoring the variability of the phenotype can be seen. Though 90% of embryos have muscles missing and 85% of embryos have muscles duplicated, the frequency of muscle loss in an individual embryo is greater than the frequency of muscle gain, for example the average number of muscles missing in an embryo is 6.05 and the range of muscles missing in an embryo is 1-24, whereas the average number of duplications in an embryo is 2.05 with a range of 1-8 (Table 7.5.2). In addition,

FIG 7.5.1 – Zfh1 loss of function disrupts muscle pattern

Zfh1 mutant embryos can show a phenotype with a predominant gain of muscles, a predominant loss of muscles or a combination of both.
Embryo B shows a predominant gain in muscles, with multiple duplications (Compare embryo B, which shows LT duplications (asterisks) with Wild Type A). These embryos are often free from many other shape and positional defects.
Embryo D shows a predominant loss of muscles, with multiple muscles missing (Compare embryo D, which shows loss of DA1 (arrow), DA2 (arrowhead) and DO2 (asterisk) with Wild Type C). These embryos tend to show other shape and positional defects in addition to muscle loss (Compare shape of DA2 (blue arrowhead) and DO2 (blue asterisk) in hemisegment A3 with Wild Type C).
Embryo F shows both gain and loss of muscle (An LT is duplicated (asterisks) and LO1 is lost (arrow) compared to Wild Type E). These embryos often show the greatest number of shape and positional defects.
The main phenotype described in the Lai et al study was the apparent reduction of the three ventral-oblique muscles (VO4, VO5, VO6) to only one muscle. These VO muscles were the most commonly missing in this studies' scoring analysis (see Table 3.4) and the phenotype is shown in Embryo H (Compare single VO (arrow) to the three in Wild Type G). This Zfh1 mutant embryo also shows a VA3 duplication (arrowhead) and loss of VA1 (asterisk) and VT1 (blue asterisk).

Zfh1 mutants were Zfh1-2 / TM3 ftz LacZ (Lai et al 1999). Homozygous mutants were selected by staining against LacZ. Muscles were stained with anti-b3 tubulin (guinea pig). Wild type embryos were Oregon R.

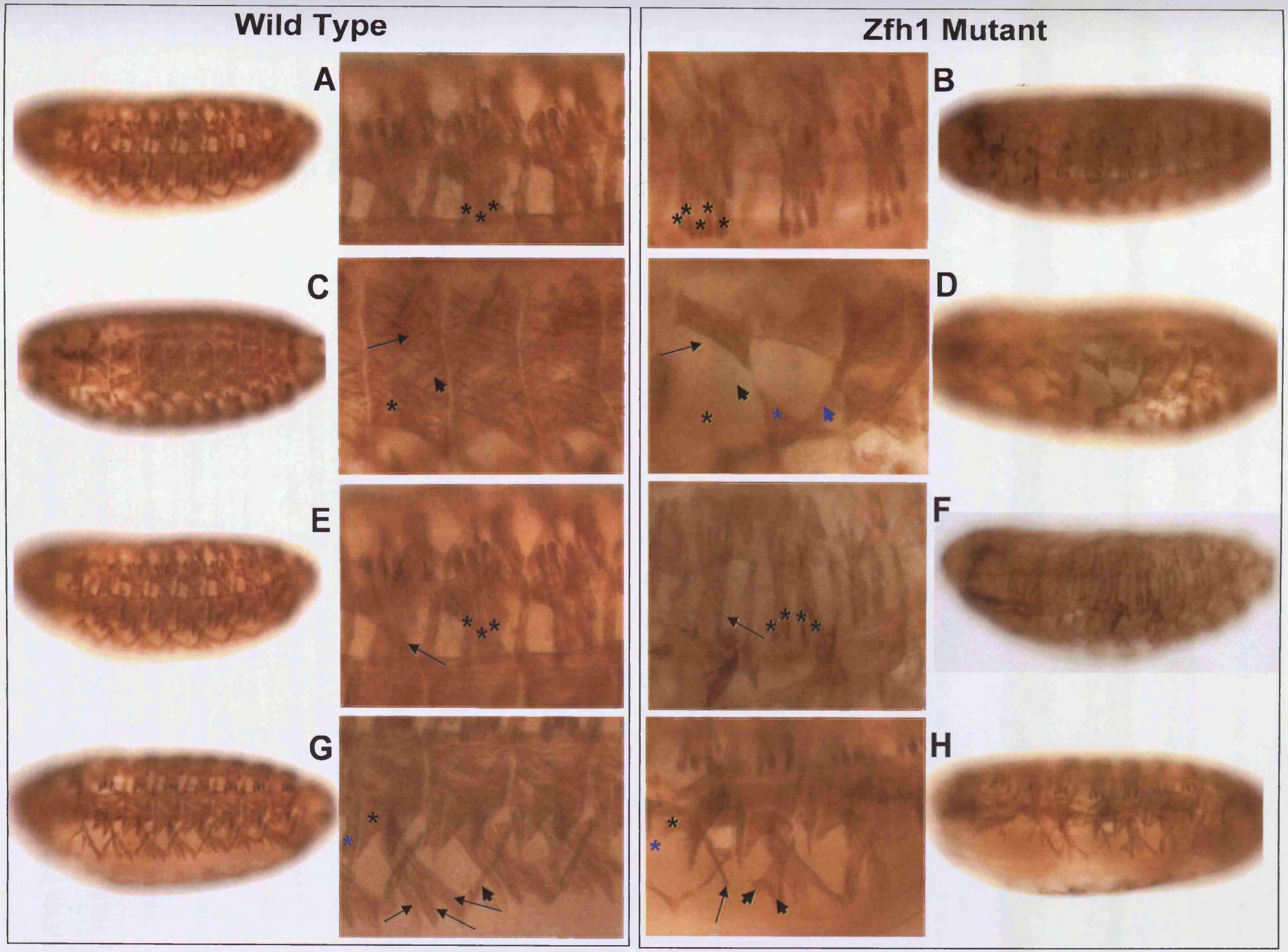

FIG 7.5.1 – Zfh1 loss of function disrupts muscle pattern

every embryo scored contains multiple shape defects in individual muscles and a large number (60%) of embryos contain attachment defects in some muscles.

Despite the variation in embryos showing either muscle loss or muscle duplication on analysis of the individual muscles distinct patterns present; as shown in FIG 7.5.2, certain individual muscles are predominantly or solely duplicated (e.g LT1, LT2, LT3 and VA3) other muscles, such as DO3, LO1, VL1-4 and VO4-VO6 are only ever missing in the embryos scored. There are also other muscles, which appear unaffected (in terms of muscle loss or duplication) such as LL1 and VO3, and others which have similar percentages of embryos with that muscle either lost or duplicated (e.g DO2). So despite the fact that on first observation the *Zfh1*^{2} mutant phenotype is variable, and that as reported in the Lai et al study there are a "wide variety of errors in the pattern and a range of severities", more detailed analysis shows that there is a definite pattern to how individual somatic muscles respond to the loss of Zfh1 activity, there are muscles which could be described as most likely to be duplicated on loss of Zfh1 and others that are most likely to be missing on loss of Zfh1 activity. FIG 7.5.3 shows a summary schematic of the muscles that are predominantly or solely duplicated, the muscles that are predominantly or solely missing and the muscles that appear predominantly unaffected (muscles that are either never missing or duplicated or are only missing in 5% of embryos) in the *Zfh1*^{2} mutant phenotype. Such an observation may suggest of a role for Zfh1 in the control of somatic muscle patterning.

In some examples of muscle patterning, a transformation of fates occurs whereby the duplication of one muscle happens at the expensive of another one. In this case the two muscles arose from an initial progenitor that gave rise to two muscles founders as is the case in the formation of the *Kruppel* positive founders that give rise to the VA1 and VA2

TABLE 7.5.1 Muscles Duplicated and Missing : Zfh1-2 (non ftz lacZ) anti-b3 tubulin @ 25

	1b	1c	1d	2a	2b	2c	2d	3c	3d	4d	5a	5c	5d	6a	6c	6d	7a	7b	7c	8a	Total	In X Embryo	Average(A2-4) In embryos affected
DO1										1											1	1	1
DA1					1					1	1					1					1 3	1 3	1 1
DO2											1						1				1 1	1 1	1 1
DA2					2		1				1					1				2	1 6	1 4	1 1.5
DO3	1			1					1		1			1							5	5	1
DO4										1								1			2	2	1
DA3																				1	1	1	1
DO5											2										2	1	2
DT1							1														1	1	1
LL1																					-		
LT1	1		1		1		1			2		1	1	1			1				8 2	7 2	1.14 1
LT2			1		1					2			1					1			5 1	4 1	1.25 1
LT3	1		1		1	1			11	2		1			1						8 2	7 2	1.14 1
LT4							1	1	1		2										1 4	1 3	1 1.33
SBM											2										2	1	2
LO1		1				2					3	1		2		1	1				11	7	1.57
VT1															1						1	1	1
VL1					1						1									1	3	3	1
VL2					1						1	1			1						4	4	1
VL3					1						2	2			1						6	4	1.5
VL4					1						2	2	1	1							7	5	1.4
VA1					1																1	1	1
VA2															1						1	1	1
VA3	1	1				1								1		2	1		1		8	7	1.14
VO1												1									1	1	1
VO2						1					2	1									4	3	1.33
VO3																					-		
VO4	1	2		3	3	1					2	1	1		1	2			2	2	21	12	1.75
VO5	1	1			2						1	1			1				1		8	7	1.14
VO6	1	1			1				1		1	1		2						1	9	8	1.13
DUP	3	1	3	-	-	2	2	1	1	8	-	1	2	2	1	2	3	1	1	1	35	17	2.06
MISS	4	5	-	3	17	4	2	-	4	1	25	12	2	6	6	5	1	1	3	6	108	18	6

Table 7.5.1 Muscle phenotype of Zfh1-2 mutants

	No. Emb with Missing	No. Embryo with Dup	No. Emb MissONLY	No. Emb DupONLY	No. Emb Shape only	No. Emb wt	Total No. Embryo
No. Emb	18	17	3	2	0	0	20
% Emb	90 %	85 %	15 %	10 %			
Muscle total	108	35					
Avg No. Muscle / Emb	6	2.06					
Range	0-25 (1-25)	0-8 (1-8)					

Cross : Zfh1-2 (non ftz lacZ) anti-b3 tubulin @ 25

ONLY means that there isn't a duplication AND a missing muscle in the same embryo. There could be other defects such as shape, attachment etc.

	Muscles **MISSING**	Muscles **DUPLICATED**	**SHAPE** DEFECTS	**ATTACHMENT** DEFECTS
% Embryos with phenotype	90 %	85 %	100 %	60 %
Average number muscles with phenotype per embryo	6.05	2.06	16.45	3.92
Range of muscles with phenotype per embryo	1 - 24	1 - 8	3 – 42	1 - 13

TABLE 7.5.2 – Zfh1 loss of function gives a complex muscle pattern phenotype

The thirty somatic muscles of a hemisegment for hemisegments A2-A4 were scored for duplication, loss, shape and attachment defects in 20 individual embryos in *Zfh1-2* mutants. The percentage of embryos that show at least one example of a defect A2-A4 , the average number of muscles of that defect per embryo (A2-A4) and the range of muscles affected (A2-A4) for all affected embryos is shown here.

Embryos were stained with β3-tubulin to visual ise muscles.

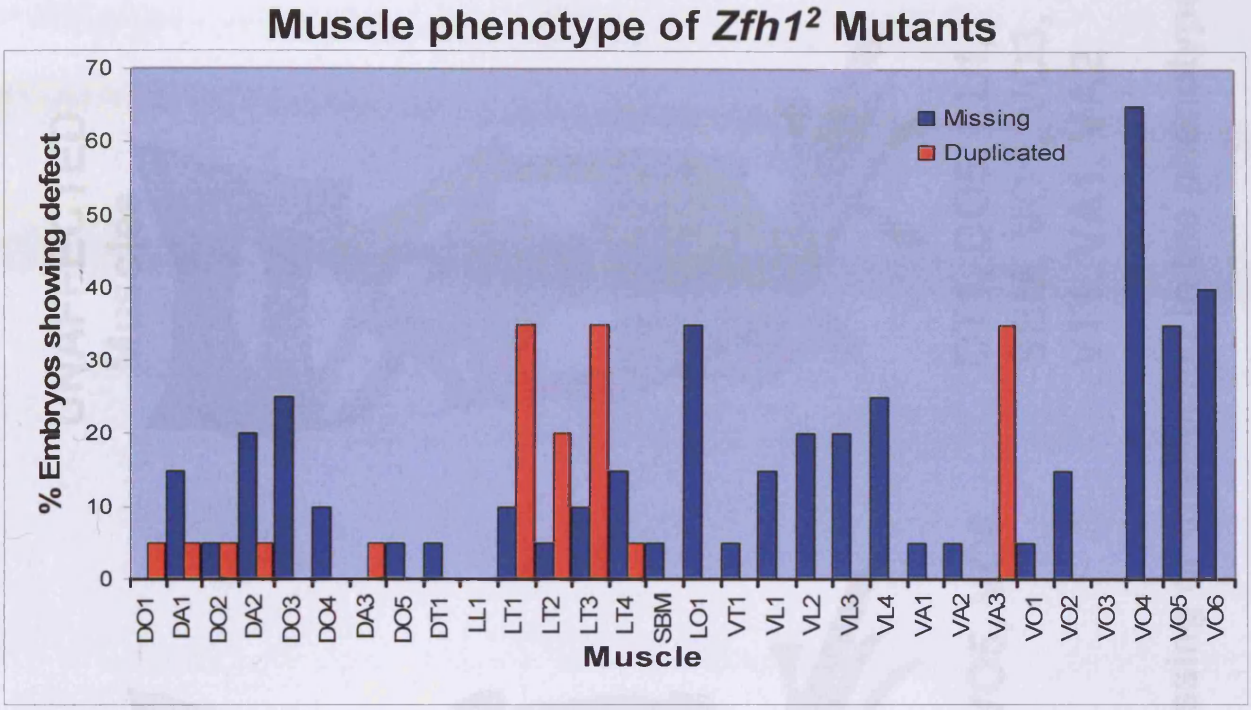

FIG 7.5.2 Muscles missing or duplicated in *Zfh1²* Mutants

Graph showing the percentage of *Zfh1²* mutant embryos that show at least one example in hemi-segments A2-A4 of muscle loss or muscle duplication for each of the thirty individual somatic muscles. Blue represents missing muscles, red represents duplicated muscles. Notice that certain individual muscles such as LT1, LT2, LT3 and VA3 are predominantly or solely duplicated, others, such as DO3, LO1, VL1-4 and VO4-VO6 are only ever missing in the embryos scored. There are also other muscles, which appear unaffected (in terms of muscle loss or duplication) and others which have similar percentages of embryos with that muscle either lost or duplicated (e.g DO2).

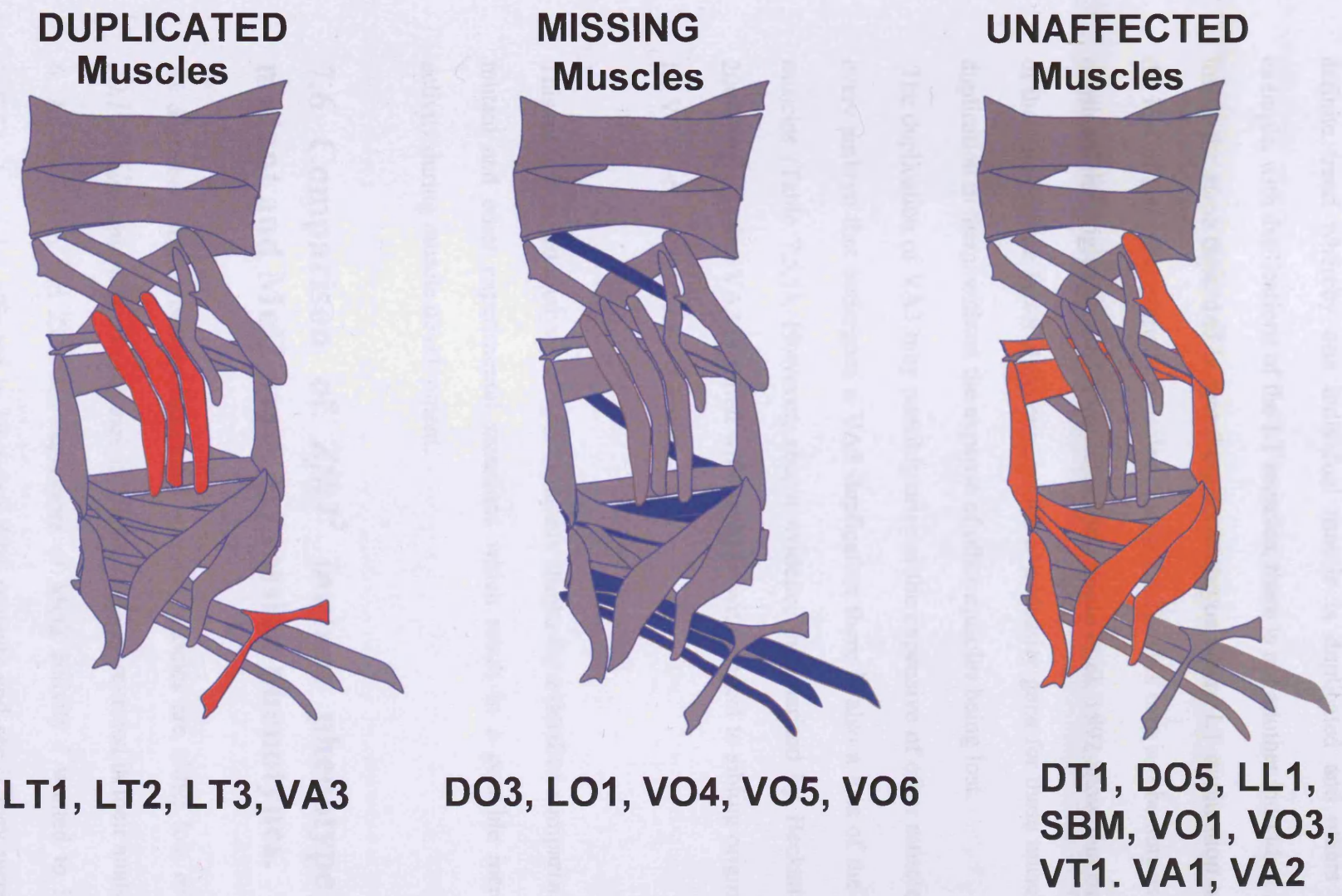

FIG 7.5.3 Muscles most frequently duplicated, missing or unaffected in the phenotype analysis of *Zfh1*^{2} mutants .

muscles (Ruiz Gomez et al, 1997). In the *Zfh1*^{2} analysis there does not appear to be a definite trend whereby one individual muscle is duplicated and others are lost. For example, with duplications of the LT muscles, there is not another individual muscle that is lost at the same time, and in fact there are embryos where LT duplication occurs without the loss of any other somatic muscles (Table 7.5.1). This may not be surprising when one considers the origins of the LT muscles; Bourgouin et al, 1992 show that over-expression of the transcription factor *Apterous* , which is a identity gene for these muscles, can cause duplication in them, without the expense of other muscles being lost.

The duplication of VA3 may possibly arise at the expensive of other muscles however; in every embryo that undergoes a VA3 duplication there is also a loss of the VO4 or VO6 muscles (Table 7.5.1). However, recent evidence summarised by Beckett and Baylies, 2009, suggests that VA3 is paired with an AMP with respect to sibling origin. The pairings for VO4-5-6, however are not known.

This more detailed analysis of *Zfh1*^{2} mutants allows for a detailed comparison of the *Him* mutant and other experimental situations which result in a possible increase of Mef2 activity during muscle development.

7.6 Comparison of *Zfh1*^{2} mutant phenotype to *Him* mutant and Mef2 over- expression phenotypes.

As described above, certain individual somatic muscles are either lost or duplicated in *Zfh1*^{2} mutants this was also the case in Him mutants as revealed in their analysis in Chapter 6. As both Him and Zfh1 are repressors of Mef2 activity I wanted to investigate the individual muscles affected in Him and Zfh1 mutants and see if they were the same. In addition, for this comparison I also scored the muscles of the abdominal hemi-segments

A2-A4 for twenty embryos in the usual way for embryos that over-expressed Mef2 in the Mef2 pattern at 29°C. The UAS Mef2 line was the "low strength" line 10T4A as described in Gunthorpe at al, 1999.

FIG 7.6.1 shows graphs of the percentage of embryos showing the loss or duplication of an individual muscle for each of the thirty muscles in abdominal hemi-segments A2-A4. Mef2 over-expression, Him loss of function and Zfh1 loss of function are all three very distinct ways of increasing Mef2 activity in muscle development, yet strikingly there are definite similarities in the phenotype for these three different experimental conditions. Most notable is the duplication of the LT muscles, which occurs at a relatively high frequency in all of the conditions. VA3 is also duplicated in all conditions, but with a much greater frequency in Zfh1 mutants. Similarly DO1 is duplicated in all three conditions but at a much greater frequency in the Him mutant.

Examples of the LT duplications for each of the three Mef2 gain-of-function experimental conditions are seen in FIG 7.6.2. Here we see two duplications of the LT muscles in each of the embryos shown. In all of these embryos there were few other defects to other muscles.

Table 7.6.1 shows a more detailed analysis of the muscle duplications in the three experimental conditions, and the muscles most frequently duplicated are represented diagrammatically in FIG 7.6.3. These data show a definite tendency towards LT duplication in experimental conditions that increase Mef2 activity.

Though a similar frequency of duplication occurs in the Zfh1 and Him mutants embryos (85% of embryos with duplications, an average of 2.06 muscles duplicated per embryo and a range of 1-8 duplications per embryo for Zfh1 mutants, compared to 95% of embryos with duplications, an average of 2.32 muscles duplicated per embryo and a range of 1-7 for Him mutants (Table 7.6.2)), a greater number and frequency of muscle loss occurs in Zfh1

mutants compared to Him mutants (Table 7.6.1 and FIG 7.6.1). Though the muscle most frequently lost in Him mutants is also one of the ones most frequently lost in Zfh1 mutants (VO6 – 15% of Him embryos, 40% of Zfh1 embryos FIG 7.6.1).

Table 7.6.3 compares aspects of the phenotypes in more detail, for example which muscles are lost and which have predominant shape defects and shows that in terms of muscles missing there appears to be little similarity between Zfh1 mutants and Mef2 over-expression embryos. And this is true for embryos over-expressing either the low or high insertion lines of UAS Mef2 (Table 7.6.2 and FIG 7.6.4).

UAS Mef2 high was driven at 25°C with Mef2 Gal4. The data for this muscle analysis came from that performed in the Mef2 dominant negative chapter comparing Mef2 over-expression to the Mef2-En phenotype (Chapter 3). The somatic muscles of hemi-segments A2-A4 of 20 embryos were scored in the usual way.

From this we can see that despite showing a large number of muscles missing and a considerable disruption to the muscle phenotype, the strong Mef2 gain-of-function condition strikingly still has the same muscle subset being duplicated; with DO1, VA3 and the LT muscles being duplicated at a relatively high frequency (FIG 7.6.5). Interestingly though, it is only the DO1 and VA3 muscles that retain the characteristic of being predominantly duplicated; though the LT muscles are duplicated at a frequency similar to the other Mef2 gain-of-function conditions (UAS Mef2 (low) over expression, the *Him* mutant and the *Zfh1* mutant), they are now missing at a similar frequency to duplication LT1 or predominantly missing with LT3 and LT4 (LT2 was not observed as missing in this analysis) (FIG 7.6.5).

FIG 7.6.1 Muscles missing or duplicated in Mef2 over-expression, *Him*^{52} mutant and *Zfh1*^{2} mutant embryos.

These graphs show the percentage of embryos showing the loss or duplication of an individual muscle for each of the thirty muscles in abdominal hemi-segments A2-A4. Mef2 over-expression, Him loss of function and Zfh1 loss of function are all three very distinct ways of increasing Mef2 activity in muscle development.

Strikingly there are definite similarities in the phenotype for these three different experimental conditions. Most notable is the duplication of the LT muscles. VA3 is also duplicated in all conditions, but with a much greater frequency in Zfh1 mutants. Similarly DO1 is duplicated in all three conditions but at a much greater frequency in the Him mutant.

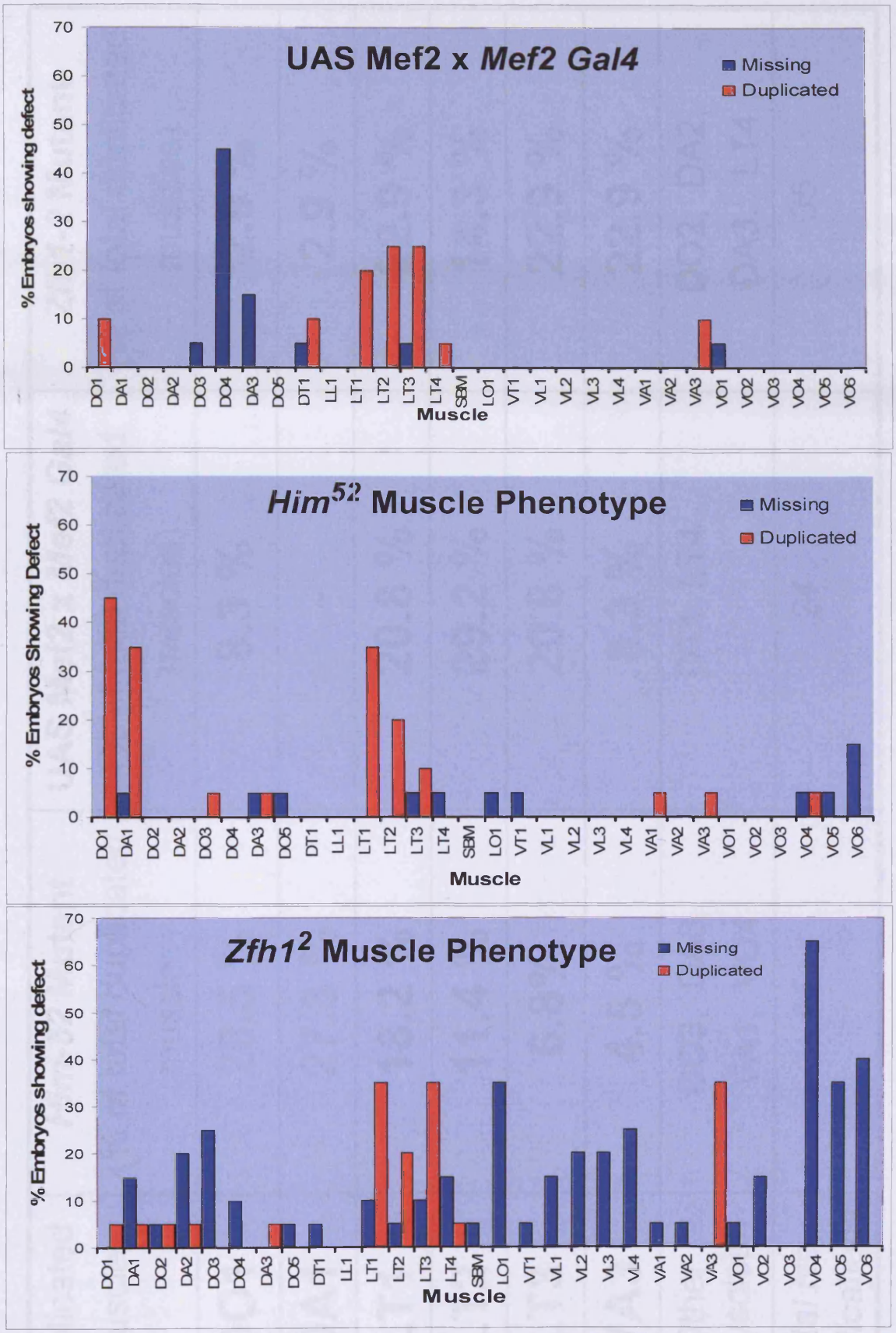

FIG 7.6.1 Muscles missing or duplicated in Mef2 over-expression, *Him*^{52} mutant and *Zfh1*^{2} mutant embryos.

Duplicated Muscles in Him mutant, UAS Mef2 and Zfh1 mutant

Duplicated Muscle	***Him-52* Mutant** (% of total duplicated muscles)	**UAS Mef2 x *Mef2 Gal4*** (% of total duplicated muscles)	***Zfh1-2* Mutant** (% of total duplicated muscles)
DO1	**20.5 %**	**8.3 %**	**2.9 %**
DA1	**27.3 %**	**-**	**2.9 %**
LT1	**18.2 %**	**20.8 %**	**22.9 %**
LT2	**11.4 %**	**29.2 %**	**14.3 %**
LT3	**6.8%**	**20.8 %**	**22.9 %**
VA3	**4.5 %**	**8.3 %**	**22.9 %**
Other muscles	DO3, DA3, VA1, VO4	DT1, LT4	DO2, DA2, DA3, LT4
Total No. Duplications	*44*	*24*	*35*

Table 7.6.1 – Increasing Mef2 activity leads to muscle duplication in the same individual somatic muscles

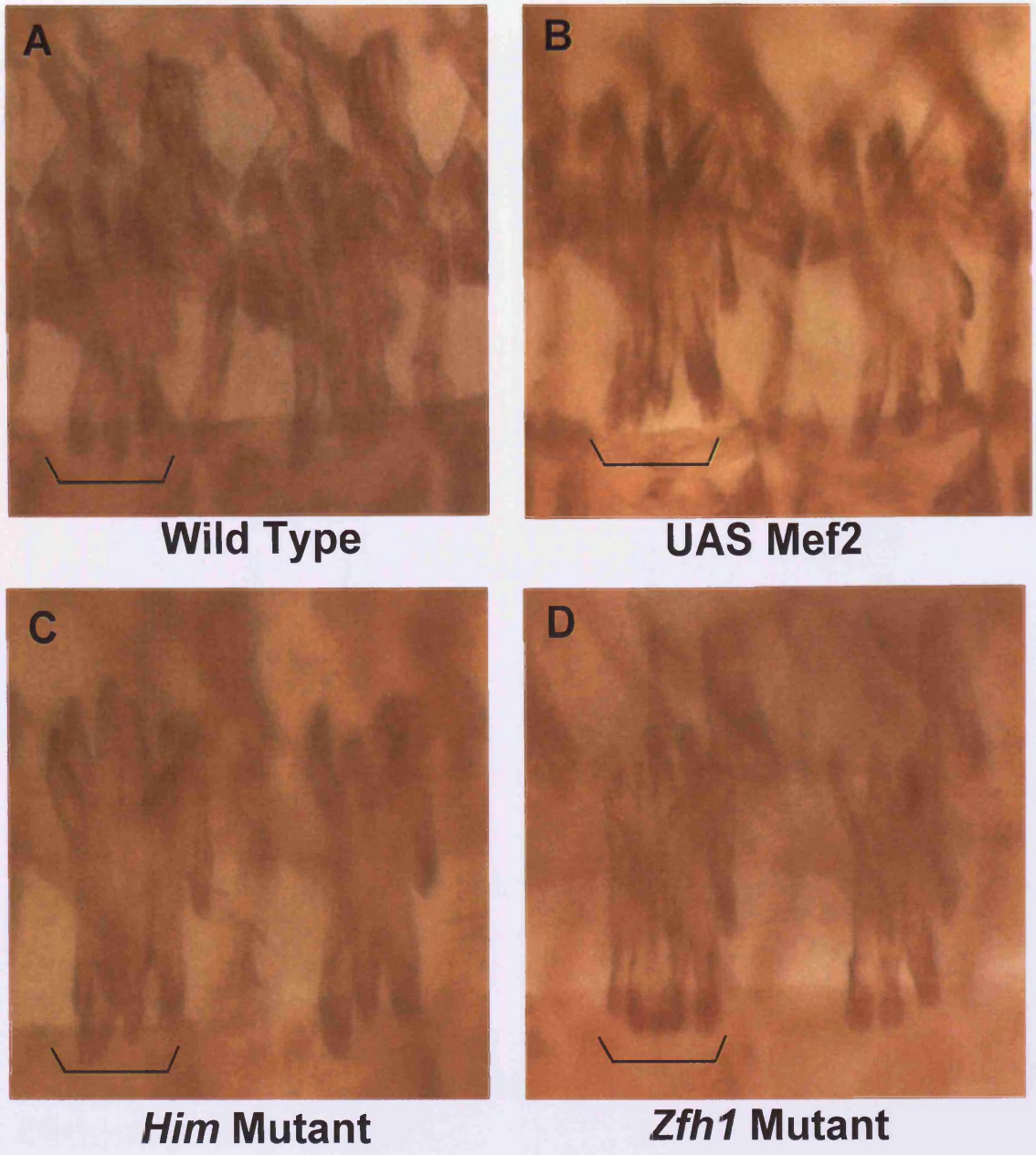

FIG 7.6.2 An increase in Mef2 activity can lead to an increase in muscle number

Increasing Mef2 activity leads to significant duplications in specific somatic muscles. This phenotype was observed with three different genetic routes : over-expression of the full length Mef2 protein using Mef2 Gal4, loss of function of *Him*, which represses Mef2 at the protein level, and loss of function of *Zfh1* which represses Mef2 at the RNA level.

Shown here are duplications in the lateral muscles, L1-L3. There are five LT muscles in an individual hemi-segment in the UAS Mef2 (B), *Him* mutant (C) and *Zfh1* mutant (D) embryos instead of the usual wild type number of three (A).

Lines used : Him-52, Zfh1-2 and UAS Mef2 low 10T4A. UAS experiment performed at 29°c. Wild type was OR.

Main muscles duplicated in Him mutants

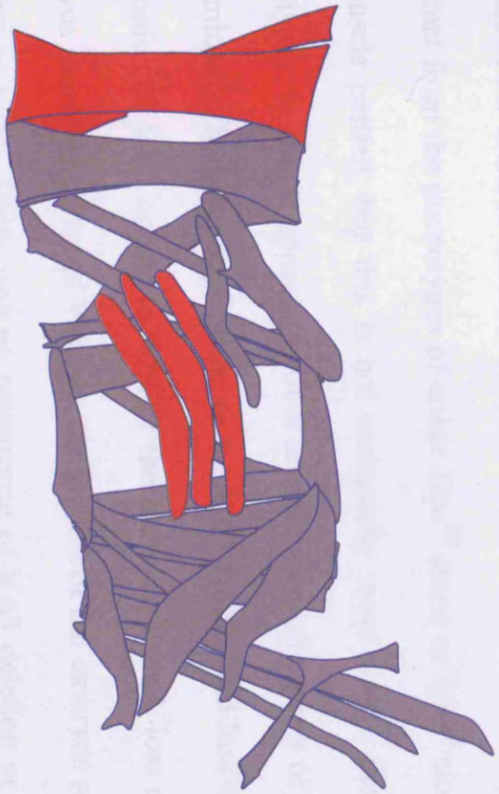

DO1, DA1, LT1/2/3

Main muscles duplicated in UAS Mef2

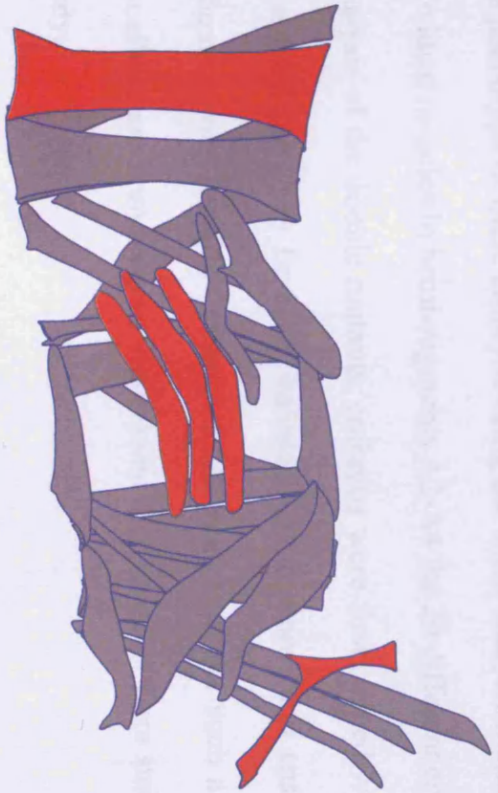

DO1, LT1/2/3, VA3

Main muscles duplicated in Zfh1 mutant

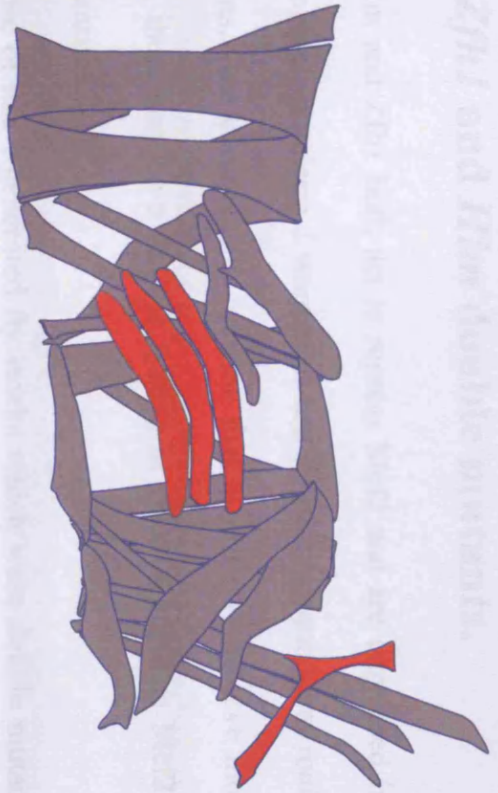

LT1/2/3, VA3

FIG 7.6.3 Most frequently duplicated muscles in Him mutant, Mef2 over-expression and Zfh1 mutant embryos.

7.7 *Zfh1* and *Him* double mutants.

As Him and Zfh1 both act to repress Mef2 and are expressed in the same pattern in the developing mesoderm I wanted to test if there is functional redundancy between the two proteins. One could easily imagine that in order to achieve most effective regulation of Mef2, there may be a failsafe system in place to regulate Mef2 activity by two different mechanisms.

Because of this I generated fly stocks which were double mutant for both Him and Zfh1 (see Materials and Methods for crossing scheme) and was then able to test the somatic muscle phenotype of these embryos using the usual analysis method (scoring of each of the 30 individual muscles in hemi-segments A2-A4 for 20 different embryos).

For analysis of the double mutants, embryos were first stained with anti-LacZ antibody to select against the TM3 ftz LacZ balancer chromosome and ensure that chosen embryos were homozygous for $Zfh1^2$ (there was no need to make such a selection for *Him* as the mutant alleles are homozygous viable) and then muscles were stained using anti-β3 tubulin antibody.

Analysis of the somatic muscles of Him^{52} ; $Zfh1^2$ double mutants reveals that the phenotype is distinct from the phenotypes of either Him^{52} alone or $Zfh1^2$ alone. There is disruption to the muscle pattern, but this is not necessarily more severe than each of the individual phenotypes, in fact it appears to be a combination of aspects of the two phenotypes. The predominant affect is a duplication of the VA3 muscle and loss of the VO4-VO6 muscles; duplication of VA3 occurs in 70% of the embryos scored, loss of VO4 occurs in 70% of embryos scored and loss of VO6 occurs in 55% of the embryos scored (loss of VO5 is less frequent at 15%). There was no occurrence of VA3 deletion or VO4-6 duplication. (FIG 7.7.1).

Cross	% Embryos with muscles MISSING	Average MISSING per embryo	Range	% Embryos with muscles DUPLICATED	Average DUPLICATED per embryo	Range	% Embryos with muscles MISSING *ONLY*	% Embryos with muscles DUPLICATED *ONLY*	% Embryos with muscles MISSING *AND* DUPLICATED
UAS Mef2 (Nguyen) X *Mef2 Gal4*	100 %	8.8	1-18	60 %	1.55	1-2	45 %	0 %	55 %
UAS Mef2 (10T4A) X *Mef2 Gal4*	65 %	1.69	1-3	70 %	1.71	1-3	25 %	30 %	40 %
Zfh1 – 2 Mutant	90 %	6.05	1 - 24	85 %	2.06	1-8	15 %	10 %	75 %
Him-52 Mutant	55 %	1.27	1-3	95 %	2.32	1-7	0 %	40 %	55 %

Table 7.6.2 – Muscles Missing or Duplicated in Mef2 gain-of function muscle phenotypes

	Muscles Missing in > 50 % Embryos	Muscles Missing in 25-49% Embryos	Muscles Missing in 10-24% Embryos	Shape Defects in >75 % Embryos	Shape Defects in 50-74% Embryos	Muscles Duplicated in >20% Embryos
UAS Mef2 High (Nguyen) x *Mef2 Gal4* (25°c)	DT1, LT4, VA1	DA1, DO2, DA2, LL1, LT1, LT2, LT3, LO1, VL4, VO4, VO6	DA3, DO5, SBM, VL1, VL3, VA2, VO3			DO1, LT1, LT3, LT4, VA3
UAS Mef2 Low (10T4A) x *Mef2 Gal4* (29°c)	-	DO4	DA3, VO4	VA3	DO3, VT1, VA1, VO4	DO1, DT1, LT1, LT2, LT3, VA3
Zfh1-2 Mutant	VO4	DO3, LO1, VL4, VO5, VO6	DA1, DA2, DO4, LT1, LT3, LT4, VL1, VL2, VL3, VO2	-	VT1, VA1, VA2, VA3, VO4, VO6	LT1, LT2, LT3, VA3
Him-52 Mutant	-	-	VO6			DO1, DA1, LT1, LT2,

Table 7.6.3 – Muscle phenotype comparison of Mef2 over-expression, Zfh1 loss of function and Him loss of function

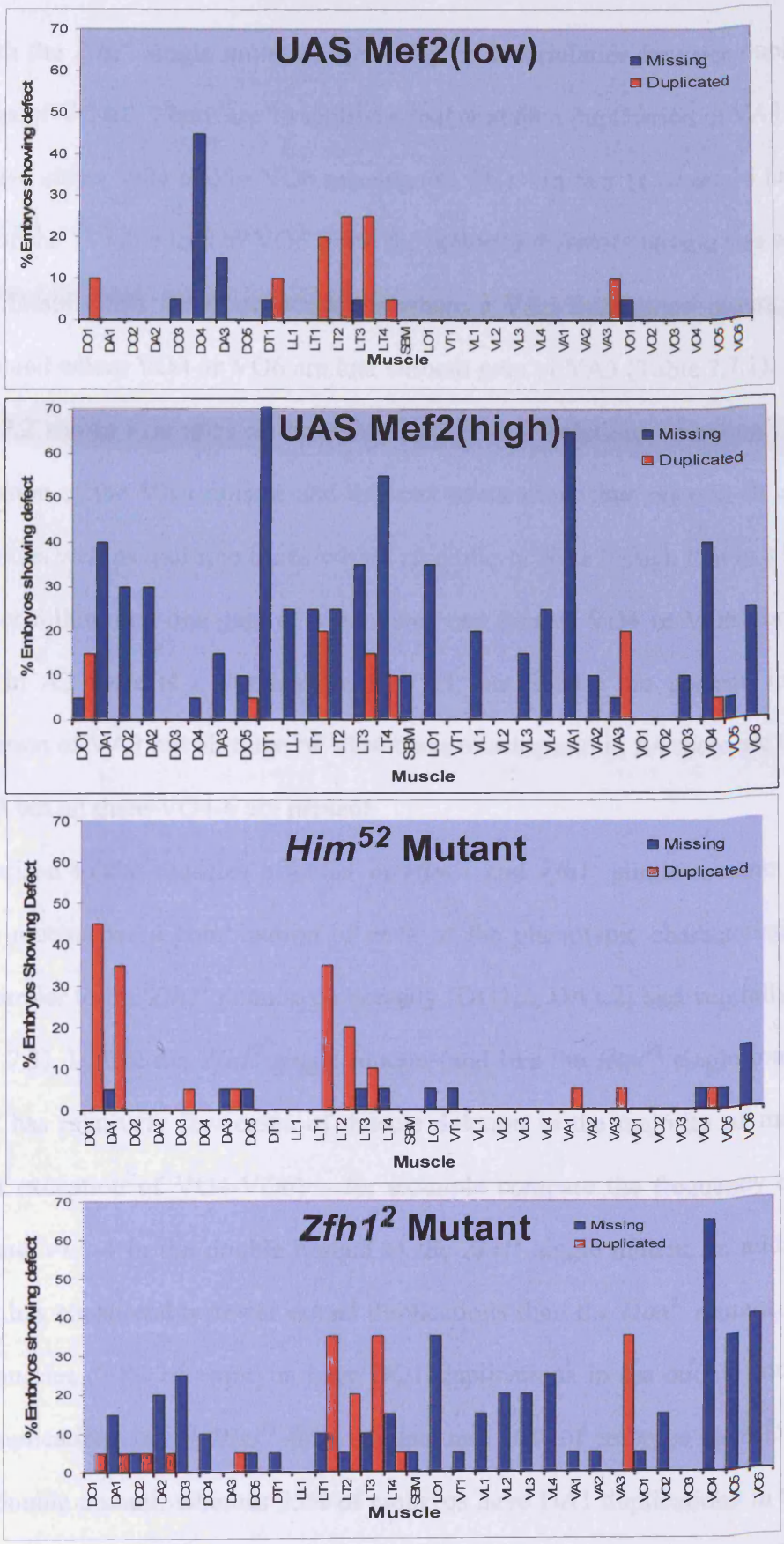

FIG 7.6.5 Muscles missing or duplicated in Mef2 over-expression, *Him*^{52} mutant and *Zfh1*^{2} mutant embryos.

As with the *Zfh1*^{2} single mutants, there may be a correlation between duplication of VA3 and loss of VO4/6; There are 14 embryos that contain a duplication of VA3 and of these 12 also have either VO4 and/or VO6 missing (85.7%) – in fact 11 of the 14 have loss of VO4 and 9 of the 14 have loss of VO6 (with the majority therefore having loss of both VO4 and VO6). Despite this there are occasions where a VA3 duplication occurs without loss of VO4-6 and where VO4 or VO6 are lost without gain of VA3 (Table 7.7.1).

FIG 7.7.2 shows examples of these duplications and deletions occurring. There is distinct duplication of the VA3 muscle and this can occur more than once in an individual hemi-segment as well as multiple times within an embryo. Note though that in a hemi-segment it does not follow that one gain of VA3 gives one loss of VO4 or VO6, for example in the figure in A2 there is a duplication of VA3, but VO4-6 are present, in A3 there is a duplication of VA3 but all three of VO4-6 are missing and in A4 there are two duplications of VA3 but all three VO4-6 are present.

Comparison to the muscles affected in *Him*^{52} and *Zfh1*^{2} single mutants shows that the double mutant has a combination of each of the phenotypic characteristics, though it is more similar to the *Zfh1*^{2} phenotype dorsally (DO1,2, DA1,2) and ventrally (VA3, VO4-6) (FIG 7.7.3). Unlike the *Zfh1*^{2} single mutant (and like the *Him*^{52} single mutant) the double mutant has relatively few cases of muscle deletion in the majority of muscles (with the distinct exception of VO4-VO6) – for example compare the frequency of loss of DO3, LO1, and VL1-4 in the double mutant to the *Zfh1*^{2} single mutant. In addition the double mutant has considerably fewer dorsal duplications than the *Him*^{52} mutant in the DO1 and DA1 muscles (20% of embryos have DO1 duplications in the double mutant, 45% have DO1 duplications in the *Him*^{52} single mutant and 10% of embryos have DA1 duplications in the double mutant, whereas 35% of embryos have DA1 duplications in the *Him*^{52} single mutant FIG 7.7.3). Possibly the most striking difference between the *Him*^{52} ; *Zfh1*^{2} double

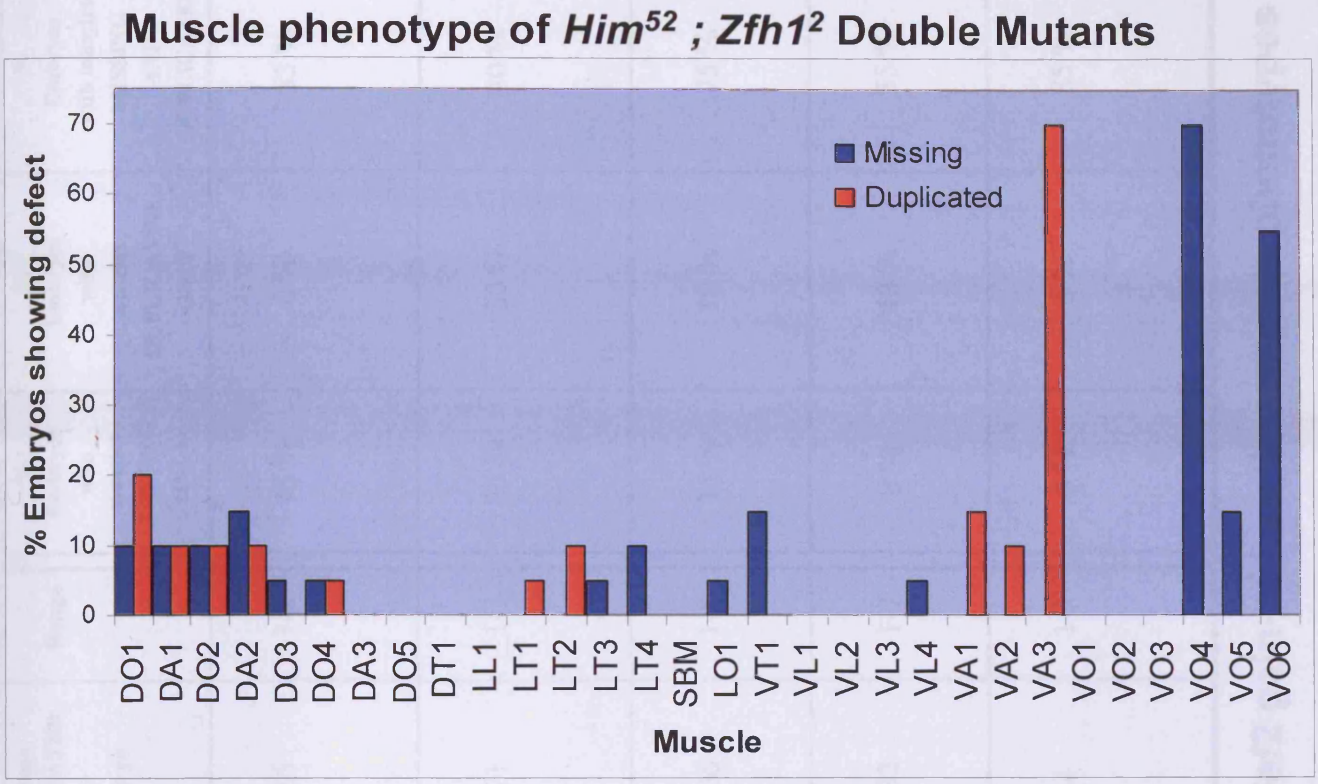

FIG 7.7.1 Muscles missing or duplicated in *Him*^{52} ; *Zfh1*^{2} Double Mutants

Graph showing the percentage of *Him*^{52} ; *Zfh1*^{2} double mutant embryos that show at least one example in hemi-segments A2-A4 of muscle loss or muscle duplication for each of the thirty individual somatic muscles. Blue represents missing muscles, red represents duplicated muscles. Notice that certain individual muscles such as VA3 solely duplicated, whereas others, such as VO4-VO6 are only ever missing in the embryos scored. There are also other muscles, which appear unaffected (in terms of muscle loss or duplication) and others which have similar percentages of embryos with that muscle either lost or duplicated (e.g DO2).

Cross	% Embryos with muscles MISSING	Average MISSING per embryo	Range	% Embryos with muscles DUPLICATED	Average DUPLICATED per embryo	Range	% Embryos with muscles MISSING *ONLY*	% Embryos with muscles DUPLICATED *ONLY*	% Embryos with muscles MISSING *AND* DUPLICATED
UAS Mef2 (Nguyen) X *Mef2 Gal4*	100 %	8.8	1-18	60 %	1.55	1-2	45 %	0 %	55 %
UAS Mef2 (10T4A) X *Mef2 Gal4*	65 %	1.69	1-3	70 %	1.71	1-3	25 %	30 %	40 %
Zfh1 – 2 Mutant	90 %	6.05	1 - 24	85 %	2.06	1-8	15 %	10 %	75 %
Him-52 Mutant	55 %	1.27	1-3	95 %	2.32	1-7	0 %	40 %	55 %
Him-52* ; *Zfh1 – 2 Double Mutant	85 %	3.7	1 - 9	90 %	2.4	1-7	0 %	5 %	85 %

Table 7.7.2 – Muscles Missing or Duplicated in Mef2 gain-of function muscle phenotypes

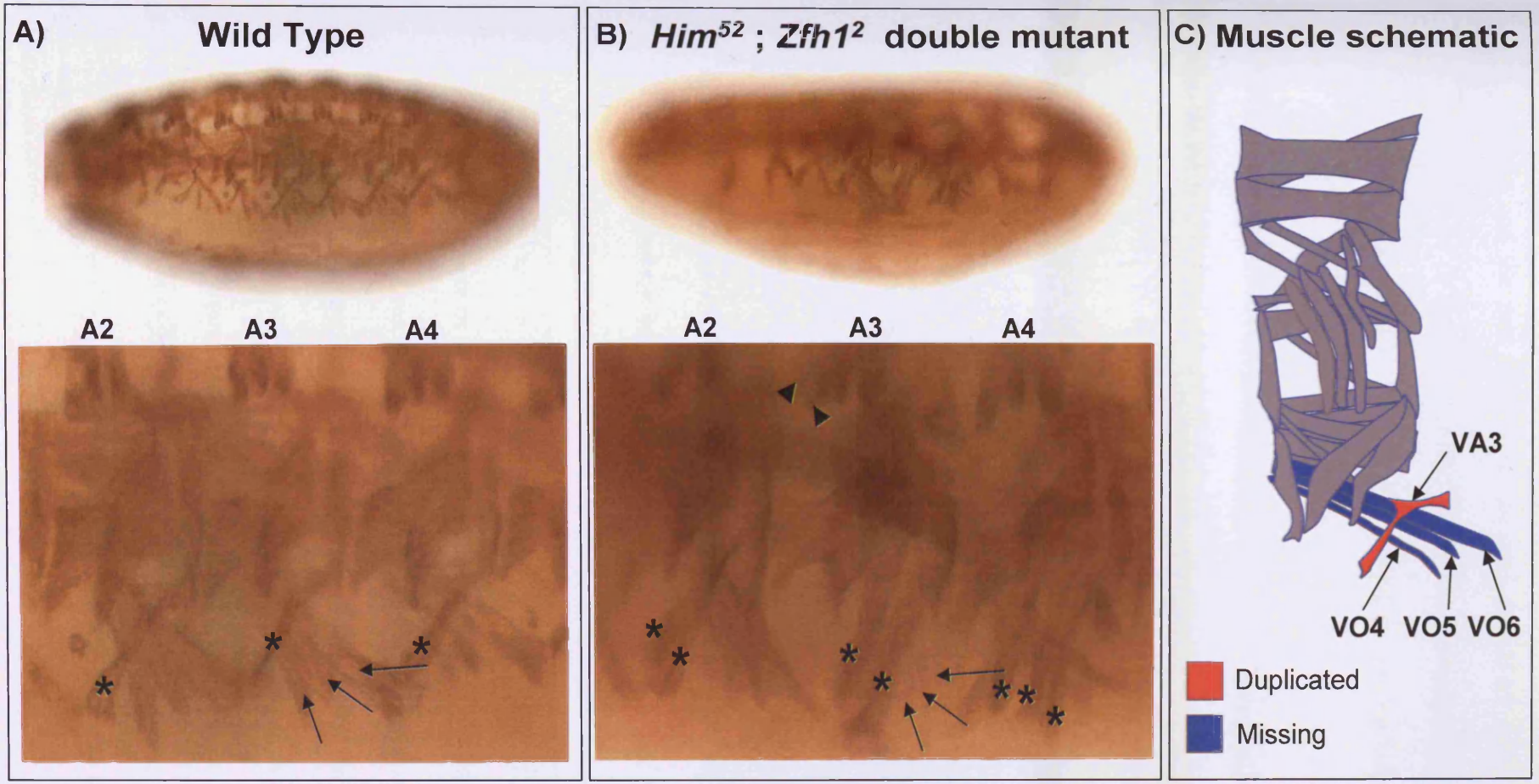

FIG 7.7.2 – *Him*^{52} ; *Zfh1*^{2} double mutants muscle phenotype

Examples of duplication and deletion of muscles in the *Him*^{52} ; *Zfh1*^{2} double mutant muscle phenotype. The VA3 muscle is frequently duplicated; there should only be one copy of the muscle per hemi-segment (see asterisks in wild type A and muscle schematic of a single hemi-segment in C) but can be seen here duplicated once in the A2, once in the A3 and twice in the A4 hemi-segments of this *Him*^{52} ; *Zfh1*^{2} double mutant embryo (asterisks in B). In addition the ventral VO4-6 muscles are frequently missing; in wild type embryos there is one of each of these muscles per hemi-segment (indicated by arrows in A and shown in the muscle schematic C), however this mutant embryo has all three missing in hemi-segment A3 (arrows in B). The VO4 or VO6 muscles are often missing in embryos that have a VA3 duplication (see data Table 7.7.2). This particular mutant embryo also contains a duplication of LT1 and LT2 in A3 (arrowheads, out of focus), but it should be noted that duplications of these muscles in the double mutant is considerably less frequent than duplication of the VA3 muscle.

Wild type embryos are Oregon R. Double mutants were first selected by staining against Ftz LacZ to ensure homozygosity of the Zfh1 mutant allele. Muscles were stained with anti β3-tubulin antibody. All experiments performed at 25°C.

mutant and the two single mutants (and also UAS Mef2 FIG 7.6.1) is the reduction of duplications in the LT muscles; in the double mutant LT1 is only duplicated in 5% of embryos, LT2 in 10% of embryos and LT3 is not duplicated, whereas in the *Him*^{52} single mutant LT1 is duplicated in 35% of embryos, LT2 in 20% and LT3 in 10%, similarly the *Zfh1*^{2} single mutant LT1 is duplicated in 35% of embryos, LT2 in 20% and LT3 in 35% (FIG 7.7.3) (for UAS Mef2 low LT1 is duplicated in 20% of embryos, LT2 in 25% and LT3 in 25%). Despite this, it appears that the frequency of duplication has not changed when comparing the *Him*^{52} mutant to the *Him*^{52}; *Zfh1*^{2} double mutant, but the muscles that get duplicated has shifted – to become predominantly VA3 in the double mutant. For example the % of embryos showing a duplication, the average number of duplications and the range of duplications per embryo are very similar for the *Him*^{52} mutant and the *Him*^{52}; *Zfh1*^{2} double mutant (95% of embryos, 2.3 muscles per embryo and 1-7 muscles per embryo for *Him*^{52} and 90% of embryos, 2.4 muscles per embryo and 1-7 muscles per embryo for the *Him*^{52}; *Zfh1*^{2} double mutant) (Table 7.7.1), but instead of the duplications occurring predominantly in DO1, DA1, LT1 and LT2 as in the *Him*^{52} mutant, they occur predominantly in VA3 (and DO1) in the *Him*^{52}; *Zfh1*^{2} double mutant (FIG 7.7.3).

In addition to the duplication of VA3 and deletion of VO4/VO6 another frequently occurring aspect to the *Him*^{52}; *Zfh1*^{2} double mutant phenotype is the occurrence of stray muscular structures which cross the ventral midline of around of 75% of embryos. These thin structures completely cross the midline and are quite deep within the embryo being situated just ventrally to the visceral muscle as opposed to closer to the surface as with the regular somatic muscles. Focussing on the microscope shows that they are not folds of the gut but are individual structures. FIG 7.7.4 shows an example of these stray muscles. They are not seen in wild type embryos, *Him*^{52} single mutants or *Zfh1*^{2} single mutants.

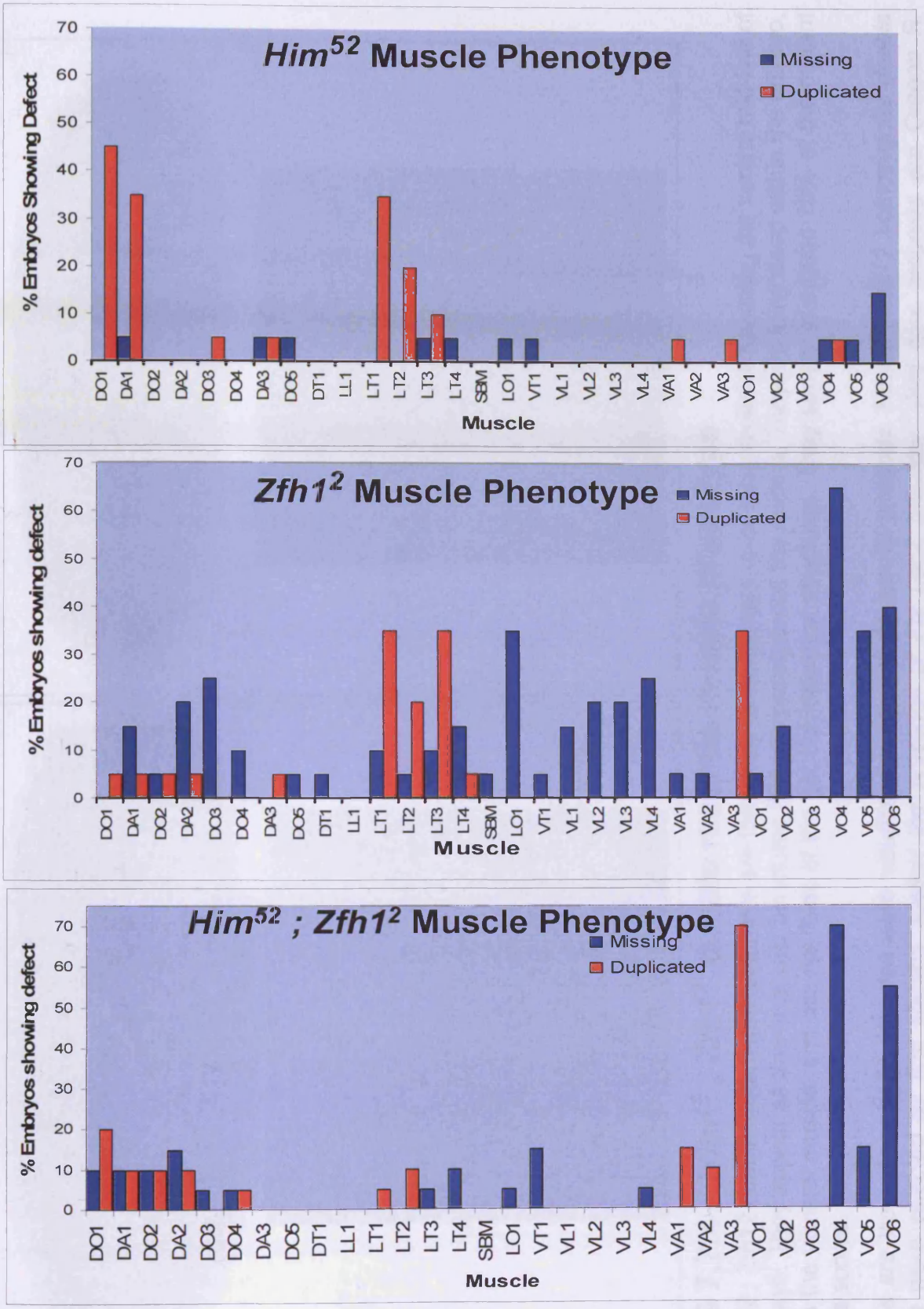

FIG 7.7.3 Comparison of muscles missing or duplicated in *Him*^{52} mutant, *Zfh1*^{2} mutant and *Him*^{52} ; *Zfh1*^{2} double mutant embryos.

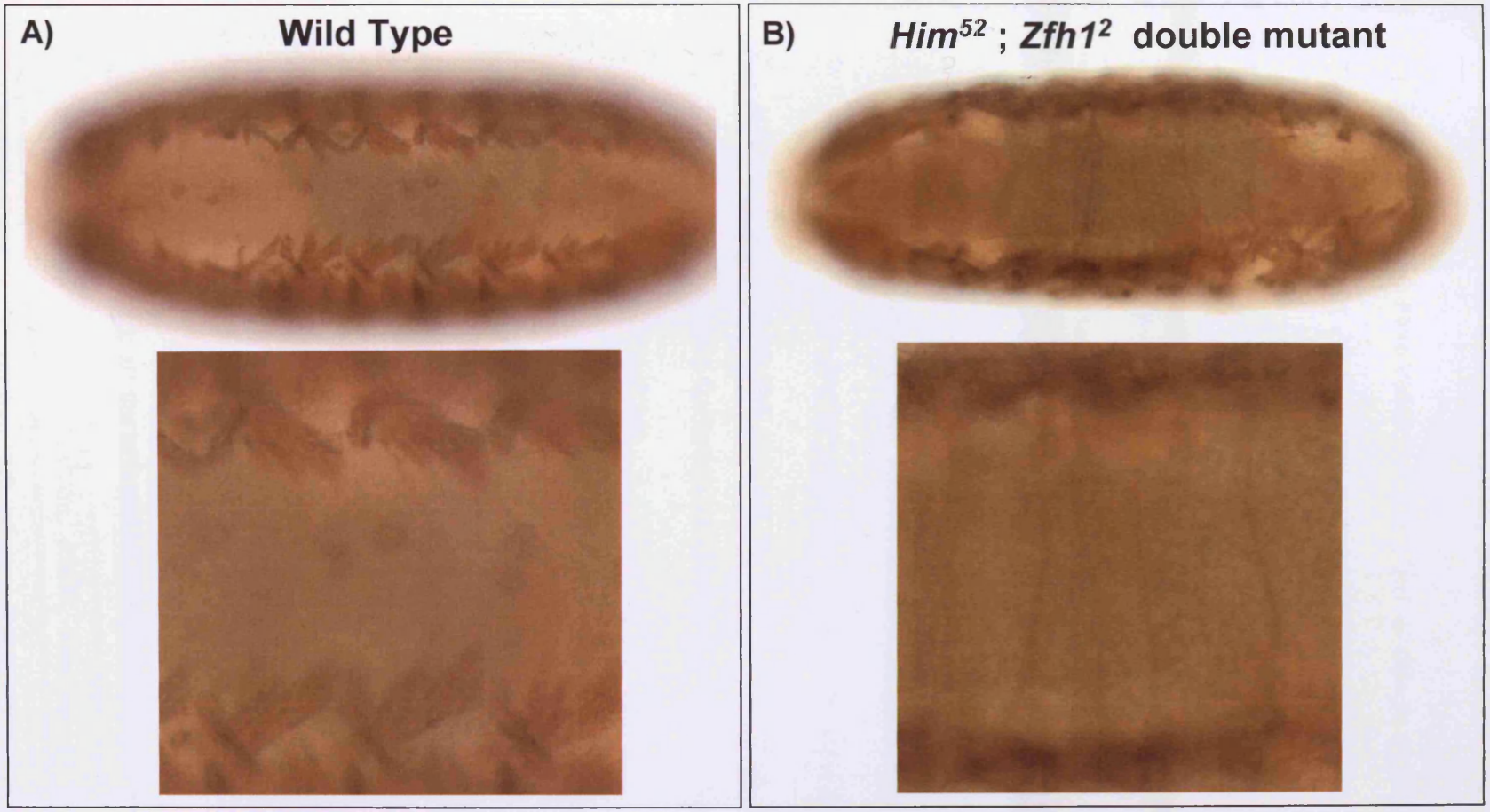

FIG 7.7.4 – *Him*^{52} ; *Zfh1*^{2} double mutants muscle phenotype

In *Him52 ; Zfh12* double mutant embryos there are frequently what appears to be stray muscles spanning the ventral mid-line of the embryo. They appear as thin muscular structures that completely cross the midline. They are fairly deep within the embryo, beneath the visceral muscle, and are not folds of the gut but individual structures. They appear in around 75% of the mutant embryos scored.

Embryos are viewed ventrally. Muscles were visualised using anti β3-tubulin antibody. Him52 ; Zfh12 homozygous double mutants were selected by first staining against the presence of Ftz LacZ balancer. Wild type embryos are Oregon R. Experiment performed at 25°C.

7.8 General Discussion; Mef2, Him and Zfh1.

In this chapter I have confirmed that Zfh1 is able to repress Mef2 at the RNA level and over-expression of Zfh1 or Him in the Mef2 pattern causes a severe reduction in somatic muscle formation. Detailed analysis of the individual somatic muscles affected shows that Him and Zfh1 have the same effect on terminal somatic muscle differentiation and that the somatic muscles can be divided up into types that are more easily lost and those that are most frequently present; an observation that has been shown previously in this work with other experimental conditions that cause a reduction in Mef2 activity, such as the Mef2 dominant negative, Mef2 RNAi and *Mef2* alleles (Chapter 3).

As discussed previously, this reinforced the idea that individual somatic muscles, or the muscle founders and identity genes that define them, have different requirements for Mef2 activity. With muscles that are lost most frequently being the ones that require the most Mef2 for their correct formation; a reduction in only a small amount of Mef2 activity results in their failure to form.

Conversely the muscles that appear unaffected under conditions of that reduce Mef2 activity, have a very low requirement for Mef2 activity as even in conditions of severe Mef2 activity reduction these muscles still form. One wouldn't expect these muscles to be Mef2-independent however, as they do not develop in complete absence of Mef2 such as seen in the Mef2 null (Bour et al, 1995; Lilly et al, 1995), and in fact one could interpret this low level of Mef2 activity required for their formation as a possible measure of the muscles' importance to the final musculature.

For example, though all the somatic muscles are similar with respect to their physiological characteristics (Bate and Rushton, 1993), they clearly have very distinct shapes and positions within the embryo. When one considers the structure of some of the individual low and high Mef2 requirement muscles there does seem to be some structural similarities

that emerges. High Mef2 requirement muscles such as DO3, DO4, VO4 and VO6 are all very similar in shape and size; being long and thin and extending diagonally across the embryo in a dorso-anterior to ventro-posterior direction.

Low Mef2 requirement muscles, however, such as DT1, VT1 and VT1 and VA2 are broader, bulky muscles that extend in an anterior to posterior direction.

From this one can wonder whether there is any advantage in these muscles having a Low Mef2 requirement. Are the muscles in this second subset more integral to the structure or function of the musculature? Would loss of muscles from the first subset be more easily tolerated by the larvae? Or from a more basic body building plan are the Mef2 low requirement muscles needed to be laid down earlier to as a basis to build up the other muscles in the structure.

So from this we could say that Mef2 requirement could either be due to the importance or the timing of formation of a muscle. Studies which delete single muscles in the musculature by either specific Gal4 targeted deletion or founder cell ablation may be a means of assessing the importance of a muscle in the larval life.

Though this provides insight into the requirements of Mef2 for individual muscles it is the Mef2-gain of function experiments that provide a novel insight into a role for Mef2 in patterning.

The observation that a distinct subset of muscles is reliably duplicated under conditions of Mef2 gain of function has never been described before. It suggests that Mef2 plays a role in their normal specification and that tight regulation of Mef2 must be maintained to ensure that additional muscles are not made. Thus though it has been established that Mef2 mutants can specify a number of founder markers (Bour et al, 1995; Lilly et al 1995), my

results suggest that there is Mef2 input into at least a subset of the founders and that this subset are the founders that define the DO1, DA1, LT1, LT2 and VA3 muscles.

An explanation for this at the founder cell level may be that Mef2 targets the activation of the specific identity gene responsible for this muscle fate. For example with the DO muscles it may be that Mef2 plays a role in the regulation of Kruppel; as shown in my work previously (Chapter 6) Him mutants and Him over-expression affects the number of Kruppel positive founder cells and it already known that Kruppel mutants and over-expression can cause the duplication or gain of this muscle (Ruiz Gomez et al, 1997), in addition Kr alongside a number of the other muscle identity genes has been identified as a potential Mef2 target (Sandmann et al, 2006).

In a similar vein the identity gene *Apterous* may be a Mef2 target suitable for investigation of the LT muscle duplications. *Ap* is expressed in LT1-4 and its over-expression causes LT duplication, whereas its loss-of-function causes LT loss (Bourgouin et al, 1992) and like Kr it appears as a potential Mef2 target (Sandmann et al, 2006). .

The idea of Mef2 playing a role in the fate of the founders may shed some light on the other observations made in Mef2 gain and loss of function conditions in my thesis. For example the identity gene S59 / Slouch is expressed in the DT1, VA2 and VT1 muscles (Knirr et al, 1999) and these three muscles are all consistently found in the subset most resistant to reductions in Mef2 activity. One may easily imagine a scenario where such "Low Mef2 Requirement Muscles" like DT1, VA2 and VT1 might be regulated by a "Low Mef2 Requirement Gene". Slouch has already been identified as having Mef2 bind to sites near its gene locus, implicating it as a potential Mef2 target (Sandmann et al, 2006), if it could be shown that Slouch was such a low requirement gene in a similar way to other

established Mef2 targets (Elgar et al, 2008) then one would be able to build upon a model for Mef2's action within muscle development. However, the model would not be as simple as "Low Mef2 Requirement Gene" gives "Low Mef2 Requirement Muscle", as despite Slouch being a potential Mef2 target, it is well established that Slouch expression in founder cells occurs in Mef2 mutants (Lilly et al, 1995) so other factors must play a role in the initial specification. Also for muscle that express a combination of identity genes a simple model like this for Mef2 activity would not suffice.

This model for the formation of founder to muscle would have Mef2 at the head of a program of muscle specific transcriptional pathways; the formation of a specific muscle would be conducted by the identity gene that Mef2 activates within the original founder and the aspects of fusion and guidance would be co-ordinated by other as yet identified transcription factors (though one such factor could be meso18E for guidance – see next chapter). These specific muscle identity genes would require certain levels of Mef2 activity to be expressed or regulated. To ensure appropriate levels of Mef2 activity are established to activate these identity genes, specific repressors that act upon Mef2 at the transcriptional level (Zfh1) and the protein level (Him) would be in place and, once the expression of the repressors is established a fine tuning of Mef2 activity can be achieved through Mef2 auto-regulation and the activation of its own repressor, Him.

meso18E

8.1 Introduction

Originally it was thought that Mef2 acted at the later stages of myogenesis; as it was shown to directly regulate the expression of a number of key structural components of the differentiated musculature (e.g Tropomyosin (Lin et al, 1996) and Paramyosin (Arrendondo et al, 2000) and the Mef2-binding site was identified in nearly all known skeletal muscle genes (reviewed in Black and Olson, 1998). However, a study in *Drosophila* by Dr.Taylor, showed that Mef2 also acted early on in the differentiation program, regulating the expression of a previously uncharacterised gene, *meso18E* (Taylor, 2000).

This study initially involved a subtractive hybridisation screen looking for genes with an early mesodermal expression pattern after subtractive hybridisation of cDNA isolated from *Twist* mutants and Wild Type embryos. From this, *meso18E* was identified as a Twist dependent gene whose expression pattern closely resembled that of Mef2 (Shown in FIG8.1.1 and Taylor, 2000).

meso18E is expressed in the developing mesoderm and in the precursors of the somatic, visceral and cardiac muscle and subsequently it is expressed in the somatic muscle, visceral muscle and the cardioblasts of the heart in an expression pattern that resembles that of *Mef2* throughout myogenesis (Taylor et al, 1995; Taylor, 2000) An RNA in-situ hybridisation profile for meso18E is shown in FIG 8.1.1 (Images taken from Taylor, 2000 Fig.3).

In his study, Dr.Taylor identified a nuclear localisation sequence in meso18E which suggests it to be putative nuclear protein. He also revealed a role for Mef2 in the regulation of *meso18E*; an RNA in-situ using *meso18E* probe in *mef2* mutants shows that *meso18E* expression is reduced in the visceral muscle precursors (from St11) and the somatic muscle

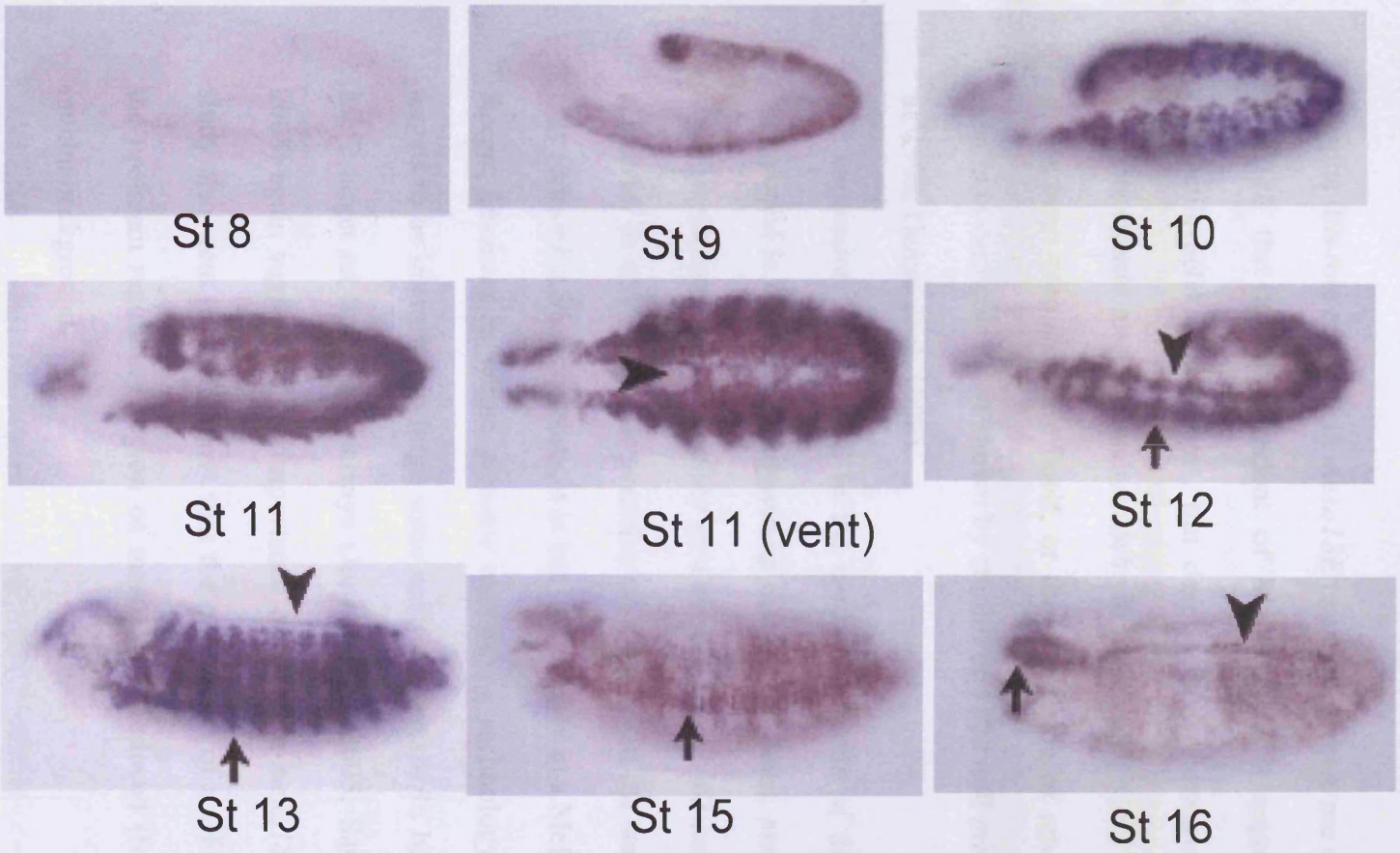

FIG 8.1 *meso18E* wild type RNA in-situ hybridisation pattern

These images are taken from Taylor, 2000 FIG5 and highlight expression in the mesodermal crossbridges of (St11 arrowhead), somatic primordia (St12 arrow),visceral primordia (St12 arrowhead), heart (St13 arrowhead), developing somatic muscle (St13 arrow), somatic muscle (St15 arrow), pharyngeal muscle (St16 arrow) and cardioblast s(St16 arrowhead).

precursors (from St12) and ectopic expression of Mef2 using a *Da*-Gal4 driver results in ectopic expression of meso18E in that pattern (Taylor, 2000).

Despite this role of Mef2 in *meso18E* expression, there are also aspects to the expression of *meso18E* that are independent of Mef2. *Mef2* is expressed in the cardioblasts, the contractile cells of the heart, but despite being necessary for the expression of some terminal muscle markers such as *Mhc* in these cells, Mef2 is not needed for the formation of the heart tube structure itself, or the expression of other muscle markers such as *β3-tubulin* in cardioblasts, as shown by studies of *Mef2* null mutants (Bour et al, 1995; Lilly et al, 1995; Damm et al, 1998).

The expression of *meso18E* in the cardioblast cells of the heart in a *Mef2* null mutant background is unaffected, suggesting that, in the heart, *meso18E* has a Mef2 independent aspect to its expression, possibly in a similar way to *β3-tubulin.* (Taylor, 2000; Damm et al, 1998). In addition, the expression of *meso18E* in the somatic and visceral mesoderm is only *reduced* in *Mef2* mutants, it is not lost entirely in a Mef2 null mutant background.

Recent advances in whole genome microarray technology have allowed potential Mef2 targets to be identified in large scale analyses. *meso18E* has been identified as a potential Mef2 target on three microarrays (Junion et al, 2005; Sandman et al, 2006; Elgar et al 2008) again suggesting the importance of Mef2 in *meso18E* regulation. The Junion et al study also went to on to show that the expression of a GFP reporter construct containing the upstream regulatory region of meso18E is reduced (but not lost entirely) in a *Mef2* mutant background.

However, it should be stressed that none of this work outlined above shows that Mef2 directly activates meso18E.

Despite knowing the expression pattern of *meso18E* and that Twist and Mef2 play a role the expression of this putative nuclear protein, little else is known about the structure and function of the gene and any role it may have in muscle development.

Consequently as part of my PhD I wanted further investigate the regulation of the gene expression and explore the role of *meso18E* through bioinformatics, gene over-expression and loss of function studies.

8.2 Expression Regulation

As outlined above there are both Mef2 dependent and Mef2 independent aspects to *meso18E* expression. I wanted to investigate the expression regulation of *meso18E* to determine whether Mef2 can be shown to activate *meso18E* directly and also to attain any insight into the Mef2 independent aspect of meso18E expression, which may suggest potential players involved in an alternative pathway to Mef2 action in muscle differentiation.

To investigate the expression regulation of *meso18E* I designed GFP reporter constructs corresponding to the non-coding regions around the gene. In a large number of genes the regions immediately upstream are the source of regulation and thus are the most obvious place to begin an investigation into transcriptional regulation. Because of this I concentrated my analysis of meso18E regulation on the region corresponding to all of the non-coding DNA immediately upstream of meso18E and up to the start the next gene, CG12531, and also the meso18E gene itself. I then divided up these regions and selected fragments for analysis upon the basis of phylogenetic footprinting. This process makes use of the complete genomic sequences established for a number of distantly-related species and through alignment and comparison of equivalent DNA regions across these species

regions can be identified that are evolutionarily conserved. Any conservation in regions of non-coding DNA, (where there is a greater degree of tolerated mutation and sequence variation than coding DNA), suggests that this site may be of particular importance, and as such is often indicative of the sites of key transcription factor binding sites involved in the regulation of the gene (for review see Zhang and Gerstein, 2003).

FIG 8.2.1 shows a phylogenetic footprint generated by the Vista tools program (Frazer et al, 2004) for the *meso18E* region. Each alignment shows the sequence comparison of a particular *Drosophila* species to *Drosophila melanogaster.* The species that are more closely related to *D.melanogaster* are shown at the top of the diagram and these show the greatest degree of sequence conservation. The species that are farther removed in evolutionary terms to *D.melanogaster*, such as *D.virilis* and *D.mojavensis* show considerably less sequence similarity (Russo et al, 1995), but it is the peaks of conservation in the non-coding DNA that do remain across evolutionary time that are of potential significance (Zhang and Gerstein, 2003; Dickmeis and Fuller, 2005).

In addition to this I also searched the potential meso18E regulatory region for Mef2 binding sites using the established consensus sequence YTAWWWWTAR (Andres et al, 1995) and found five.

8.2.1 Design of GFP Reporter constructs

FIG 8.2.2a shows how I divided the *meso18E* region into reporter constructs. Note how the orientation of the region differs from the orientation of the phylogenetic footprint figure; the reporter construct map depicts the region with the gene of interest in the conventional 5' to 3' orientation, whereas the same region is depicted in the opposite way in the phylogenetic footprint, because Vista orientates the comparisons in the direction that the *D. melanogaster* genome was sequenced.

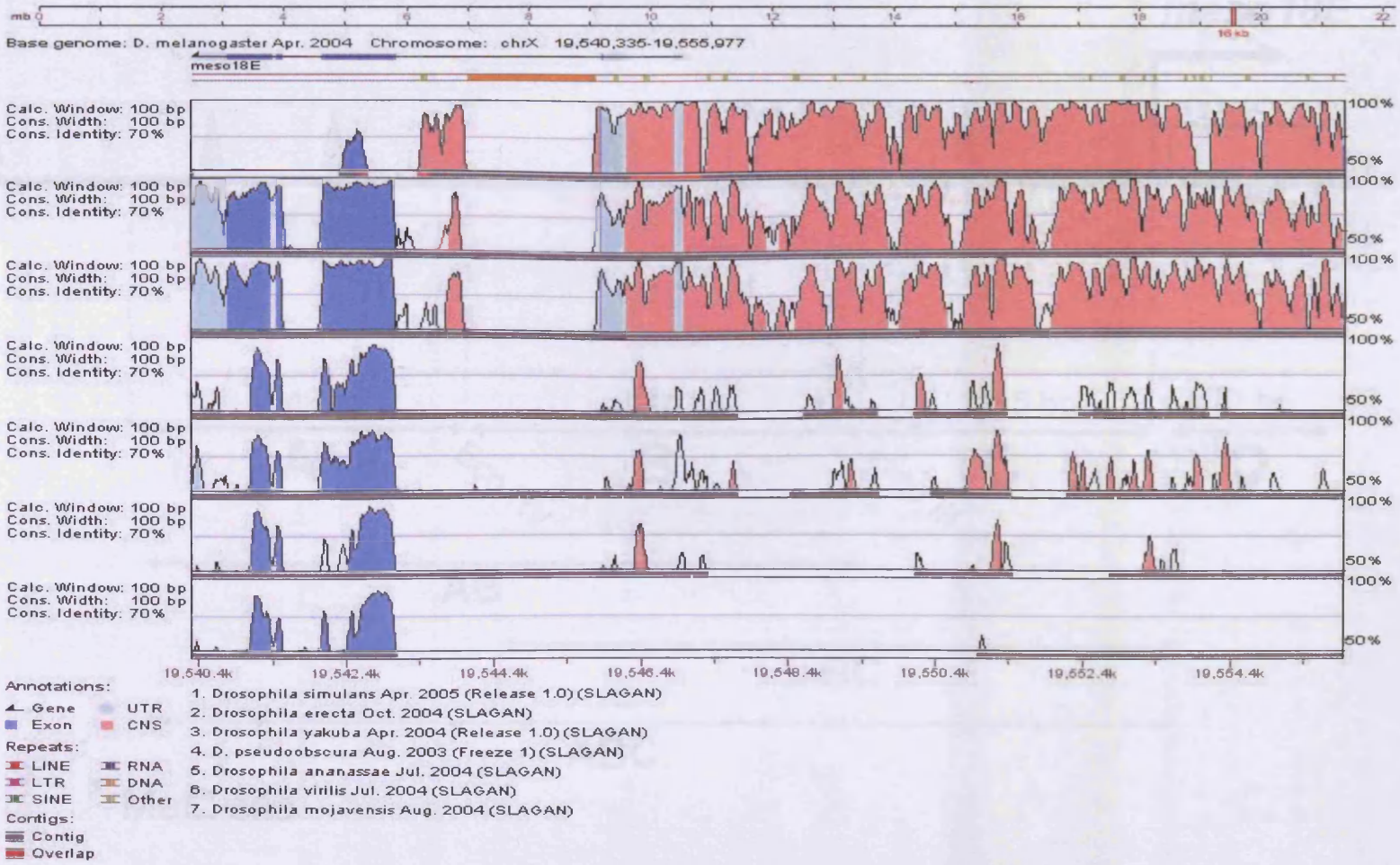

FIG 8.2.1 Phylogenetic conservation footprint for the *meso18E* regulatory region

Vista tools genome comparison (Frazer et al, 2004) of aligned genomic sequences for different *Drosophila* species. Red peaks correspond to regions of conservation in non-coding sequence. Dark blue represents exons of the meso18E Gene and turquiose represents Untranslated Regions of the meso18E gene. Each row represents a different species alignment relative to the meso18E region of *Drosophila melanogaster*. The species lower down the graph are more distantly related to *D. melanogaster,* (Russo et al, 1995), suggesting that any conservation in the non-coding region in these alignments may have a greater functional significance (Zhang and Gerstein, 2003).

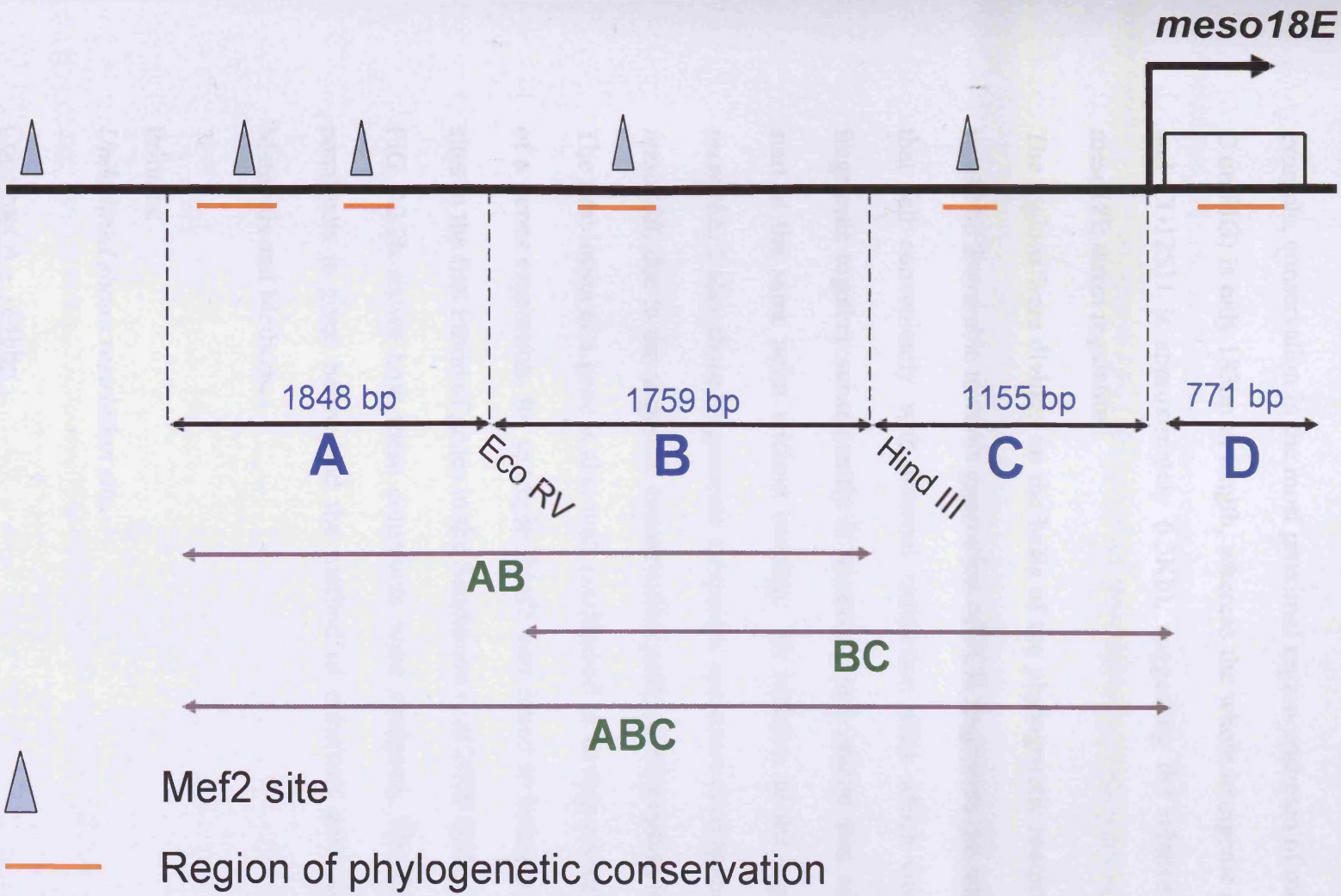

FIG 8.2.2a Reporter construct analysis for the *meso18E* regulatory region

I divided the upstream region of meso18E into different regions for the generation of GFP reporter constructs for transcriptional regulation analysis of the meso18E gene. I based the division upon the identified peaks of phylogenetically conserved regions identified by species sequence alignment (FIG 4.1.2) In addition I also searched the region for potential Mef2 sites using the sequence binding motif YTAWWWWTAR. Reporters A, B and C lie upstream of the meso18E gene. Reporter D lies in the first intron of the gene, but shows some degree of phylogenetic conservation. Sequence analysis shows that all of the Mef2 sites included in the constructs lie within regions that are phylogenetically conserved.

The regions of phylogenetic conservation are highlighted as orange lines positions of the Mef2 sites are shown in the figure as blue triangles. Note how the Mef2 sites fall into the regions of conservation even though the regions of conservation can be relatively small (for example, conservation in the most proximal region upstream of meso18E (within Construct C on FIG) is only 183bp in length, whereas the whole intergenic region between meso18E and CG12531 is approximately 6.5Kb), suggesting the relative importance of Mef2 in meso18E direct regulation.

The regions were divided on the basis of the phylogenetic footprinting, reporter sizes that would be favourable towards generation of PCR fragments (i.e not greater than 2-3Kb) and that fell conveniently with internal restriction sites which could be used to fuse the fragments together subsequently if necessary and ensure that adjacent constructs end or start at the same point without overlap. In addition to the region directly upstream of *meso18E*, I also chose to generate a reporter construct corresponding to the first intron of *meso18E*, due to the sequence conservation peak corresponding to this region (FIG 8.2.2). The first intron of a gene is also well established as having responsibility for the regulation of a genes expression, for example, Mef2 was found to bound a significant proportion of sites in the first intron of genes in the Sandmann et al 2006 study.

FIG 8.2.2b shows how these constructs were designed. The Primer sequence for these constructs is given below and the method of construct generation can be found in the Materials and Methods.

Primers:

Underlined shows restriction site.

Construct A – 1848bp :

18E-A fwd:SphI GCATGCCAAGAATAAGAATCCACC Tm = 61.0°C

18E-A rev :BglII AGATCTTCGACTGGATAAAATCGGTC Tm = 61.6°C

Construct B - 1759bp :

18E-B fwd:BglII AGATCTGAAAGATTGAAAGATACAAGCAG
Tm = 61.0°C

18E-B rev:EcoRI GGAATTCGTATTAACAAAGTAATATCCAAGG
Tm = 61.0°C

Construct C – 1155bp :

18E-C Fwd (EcoRI) - GAATTCATTATACCCGCCTGTTGG Tm 61.1°C

18E-C Rev (BamHI) - GGATCCCGTTGCCGATACTAAC Tm = 62.1°C

Construct D – 771bp :

18E-C Fwd (BglII) – AGATCTCAGGACGGCGGACTAC Tm = 63.9°C

18E-C Rev (BamHI) - GGATCCTTTGTGACACTTAACGTCTAG Tm = 63.5°C

During my PhD I successfully generated reporter constructs and subsequent transgenic lines for the 1155bp region immediately upstream of the start site of *meso18E* and the 771bp region covering the first intron of the gene; meso18E C GFP pStinger and meso18E D GFP pHStinger respectively. (The difference between pStinger and pHStinger is that pHStinger contains a TATAA box, whereas pStinger doesn't. For reporter fragments that contain an endogenous TATAA box such as those immediately upstream of a gene start site, as in the 18E C fragment, the pStinger vector is used (Barolo et al, 2000)).

At least three transgenic lines were tested for each of these reporter constructs and representative lines are shown in the figures.

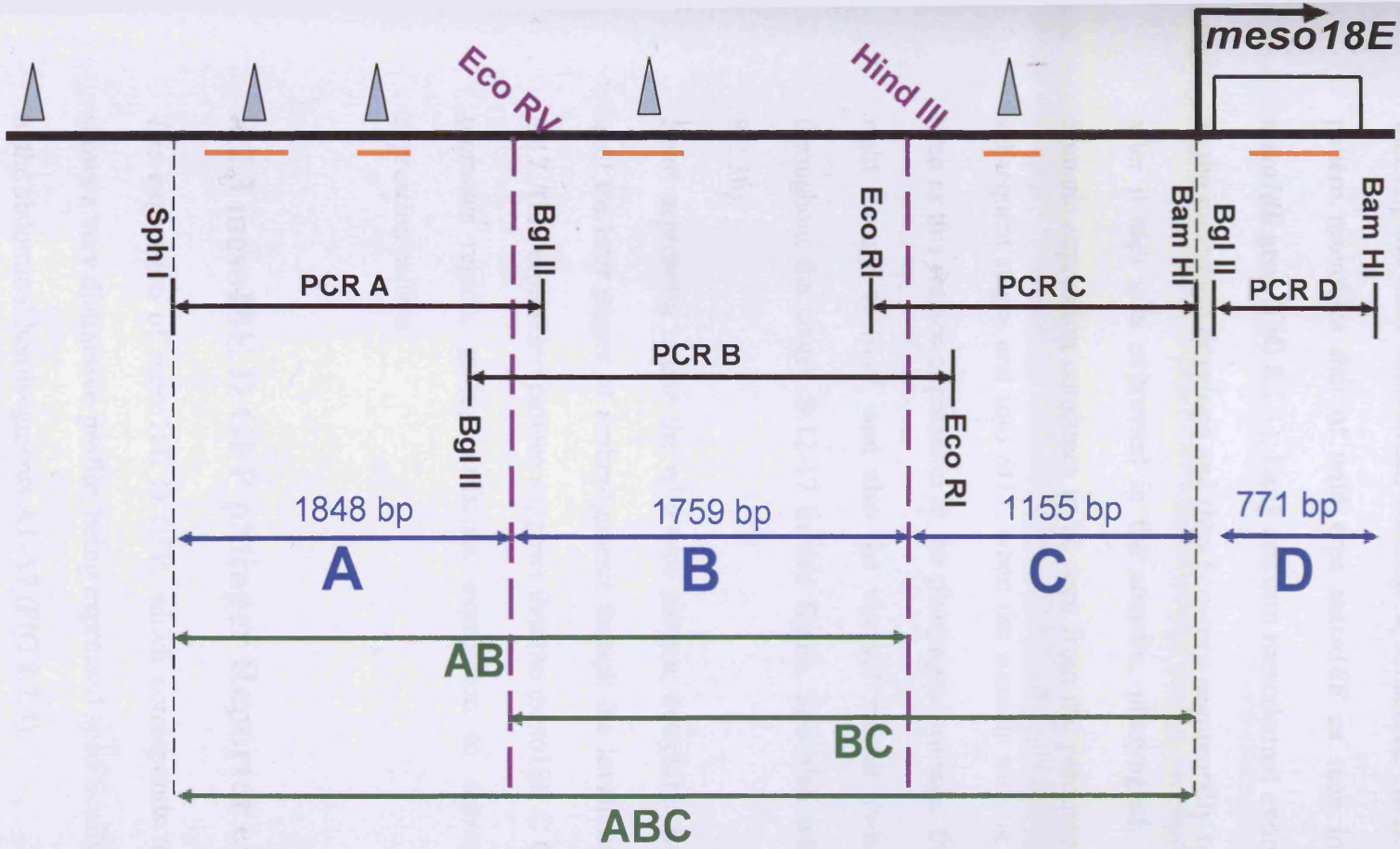

FIG 8.2.2b Generation of the reporter constructs for the *meso18E* regulatory region

I used two internal restriction sites, Eco RV and Hind III, (purple on diagram) that were unique to the region and compatible with the pStinger GFP or pH Stinger GFP vectors used. Primers were designed that overlapped these sites appropriately and introduced unique restriction sites at the end of the PCR fragment (Black on diagram) that allowed for cloning into the vectors in an appropriate orientation that would also allow for subsequent joining up of the fragments as required. On cloning, PCR fragments could then be cut with EcoRV and HindIII as necessary so that reporter constucts A, B and C would have no overlapping sequence as individual constructs (Blue on diagram). These fragments could then also be easily cloned together to generate the larger reporter constructs AB, BC and ABC (Green on diagram) if analysis of A, B, and C required it. As reporter D is a stand alone construct, the PCR fragment could be cloned directly into pH Stinger and used directly as a GFP reporter.

8.2.2 meso18E C GFP pStinger Reporter expression

FIG 8.2.3 shows the expression pattern for meso18E C GFP, the proximal region to the transcription start site, which contains a conserved Mef2 site within its sequence. The pattern resembles that of wild type *meso18E* as seen in the RNA in-situ against the *meso18E* gene (FIG 8.1.1). Early uniform mesodermal expression is seen, which continues as the mesoderm develops and then becomes segmentally repeated at around St10, shortly after it also gets expressed in the somatic, pharyngeal, visceral and heart precursors. Somatic expression continues to be seen from the precursors at St10 right through all the subsequent stages and into St17, when the somatic muscle has fully formed. At the same time as this we see expression in the pharyngeal muscle, from the precursors seen at St10 right through to St17, and also the visceral muscle (which can be seen out of focus throughout the stages St12-17 in this figure, and also when brought into focus in FIG 8.2.3b).

Heart expression is like the wild type pattern; detectable in the cardioblasts from St10 up until the later stages of embryogenesis though the levels of expression are quite weak by St17. This expression pattern suggests that the meso18E C GFP reporter may be a minimal promoter region, giving sufficient expression to represent the wild type *meso18E* expression pattern.

8.2.3 meso18E D GFP pStinger Reporter expression

The expression of meso18E D GFP, which corresponds to the first intron of *meso18E,* shows a very distinctive profile, being expressed specifically in small clusters of large cells in the abdominal hemisegments A1-A7 (FIG 8.2.4).

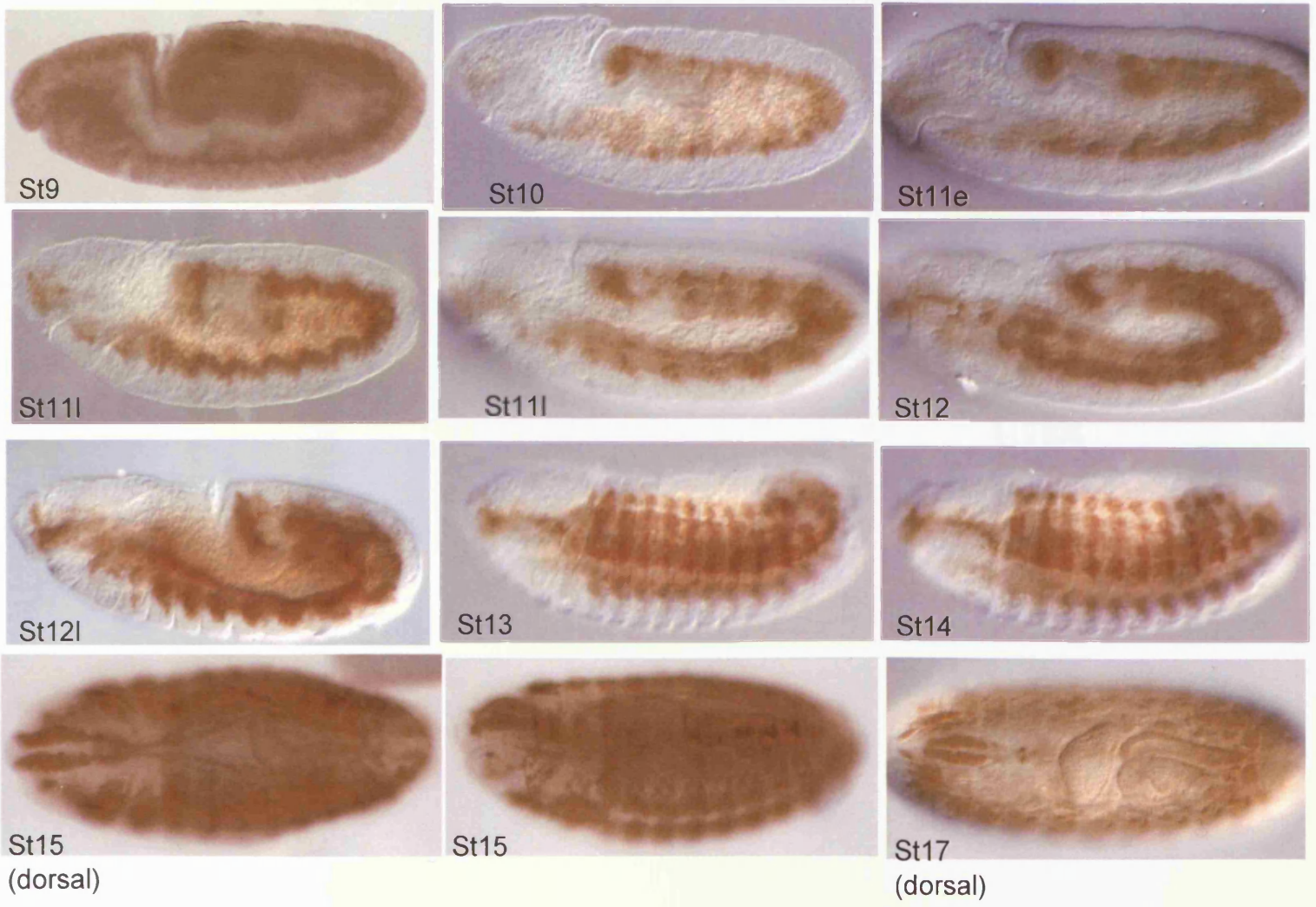

FIG 8.2.3a meso18E C GFP Reporter construct expression pattern mimics wild type meso18E

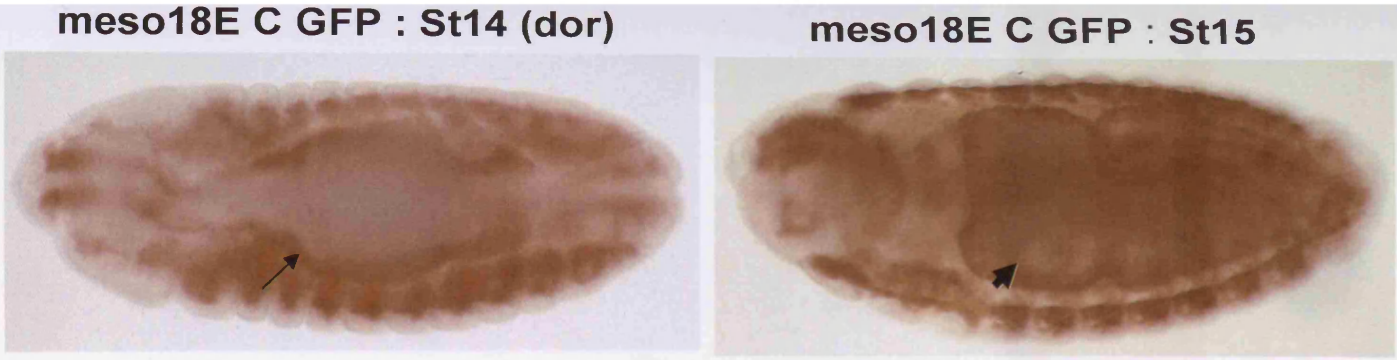

FIG 8.2.3b Examples of meso18E C GFP Reporter construct expression in the visceral muscle

The expression pattern of the meso18E C reporter fragment mimics (FIG 8.2.3a) mimic that of wild type meso18E expression (see in-situ FIG 8.1). Embryos are shown from St9-St17 and are representative. The line shown was one of three others tested, all that show the same pattern. GFP reporter construct pattern visualised using anti-GFP antibody.

FIG8.2.3b shows visceral expression in at St14 (arrow) and St15 (arrowhead) in this line

The staining of the cells is initially seen at St11 and continues through to St17. The large cells are in clusters of around 2-9 cells, which varies from embryo to embryo and hemi-segment to hemi-segment, but have an average of around 6 cells. The image in FIG 8.2.4 shows a representative St15 embryo for the reporter expression.

Initial description of similar cells in the Hartenstein Atlas of *Drosophila* Development (Hartenstein, 1993 and www.sdbonline.org/fly/atlas/00atlas.htm) suggested that these may be the oenocytes. Subsequent personal communication with Alex Gould, NIMR and Adi Salzberg, Technion, Israel and comparison to the Drifter LacZ pattern and Spalt localisation, which are both markers of the oenocytes (Elstob et al, 2001) reinforced this. The oenocytes are secretory cells derived from the peripheral nervous system (Gould et al 2001 review) which may have a role in regulation of the transition between developmental stages in *Drosophila* development (i.e moults and pupation) (Thummel, 2001) and in the final size of a fly (Columbani et al, 2005) through their secretion of the ecdysteroid hormone Ecdysone (Kozlova and Thummel, 2003). In addition these cells have recently been identified as having an essential role in lipid metabolism, where they function as hepatocyte cells giving them a role similar to the liver (Gutierrez et al, 2006).

Though there are links between the ecdysone pathway and Mef2 that may be of significance, (for example it has been shown that ecdysone steroid hormone induces transcription of *Mef2* in the adult *Drosophila* myoblasts (Lovato et al, 2005)), I decided to concentrate my studies on the immediate investigation of meso18E in muscle differentiation.

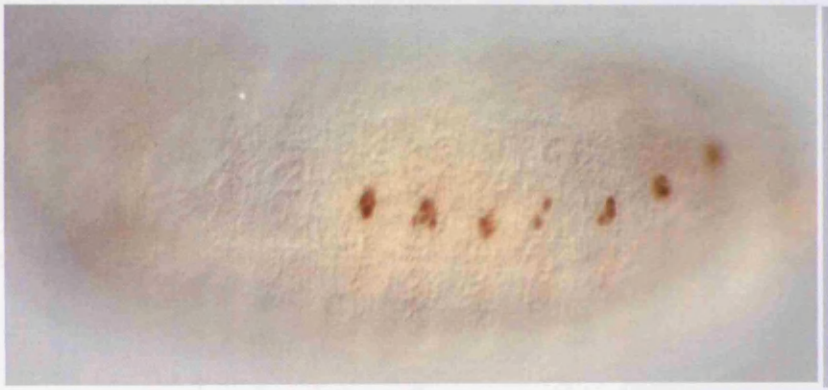

meso18E D GFP

(St15 lateral view, antiGFP staining)

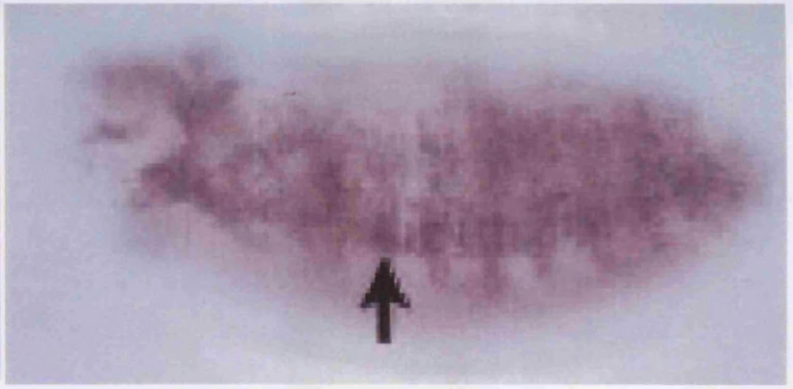

meso18E wt

(St15 lateral view, RNA in-situ)

Oenocytes; secretory cells present in abdominal hemisegments A1-A7

FIG 8.2.4 meso18E D GFP reporter construct expresses specifically in the oenocytes

8.2.4 Site Directed Mutagenesis to the Mef2 site in the meso18E C GFP reporter reveals meso18E to be a direct target of Mef2.

As the expression of the meso18E C GFP pStinger reporter is representative of the wild type pattern meso18E pattern (FIG 8.2.3) and that this wild type pattern itself is reminiscent of the Mef2 pattern in its later stages of embryogenesis I wanted to investigate the significance of the conserved Mef2 transcription factor binding site within the region.
It has already been shown that Mef2 plays a role in the regulation of *meso18E* expression (Taylor, 2000; Junion et al, 2005) but it has never been established if this regulation is through the direct action of Mef2 on the *meso18E* promoter, or indirect, through the interaction or upstream action upon some other regulatory gene.
Deletion of the binding site in reporter constructs via Site Directed Mutagenesis (SDM) is the classic way of determining whether a gene is a direct target for a specific transcription factor, and this has been used as a means of determining a number of direct targets for Mef2 in the past. For example, *Tropomyosin* (Lin et al, 1996), *β3-tubulin* (Damm et al, 1998) , *Paramyosin* (Arrendondo et al, 2000), *Act57B* (Kelly et al, 2002) and *Mef2* itself (Cripps et al, 2004) were all established as direct Mef2 targets in this way.

The sequence of the Mef2 site in the meso18E C region is CTATTTTTAG, which fits to the Mef2 site consensus of YTAWWWWTAR (Andres et al, 1995), where Y = C or T, W = A or T and R = A or G and is the exact same sequence of another Mef2 site previously established as essential for the expression of the Mef2 target, *Act57B* (Kelly et al, 2002).

It has been previously established that an A to C change in the third base of the consensus sequence, is sufficient to abolish Mef2 protein binding to the transcription factor binding site (Serjesi and Olson, 1991), though more recently more changes were introduced in the

central region of the site also, changing the A/Ts (W) to C/Gs, sometimes through the introduction of a CG rich restriction site such as SacII (CGGCGG) (Cripps et al, 2004) or Not I (GCGGCCGC) (Kelly et al, 2002). For site-directed mutagenesis to the Mef2 site in the meso18E C region of the GFP reporter I decided to introduce a SacII site changing the site from CTATTTTTAG to CCCGCCGTAG, which should completely destroy the binding activity of the site. As the Mef2 site is identical to the key Mef2 site in *Act57B* I did consider introducing a NotI site into the sequence, as was done for that study (Kelly et al 2002), but on further investigation, the potential for forming hairpin loops, dimers and bulge loops in the primers at key PCR extension temperatures was considerable (GeneRunner program) and I decided to use SacII instead which seemed less potentially problematic. I also checked that what would be the new sequence in the region of the site would not inadvertently introduce any new transcription factor binding sites using the Patch program (gene-regulation.com).

I then successfully generated, sequenced and confirmed this construct (see Materials and Methods) and named it meso18E C ΔMef2 SDM.

Subsequently it was injected by Jun Han in the lab, and she established transgenic lines that were recently investigated by her. On investigation of these multiple lines, she showed that the reporter gave a complete absence of GFP expression, showing that Mef2 is responsible for the pattern generated by this construct and revealing meso18E to be a direct target of Mef2.

8.3 Structure of the meso18E gene.

Little was known at the beginning of my PhD about the meso18E protein. It was established that the protein is 553 amino acids in length and is described as a putative nuclear protein due to the presence of a bipartite nuclear localisation sequence (NLS) at

residues 86-102 and analysis by the PSORT program (Taylor, 2000). In addition, at this time Blast protein database searches revealed little in the way of significant similarity to other proteins and found no functional protein domains which may suggest any role for the protein (Taylor, 2000).

In the last ten years there have been considerable advances in bioinformatic technologies and expansion in protein and nucleotide databases as more sequencing occurs. Consequently, it was an appropriate time for me to revisit the analysis of meso18E to search for homology, protein domains and protein structure as a way of elucidating more about the protein and possibly from this, a suggestion of its function.

8.3.1 meso18E homology searches

A Blast search of the meso18E amino acid sequence against the non-redundant protein database at Swiss Prot (www.ch.embnet.org) reveals that the meso18E protein is highly conserved among the *Drosophila* species, but outside of this genus has no proteins that show significant homology to the complete protein (FIG 8.3.1). However, the Blast search does repeatedly bring up a lower level of similarity to one specific region of around 80 amino acids long at the N terminal end of the meso18E protein and that on closer inspection of the sequence alignments reveals that it is the same residues that keep occurring across a range of various proteins from different species. This suggests that the region could correspond to a conserved protein domain and that the residues that keep reoccurring in the alignment are key residues for the function of the protein domain.

The proteins that show homology to this region are all nuclear and seem to have some degree of transcription factor activity; for example, the p400 SWI / SNF related protein in humans, the Domino protein highlighted in mouse, humans and also *Drosophila* in this

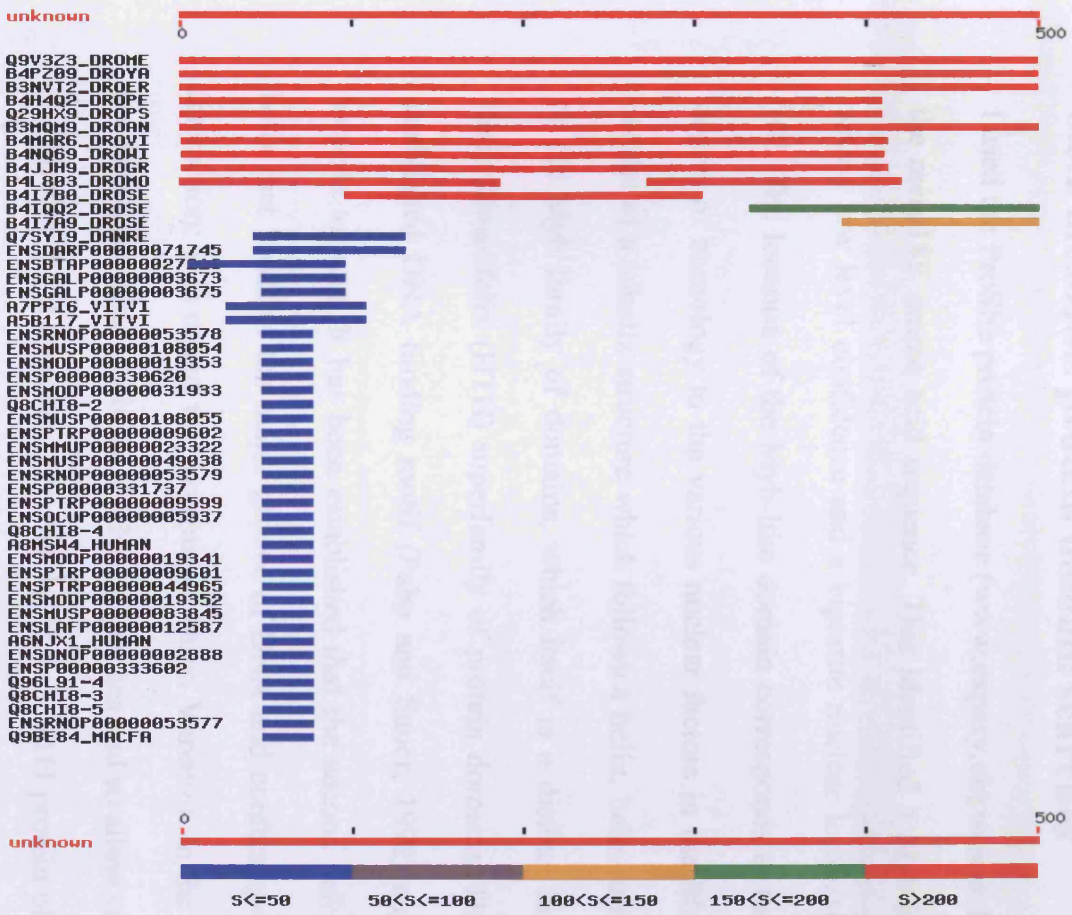

H W++V++V+N S R++KQC NRYEN+

FIG 8.3.1 meso18E is conserved among the *Drosophila* species and contains an evolutionally conserved myb-like domain

search, and GT2 and GT3a, plant transcription factors found in *Arabidopsis*. The residue sequence that is recurring in the alignment is :

HW++V++V+NSR++KQCNRYEN+

8.3.2 meso18E protein domain searches

I used the ProSite protein database (www.expasy.ch) to search for potential domains within the meso18E amino acid sequence. This identified a Myb-like domain at residues 18-86 with a low level confidence and a bipartite nuclear localization sequence at residues 86-102. The location of the Myb-like domain corresponds to the same region that shows the degree of homology to the various nuclear factors in the Blast search. Myb-like domains consist of a trihelix structure which follows a helix, helix-turn-helix pattern. They are part of the Myb family of domains, which itself is a distinct branch of the well established Helix-Turn-Helix (HTH) superfamily of protein domains. The HTH domain was the first established DNA binding motif (Pabo and Sauer, 1992) and is found in proteins from bacteria to man. It has been established that the second helix of the HTH domain is the helix that binds to the major groove of DNA and confers specificity in the DNA binding interaction; it is called the recognition helix. Variation in the recognition helix allows for the domain to bind to different DNA sequences and so allow variation in binding properties in different HTH proteins. The first helix in a HTH protein plays a role in the stability of the binding in the interaction.

The Myb family is a distinct branch of the HTH family; the domain contains an additional helix and as such has a helix, helix-turn-helix structure. As with the regular HTH domains, it is the second helix of the helix-turn-helix section that confers DNA binding specificity and is the recognition helix. (i.e in the Myb domain, the third helix is the recognition helix).

The Myb domain is named after the first proteins that were discovered to contain this tri-helix structure; the viral and cellular Myb proteins (Peters et al, 1987; Biedenkapp et al, 1988). Myb-type domains are DNA binding, and proteins containing them have been shown to function as transcription factors in a number of diverse roles from cell growth, differentiation and apoptosis (Oh and Reddy, 1999), to regulation of the cell cycle (Hirai and Sherr, 1996) and the maintenance of telomeres (Broccoli et al, 1997). The Myb domain itself is around 50 amino acids in length and is frequently found in a series of tandem repeats of the domain; for example in the c-Myb protein itself there are three adjacent repeats of the tri-helical Myb domain; R1, R2 and R3 (Gabrielson et al, 1991), though of these only R2 and R3 are essential for Myb function (Saikumar et al, 1990; Ogata et al, 1994). In other Myb containing proteins only two tandem Myb domains are found; R2 and R3, and in fact there is a distinct class of Myb related proteins found in plants called the R2R3 class which have this specific make up (Oh and Reddy, 1999; Jin and Martin, 1999). There are also members of the Myb family which only contain one copy of the Myb domain within the protein (effectively R3 only containing proteins) (Oh and Reddy, 1999). meso18E only contains one Myb-like domain and this is discussed later in this section.

Other members of the Myb domain family are the SANT domain and the Myb-like domain; like the Myb domain they consist of a helix, helix-turn-helix structure and are both similar to the Myb domain in terms of sequence and structure.

Unlike the Myb domain the SANT domain has protein binding properties as opposed to DNA binding properties, and this difference is thought to be down to variation in specific amino acid residues in the recognition helix of the domain; the SANT domains tend to contain a number of bulky aromatic and acidic residues whereas the Myb domain shows a greater number of positively charged residues making binding with the negatively charged backbone of the DNA more favourable (Aasland et al, 1996; Martin and Paz-Ares, 1997).

The SANT domain takes it name from a number of nuclear receptor co-repressors that were found to contain it (Switching Defective Protein (Swi3), Adaptor 2 (Ada2), Nuclear Receptor Co-Repressor (N-CoR) and Transcription Factor (TF)IIIB) (Aasland et al, 1996). SANT domain-containing proteins tend to show chromatin remodeling properties (Aasland et al, 1996) or an ability to bind to histone tails (Boyer et al, 2004).

Myb-like domains contain structural and sequence similarity to the Myb and SANT domains but vary sufficiently in specific residues in the helices to make them distinct from these domains. This category is in some ways quite varied as it appears that any domain that appears similar to, but distinct from, the Myb domain is described as Myb-like. With time it may be that they get a more distinct categorization however.

Myb-like domains have been shown to have either DNA binding or protein binding properties. A lot of recently identified Myb-like domains appear as single domains (as opposed to the tandem repeats such as with the R1, R2, R3 of c-Myb) and are longer than the Myb or SANT domains, typically being around 80 amino acids in length as opposed to around 50; as such they are sometimes described as extended Myb domains (Mohrmann et al, 2002; Barg et al, 2005; Zimmerman et al, 2007). The Myb-type domain can be further categorized into different subgroups, for example the Myb-like domain in mes2 is described as a MADF domain (Myb / SANT like domain in Adf1, the first protein it was described in (England et al, 1990; England et al, 1992)).

The ProSite database generates a Sequence Logo for each established protein domain and this Sequence Logo is a means of showing the key conserved residues in a protein domain. It does this by assigning a weight to a particular residue based upon the frequency of its occurrence in alignments of numerous proteins containing the domain. The taller the height of a residue in the Logo the more highly conserved it is, and so, one expects, the more

functionally important it is. The Sequence Logo to the Myb-like domain is shown in FIG 8.3.2 A) and a comparison of the meso18E amino acid sequence to this is shown in B). Though meso18E does not give a complete match, a high proportion of the key residues that defines a Myb-like domain are present in this region of meso18E. Conserved residues in the meso18E sequence are highlighted in bold in the corresponding colour to the key residue in the Myb-like domain Sequence Logo. The Tryptophan residue (W) at position 29 of the Sequence Logo is not conserved and this is part of the reason that meso18E does not score highly as a typical Myb-like domain. Tryptophan residues have been established as key residues in the Myb domain as their hydrophobic properties form a scaffold which maintains the conformation of the Myb type helix (Saikumar et al, 1990). In C) of the figure, the residues that were conserved and kept occurring in the Blast results are shown. These Blast conserved residues are underlined in the full meso18E sequence to the region in B). A residue that is underlined and highlighted in bold therefore is conserved across species (Blast) and shown to be key in the Myb-like domain (Sequence Logo); there are a number of residues like this, especially in the more 3' region of the meso18E sequence in this region (KQC NRYEN), suggesting that this part of the domain may be of particular importance, which is what one would expect as this region would correspond to the third helix (the recognition helix) of the Myb-like tri-helix.

A feature of the ProSite database is that it allows you to search all of the proteins that it classes as Myb-like domain containing, the database shows 1,818 proteins containing a myb-like domain from species as diverse as bacteria to man and reassuringly proteins such as Domino, ISI SWI and GT2 that were identified in Blast homology searches also feature in this list.

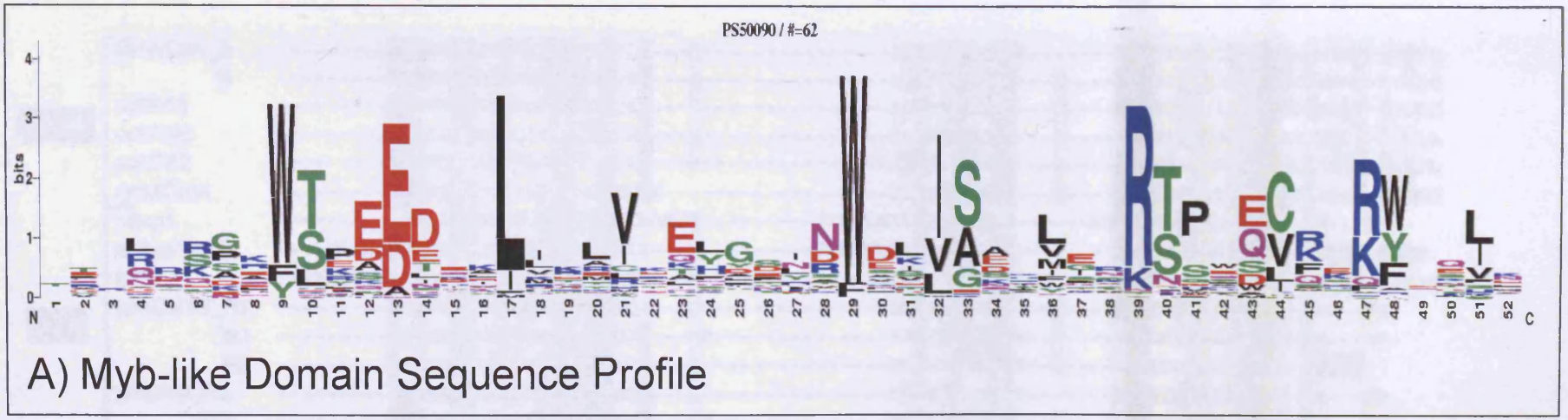

A) Myb-like Domain Sequence Profile

HASV**W**EM**V**AE**V**L**N**RF**S**ARK**R**TAK**Q**C**C**N**R**Y**E**N**L**

B) meso18E sequence

H W++V++V+N S R++KQC NRYEN+

C) meso18E Blast conserved residues

FIG 8.3.2 Comparison of the meso18E sequence to the ProSite Sequence Logo for the Myb-like domain

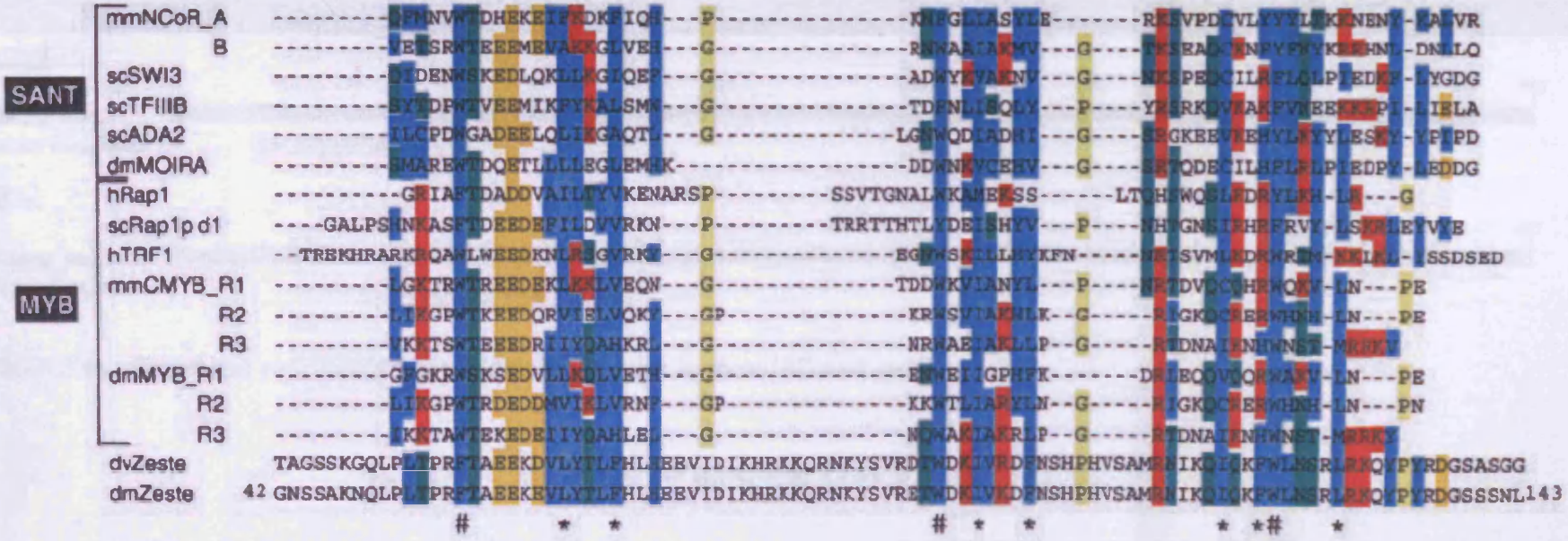

Zeste myb-like region

RFTAEEKEVLYTLFHLHEEVIDIKHRKKQRNKYSVRETWDKIVKDFNSHPHVSAMRNIKQIQKFWLNSRLRK

meso18E myb-like region

RTPESYFNVPESVALLNIVKSERIQSAFQSNRKNHASVWEMVAEVLNRFSARKRTAKQCCNRYENLKKIYTQLKKNP

FIG 8.3.3 meso18E comparison to other known myb/SANT domain containing proteins shows conservation of key residues

Image taken from Zeste myb domain study

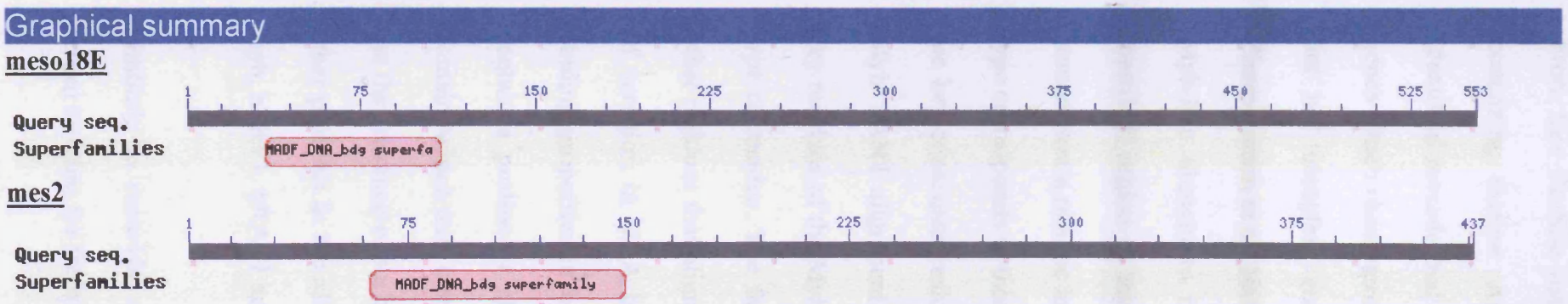

FIG 8.3.4a Graphical representation of domains present in meso18E and mes2

meso18E : CD Length: 89 **Bit Score:** 33.49 **E-value:** 0.11

```
                                10        20        30        40        50        60        70        80        90
                                ....*....|....*....|....*....|....*....|....*....|....*....|....*....|....*....|....*....|
meso18E sequence   34 LLNIVKSERI----QSAFQSNRKNHASVWEMVAEVLNrfsarkRTAKQCCNRYENLKKIYT-QLKKNPERHVRRN----WPY----MFL 109
Adf1 sequence       2 LIELVRERPClwdrRHPDYRNKEEKRKAWEEIAEELG------LSVEECKKRWKNLRDRYRrELKRLQNGKSGGGkkskWEYfdrlSFL 84
```

mes2 : CD Length: 89 **Bit Score:** 98.20 **E-value:** 3e-21

```
                                10        20        30        40        50        60        70        80        90
                                ....*....|....*....|....*....|....*....|....*....|....*....|....*....|....*....| ....*....|
mes2 sequence      62 KLIQMVHDNPILWDSRLPNFKGAEEeKNRAWEHIGREFNAPGRRVARAFKSLRESYRRELAHVKL--MGNGFKPKWSLYEAMDFLRDVIR 149
Adf1 sequence       1 RLIELVRERPCLWDRRHPDYRNKEE-KRKAWEEIAEELGLSVEECKKRWKNLRDRYRRELKRLQNgkSGGGKKSKWEYFDRLSFLRPVIR  89
```

FIG 8.3.4b Sequence alignment of identified MADF (Myb-like Adf1) Domain of meso18E and mes2 with Adf1.

From this ProSite list, a number of *Drosophila* proteins that are classed as Myb-like containing feature. Among these are the transcription factor Zeste and the recently identified mesodermal factor mes2. There have been recent publications on each of these genes which characterises their Myb-like domains and which stresses the general similarity but not complete conservation to the Myb-like domain (Mohrmann et al, 2002; Zimmermann et al, 2006). From this I was able to make direct comparisons of the meso18E Myb-like domain to the data in these papers. FIG 8.3.3 shows a comparison of the meso18E region to the Myb and SANT domain alignments for the Zeste study. In this comparison a residue in the meso18E sequence is highlighted in a colour if its position and type corresponds to those in the Myb/ SANT alignment. Residues with a hash beneath them are key consensus residues. Comparison of how the meso18E sequence lines up with the Myb/ SANT alignment compared to the Zeste alignment shows that meso18E also has the key residues of the Myb and SANT domain conserved in terms of either specific residue or type of residue. The fact that there is variation between meso18E and Zeste in terms of other residues that align with the Myb/ SANT domain alignment is likely to be a reflection of variation in DNA binding properties (assuming that, like Zeste, meso18E has DNA binding properties of course). It also worth noticing that unlike zeste meso18E does not contain a proline or glycine residue which separates the second and third helix of the domain, which may confer a difference in the way the region turns between the two helices, but the presence of such a residue is not essential to the Myb/SANT domain as a number of other proteins in the alignment also do not contain these (e.g the R1 repeat of drosophila myb, hTRF1, hRAP1 and mmNCoRA).

Similarly to meso18E mes2 is a mesodermal protein that was originally identified in a screen looking for factors affected in Twist mutants (Furlong et al, 2001). In the subsequent

mes2 study, the Myb-like domain is presented as a MADF domain (Zimmermann et al, 2006). The MADF domain was first described in *Drosophila* Adf1 (England et al, 1992) and its name derives from Myb/SANT like in Adf1 (and should not be confused with the MADS domain present in Mef2 as described previously). The MADF domain is DNA binding and examples there are a number of MADF domain containing proteins found in *Drosophila*, including Adf1 (England et al, 1992), Dorsal interacting protein, Dip3 (Bhaskar and Courey, 2002), Stonewall (Clark and McKearin, 1996) and mes2 (Zimmermann et al, 2006). All of these have DNA binding ability, transactivational activity and have a single Myb-like MADF domain at the N terminal end. Analysis of the protein sequence of the mesodermally expressed mes2 by Zimmermann et al was performed using the Conserved Domain Database (CDD) (Marchler-Bauer and Bryant, 2004). Analysis of the meso18E sequence with this program detects a MADF domain in the N terminus of the protein FIG 4.2.4a and a comparison of this with the mes2 alignment is shown in FIG 4.2.4b. The alignments are made using the sequence of the *Drosophila* Adf1 protein, which is the defining sequence for the MADF domain in this program.

Note that although the alignment of meso18E with Adf1 shows less similarity than mes2 does (an e-value of 0.11 as opposed to 3e-21), there is still significant conservation, especially in residues that have already been established to be key defining parts of the helices of Myb-like domains (Hulo et al, 2007).

In addition to this sequence analysis which suggests meso18E consists of a tri-helix Myb related domain I also performed a prediction of potential protein structure through sequence analysis using the JPRED program (Cole et al, 2008). This also predicts a trihelix structure with high confidence within the region corresponding to the MADF domain predicted by CDD (amino acids 34-109) (or alternatively the Myb-like domain predicted by Prosite (amino acids 18-86). And additionally as one might expect, the residues that are

conserved in alignment fall specifically within these predicted helix regions (FIG 8.3.5a, FIG 8.3.5b and FIG8.3.5c).

From this structural analysis and the alignments with the Prosite Myb-like sequence logo, the Zeste Myb-like comparison and the MADF comparison it can be seen that by sequence analysis meso18E contains a tri-helical protein domain at its N-terminal end which certainly lies within the Myb family and whose similarity but not complete conservation with established Myb-like and MADF domains suggests it may have similar transcriptional activity to these.

From this data I designed UAS constructs to investigate the functional significance of this domain in the context of over-expression using the Gal4 UAS system.

8.4 meso18E UAS constructs

FIG 8.4.1 shows a graphic representation of the meso18E over-expression constructs designed to investigate the role of the protein and the significance of domains within it. The full length over-expression construct was previously designed and generated in the lab by Dr.Taylor, it over-expresses the full 553 amino acids of the meso18E protein. The other constructs were designed based upon the protein sequence analysis above to investigate the significance of the Myb-like / MADF domain at the N terminus and also the predicted bipartite NLS and a Serine rich region at amino acids 165-191. I designed a construct which takes a considerable truncation to the C terminus. It consists of the first 125 amino acids of the protein and contains the Myb-like region (18-86), the predicted NLS (86-102) and continues further to ensure that these domains are completely included in the protein and also to include some amino acids which had some weak conservation homology based on Blasted sequence.

MDTKNPPPVTSSYHHQRAPRTPESYFNVPESVALLNIVKSERIQSAFQSN
RKNHASVWEMVAEVLNRFSARKRTAKQCCNRYENLKKIYTQLKKNPERHV
RRNWPYMFLFKEIEEQRGECWGSNGKRLALITKNHNELSYYQRRRQAAEL
GVLLNKDNLTPHQHSLLQSLSQSQSQSHSHAHSTDSSQSGSKLDRFLPNH
FVEAQLSEVAGPVGGSASGVSGMSAGGFDENPLQMQMVQAAAAAAAVAAH
KRHELQMASVGGVQMTPEDDDEDEPQRPAFKNHLHVLGHGHGLGLGHAPM
DDSGEAPDFEKDCNGALNMHHQNNNHNENHISMKSEPLSEGEFNPDDIQL
MQTNYNGAQNYYSPGMDANILHPDVIVDTDILSDCSSSTTLKKKRKMSTS
TDGDSTNYELIEYLKRREKRDEELLKRMDAREDRLMNLLERTVVAIETLA
VKRALTFPVNPTKENAPATARPLSPPPPEAQFAAPPATQEQPTSPERNGI
ATGRSGTIPVANQDAAIEVPDDGDSGDDVQVKDKLAKLTPKAGGDERTDG
RQT

FIG 8.3.5a Summary of meso18E protein analysis with respect to predicted MADF domain.

meso18E amino acid sequence 1-553 (Flybase)
Blue text : Region predicted as MADF domain - amino acids 34-109 (e value 0.11) (CDD)
Red text : Conserved residues within the predicted MADF domain from Adf1 alignment
Underlined : Predicted Helix structures (JPRED)

MDTKNPPPVTSSYHHQRAPRTPESYFNVPESVALLNIVKSERIQSAFQSN
RKNHASVWEMVAEVLNRFSARKRTAKQCCNRYENLKKIYTQLKKNPERHV
RRNWPYMFLFKEIEEQRGECWGSNGKRLALITKNHNELSYYQRRRQAAEL
GVLLNKDNLTPHQHSLLQSLSQSQSQSHSHAHSTDSSQSGSKLDRFLPNH
FVEAQLSEVAGPVGGSASGVSGMSAGGFDENPLQMQMVQAAAAAAAVAAH
KRHELQMASVGGVQMTPEDDDEDEPQRPAFKNHLHVLGHGHGLGLGHAPM
DDSGEAPDFEKDCNGALNMHHQNNNHNENHISMKSEPLSEGEFNPDDIQL
MQTNYNGAQNYYSPGMDANILHPDVIVDTDILSDCSSSTTLKKKRKMSTS
TDGDSTNYELIEYLKRREKRDEELLKRMDAREDRLMNLLERTVVAIETLA
VKRALTFPVNPTKENAPATARPLSPPPPEAQFAAPPATQEQPTSPERNGI
ATGRSGTIPVANQDAAIEVPDDGDSGDDVQVKDKLAKLTPKAGGDERTDG
RQT

FIG 8.3.5b Summary of meso18E protein analysis with respect to predicted Myb-like domain and ProSite Logo conservation.

meso18E amino acid sequence 1-553 (Flybase)
Blue text : Predicted Myb-like region (aminoacids 18-86) (Prosite)
Red text : Conserved residues in Myb-like domain as identified in ProSite Logo comparison (Prosite)
Underlined : Predicted Helix structures (JPRED)

MDTKNPPPVTSSYHHQRAPRTPESYFNVPESVALLNIVKSERIQSAFQSN
RKNHASVWEMVAEVLNRFSARKRTAKQCCNRYENLKKIYTQLKKNPERHV
RRNWPYMFLFKEIEEQRGECWGSNGKRLALITKNHNELSYYQRRRQAAEL
GVLLNKDNLTPHQHSLLQSLSQSQSQSHSHAHSTDSSQSGSKLDRFLPNH
FVEAQLSEVAGPVGGSASGVSGMSAGGFDENPLQMQMVQAAAAAAAVAAH
KRHELQMASVGGVQMTPEDDDEDEPQRPAFKNHLHVLGHGHGLGLGHAPM
DDSGEAPDFEKDCNGALNMHHQNNNHNENHISMKSEPLSEGEFNPDDIQL
MQTNYNGAQNYYSPGMDANILHPDVIVDTDILSDCSSSTTLKKKRKMSTS
TDGDSTNYELIEYLKRREKRDEELLKRMDAREDRLMNLLERTVVAIETLA
VKRALTFPVNPTKENAPATARPLSPPPPEAQFAAPPATQEQPTSPERNGI
ATGRSGTIPVANQDAAIEVPDDGDSGDDVQVKDKLAKLTPKAGGDERTDG
RQT

FIG 8.3.5c Summary of meso18E protein analysis with respect to predicted Myb-like domain and conserved BLAST residues.

meso18E amino acid sequence 1-553 (Flybase)
Blue text : Predicted Myb-like region (aminoacids 18-86) (Prosite)
Red text : Conserved residues across species as identified in BLAST search (Expasy)
Highlighted dark blue : Predicted Helix structures (JPRED)
Predicted Bipartitite NLS **KIYTQLKKNPERHVRR** (Prosite)

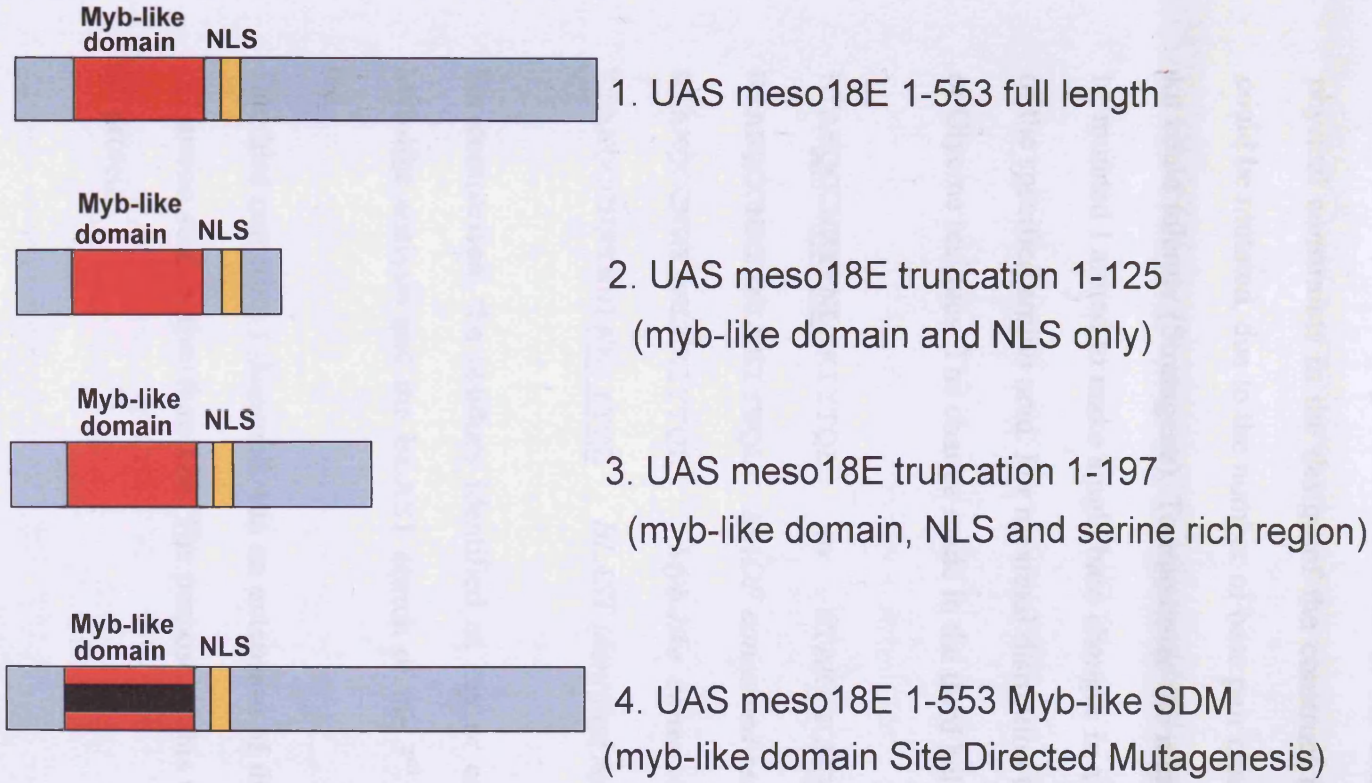

FIG 8.4.1 Planned UAS constructs for analysis of meso18E function

To investigate the role of meso18E I designed UAS constructs that could be over-expressed using the Gal4 system. The diagram shows a graphic representation of these (not to scale). Full length meso18E protein is 553 amino acids and should show any phenotype associated with gain-of-function of the gene. Based on my analysis of the protein sequence (Chapter 4.2) I also designed constructs which might provide insight into the role of the identified Myb-like / MADF domain at the N terminus of the protein. Through identification of the key conserved residues within this region I also designed a construct to target the deletion of these residues specifically via site directed mutagenesis in the predicted recognition helix of the domain. All proteins are shown with the N terminus at the left.

I also designed a construct which would change key residues within the Myb-like domain. I wanted to make that made the most potentially significant changes within the domain, so consequently chose to mutate residues that were within the third predicted helix, the recognition helix, and that were conserved within the alignment comparison to the Myb-like domain protein logo and conserved in the Blast homology alignments. There were physical constraints in the design of the construct regarding the number of residues that could be mutated, due to the number of base pair changes that the site directed mutagenesis kit could tolerate (Stratagene). To maximize the number of amino acid residues that could be mutated I aimed to make single base changes in a codon that would result in the change of the specified amino acid. For maximal disruption to the helix I tried to introduce Proline or Glycine residues. The change made in the third helix were as follows :

RTAK**QC**CN**RY**E**NL**KKIYTQL to RTAK**PG**CN**GP**E**GP**KKIYTQL

RTAKQCCNRYENLKKIYTQL *MADF conserved residues in the 3rd helix*

RTAKQCCNRYENLKKIYTQL *Myb-like conserved residues in the 3rd helix*

RTAKQCCNRYENLKKIYTQL *BLAST identified residues in the 3rd helix*

For comparison, the residues identified as key or conserved in the MADF analysis, the Myb-like analysis and the BLAST search of the 3rd helix of meso18E are highlighted in red.

The third construct I designed was an extension of the truncated protein which extends to 197 amino acids rather than 125. The purpose of this was to include a Serine rich region of the protein.

Of the four constructs described here, only full length meso18E was analysed as part of my thesis. The meso18E 1-125 truncation was made, injected and fly lines established but not

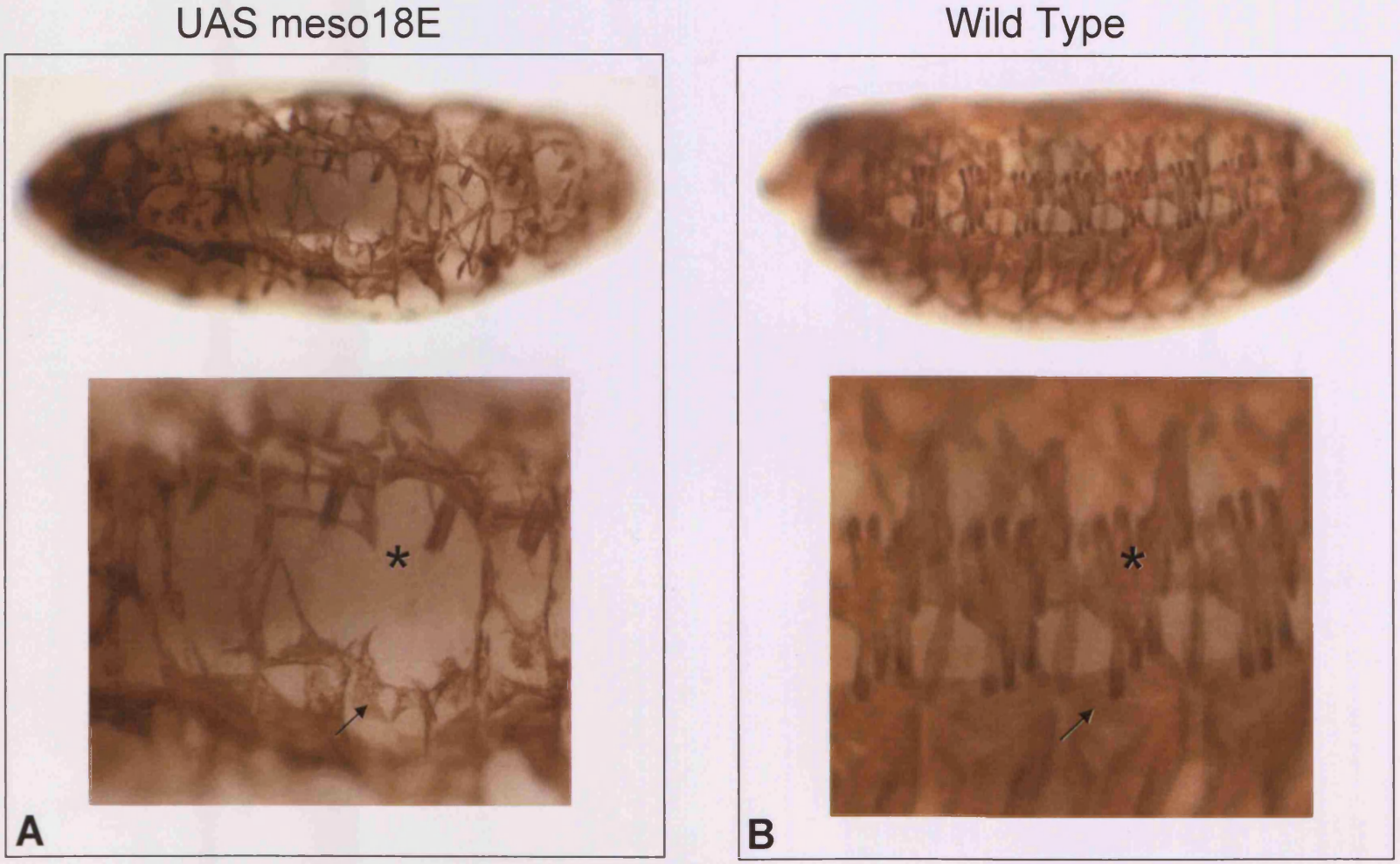

FIG 8.5.1 Over-expression of full length *meso18E* in the mesoderm causes a severe disruption to muscle pattern

investigated at the time of writing and the meso18 1-197 truncation and Myb-like domain SDM constructs were not completed. Description of the construct design can be found in the materials and methods.

8.5 meso18E gain-of-function analysis.

Three independent, homozygous viable lines carrying the UAS meso18E 1-553 full length transgene were generated previously in the lab by Dr.Taylor and I investigated their effect on muscle development through overexpression with various Gal4 lines.

Because of the similarity in expression pattern of meso18E to Mef2 (Taylor et al, 1995; Taylor, 2000 and section 8.1), I chose to use the Mef2 Gal4 driver to initially investigate a role for meso18E in muscle development. Mef2 Gal4 also has the advantage of being a particularly strong mesodermal driver.

8.5.1 Over-expression of meso18E has a severe effect on muscle development.

FIG 8.5.1 shows an example of how over-expression of meso18E in the Mef2 pattern causes a severe disruption to the muscle pattern of St17 embryos. The order of the somatic musculature is lost and there are a high proportion of muscles appearing misattached and particularly spindly and misshapen in comparison to wild type. In addition there are a number of muscles that appear to be missing completely, for example in the representative embryo shown in FIG 8.5.1, the LT1-4 muscle are missing in the majority of hemi-segments, leaving large gaps in the muscle pattern.

The UAS meso18E line used in this figure was meso18E 20T2. The three established lines were called meso18E 20T2, meso18E 29T1 and meso18E 29T24 and each of them was investigated as part of the analysis of meso18E gain-of-function.

FIG 8.5.1 Over-expression of full length *meso18E* in the mesoderm causes a severe disruption to muscle pattern

The regular somatic muscle pattern seen in Wild Type embryos (B) is severely disrupted when full length meso18E is over-expressed in the mesoderm (A). The embryo here had the UAS meso18E 20T2 line driven in the Mef2 pattern at 29°C and shows a representative phenotype of all those seen.
There is a severe loss of organisation to the musculature with a high proportion of muscles appearing misattached and especially spindly and misshapen in comparison to Wild Type. For example this is particularly noticeable in the ventral region where the VL1-4 and VO1-3 muscles are situated (arrow).
In addition there are also subsets of muscles that appear to be completely missing in each of the hemi-segments within the meso18E over-expression embryo, for example absence of the LT1-4 muscles causes distinctive gaps in the muscle pattern of the embryo (compare asterisk region in A with Wild type B).
The embryos are St17, viewed laterally and stained with anti-β3 tubulin antibody to visualise muscles.

All of the lines give a similar effect upon muscle development, disrupting the shape and attachment of a large proportion of muscles and also causing muscle loss. However, there is variation in strength between the transgenic lines, which is not unusual and probably due to differences in insertion position. meso18E 20T2 is the strongest line whereas meso18E 29T1 and meso18E 29T24 are of a more comparable level. This is reflected by the extent of muscle loss in embryos that were scored for presence, absence, shape and attachment defects in A2-A4 of ten individual embryos; FIG 8.5.2 shows how the average number of muscles lost in hemi-segments A2-A4 is distinctly higher in the meso18E 20T2 line (58.8) than the meso18E 29T1 and meso18E 29T24 lines (12.4 and 10.9 respectively) when the lines are driven by Mef2 Gal4 at 29°C. In a similar manner the range of muscles affected in any one embryo (A2-A4) is also higher in the meso18E 20T2 than the other lines, (45-74 muscles missing as opposed to 4-19 missing for meso18E 29T1 and 1-24 missing in meso18E 29T24 embryos).

Despite the differences in strength, the lines show clear similarities in their phenotype in the way over-expression of meso18E effects the derivatives of the mesoderm, with the 29T1 and 29T24 lines showing milder phenotypes as opposed to different phenotypes to the 20T2 line. This can be seen in the tables showing the data for the analysis of somatic muscle phenotype of the three lines (TABLE 8.5.1a and 8.5.1b) and seen in the representative embryos shown in FIG 8.5.3.

Over-expression of meso18E causes a strong phenotype in all of the mesoderm derivatives it is expressed in. As shown in FIG 8.5.1 over-expression of meso18E causes a severe derangement to the somatic muscles. In addition, the gut is frequently severely misshapen in meso18E 20T2 over-expression embryos; it fails to constrict and instead forms a rounded bloated structure, which consequently appears to affect the shape of the embryo itself, deforming it where the gut blisters out and also causing the somatic musculature in

Muscle phenotype	**UAS 18E (20T2)** x *Mef2 Gal4* (29°C)	**UAS 18E (29T1)** x *Mef2 Gal4* (29°C)	**UAS 18E (29T24)** x *Mef2 Gal4* (29°C)
% embryos with muscle missing	100 %	100 %	100 %
Average No. muscles missing per embryo	58.8	12.4	10.9
Range of muscles missing per embryo	45 - 74	4 - 19	1 -24

Table 8.5.2 - Muscle missing phenotype of meso18E over-expression lines

The thirty individual somatic muscles per hemisegment scored A2-A4 for 15 individual embryos for each meso18E overexpression line. The average number of muscles A2-A4 missing per embryo is shown and the range of muscles missing A2-A4 for the embryos scored for that experimental condition are shown. There is a total possible muscles missing of 90 (30 per hemisegment) for each embryo tested. All three UAS meso18E lines driven by Mef2 Gal4 at 29°C.

	Muscles Missing in > 50 % Embryos	Muscles Missing in 25 – 49 % Embryos	Muscles Missing in 10 -24% Embryos	Muscle Duplication in 10 – 30 % Embryos	Shape Defects in > 70 % Embryos	Shape Defects in 50 -69 % Embryos
UAS 18E (20T2) X *Mef2 Gal4* (29°C)	All others (see Table 4.4.3b)	DT1	LL1, DO5	-	DA3, DO5, DT1, LL1, VT1, VL1, VL2, VL3, VL4, VA1	SBM, VO1, VO2
UAS 18E (29T1) *X* *Mef2 Gal4* (29°C)	DO3, DO4, LT1, LT4, LO1, VT1, VA3, VO4, VO6	LT2, LT3, SBM	DA1, DO2, DA2, DA3, DO5, LL1, VL2, VL3, VA1, VA2, VO1, VO2, VO5	DO1, LT1, VA3	DO4, DA3, LL1, LT1, LT2, LT3, VT1, VA1, VA2, VA3, VO4, VO5, VO6	DA2, DO3, DO5, LT4, SBM
UAS 18E (29T24) X *Mef2 Gal4* (29°C)	DA2, LT3, LT4, VL2, VL3, VO4	DO3, DO4, DO5, LT2, LO1, VA3, VO1, VO5, VO6	DA1, DA3, DT1, LT1, SBM, VT1, VL1, VL4, VA1, VO2 VO3	DO1, DA1, VO4, VO6	DO2, DO3, DO4, DA3, LT2, LT3, VT1, VA1, VA3, VO4, VO5, VO6	DO1, DA1, DA2, LT1, LT4, LO1, VA2

Table 8.5.1a Individual muscle phenotype analysis of meso18E over-expression lines

Cross	Muscles Missing in 100 % Embryos	Muscles Missing in 90-99 % Embryos	Muscles Missing in 80-89% Embryos	Muscles Missing in 70 - 79% Embryos	Muscles Missing in 10 – 30% Embryos
UAS 18E (20T2) x *Mef2 Gal4* (29°C)	**DO3, LT1, LT2, LT3, LT4, LO1, VA2, VA3, VO3, VO4, VO5, VO6**	**DO4, VL3, VO2,**	**SBM, VL1, VL2, VO1**	**DA3, VT1, VL4**	**DO5, DT1, LL1,**

Table 8.5.1b - Meso18E 20T2 over-expression muscle phenotype analysis

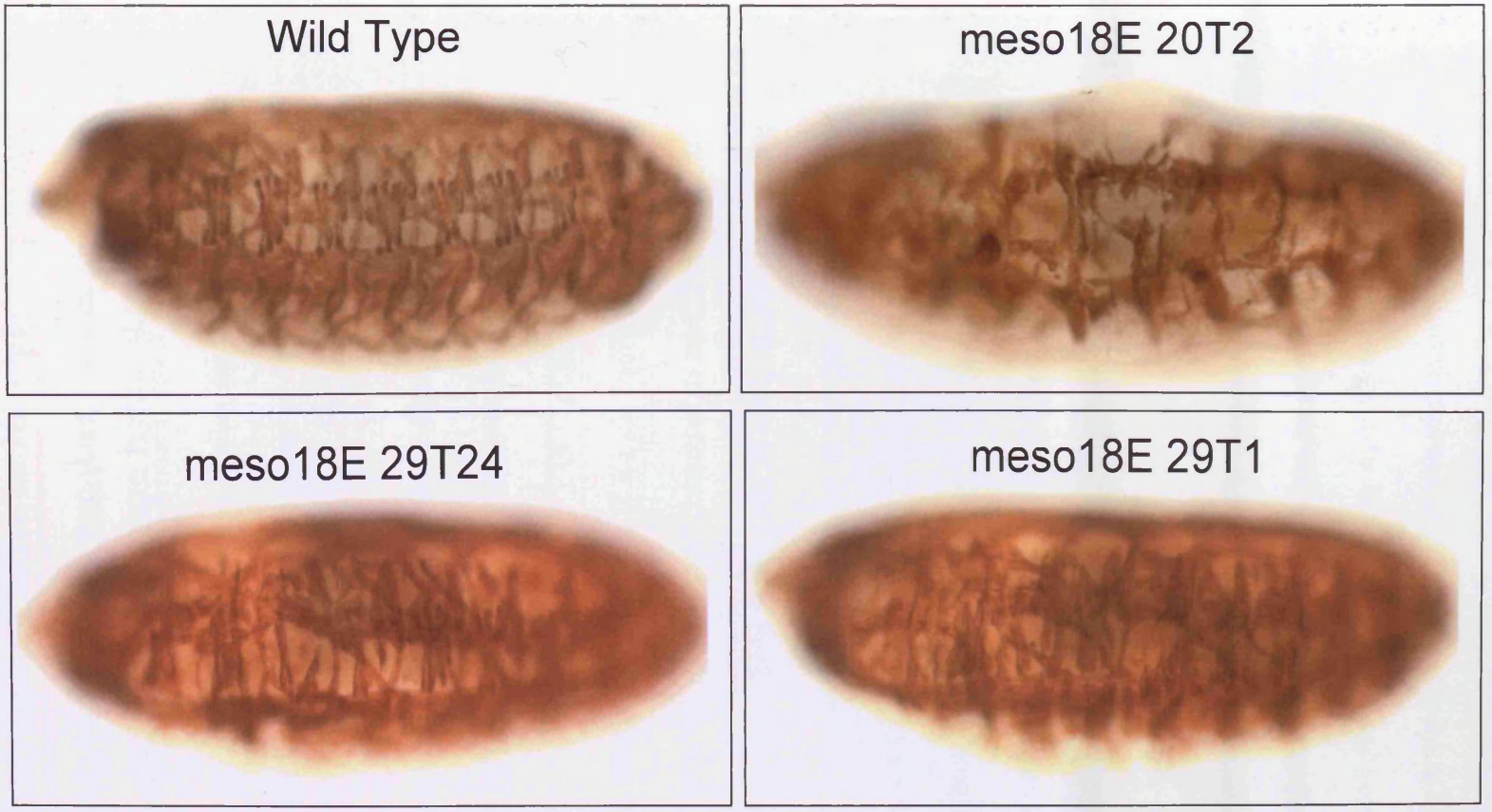

FIG 8.5.3 There is some variation in strength, but not type of muscle phenotype when over-expression of the three full length *meso18E* transgenic lines are compared.

meso18E20T2, meso18E 29T24 and meso18E 29T1 driven by Mef2 Gal4 at 29°C all give a muscle phenotype which shows disruption to the muscle pattern with predominantly muscles being missing or misattached (see Table 8.5.1 for details). The images shown here are representative of the strength of phenotype observed, with meso18E 20T2 being Muscles stained with anti β3-tubulin.

the region it extends into to be misshapen (FIG 8.5.4a). This gut phenotype is also seen in the weaker meso18E lines at a lower frequency. An example of this gut structure in meso18E 29T1 over-expression embryos is shown in FIG 8.5.4b.

Another striking aspect to the meso18E gain-of-function phenotype is the failure of a proper heart structure to form. This is particularly profound in the meso18E 20T2 over-expression embryos where there can be a complete absence of a heart structure except for a few remaining clumps of misshapen cardioblast cells (FIG 8.5.5). Slightly milder phenotypes also occur with meso18E 20T2, whereby only partial sections of tubular heart form or their appears to a large number of misshapen cardioblasts either side of the dorsal midline where the heart should be but no dorsal tube forms, as if the cells were unable to find their position or maintain their integrity (FIG 8.5.5). This embryo that shows no dorsal tube also shows defects in the shape and pattern of the cells within pharyngeal muscle, though the general shape of the muscle itself remains distinguishable (FIG 8.5.5). With the lower strength over-expression lines, a milder heart phenotype occurs; the heart tube forms, but their can be kinks within it or incorrect numbers of β3-tubulin positive cardioblasts in the heart pattern (FIG 8.5.6).

In addition to somatic muscles appearing misguiding and misshapen in the body wall of the embryo (FIG 8.5.1 and 8.5.3), they can also stray across into the ventral midline as shown in FIG 8.5.7.

A small proportion of embryos examined from the staining show a very distinctive phenotype where they appear to have differentiated somatic musculature resembling that of St17 (albeit with shape defects), but the shape of the embryo more closely resembles a St12 embryo with respect to germ band retraction (FIG 8.5.8). The embryo shown here used the meso18E 29T1 line, it was not seen with the meso18E 20T2 line in the embryos examined.

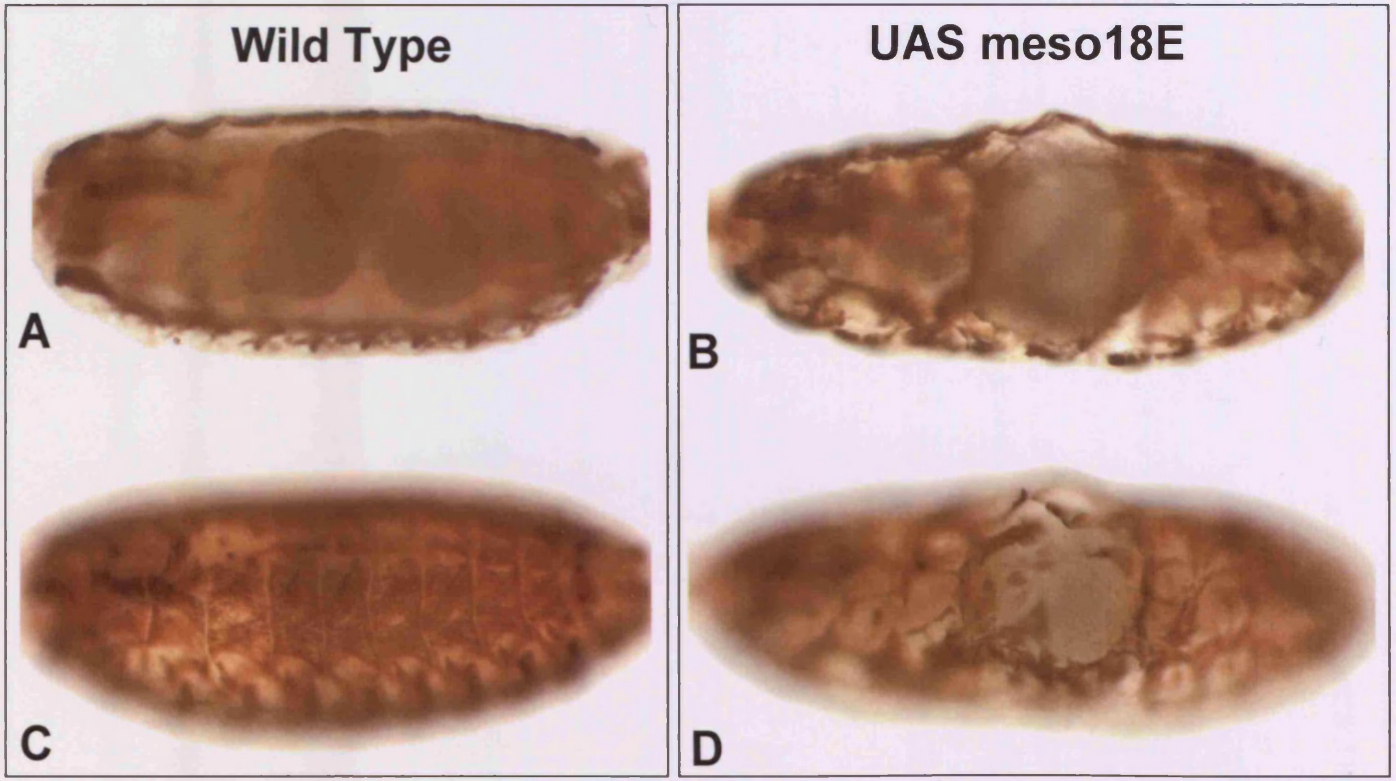

FIG 8.5.4a The gut fails to restrict in meso18E over-expression embryos, which results in a bloated phenotype

In the majority of embryos strongly over-expressing meso18E there is a failure of the gut to constrict properly and instead it forms a rounded blister like structure which bloats the embryo causing the shape of the embryo itself to become deformed and also the somatic muscles and heart to not form in this area or be severely misshapen.

The embryos here are St17 and viewed dorso-laterally. In the meso18E over-expression embryo, B, the focus is on the visceral muscle and shows the mishapen rounded gut in comparison to the tubular constricted gut of Wild Type in A. Shifting focus at this position shows that the somatic muscles are especially affected where the abdomen distends, with muscles missing or seemingly stretched to the shape of the rounded gut where the somatic muscles are present (compare D with wild type C).

Line used meso18E 20T2, driven by Mef2 Gal4 at 29°C, stained with anti β3-tubulin.

FIG 8.5.4b The gut fails to restrict in both meso18E high and low strength over-expression embryos.

FIG 8.5.5 Strong over-expression of meso18E causes loss of heart structure

Over-expression of meso18E causes a severe heart phenotype, which can result in almost complete loss of the heart.

Embryo B shows only a few cardioblasts, which are misshapen and in a small isolated clump (arrow in B).

In embryo C there is some tubular structure that forms, but this is only a partial section of heart, in which the cardioblasts are also misshapen (bracket in C). This heart section is also mis-positioned within the embryo compared to wild type, having strayed away from the dorsal midline (marked by an arrowhead in the full embryo image of C).

Embryo D shows a no heart structure at all in the dorsal midline, but has a large number of severely disorganised cardioblast-like cells either side of the midline (arrow in D). The general shape of the pharyngeal in this embryo wild type but the shape of the cells and their pattern seems disorganised (arrowhead, D).

All embryos are St17, aligned dorsally and stained with β3-tubulin antibody. UAS meso18E line used is 20T2 and was driven by Mef2 Gal4 at 29 ℃. Wild type embryos are OR.

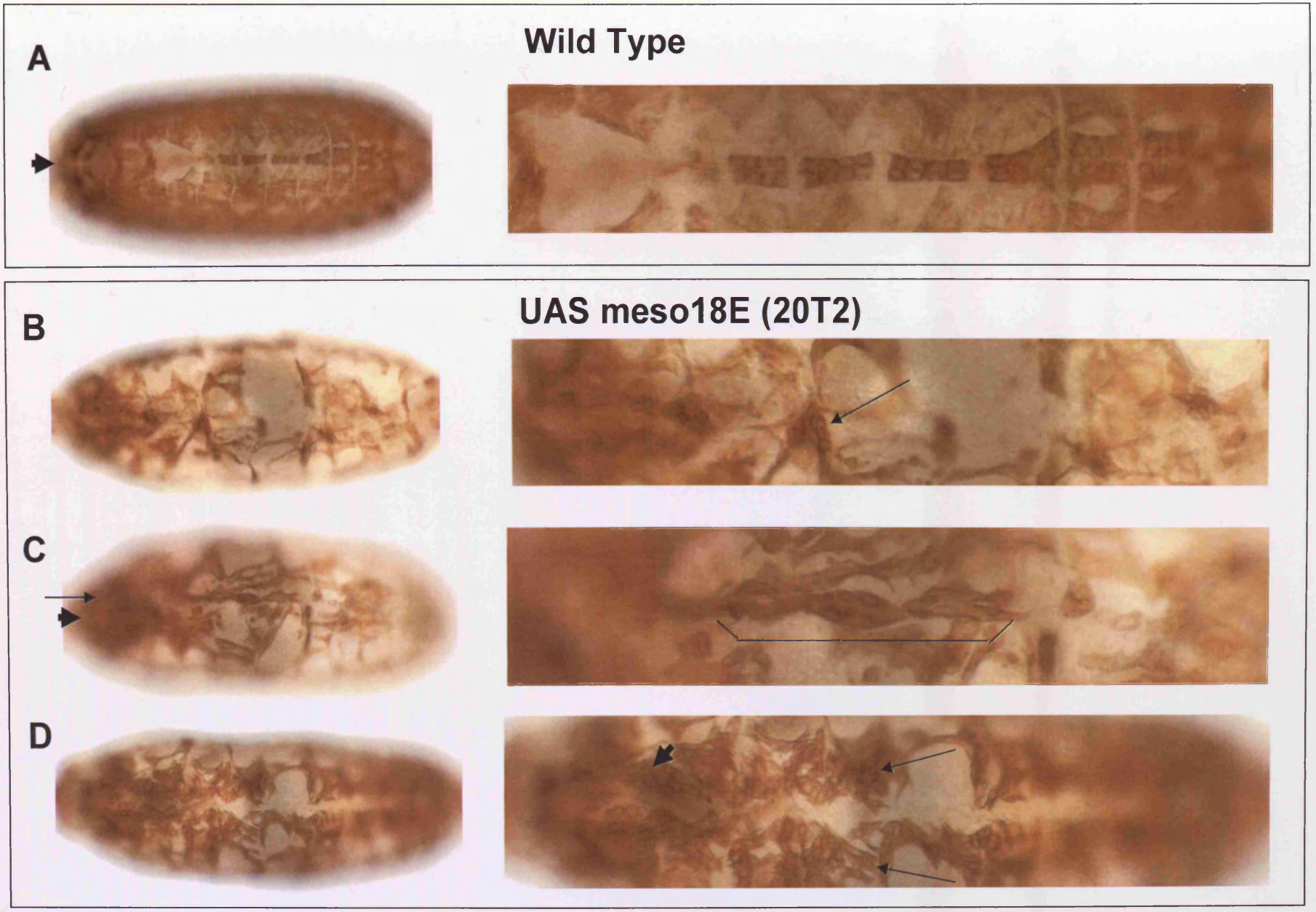

FIG 8.5.5 Strong over-expression of meso18E causes loss of heart structure

FIG 8.5.6 Milder over-expression of meso18E disrupts heart pattern

When meso18E is over-expressed with the weaker UAS insertion lines (29T24 or 29T1) the heart phenotype is less severe than that seen with 20T2 which can result in loss of heart structure.

Instead with these lines the heart forms, but shows structural or pattern defects. Embryo B shows a linear heart, consisting of two rows of cardioblasts, but that has defects in cardioblast pattern.

The wild type heart consists of two rows of cardioblasts which have a repeating pattern of four out of six β3-tubulin positive cardioblasts per hemisegment (see A). With meso18E overexpression the pattern is disrupted, with a group of two in one row (arrows in B) and a group of nine in another row (bracket in B).

Embryo C shows a stronger phenotype consisting of sections of cells being missing (arrow, C) and circular clumps of misshapen cardioblasts (arrowhead, C) – a phenotype which was also seen with the stronger UAS meso18E line (FIG 4.4.3 – B)

Embryo D shows a group of misshapen and disorganised cardioblasts (arrow, D) and a kink in the tubular structure of the heart (line D).

All embryos are St17, aligned dorsally and stained with β3-tubulin antibody. UAS meso18E lines used were 29T24 and 29T1 and were driven by Mef2 Gal4 at 29 °C. Wild type embryos are OR.

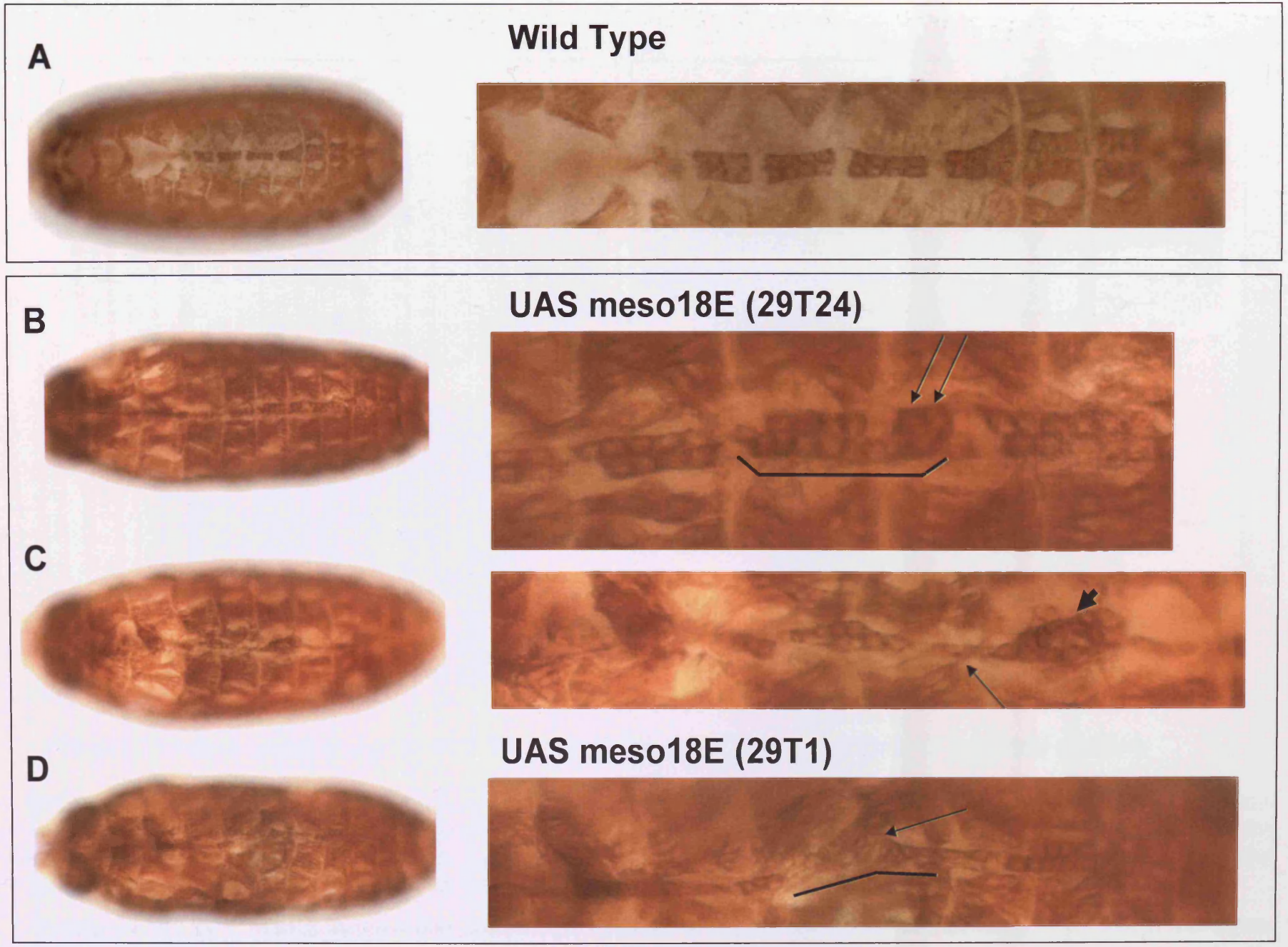

FIG 8.5.6 Milder over-expression of meso18E disrupts heart pattern

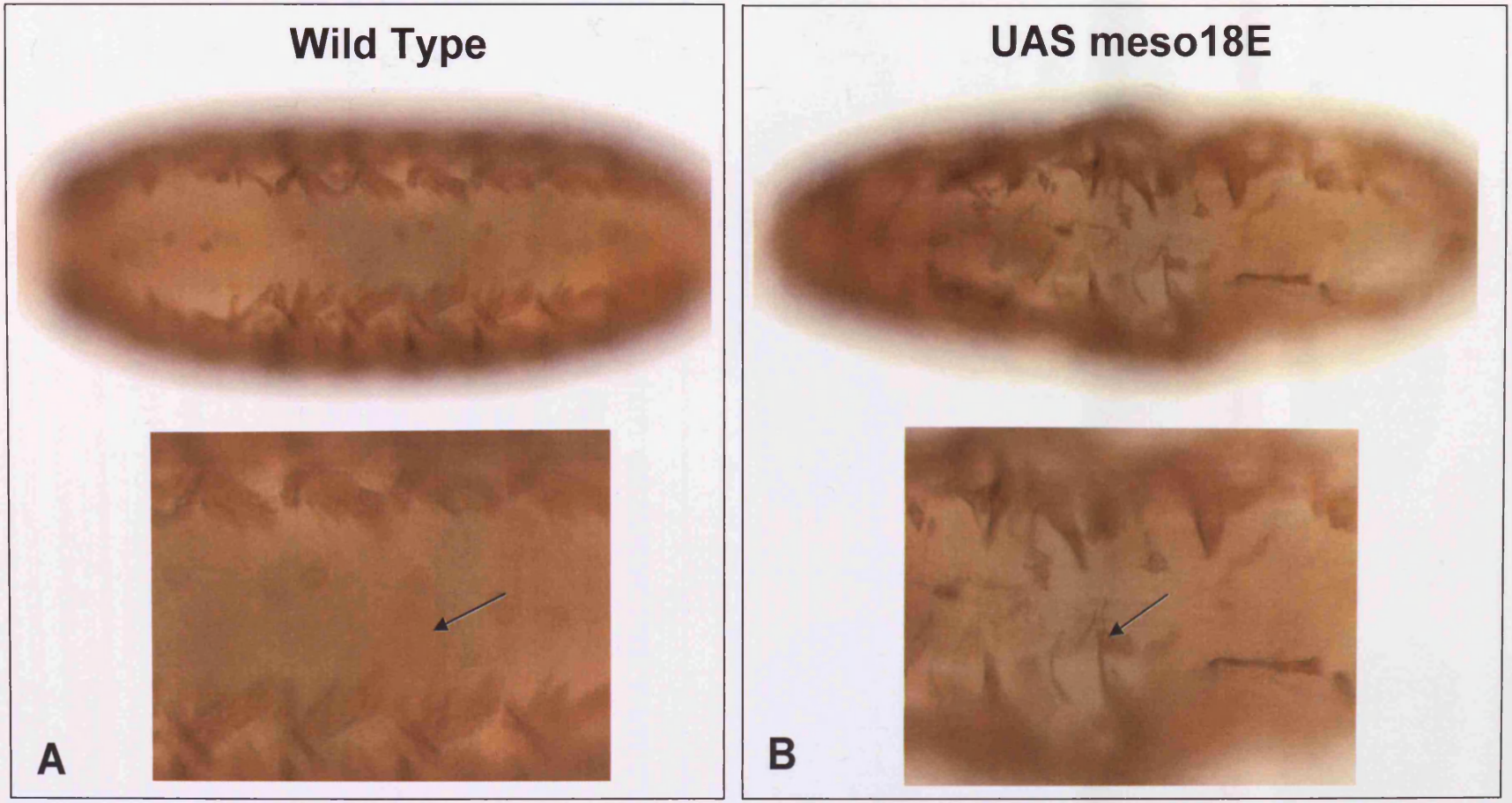

FIG 8.5.7 Over-expression of meso18E causes muscles to stray across the ventral midline

Embryos overexpressing meso18E show a severe disruption to muscle pattern with some muscles straying across the ventral midline as seen in the image above. Compare the ventrally viewed embryo B, where spindly muscles can be seen spanning the midline (arrow B) to wild type A). No muscles do this in the wild type condition (arrow A). More examples of muscles crossing the midline in this way can be seen in FIG 8.5.10

All embryos are St17, aligned ventrally and stained with β3-tubulin antibody. UAS meso18E lines used is 20T2 and was driven by Mef2 Gal4 at 29 ℃. Wild type embryos are Oregon R.

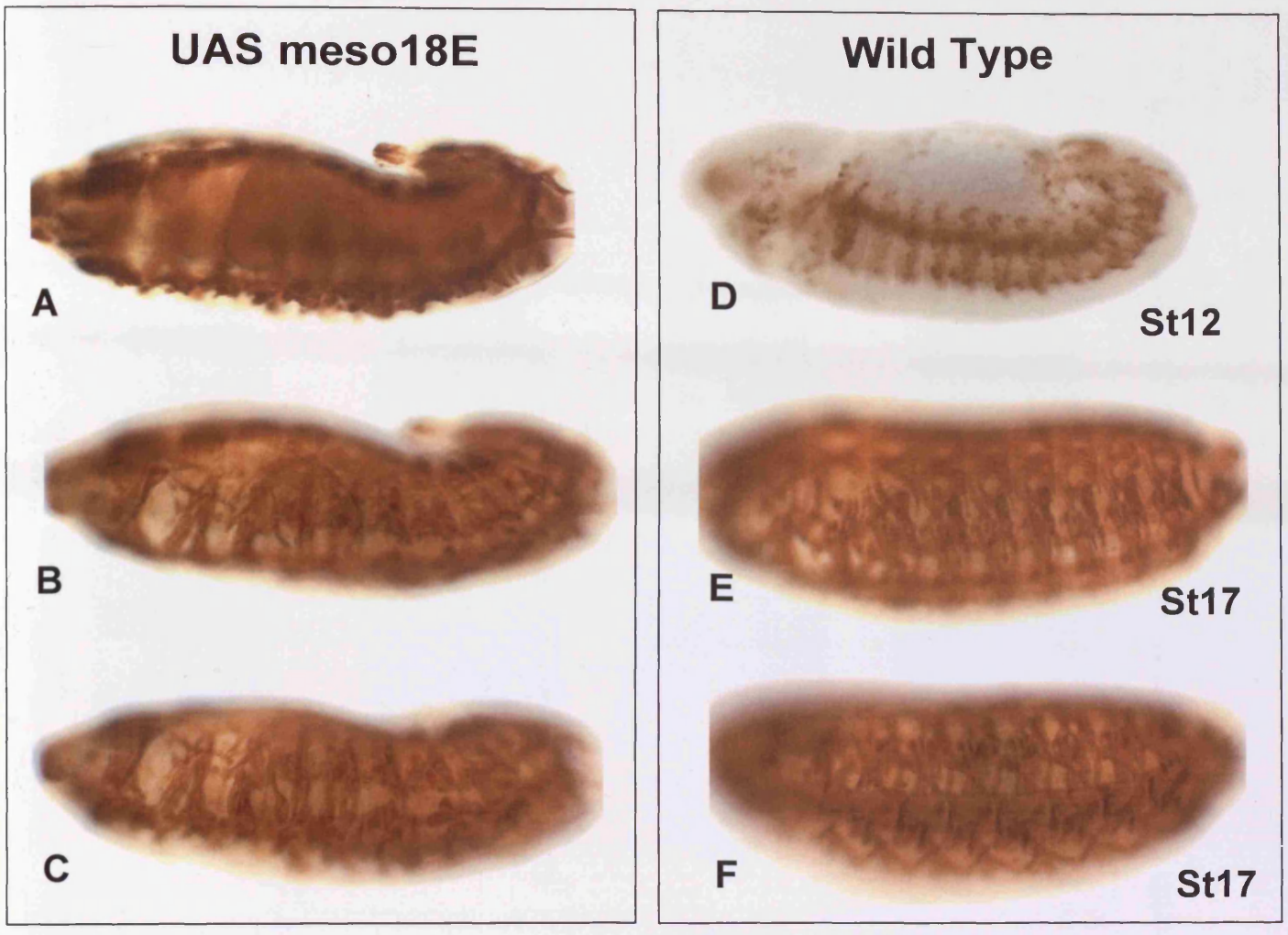

FIG 8.5.8 Over-expression of meso18E can cause severe developmental defects in some embryos

In a small percentage of meso18E (20T2) over-expression embryos a phenotype is seen where the embryo has the appearance of a St12 embryo, with the germ band not yet retracted (arrow) but the musculature of a St17 embryo where distinct individual muscles have formed.

This phenotype could occur as a result of premature muscle differentiation or delayed germ band retraction.

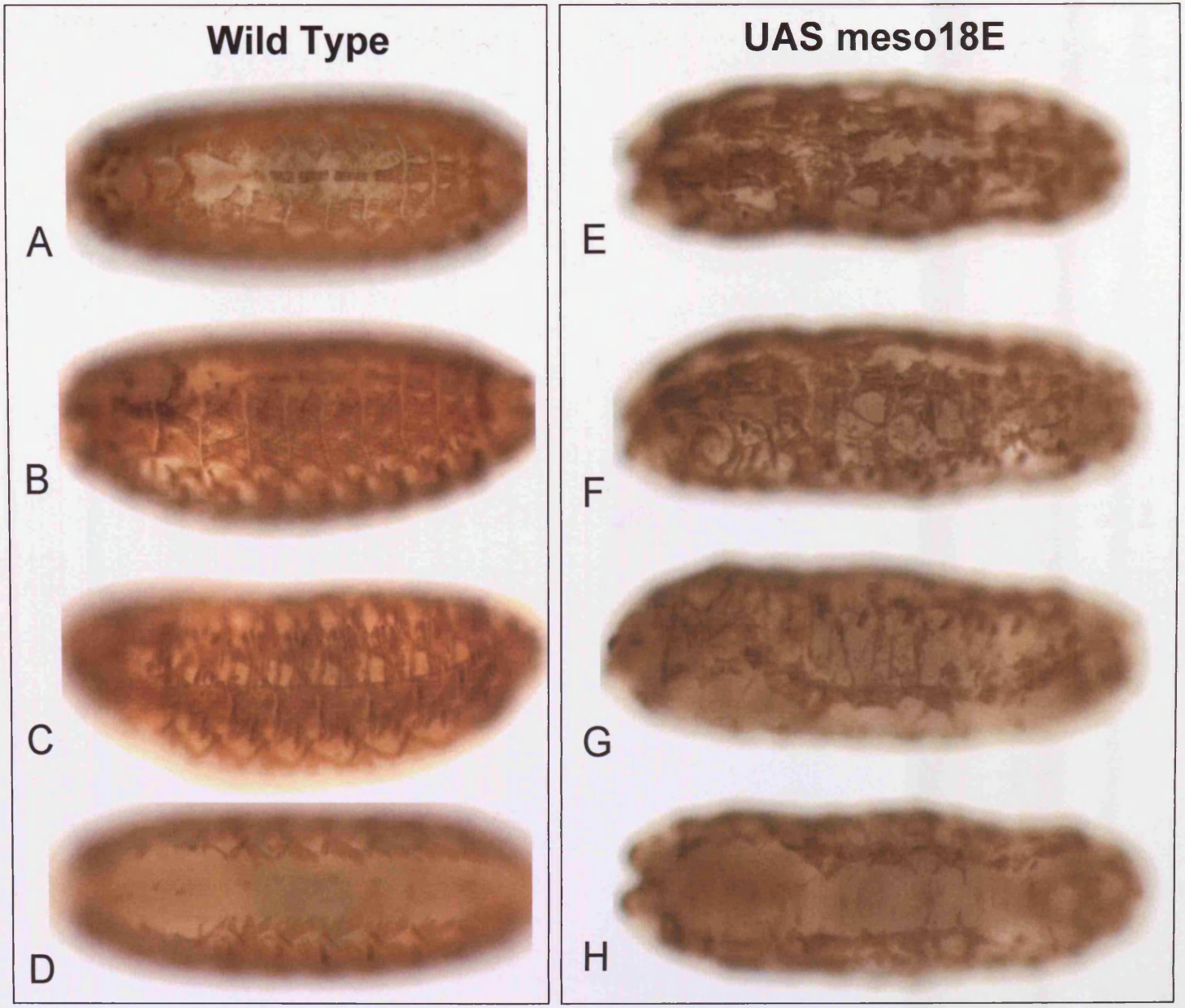

FIG 8.5.9 Over-expression of meso18E with Twist Gal4 also severely disrupts muscle pattern

FIG 8.5.10 Examples of muscles crossing the ventral midline in meso18E overexpression embryos.

A proportion of embryos (approx 30%) overexpressing meso18E show muscles that span either partially or completely the ventral midline. These muscles are also misshapen and thin. The line used in all of these images is meso18E 20T2 and was driven by Twi ; Twi Gal4 at 25°C. The muscles were visualised by staining with anti β3-tubulin antibody. All embryos St17 and viewed ventrally. Wild type is Oregon R.

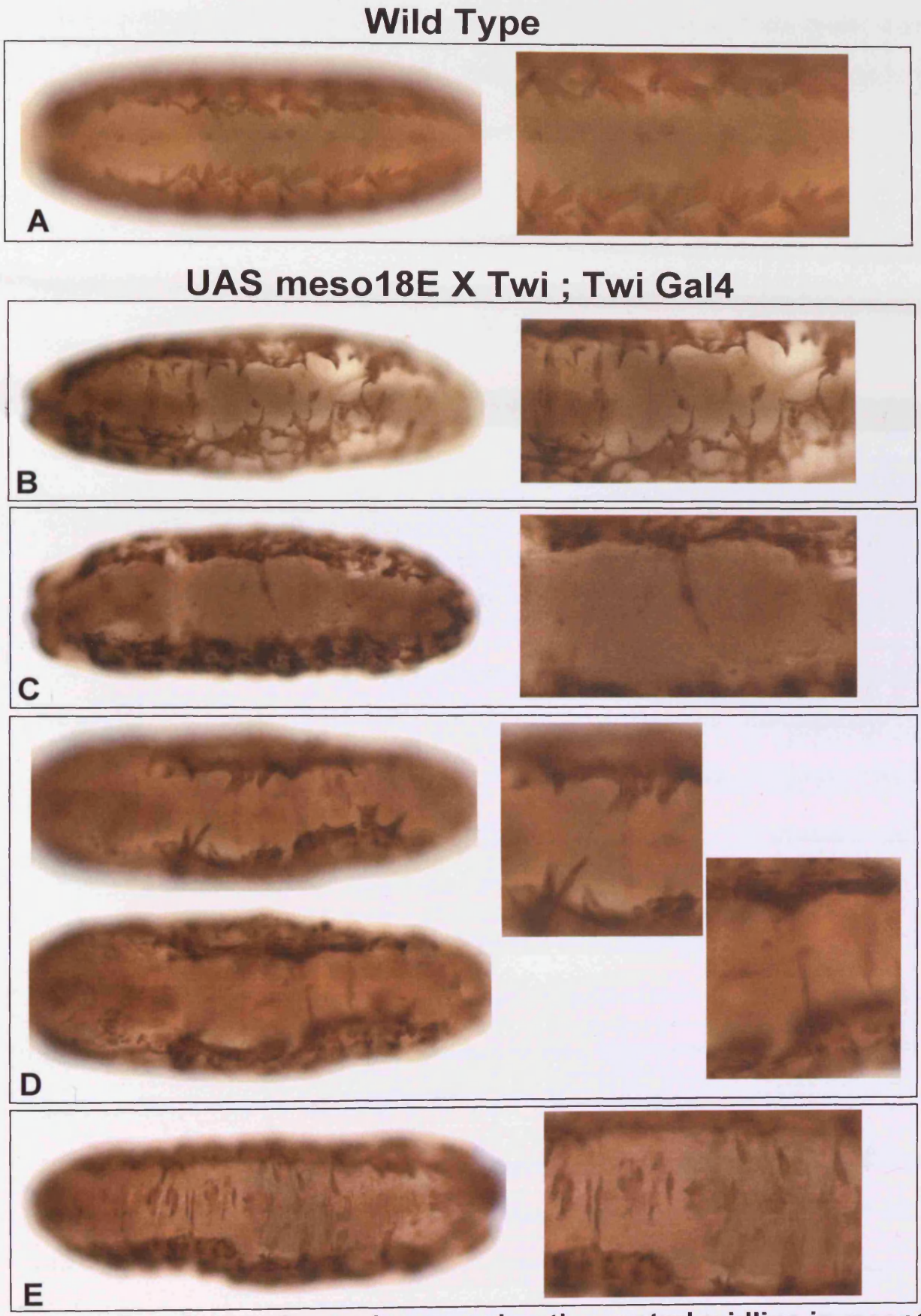

FIG 8.5.10 Examples of muscles crossing the ventral midline in meso18E over-expression embryos

Over-expression of meso18E slightly earlier in muscle development also causes a very severe disruption to muscle development. Driving the lines in the Twist pattern (with Twi ; Twi Gal4) can cause muscle loss, and severe shape and attachment defects in somatic musculature, disruption to the formation of the heart, failure of the gut to restrict (not shown) and muscles to stray into the ventral midline (FIG 8.5.9); these muscles can occasionally completely span the ventral midline (FIG 8.5.10). The line shown here is the stronger meso18E 20T2 UAS line and was driven with Twi; Twi Gal4 at 25°C. The meso18E 29T1 and 29T24 also gave a similar phenotype (not shown) in a manner resembling that seen when the lines were driven by Mef2 Gal4 (FIG 8.5.3).

8.6 meso18E loss-of-function.

After the discovery that meso18E gain-of-function gives a severe muscle phenotype in all the tissues it is normally expressed in (somatic : muscle loss, missattachment and misguidance, cardiac : complete loss of heart structure or cardioblast pattern, visceral : failure of gut to constrict, forming rounded bloated shape which can effect embryo shape, and pharyngeal : muscle cell shape and pattern) I wanted to investigate any potential phenotype associated with loss-of-function of meso18E in the embryo.

Investigation of the genomic region around meso18E (Flybase) showed that the region was rich in transposable element insertion stocks. FIG 8.6.1 shows a GBrowse map of the 18E region on the X chromosome which the meso18E gene lies in and highlights all the transposable element stocks available in the region. Analysis of the orientation and structure of the transposable elements revealed two which were appropriately aligned and positioned to enable the targeted deletion of meso18E alone through the technique of transposable element mediated recombination

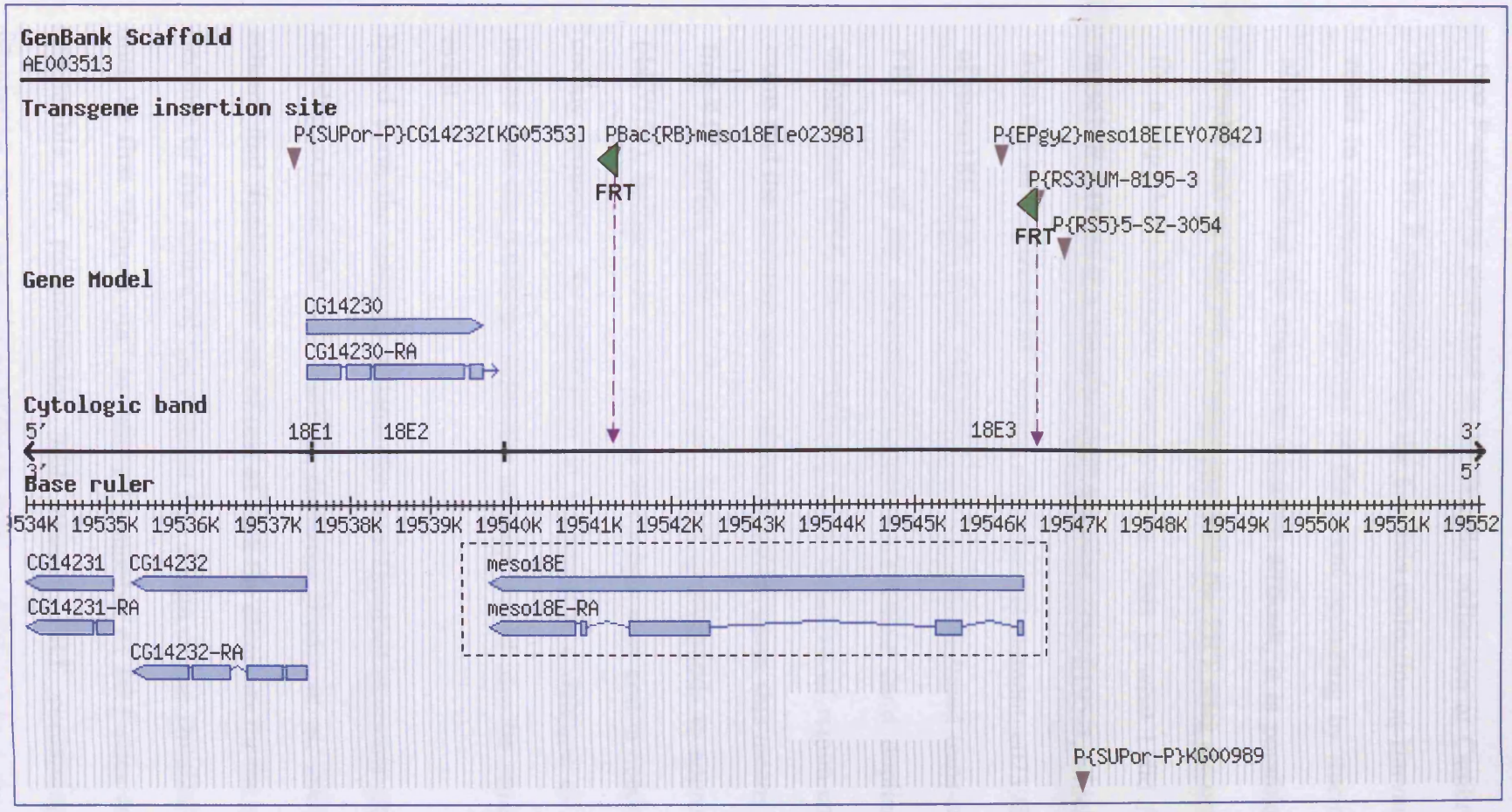

FIG 8.6.1 meso18E gene region and transposable element insertions

The Flybase GBrowse data for the region of the meso18E gene showing the pBac RB e02398 exelixis element and pRS3 UM-8195-3 DrosDel elements that can be used together to make a deficieny specific to meso18E.

(FlyBase)

Crossing schemes have been developed for generating an FRT mediated deletion between two P-elements generated in the Drosdel collection at Cambridge (Ryder et al, 2001) or between two P-elements from the Exelixis collection at Harvard (Parks et al, 2001) which result in convenient analysis of the event occurring by tracing a w+ marker. However, although tracing the event can be more difficult, it is possible to use a combination of a Drosdel and an Exelixis element provided the FRT sites are oriented in the same direction for a flip event between them to occur. This is what I did for the targeted deletion of meso18E. There is a DrosDel RS3 element, UM-8195-3, which is situated 59bp upstream from the start of meso18E and the Exelixis RB element, e02398, situated in the third intron of meso18E (FIG 8.6.1 and 8.6.2). A Flippase induced trans-recombination event via the FRT sites of the elements results in a deletion (and duplication) of the 5220bp's of endogenous DNA situated between them. Deletion of region corresponds to the first three exons and the first two introns of the meso18E gene, this means that a deletion removes the first 447 amino acids of the gene, which corresponds to approximately 80% of the gene (447/553), before even considering that a new start codon needs to be found in the remain coding sequence. As established in section 8.3, a deletion of the first 447 amino acids means that the predicted Myb-like domain would also be removed in the recombination event.

Based upon the crossing scheme for two DrosDel elements (Ryder et al, 2001) and the crossing scheme for two Exelixis elements (Parks et al, 2001), I designed a crossing scheme that would allow use of one of each the elements for the meso18E situation.

Because of the nature of the element and design of the DrosDel system, the RS3 element must be first "flipped out" to reduce its number of FRT sites from two to one making it compatible for recombination with another FRT containing element in the same orientation. The consequence of this is that an additional heat shock step is required and the

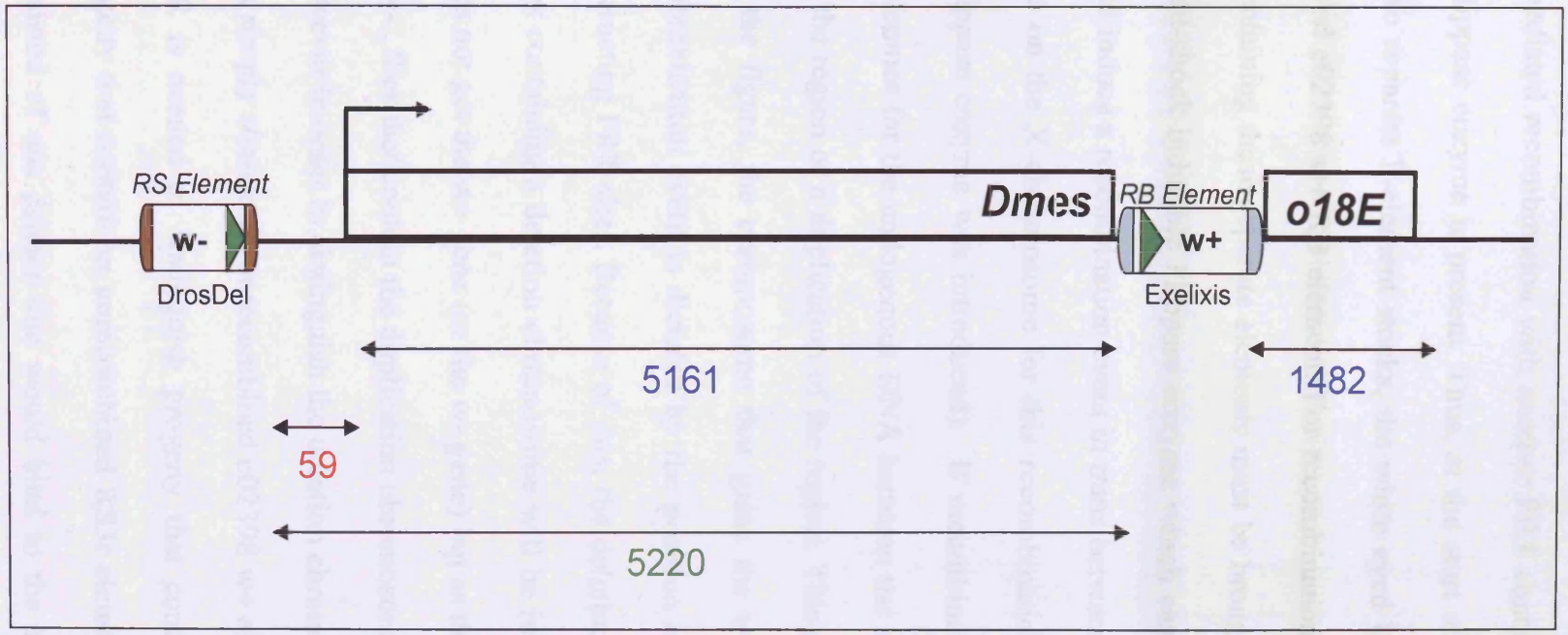

FIG 8.6.2 meso18E FRT element map

Graphic representation of the meso18E gene and the transposableelements in the region that can be used to generate a deletion of the gene. The RS element is UM-8195-3 (DrosDel) and the pBacRB element is e02398 (Exelixis).

On recombination between the FRT sites within elements 5220bp's of Endogenous DNA will be removed from the region that they span. This corresponds to the majority of the meso18E gene including the predicted myb-like domain towards the N terminus of the protein.

Around 1/5th of the gene will remain at the 3' end.

RS3 element loses its w+ marker gene, becoming a RS3r w- element at the same position in the genome. The e023898 RB element contains a w+ element is capable of FRT mediated recombination with another FRT containing element immediately, provided the Flippase enzyme is present. Thus, at the start of the recombination cross you begin with two separate P-element stocks, the white eyed UM-8195-3 RS3r w- element and the red eyed e02398 w+ RB element. For recombination to occur the individual X chromosomes containing these separate elements must be brought together in the presence of a copy of a heat-shock inducible Flippase enzyme which can act upon the FRT sites of the elements and induce a recombination event in trans between the two chromosomes. (As the elements are on the X chromosome for this recombination, an autosomal copy (on the II) of the Flippase enzyme was introduced). If recombination is successful there are two possible outcomes for the endogenous DNA between the two FRT sites of the elements, a deletion of the region or a duplication of the region. This event is outlined in FIG 8.6.4. As shown in the figure, the chromosome that gains the w+ gene from the RB element after the recombination event is dictated by the position of the eye colour gene in relation to the interacting FRT sites. Because of this, the deletion chromosome gains the w+ gene and so flies containing a deletion chromosome will be red eyed and the duplication chromosome does not get the w+ gene (or the w- gene) but as the genetic background for the cross stock is w- , flies that contain the duplication chromosome will be white eyed.

However in order to distinguish the deletion chromosome containing progeny with progeny that simply contain an unrecombined e02398 w+ element, PCR is needed. In the same way PCR is needed to distinguish progeny that contain a duplication chromosome with a progeny that contain an unrecombined RS3r element. Primers were designed in pairs that consisted of one primer that would bind to the end of an element and the other being specific to the endogenous DNA adjacent to it as outlined in FIG 8.6.4. As the figure

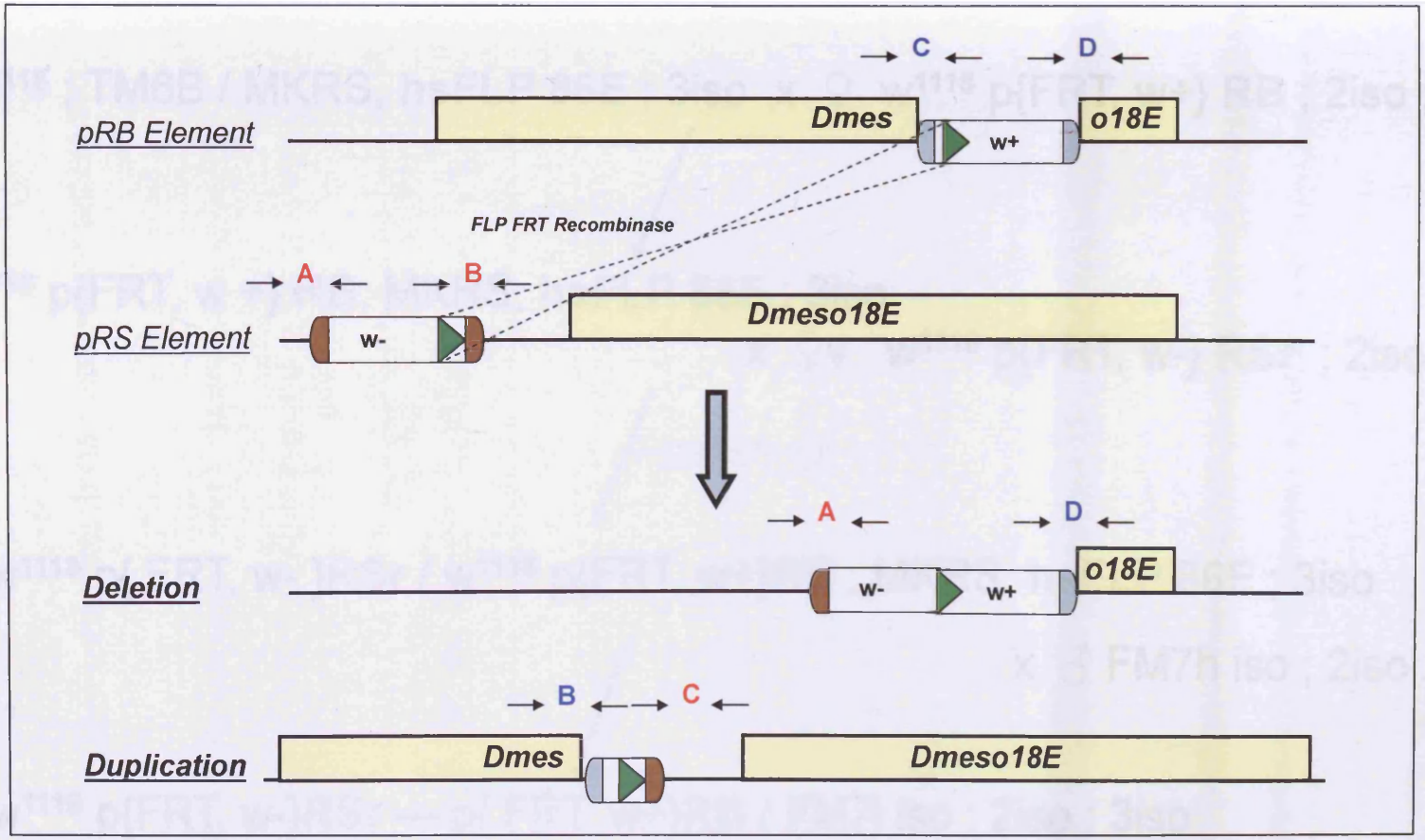

FIG 8.6.3 FRT element mediated trans recombination of the meso18E gene region

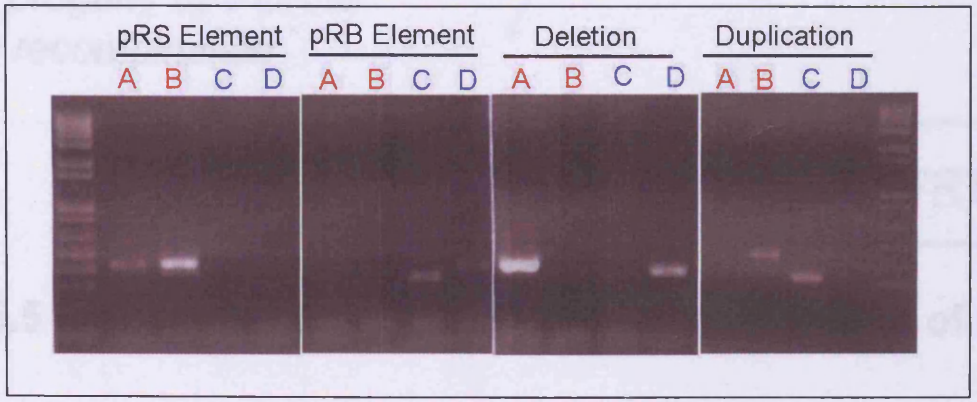

FIG 8.6.4 PCR confirmation of successful deletion and duplication recombination events

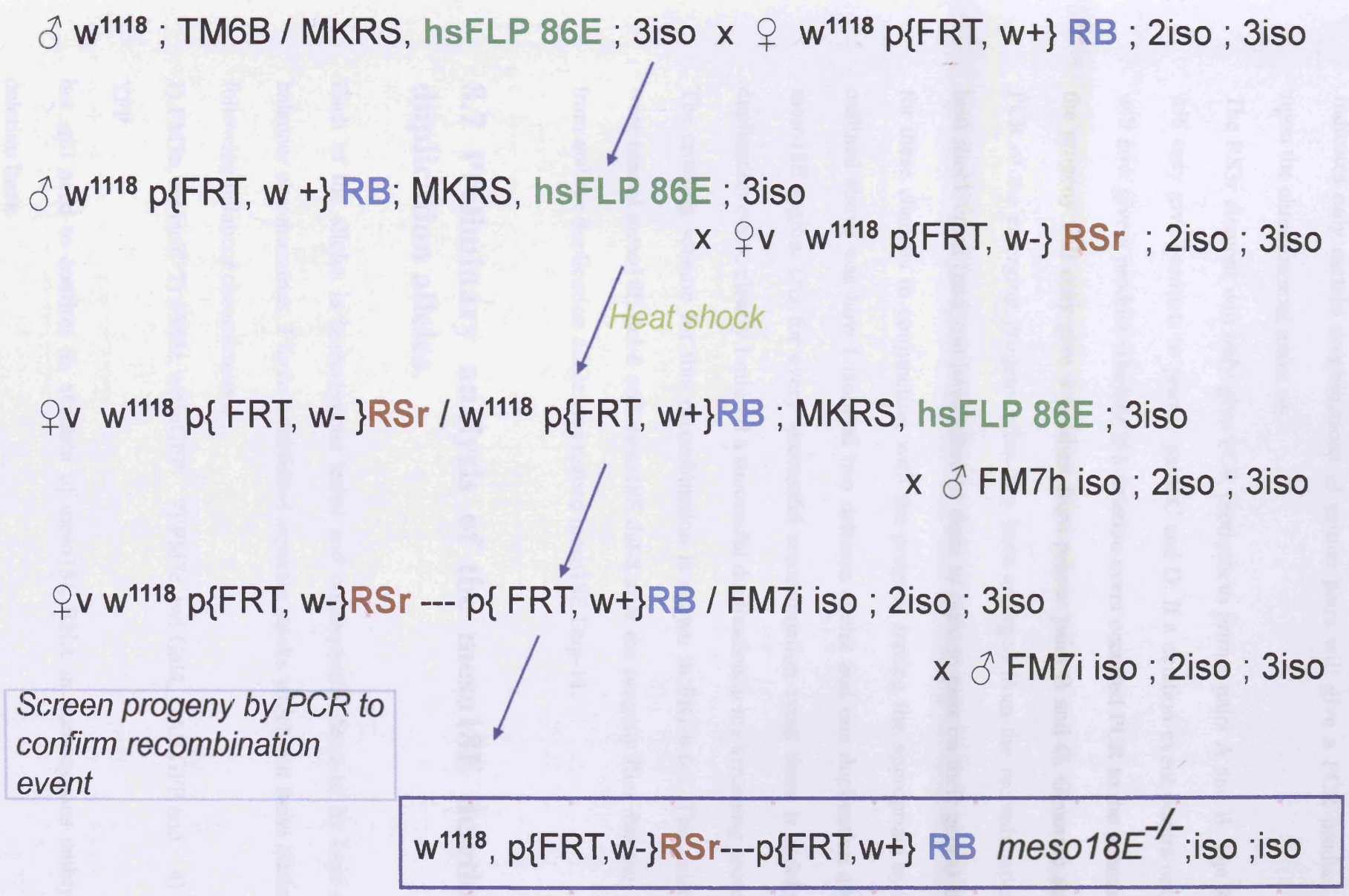

FIG 8.6.5 FRT element mediated trans-recombination of the *meso18E* gene region

indicates only certain combinations of primer pairs will give a PCR product depending upon the chromosomal make up.

The RS3r element will only give PCR products to primer pairs A and B. The RB element will only give products to primer pairs C and D. If a deletion event occurs only A and D will now give a product whereas if a deletion event occurred PCR to the genomic DNA of the progeny will only give a product from primer pairs B and C. Genomic screening by PCR of the emerging progeny after they have emerged from the recombination inducing heat shock cross (and you have allowed them to mate to pass on their genes) and looking for these changes in conjunction with the progeny having the appropriate eye colour as outlined above was how I isolated two deletion alleles and one duplication allele for the meso18E region. (As for every successful recombination event there is a deletion and a duplication event, clearly I missed a successful duplication in my screening process).

The crossing scheme for this recombination is shown in FIG 8.6.5. The deletion alleles were named meso18E del-6 and meso18E del-8 after the progeny flies that they originated from and the duplication allele was named meso18E Dup-11.

8.7 Preliminary analysis of the meso18E deletion and duplication alleles.

Each of the alleles is homozygous lethal and consequently have to be kept over FM7 balancer chromosomes. I have established separate stocks which put these alleles over the following balancer chromosomes :

1) FM7c, ftz lacZ 2) FM7c, actinGFP 3) FM7c, twi Gal4, UAS GFP and 4) FM7c dfd YFP

but still need to confirm an absence of meso18E RNA in homozygous embryos of the deletion lines.

Experiment	Embryo Hatching	Survival to adult fly
Wild Type	99 %	87 %
meso18E Del-6	100 %	4 %
meso18E Del-8	100 %	5 %
meso18E Dup-11	96 %	8 %
meso18E RNAi x Dicer II ; Mef2 Gal4 (29°c)	92 %	0 %

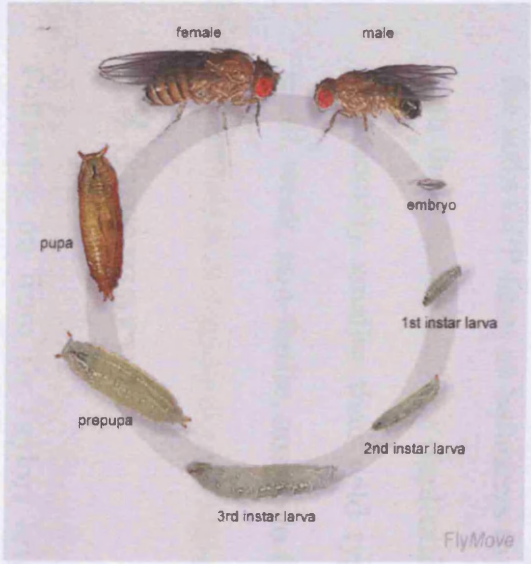

FIG 8.7.1 *meso18E* mutant phenotype analysis

Hatching and survival data for the established deletion and duplication lines for the meso18E recombination. The data suggests that the mutants are lethal with only a small number of escapers surviving to adulthood. These that survive are infertile and die within a day of eclosing. The majority of the mutants die at the pupal stage for both the deletion and duplication lines.

All three of the lines themselves are homozygous lethal. Hatching and survival tests using the actin GFP lines as balancers to test for homozyosity reveal that the majority of flies for both the deletion and the duplication lines die at the late larval / pupal stages. Pupae are considerably smaller than wild type. There are occasional adult escapers and these are small, weak, non-fertile, unable to fly and die within one day of eclosion (FIG 8.7.1).

8.8 Summary

Following on from Dr.Taylors original investigation I have found the following in my characterisation of meso18E;

It is a putative nuclear factor that contains a conserved helix-helix-turn-helix Myb-like domain at its N terminus.

That it is a direct target of Mef2; a 1Kb region upstream of the gene is capable of recapitulating meso18E expression, and a Mef2 site located in a region of phylogenetically conserved non-coding DNA within this region is essential for this expression, as revealed by Site Directed Mutagenesis to the binding site of a GFP reporter construct.

Over-expression of meso18E causes a severe disruption to the formation of the somatic musculature, heart and visceral muscle. A predominant phenotype of misguided muscles in the abdominal wall is seen as well a number of muscles than can stray across the ventral midline and others that can cross the dorsal midline. In addition overexpression in the heart causes a severe disruption to the formation of the vessel as seen with loss of b3 tubulin expressing cardioblasts.

That a distinct subset of muscles are seen to be missing in meso18E over-expression embryos that are different to the high mef2 requirement subset as seen in Mef2 loss of function conditions.

In addition I have generated and confirmed by PCR two deletion alleles and one duplication allele for *meso18E* that were made by P-element mediated recombination.

All of these alleles are lethal at the pupal stage; the flies are smaller than wild type and fail to get out of their pupal case.

In addition to these new mutant alleles, I have also generated a UAS meso18E 1-125 overexpression construct for which transgenic lines have recently been generated.

8.9 Discussion

As a potential transcription factor that is directly activated early in myogenesis by Mef2 meso18E is a good candidate for a role as a Mef2 effector; a factor which would subsequently activate its own cohort of genes to help regulate a specific process.

The phenotype associated with meso18E over-expression suggests that this could be as an effector of the muscle guidance program. If this was the case one might expect evidence of regulation by meso18E or genetic interaction of meso18E with factors already known to be players in this process, be this at the level of signalling between the tendons and myotube or in defining the midline with genes such as roundabout.

Concluding Remarks and Models for Mef2 action.

The aim of this study was to gain insight on the role of Mef2 in muscle development. I did this through changing Mef2 activity levels throughout the embryo by a variety of distinct methods and then carefully characterising the terminal somatic muscle phenotype and investigating any trends.

From the observations this study has presented I feel that two models can be made which provide an explanation for the role of Mef2 in the patterning of the somatic musculature. The first comes from the observation that, unlike previously thought, there is a role for Mef2 in the specification of founder cells – though only a specific subset of founders. The model, outlined below (and expanded from observations by Park et al, 1998), provides an explanation placing the actions Mef2 and Him in the fate specification of the affected subset of founder cells.

The second model is the idea that individual somatic muscles have a specific requirement for Mef2 for their correct formation and that this requirement may be dictated by the identity genes that the muscle derives from. Though this second aspect can be an explanation for a role for Mef2 in founder cell specification, it is also an explanation for the correct formation of muscles whose founders appear to have formed independently of Mef2.

9.1 The specification of particular founder cells

I identified a possible role for Mef2 in the specification of the founder cells that specify the DO1, LT1, LT2, LT3 and VA3 muscles.

Experiments looking at the Kruppel positive founders for the DO1/DA1 muscle show that these founder cells can undergo an increase in number under conditions of increased Mef2

activity and that this manifests as a duplication in the corresponding muscle in the terminal St17 phenotype. The sibling for this DO1 founder is a pericardial cell. The two cells derive from a progenitor that is initially positive for Mef2, but on division and distribution of the asymmetric determinant Numb, the cells adopt two different fates; the cell that acquires Numb maintains Mef2 expression and becomes a DO1 founder (that will subsequently differentiate into the DO1 muscle), whereas the cell that does not acquire numb loses Mef2 expression and becomes an eve positive pericardial cell of the heart (Park et al, 1998).

In FIG 9.1.1, I add to this model by suggesting that it is Him that is responsible for this loss of Mef2 expression and that this action is mediated by Notch maintaining expression of Him. The other muscles such as the VA3, which is derived from a muscle / non-muscle sibling pair (VA3 founder and AMP – Beckett and Baylies, 2009) can also be explained in this way. Such a model would provide an explanation for the maintenance of Him expression observed in the AMPs and pericardial cells (Chapter 4) and is supported by a number of factors such as over-expression of Him causing increased pericardial cell number (Liotta, PhD thesis 2006), the presence of numerous SuH sites in the Him regulatory region (Chapter 4.3 and Rebeiz et al, 2002) and the observation that Him appears as a potential Notch target on a recent microarray (Krejci and Bray, 2007).

As can be seen from FIG 9.1.1, the distribution of the factors provides an explanation for both an increase in these muscle numbers seen in Him mutants or Mef2 overexpression and also an explanation for decrease in muscle number in Him overexpression or Mef2 mutant backgrounds. FIG 9.1.2 shows fates adopted in various experimental conditions and an explanation for these fates according to the model. From this it is clear that a number of further investigations are required in order to validate the model. One of the key experiments would be to show that when a muscle duplication occurs (in Him mutants or

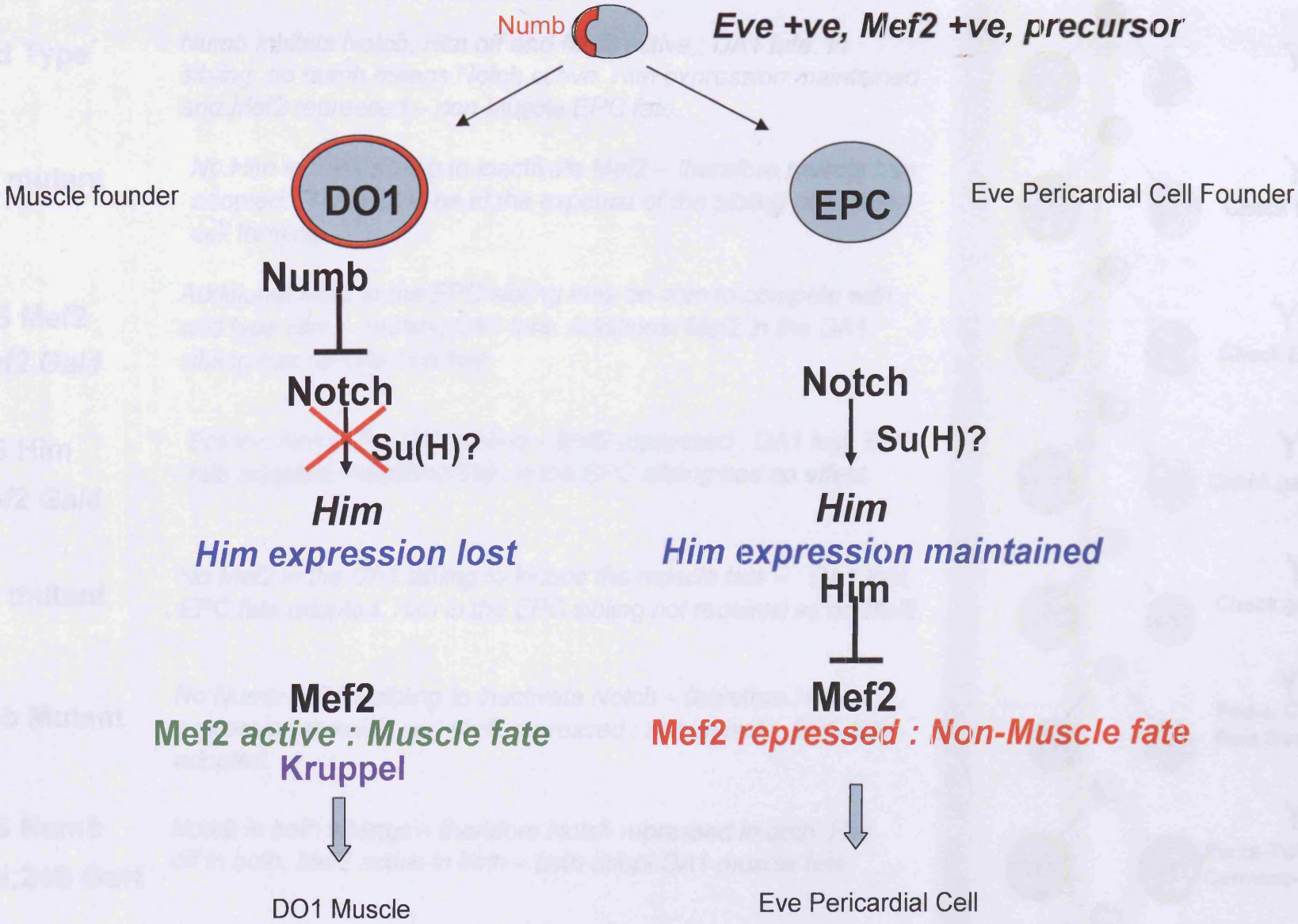

FIG 9.1.1 A model for the role of Mef2 in asymmetric founder division

Experiment	Comments	Cell fate outcome	Seen?
Wild Type	*Numb inhibits Notch, Him off and Mef2 active : DA1 fate. In sibling, no numb means Notch active, Him expression maintained and Mef2 repressed – non Muscle EPC fate.*	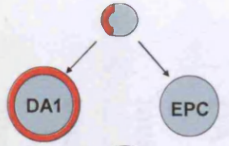	Y
Him mutant	*No Him in EPC sibling to inactivate Mef2 – therefore muscle fate adopted. This would be at the expense of the sibling pericardial cell forming.*	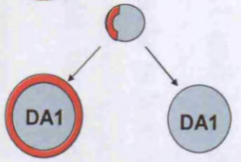	Y **Check EPC loss**
UAS Mef2 x *Mef2 Gal4*	*Additional Mef2 in the EPC sibling may be able to compete with wild type Him – causing DA1 fate. Additional Mef2 in the DA1 sibling has no effect on fate.*	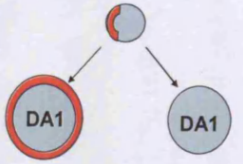	Y **Check EPC loss**
UAS Him x *Mef2 Gal4*	*Ectopic Him in the DA1 sibling – Mef2 repressed : DA1 lost, EPC fate adopted. Additional Him in the EPC sibling has no effect.*	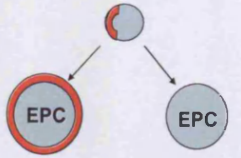	Y **Check gain of EPC**
Mef2 mutant	*No Mef2 in the DA1 sibling to induce the muscle fate – : DA1 lost, EPC fate adopted. Him in the EPC sibling not required as no Mef2.*	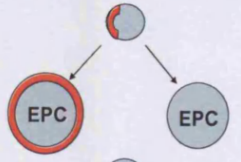	Y **Check gain of EPC**
Numb Mutant	*No Numb in DA1 sibling to inactivate Notch – therefore Him expression remains and Mef2 repressed : non-muscle, EPC fate adopted.*	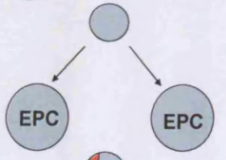	Y **Parks. Carmena. Ruiz Gomez**
UAS Numb xTwi;24B Gal4	*Numb in both siblings – therefore Notch repressed in both, Him off in both, Mef2 active in both – both adopt DA1 muscle fate.*	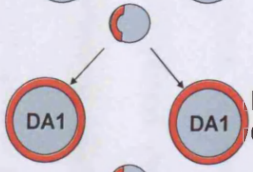	Y **Parks-Twi;24B Gal4 Carmena-Twi Gal4**
Notch mutant	*Him expression not maintained in the EPC sibling as Notch not present to activate. Thus the DA1 fate is adopted as Mef2 is not repressed in the EPC sibling*	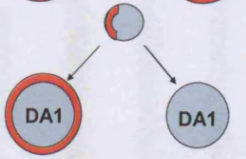	Y **Parks.**

FIG 9.1.2 Cell fate outcome for Mef2 founder cell specification model

UAS Mef2 experiments) a pericardial cell is lost (or AMP is lost, if that is the sibling cell of the pair such as with VA3). The most suitable way to achieve this would be by double florescent labelling for Eve and Kruppel as this would be able to show distinctly each DO1, DA1 and eve positive pericardial cell in an experimental condition. Conversely, when a muscle is lost it would be good to show that a pericardial cell is gained. Additionally if it could be shown that overexpression of Mef2 was able to rescue the *Numb* mutant phenotype and Him overexpression was able to rescue the *Notch* mutant phenotype, this would both reinforce the validity of the model and help place factors in the correct position in the pathway.

It should also be noted that despite the plausibility of this model other explanations exist for a possible muscle duplication at this stage; for example if there is a division of the founder cell before myoblast recruitment this could explain the formation of two muscles of the same fate forming in the same area as is seen. The main difference between this and the model is that the sibling cell of the precursor should develop normally in this situation.

9.2 The Role of Mef2 activity requirement for general muscle patterning

The other model I propose is based upon the fact that certain muscles have a specific requirement for Mef2 activity; with High Mef2 Requirement Muscles being easily lost and Low Mef2 Requirement Muscles remaining present under conditions of decreased Mef2 activity. Analysis of the individual muscles that fall into these categories in conjunction with the expression patterns of known identity genes allows for a model that proposes the identity genes in turn have various requirements for Mef2 activity. The fact that the identity

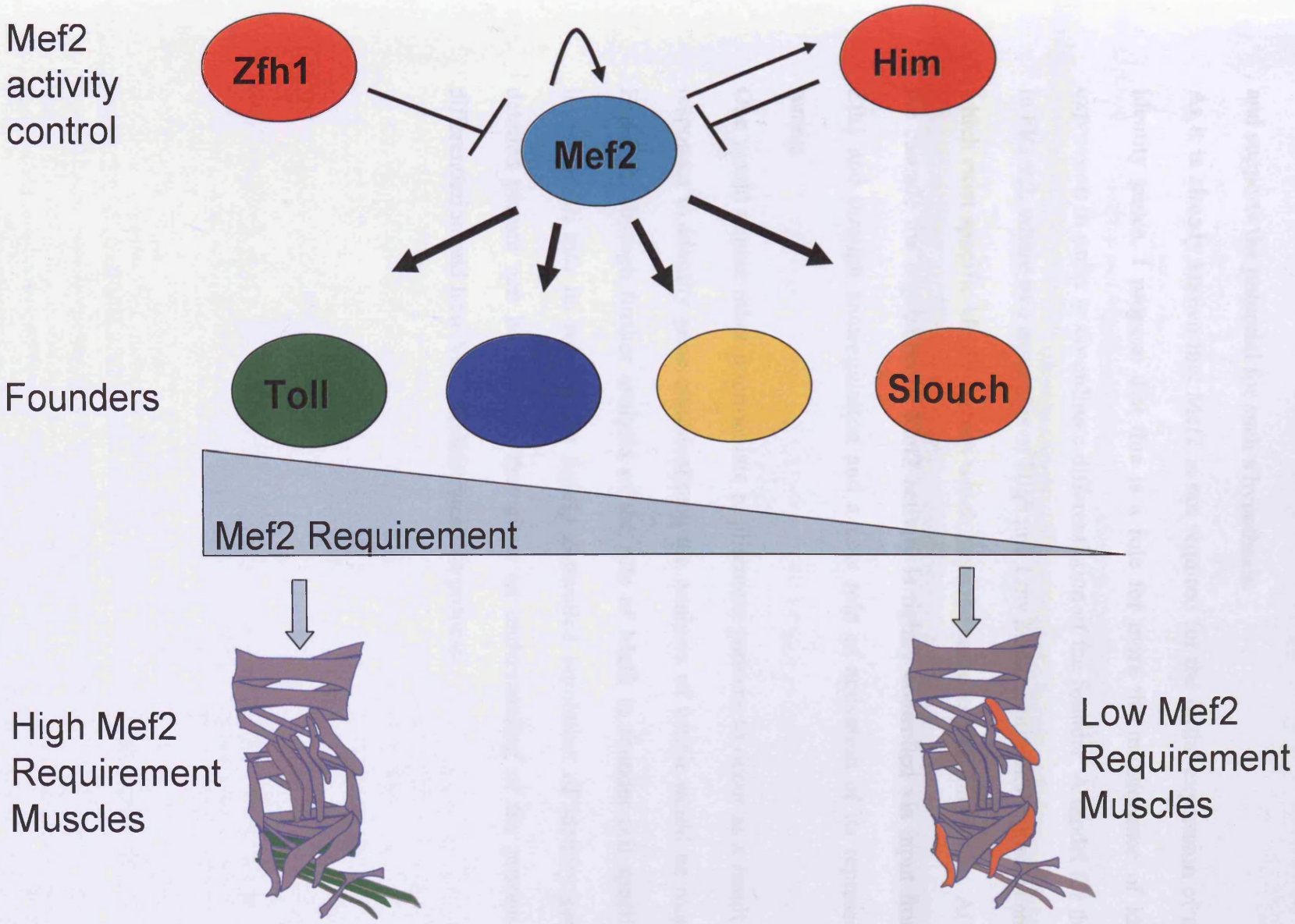

FIG 9.2 A model for the role of Mef2 activity requirement for general muscle patterning

genes are potential Mef2 targets has only recently been established (Sandmann et al, 2006) and supports the potential for such a hypothesis.

As it is already known that Mef2 is not required for the initial expression of many of the identity genes, I propose that this is a role for more the maintenance of identity gene expression in order to co-ordinate differentiation of the founder. A model for this is shown in FIG 9.2, where two examples of High and Low Mef2 requirement muscles are shown for which exist specific identity genes which have the same expression pattern. At the head of the cascade the regulation of Mef2 activity is tightly controlled via input from Him and Zfh1 and through autoregulation and a new role of activation of its repressors for fine tuning.

One would expect other intermediate requirement patterns to occur as a result of possible responses to identity gene combinations, the analysis of which would be more complex. However, through further analysis of the role of Mef2 in founder cell specification and investigation into its role in the tightly controlled regulation of identity genes a more detailed picture can be built up that gives an understanding of the process of muscle differentiation and how Mef2 orchestrates this process.

References

Aasland R., Stewart A.F., Gibson T. (1996) The SANT domain: a putative DNA-binding domain in the SWI-SNF and ADA complexes, the transcriptional corepressor N-CoR and TFIIIB. Trends Biochem. Sci. 21:87-88.

Adams MD, Celniker SE, Holt RA, Evans CA, Gocayne JD et al. (2000) The genome sequence of *Drosophila melanogaster*. Science 287(5461): 2185-2195.

Adams MD and Sekelsky JJ (2002) From sequence to Phenotype : Reverse Genetics in *Drosophila melanogaster* Nature Rev. Genet. 3, 189–198

Ambros V (2004) The functions of animal microRNAs. Nature 431(7006): 350-355.

Anant S, Roy S, VijayRaghavan K (1998) Twist and Notch negatively regulate adult muscle differentiation in *Drosophila*. Development 125(8): 1361-1369.

Andres, V., Cervera, M. and Mahdavi, V. (1995). Determination of the consensus binding site for MEF2 expressed in muscle and brain reveals tissue specific sequence constraints. J. Biol. Chem. 270, 23246-23249.

Arredondo, J. J., Ferreres, R. M., Maroto, M., Cripps, R. M., Marco, R., Bernstein, S. I. and Cervera, M. (2001). Control of *Drosophila paramyosin/miniparamyosin* gene expression. Differential regulatory mechanisms for muscle-specific transcription. J Biol Chem 276, 8278-87

Artavanis-Tsakonas S MK, Fortini ME. (1995) Notch signaling. Science 268(5208): 225-232.

Artero, R. D., Castanon, I. and Baylies, M. K. (2001). The immunoglobulin-like protein Hibris functions as a dose-dependent regulator of myoblast fusion and is differentially controlled by Ras and Notch signaling. Development 128, 4251-64.

Ashburner M, Drysdale R (1994). FlyBase-the *Drosophila* genetic database. Development. 1994 Jul;120(7):2077-9

Ashburner M, Golic K and Hawley S (2004) *Drosophila* : A Laboratory handbook (2nd Edition) Cold Spring Harbor Laboratory Press ISBN-10: 0879697067

Ashburner M and Bergman CM (2005) *Drosophila melanogaster*: a case study of a model genomic sequence and its consequences. Genome Res. Dec;15(12):1661-7

Azpiazu, N. and Frasch, M. (1993). *tinman* and *bagpipe*: two homeo box genes that determine cell fates in the dorsal mesoderm of *Drosophila*. Genes Dev 7, 1325-40.

Azpiazu, N., Lawrence, P. A., Vincent, J. P. and Frasch, M. (1996). Segmentation and specification of the *Drosophila* mesoderm. Genes Dev 10, 3183-94.

Baker PW TK, Klitgord N, Cripps RM. (2005) Adult myogenesis in *Drosophila melanogaster* can proceed independently of *myocyte enhancer factor-2*. Genetics 170(4): 1747-1759.

Barolo S, Carver LA, Posakony JW (2000) GFP and beta-galactosidase transformation vectors for promoter/enhancer analysis in *Drosophila*. Biotechniques. Oct;29(4):726

Bate M (1990) The embryonic development of larval muscles in *Drosophila*. Development 110(3): 791-804.

Bate M (1993) The mesoderm and its derivaties. In: Bate M, Arias AM (eds) The development of *Drosophila melanogaster*. Cold Spring Harbor Laboratory Press, Cold Spring Harbor, NY, Vol 3, pp 1013–1090

Bate M, Rushton E, Currie DA (1991) Cells with persistent *twist* expression are the embryonic precursors of adult muscles in *Drosophila*. Development 113(1): 79-89.

Bate, M. and Rushton, E. (1993). Myogenesis and muscle patterning in *Drosophila*. C R Acad Sci III 316, 1047-61.

Baylies MK, Bate M (1996) *twist*: a myogenic switch in *Drosophila*. Science 272(5267): 1481-1484.

Baylies MK, Bate M, and Ruiz Gomez M (1998) Myogenesis: a view from *Drosophila*. Cell 93(6): 921-927.

Becker, S., Pasca, G., Strumpf, D., Min, L., and Volk, T. (1997). Reciprocal signaling between *Drosophila* epidermal muscle attachment cells and their corresponding muscles. Development 124,2615–2622.

Beckett K and Baylies MK (2007) 3D analysis of founder cell and fusion competent myoblast arrangements outlines a new model of myoblast fusion. Developmental Biology 309 (2007) 113–125

Beinert N WM, Dowe G, Chung HR, Jackle H, Schafer U. (2004) Systematic gene targeting on the X chromosome of *Drosophila melanogaster*. Chromosoma 113(6): 271-275.

Bellaiche Y MV, Perrimon N. (1999) *I-SceI* endonuclease, a new tool for studying DNA double-strand break repair mechanisms in *Drosophila*. Genetics 152(3): 1037-1044.

Bellen HJ LR, Liao G, He Y, Carlson JW, Tsang G, Evans-Holm M,, Hiesinger PR SK, Rubin GM, Hoskins RA, Spradling AC. (2004) The BDGP gene disruption project: single transposon insertions associated with 40% of *Drosophila* genes. Genetics 167(2): 761-781.

Berg CA SA (1991). Studies on the rate and site-specificity of P element transposition. Genetics 127(3): 515-525.

Bernstein SI ODP, Cripps RM. (1993) Molecular genetic analysis of muscle development, structure, and function in *Drosophila*. Int Rev Cytol 143: 63-152.

Bernstein SI, O'Donnell PT, Cripps RM. (1993). Molecular genetic analysis of muscle development, structure, and function in *Drosophila*. Int Rev Cytol.;143:63-152

Blanchard FJ, Shawn A, Cyran SA, Hancock DH, Taylor MV, Blau J (2010). The transcription factor Mef2 is required for normal circadian behavior in *Drosophila*. J.Neuroscience.

Black, B. L. and Olson, E. N. (1998). Transcriptional control of muscle development by myocyte enhancer factor-2 (MEF2) proteins. Annu Rev Cell Dev Biol 14, 167-96

Bour BA, O'Brien MA, Lockwood WL, Goldstein ES, Bodmer R et al. (1995) *Drosophila* MEF2, a transcription factor that is essential for myogenesis. Genes Dev 9(6): 730-741.

Bour, B. A., Chakravarti, M., West, J. M. and Abmayr, S. M. (2000). *Drosophila* SNS, a member of the immunoglobulin superfamily that is essential for myoblast fusion. Genes Dev 14, 1498-511.

Bourgouin, C., Lundgren, S. E. and Thomas, J. B. (1992). *Apterous* is a *Drosophila* LIM domain gene required for the development of a subset of embryonic muscles. Neuron 9, 549-61.

Boyer L.A., Latek R.R., Peterson C. (2004). The SANT domain: a unique histone-tail-binding module? Nat. Rev. Mol. Cell Biol. 5:158-163.

Bray S FM (2001) Notch pathway: making sense of suppressor of hairless. Curr Biol 11(6): 217-221.

Brewer PB HP, Dorian K, Griffith ME, Ishida T, Kaplan-Levy RN, Kilinc A,, DR. S (2004) PETAL LOSS, a trihelix transcription factor gene, regulates perianth architecture in the *Arabidopsis* flower. Development 131(16): 4035-4045.

Broihier HT, Moore LA, Van Doren M, Newman S, Lehmann R.(1998) *zfh-1* is required for germ cell migration and gonadal mesoderm development in *Drosophila*. Development.;125(4):655-66.

Brown, N.H., Gregory, S.L., and Martin-Bermudo, M.D. (2000). Integrins as mediators of morphogenesis in *Drosophila*. Dev. Biol. 223,1–16.

Carmena, A., Bate, M. and Jimenez, F. (1995). *Lethal of scute,* a proneural gene, participates in the specification of muscle progenitors during *Drosophila* embryogenesis. Genes Dev 9, 2373-83.

Carmena, A., Murugasu-Oei, B., Menon, D., Jimenez, F. and Chia, W. (1998). *Inscuteable* and *numb* mediate asymmetric muscle progenitor cell divisions during *Drosophila* myogenesis. Genes Dev 12, 304-15.

Castro JP and Carareto CMA (2004) *Drosophila melanogaster P* transposable elements: mechanisms of transposition and regulation. Genetica 121: 107–118, 2004.

Chavez VM MG, Delbecque JP, Kobayashi K, Hollingsworth M, Burr J, Natzle, JE OCM (2000) The *Drosophila* disembodied gene controls late embryonic morphogenesis and codes for a cytochrome P450 enzyme that regulates embryonic ecdysone levels. Development 127(19): 4115-4126.

Chen, E. H. and Olson, E. N. (2001). Antisocial, an intracellular adaptor protein, is required for myoblast fusion in *Drosophila*. Dev Cell 1, 705-15.

Chen, E. H., Pryce, B. A., Tzeng, J. A., Gonzalez, G. A. and Olson, E. N. (2003). Control of myoblast fusion by a guanine nucleotide exchange factor, loner, and its effector ARF6. Cell 114, 751-62.

Colombani J BL, Layalle S, Pondeville E, Dauphin-Villemant C,, Antoniewski C CC, Noselli S, Leopold P. (2005) Antagonistic actions of ecdysone and insulins determine final size in *Drosophila*. Science 310(5748): 667-670.

Cripps, R. M., Black, B. L., Zhao, B., Lien, C. L., Schulz, R. A. and Olson, E. N. (1998). The myogenic regulatory gene *Mef2* is a direct target for transcriptional activation by Twist during *Drosophila* myogenesis. Genes Dev 12, 422-34.

Cripps RM LT, Olson EN. (2004). Positive autoregulation of the Myocyte enhancer factor-2 myogenic control gene during somatic muscle development in *Drosophila*. Dev Biol 267(2): 536-547.

Crozatier M, Vincent A (1999) Requirement for the *Drosophila* COE transcription factor Collier in formation of an embryonic muscle: transcriptional response to Notch signalling. Development. 126:1495-1504.

Damm, C., Wolk, A., Buttgereit, D., Loher, K., Wagner, E., Lilly, B., Olson, E. N., Hasenpusch-Theil, K. and Renkawitz-Pohl, R. (1998). Independent regulatory elements in the upstream region of the *Drosophila beta 3 tubulin* gene (*beta Tub60D*) guide expression in the dorsal vessel and the somatic muscles. Dev Biol 199, 138-49.

Dietzl G, Chen D, Schnorrer F, Su KC, Barinova Y, Fellner M, Gasser B, Kinsey K, Oppel S, Scheiblauer S, Couto A, Marra V, Keleman K, Dickson BJ (2007). A genome-wide transgenic RNAi library for conditional gene inactivation in Drosophila. Nature. Jul 12;448(7150):151-6

Dohrmann, C., Azpiazu, N. and Frasch, M. (1990). A new *Drosophila* homeo box gene is expressed in mesodermal precursor cells of distinct muscles during embryogenesis. Genes Dev 4, 2098-111.

Dorn A, Romer F (1976) Structure and Function of prothoracic glands and oenocytes in embryos and last larval instars of *Oncopeltus fasciatus*. Cell and Tissue Research 171: 331-350.

Drysdale R; FlyBase Consortium (2008) FlyBase : a database for the *Drosophila* research community Methods Mol Biol. ;420:45-59.

Dubois L, Enriquez J, Daburon V, Crozet F, Lebreton G, Crozatier M and Vincent A (2007) *collier* transcription in a single *Drosophila* muscle lineage : the combinatorial control of muscle identity. Development 134, 4347-4355

Duffy JB (2002) GAL4 system in *Drosophila*: a fly geneticist's Swiss army knife. Genesis. Sep-Oct;34(1-2):1-15

Dunin-Borkowski OM., Brown NH. and Bate M. (1995). Anterior-posterior subdivision and the diversification of the mesoderm in *Drosophila*. Development 121, 4183-93.

Dworak HA and Sink H (2002) Myoblast fusion in *Drosophila*. Bioessays 24:591–601, 2002.

Edmondson, D. G., Lyons, G. E., Martin, J. F. and Olson, E. N. (1994). *Mef2* gene expression marks the cardiac and skeletal muscle lineages during mouse embryogenesis. Development 120, 1251-63.

Eissenberg JC WM, Chrivia JC. (2005) Human SRCAP and *Drosophila melanogaster* DOM are homologs that function in the notch signaling pathway. Mol Cell Biol 25(15): 6559-6569.

Elgar SJ, Han J, and Taylor MV (2008) mef2 activity levels differentially affect gene expression during *Drosophila* muscle development. PNAS 918–923 vol.105-3

Elstob PR BV, Gould AP (2001) Spalt-dependent switching between two cell fates that are induced by the *Drosophila* EGF receptor. Development 128(5): 723-732.

Engels, W.R., (1983). The *P* family of transposable elements in *Drosophila.* Ann. Rev. Genet. 17: 315–344.

Engels W (1992) The origin of P elements in *Drosophila melanogaster*. Bioessays 14(10): 681-686.

England BP, Admon A, and Tjian R(1992) Cloning of *Drosophila* transcription factor Adf-1 reveals homology to Myb oncoproteins Proc. Nati. Acad. Sci. USA Vol. 89, pp. 683-687

Fire A, Xu S, Montgomery MK, Kostas SA, Driver SE, and Mello, CC. (1998) Potent and specific genetic interference by double-stranded RNA in *Caenorhabditis elegans*. Nature 391, 806-811

Fortini, M. E., Lai, Z. C. and Rubin, G. M. (1991). The *Drosophila zfh-1* and *zfh*-2 genes encode novel proteins containing both zinc-finger and homeodomain motifs. *Mech Dev* 34, 113-22.

Frasch, M., Hoey, T., Rushlow, C., Doyle, H. and Levine, M. (1987). Characterization and localization of the even-skipped protein of *Drosophila*. Embo J 6, 749-59.

Frasch, M. (1995). Induction of visceral and cardiac mesoderm by ectodermal Dpp in the early *Drosophila* embryo. Nature 374, 464-7.

Frasch M (1999) Control in patterning and diversification of somatic muscles during *Drosophila* embryogenesis. Curr. Opin. Gene & Dev. 9:522-529

Frazer KA, Pachter L, Poliakov A, Rubin EM, Dubchak I.(2004) VISTA: computational tools for comparative genomics. Nucleic Acids Res. Jul 1;32(Web Server issue):W273-9.

Frommer, G., Vorbruggen, G., Pasca, G., Jackle, H., and Volk, T.(1996). Epidermal egr-like zinc finger protein of *Drosophila* participates in myotube guidance. EMBO J. 15, 1642–1649.

Fu YW, Mohun TJ, Evans SM (1998) Vertebrate *tinman* homologues *XNkx2-3* and *XNkx2-5* are required for heart formation in a functionally redundant manner. Development 125(22): 4439-4449.

Furlong EE, Andersen EC, Null B, White KP, Scott MP. (2001). Patterns of gene expression during *Drosophila* mesoderm development. Science 293:1629–1633.

Goldstein ES TS, Stephenson AE, Gramstad GD, Keilty A, Kirsch L,, Imperial M GS, Hudson SG, LaBell AA, O'Day M, Duncan C, Tallman M,, Cattelino A LJ (2001) A genetic analysis of the cytological region 46C-F containing the *Drosophila melanogaster* homolog of the jun proto-oncogene. Mol Genet Genomics 266(4): 695-700.

Golic KG, GM (1996) Engineering the *Drosophila* genome: chromosome rearrangements by design. Genetics 144(4): 1693-1711.

Gong WJ and Golic GK (2003) Ends-out, or replacement, gene targeting in *Drosophila*. Proc Natl Acad Sci U S A 100(5): 2556-2561.

Gong WJ and Golic GK (2004) Genomic deletions of the *Drosophila* melanogaster Hsp70 genes. Genetics 168(3): 1467-1476.

Gould AP EP, Brodu V. (2001) Insect oenocytes: a model system for studying cell-fate specification by *Hox* genes. J Anat 199: 25-33.

Grad YH, Roth FP, Halfon MS, Church GM, Silver LM, Elgin SC. (2004) Prediction of similarly acting cis-regulatory modules by subsequence profiling and comparative genomics in *Drosophila* melanogaster and D.pseudoobscura. Bioinformatics. Nov 1;20(16):2738-50. Epub 2004 May 14

Gray YH TM, Sved JA. (1996) P-element-induced recombination in *Drosophila* melanogaster: hybrid element insertion.. Genetics 144(4): 1601-1610.

Greenspan RJ (1997) Fly Pushing: Theory and Practice of *Drosophila* Genetics. Cold Spring Harbor Laboratory Press. ISBN-10: 0879694920

Gubb D, Roote J, Trenear J, Coulson D, Ashburner M. (1997) Topological constraints on transvection between white genes within the transposing element TE35B *in Drosophila melanogaster*. Genetics. Jul;146(3):919-37.

Gunthorpe D, Beatty KE, Taylor MV (1999) Different levels, but not different isoforms, of the *Drosophila* transcription factor DMEF2 affect distinct aspects of muscle differentiation. Dev Biol 215(1): 130-145.

Haflon, M.S., Hashimoto, C. and Keshishian, H. (1995). The *Drosophila Toll* gene functions zygotically and is necessary for proper motoneuron and muscle development. Dev. Biol. 169: 151-167.

Han K, Manley JL(1993). Functional domains of the *Drosophila* Engrailed protein. EMBO J.12(7):2723-33.

Han, Z., Fujioka, M., Su, M., Liu, M., Jaynes, J. B. and Bodmer, R. (2002). Transcriptional integration of competence modulated by mutual repression generates cell-type specificity within the cardiogenic mesoderm. Dev. Biol. 252, 225-240.

Han Z, Olson EN (2005) Hand is a direct target of Tinman and GATA factors during *Drosophila* cardiogenesis and hematopoiesis. Development 132(15): 3525-3536.

Hardin PE (2005) The circadian timekeeping system of *Drosophila*. Curr Biol. 6;15(17):R714-22

Hartl, D.L. and Lozoskaya, E.R. (1994). Genome evolution: between the nucleosome and the chromosome. EXS 69, 579-92.

Hiesinger PR BH (2004) Flying in the face of total disruption. Nat Genetics 36(3): 211-212.

Hulo N., Bairoch A., Bulliard V., Cerutti L., Cuche B., De Castro E., Lachaize C., Langendijk-Genevaux P.S., Sigrist C.J.A.(2007) *The 20 years of PROSITE.* Nucleic Acids Res. 2007 Nov 14.

Introna M LM, Castellano M, Arsura M, Golay J. (1994) The myb oncogene family of transcription factors: potent regulators of hematopoietic cell proliferation and differentiation. Semin Cancer Biol 5(2): 113-124.

Ip, Y. T., Park, R. E., Kosman, D., Yazdanbakhsh, K. and Levine, M. (1992). dorsal-twist interactions establish *snail* expression in the presumptive mesoderm of the *Drosophila* embryo. Genes Dev 6, 1518-30.

Jagla T, Bellard F, Lutz Y, Dretzen G, Bellard M, Jagla K (1998) ladybird determines cell fate decisions during diversification of *Drosophila* somatic muscles. Development. 125:3699-3708.

Jasin M BP (1988) Homologous integration in mammalian cells without target gene selection. Genes Dev 2(11): 1353-1363.

Jiang J, Kosman D, Ip YT, Levine M (1991) The dorsal morphogen gradient regulates the mesoderm determinant twist in early *Drosophila* embryos. Genes Dev 5(10): 1881-1891.

Johnson AN, Burnett LA, Sellin J, Paululat A, Newfeld SJ.(2007) Defective decapentaplegic signaling results in heart overgrowth and reduced cardiac output in *Drosophila*. Genetics.;176(3):1609-24

Junion G JT, Duplant S, Tapin R, Da Ponte JP, Jagla K. (2005) Mapping Dmef2-binding regulatory modules by using a ChIP-enriched in silico targets approach. Proc Natl Acad Sci U S A 102(51): 18479-18484.

Karamboulas C, Swedani A, Ward C, Al-Madhoun AS, Wilton S, Boisvenue S, Ridgeway AG, Skerjanc IS. (2006a) HDAC activity regulates entry of mesoderm cells into the cardiac muscle lineage. J Cell Sci. 15;119(Pt 20):4305-14.

Karamboulas C, Dakubo GD, Liu J, De Repentigny Y, Yutzey K, Wallace VA, Kothary R, Skerjanc IS. (2006b) Disruption of MEF2 activity in cardiomyoblasts inhibits cardiomyogenesis. J. Cell Sci. 15;119(Pt 20):4315-21

Kavi HH, Fernandez H, Xie W, Birchler JA.(2008) Genetics and biochemistry of RNAi in *Drosophila*. Curr Top Microbiol Immunol. 320:37-75

Keller, C.A., Erickson, M.S. and Abmayr, S.M. (1997). Misexpression of nautilus induces myogenesis in cardioblasts and alters the pattern of somatic muscles fibers. Dev. Biol. 181: 197-212.

Kelly, K. K., Meadows, S. M. and Cripps, R. M. (2002). *Drosophila* MEF2 is a direct regulator of *Actin57B* transcription in cardiac, skeletal, and visceral muscle lineages. Mech Dev 110, 39-50.

Krejcí A, Bray S (2007) Notch activation stimulates transient and selective binding of Su(H)/CSL to target enhancers Genes Dev. Jun 1;21(11):1322-7

Kidwell M (1983) Evolution of hybrid dysgenesis determinants in *Drosophila* melanogaster. Proc Natl Acad Sci U S A 80(6): 1655-1659.

Kidwell, M.G., (1985). Hybrid dysgenesis in *Drosophila melanogaster*: nature and inheritance of *P* element regulation. Genetics 111: 337–350.

Klinedinst SL and Bodmer R (2003) Gata factor Pannier is required to establish competence for heart progenitor formation. Development 130(13): 3027-3038

Kolodziejczyk, S. M., Wang, L., Balazsi, K., DeRepentigny, Y., Kothary, R. And Megeney, L. A. (1999). MEF2 is upregulated during cardiac hypertrophy and is required for normal post-natal growth of the myocardium. Curr. Biol. 9, 1203-1206.

Knirr S, Azpiazu N, Frasch M (1999) : The role of the NK-homeobox gene slouch (S59) in somatic muscle patterning. Development, 126: (20):4525-4535.

Knirr S, Frasch M (2001) Molecular integration of inductive and mesoderm-intrinsic inputs governs even-skipped enhancer activity in a subset of pericardial and dorsal muscle progenitors. Dev Biol 238(1): 13-26.

Kopczynski CC, Noordermeer JN, Serano TL, Chen WY, Pendleton JD, Lewis S, Goodman CS, Rubin GM. (1998) A high throughput screen to identify secreted and transmembrane proteins involved in *Drosophila* embryogenesis. Proc Natl Acad Sci U S A. 95(17):9973-8.

Krainc D BG, Okamoto S, Carles M, Kusiak JW, Brent RN, Lipton SA. (1998) Synergistic activation of the N-methyl-D-aspartate receptor subunit 1 promoter by myocyte enhancer factor 2C and Sp1. J Biol Chem 273(40): 26218-26224.

Kumar S and FlyExpress Consortium (2009) A Knowledge-base of Spatiotemporal Expression Patterns at a Genomic-scale in the Fruit-fly Embryogenesis (www.flyexpress.net). Arizona State University, Tempe, Arizona 85287, USA.

Lai, Z. C., Fortini, M. E. and Rubin, G. M. (1991). The embryonic expression patterns of *zfh-1* and *zfh-2*, two *Drosophila* genes encoding novel zinc-finger homeodomain proteins. Mech Dev 34, 123-34.

Lai, Z. C., Rushton, E., Bate, M. and Rubin, G. M. (1993). Loss of function of the *Drosophila zfh-1* gene results in abnormal development of mesodermally derived tissues. Proc Natl Acad Sci U S A 90, 4122-6.

Lang AB, Wyss C, Eppenberger HM (1980). Localization of arginine kinase in muscles fibres of *Drosophila* melanogaster. J Muscle Res Cell Motil. 1980 Jun;1(2):147-61

Layden MJ, Odden JP, Schmid A, Garces A, Thor S, Doe CQ.(2006) Zfh1, a somatic motor neuron transcription factor, regulates axon exit from the CNS. Dev Biol. 15;291(2):253-63

Leatherman JL, Dinardo S (2008) Zfh-1 controls somatic stem cell self-renewal in the *Drosophila* testis and nonautonomously influences germline stem cell self-renewal. Cell Stem Cell. 3;3(1):44-54.

Lee HK, Lundell MJ.(2007) Differentiation of the *Drosophila* serotonergic lineage depends on the regulation of Zfh-1 by Notch and Eagle. Mol Cell Neurosci.;36(1):47-58

Lee RC FR, Ambros V. (1993) The *C. elegans* heterochronic gene lin-4 encodes small RNAs with antisense complementarity to lin-14. Cell 75(5): 843-854.

Lehmann R, Tautz D. (1994) In situ hybridization to RNA. Methods Cell Biol. 44:575-98

Leptin M (1991) twist and snail as positive and negative regulators during Drosophila mesoderm development. Genes Dev 5(9): 1568-1576.

Leptin M, Grunewald B (1990) Cell shape changes during gastrulation in *Drosophila*. Development 110(1): 73-84.

Lilly B, Galewsky S, Firulli AB, Schulz RA, Olson EN (1994) D-MEF2: a MADS box transcription factor expressed in differentiating mesoderm and muscle cell lineages during *Drosophila* embryogenesis. Proc Natl Acad Sci U S A 91(12): 5662-5666.

Lilly, B., Zhao, B., Ranganayakulu, G., Paterson, B. M., Schulz, R. A. and Olson, E. N. (1995). Requirement of MADS domain transcription factor D-MEF2 for muscle formation in *Drosophila*. Science 267, 688-93

Lin, M. H., Nguyen, H. T., Dybala, C. and Storti, R. V. (1996). Myocyte-specific enhancer factor 2 acts cooperatively with a muscle activator region to regulate *Drosophila tropomyosin* gene muscle expression. Proc Natl Acad Sci USA 93, 4623-8.

Lin, M. H., Bour, B. A., Abmayr, S. M. and Storti, R. V. (1997). Ectopic expression of MEF2 in the epidermis induces epidermal expression of muscle genes and abnormal muscle development in *Drosophila*. Dev Biol 182, 240-55.

Liotta D (2006) *Dmeso17A ;* A Novel inhibitor of muscle differentiation. PhD Thesis, Cardiff University.

Liotta D, Han J, Elgar S, Garvey C, Han Z and Taylor MV (2007) The *Him* Gene Reveals a Balance of Inputs Controlling Muscle Differentiation in *Drosophila*. Current Biology 17, 1409–1413.

Liu M, Su M, Lyons GE, Bodmer R.(2006) Functional conservation of zinc-finger homeodomain gene *zfh1/SIP*1 in *Drosophila* heart development. Dev Genes Evol.;216(11):683-93

Locke M (1969) The Ultrastructure of the oenocytes in the moult/intermoult cycle of an insect. . Tissue and Cell 1: 103-154.

Lovato TL BA, Cripps RM. (2005) Transcription of Myocyte enhancer factor-2 in adult *Drosophila* myoblasts is induced by the steroid hormone ecdysone. Dev Biol 288(2): 612-621.

Maqbool T and Jagla K (2007) Genetic control of muscle development : learning from *Drosophila*. J. Muscle Res. Cell. Motil. 28:397-407

Markstein M, Zinzen R, Markstein P, Yee KP, Erives A, Stathopoulos A, Levine M. (2004). A regulatory code for neurogenic gene expression in the *Drosophila* embryo. Development. 131(10):2387-94.

Menon, S.D. and Chia, W. (2001). *Drosophila* Rolling pebbles. a Multidomain protein required for myoblast fusion that recruits D-Titin in response to the myoblast attractant Dumbfounded. Dev. Cell 1,691–703.

Miller A (1950) The internal anatomy and histology of the imago of *Drosophila melanogaster*. In: Demerec M, editor. Biology of *Drosophila*. Facsimile ed: CSHL Press. pp. 420-534.

Molkentin JD BB, Martin JF, Olson EN. (1996) Mutational analysis of the DNA binding, dimerization, and transcriptional activation domains of MEF2C. Mol Cell Biol 16(6): 2627-2636.

Moore LA, Broihier HT, Van Doren M, Lehmann R.(1998) Gonadal mesoderm and fat body initially follow a common developmental path in *Drosophila*. Development ;125(5):837-44.

Morgan TH (1910). Sex Limited Inheritance in *Drosophila*. Science. Jul 22;32(812):120-122

Murre C, McCaw PS, Baltimore D (1989). A new DNA binding and dimerization motif in immunoglobulin enhancer binding, daughterless, MyoD, and myc proteins. Cell. 56(5):777-83.

Nagano Y (2000) Several features of the GT-factor trihelix domain resemble those of the Myb DNA-binding domain. Plant Physiol 124(2): 491-494.

Nguyen HT, Bodmer R, Abmayr SM, McDermott JC and Spoerelii NA (1994) D-mef2: A *Drosophila* mesoderm-specific MADS box-containing gene with a biphasic expression profile during embryogenesis. Proc. Natl. Acad. Sci. USA Vol. 91, pp. 7520-7524

Nguyen T, Wang J and Schulz RA (2002) Mutations within the conserved MADS box of the D-MEF2 muscle differentiation factor result in a loss of DNA binding ability and lethality in *Drosophila*. Differentiation 70:438–446

Nose, A., Mahajan, V. B. and Goodman, C. S. (1992) Connectin: a homophilic cell adhesion molecule expressed on a subset of muscles and the motoneurons that innervate them in *Drosophila*. Cell 70, 553-67.

Nose A, Isshiki T, Takeichi M (1998) Regional specification of muscle progenitors in *Drosophila*: the role of the *msh* homeobox gene. Development. 125:215-223.

Nüsslein-Volhard C, Wieschaus E. (1980) Mutations affecting segment number and polarity in *Drosophila*. Nature 287(5785):795-801.

Ogawa H UT, Aoyama T, Aronheim A, Nagata S, Fukunaga R. (2003) A SWI2/SNF2-type ATPase/helicase protein, mDomino, interacts with myeloid zinc finger protein 2A (MZF-2A) to regulate its transcriptional activity. Genes Cells 8(4): 325-339.

Okamoto S KD, Sherman K, Lipton SA. (2000) Antiapoptotic role of the p38 mitogen-activated protein kinase-myocyte enhancer factor 2 transcription factor pathway during neuronal differentiation. Proc Natl Acad Sci U S A 97(13): 7561-7566.

Ornatsky OI AJ, McDermott JC. (1997) A dominant-negative form of transcription factor MEF2 inhibits myogenesis. J Biol Chem 272(52): 33271-33278.

Orr-Weaver TL SJ, Rothstein RJ (1981) Yeast transformation: a model system for the study of recombination. Proc Natl Acad Sci U S A 78(10): 6354-6358.

Pan DJ, Huang JD, Courey AJ (1991) Functional analysis of the *Drosophila* twist promoter reveals a dorsal-binding ventral activator region. Genes Dev 5(10): 1892-1901.

Park M, Yaich LE, and Bodmer R (1998) Mesodermal cell fate decisions in *Drosophila* are under the control of the lineage genes numb, Notch, and sanpodo Mech. of Dev. 75 117–126

Parks AL CK, Belvin M, Dompe NA, Fawcett R, Huppert K, Tan LR, Winter CG,, Bogart KP DJ, Deal-Herr ME, Grant D, Marcinko M, Miyazaki WY, Robertson S,, Shaw KJ TM, Vysotskaia V, Zhao L, Andrade RS, Edgar KA, Howie E, Killpack, K MB, Norton A, Thao D, Whittaker K, Winner MA, Friedman L, Margolis J,, Singer MA KC, Curtis D, Kaufman TC, Plowman GD, Duyk G, Francis-Lang et al. (2004) Systematic generation of high-resolution deletion coverage of the Drosophila melanogaster genome. Nat Genetics 36(3): 288-292.

Paululat A, Breuer S, and Renkawitz-Pohl R (1999) Determination and development of the larval muscle pattern in *Drosophila melanogaster*. Cell Tissue Res 296:151–160

Postigo, AA. and Dean, DC. (1997). ZEB, a vertebrate homolog of *Drosophila* Zfh-1, is a negative regulator of muscle differentiation. Embo J 16, 3935-43.

Postigo, AA., Ward, E., Skeath, JB. and Dean, DC. (1999). *zfh-1*, the *Drosophila* homologue of ZEB, is a transcriptional repressor that regulates somatic myogenesis. Mol Cell Biol 19, 7255-63.

Pothoff MJ and Olson EN (2007) MEF2 : A central regulator of diverse developmental programs. Development 134, 4131-4140

Prokop A, Landgraf M, Rushton E, Broadie K, Bate M.(1996) Presynaptic development at the *Drosophila* neuromuscular junction: assembly and localization of presynaptic active zones. Neuron. Oct;17(4):617-26

Ranganayakulu G, Zhao B, Dokidis A, Molkentin JD, Olson EN et al. (1995) A series of mutations in the D-MEF2 transcription factor reveal multiple functions in larval and adult myogenesis in *Drosophila*. Dev Biol 171(1): 169-181.

Ranganayakulu, G., Schulz, R. A. and Olson, E. N. (1996). Wingless signaling induces nautilus expression in the ventral mesoderm of the *Drosophila* embryo. Dev Biol 176, 143-8.

Rau, A., Buttgereit, D., Holz, A., Fetter, R., Doberstein, S.K., Paululat, A., Staudt, N., Skeath, J., Michelson, A.M. and Renkawitz-Pohl,R. (2001). rolling pebbles (rols) is required in *Drosophila* muscle precursors for recruitment of myoblasts for fusion. Development 128,5061–5073.

Rebeiz M, Reeves NL, Posakony JW (2002) SCORE: a computational approach to the identification of cis-regulatory modules and target genes in whole-genome sequence data. Site clustering over random expectation. Proc Natl Acad Sci U S A 99(15): 9888-9893.

Reichhart, J. M., Ligoxygakis, P., Naitza, S., Woerfel, G., Imler, J. L. and Gubb, D. (2002). Splice-activated UAS hairpin vector gives complete RNAi knockout of single or double target transcripts in *Drosophila* melanogaster. *Genesis* 34, 160-4.

Reiter, L. T., Potocki, L., Chien, S., Gribskov, M. and Bier, E. (2001). A systematic analysis of human disease-associated gene sequences in *Drosophila* melanogaster. *Genome Res* 11, 1114-25

Romer F (1971) Molting hormones in oenocytes of the flour beetle. Naturwissenschaften 58: 324-325.

Romer F GW (1981) Arachnid oenocytes: ecdysone synthesis in the legs of harvestmen (Opilionidae). Cell Tissue Res 216(2): 449-453.

Rong YS and Golic GK (2000) Gene targeting by homologous recombination in *Drosophila*. Science 288(5473): 2013-2018.

Rong YS and Golic GK (2001) A targeted gene knockout in *Drosophila*. Genetics 157(3): 1307-1312.

Rong YS TS, Xie HB, Golic MM, Bastiani M, Bandyopadhyay P, Olivera, BM BM, Rubin GM, Golic KG. (2002) Targeted mutagenesis by homologous recombination in *D. melanogaster*. Genes Dev 16(12): 1568-1581.

Rubin, G. M. (2001). The draft sequences. Comparing species. *Nature* 409, 820-1.

Ruiz-Gomez, M. and Bate, M. (1997). Segregation of myogenic lineages in *Drosophila* requires *numb*. Development 124, 4857-66.

Ruiz-Gomez, M., Romani, S., Hartmann, C., Jackle, H. and Bate, M. (1997). Specific muscle identities are regulated by Kruppel during *Drosophila* embryogenesis. Development 124, 3407-14.

Ruiz-Gomez M (1998) Muscle patterning and specification in *Drosophila*. Int. J. Dev.Biol. 42:283-290.

Ruiz-Gomez, M., Coutts, N., Price, A., Taylor, M. V. and Bate, M. (2000). *Drosophila dumbfounded*: a myoblast attractant essential for fusion. Cell 102, 189-98.

Rushton, E., Drysdale, R., Abmayr, S. M., Michelson, A. M. and Bate, M. (1995). Mutations in a novel gene, *myoblast city*, provide evidence in support of the founder cell hypothesis for *Drosophila* muscle development. Development 121, 1979-88.

Russo, C.A.M., Takezaki, N. and Nei, M. (1995). Molecular phylogeny and divergence times of drosophilid species. *Mol Biol Evol* 12, 391-404.

Ryder E and Russell S (2003) Transposable elements as tools for genomics and genetics in *Drosophila*. Briefings in Functional Genomics and Proteomics. VOL 2. NO 1. 57–71.

Ryder E BF, Ashburner M, Bautista-Llacer R, Coulson D, Drummond J, Webster, J GD, Gunton N, Johnson G, O'Kane CJ, Huen D, Sharma P, Asztalos Z, Baisch, H SJ, Kube M, Kittlaus K, Reuter G, Maroy P, Szidonya J,, Rasmuson-Lestander A EK, Dickson B, Hugentobler C, Stocker H, Hafen E,, Lepesant JA PG, Heisenberg M, Mechler B, Serras F, Corominas M, et al. (2004) The DrosDel collection: a set of P-element insertions for generating customchromosomal aberrations in *Drosophila* melanogaster. Genetics 167(2): 797-813.

Sandmann T JL, Jakobsen JS, Karzynski MM, Eichenlaub MP, Bork P, Furlong, EE. (2006) A temporal map of transcription factor activity: mef2 directly regulates target genes at all stages of muscle development. Dev Cell 10(6): 797-807.

Schnorrer, F. and Dickson, B. J. (2004). Muscle building; mechanisms of myotube guidance and attachment site selection. Dev Cell 7, 9-20.

Sellin J, Drechsler M, Nguyen HT, Paululat A.(2009) Antagonistic function of Lmd and Zfh1 fine tunes cell fate decisions in the Twi and Tin positive mesoderm of *Drosophila* melanogaster. Dev Biol. 15;326(2):444-55.

Shalizi AK, and Bonni A.(2005) brawn for brains: the role of MEF2 proteins in the developing nervous system. Curr Top Dev Biol. 2005;69:239-66

Shin HH SJ, Chung HY, Choi SJ, Hahn MJ, Kang JS, Choi MS, Han TH. (1999) Requirement of MEF2D in the induced differentiation of HL60 promyeloid cells. Mol Immunol 36(18): 1209-1214.

Shore, P. and Sharrocks, A. D. (1995). The MADS-box family of transcription factors. Eur. J. Biochem. 229, 1-13.

Smith ST, Jaynes JB.(1996) A conserved region of engrailed, shared among all en-, gsc-, Nk1-, Nk2- and msh-class homeoproteins, mediates active transcriptional repression in vivo. Development.;122(10):3141-50.

Sokol NS, Ambros V (2005). Mesodermally expressed *Drosophila microRNA-1* is regulated by Twist and is required in muscles during larval growth. Genes Dev. 19(19):2343-54.

Soler C, Taylor MV. (2009) The *Him* gene inhibits the development of *Drosophila* flight muscles during metamorphosis. Mech Dev. 2009 Jul;126(7):595-603

Spradling AC, Stern DM, Kiss I, Roote J, Laverty T and Rubin GM (1995) Gene disruptions using P transposable elements : An integral component of the *Drosophila* genome project. PNAS : 92, 10824-10830.

St Johnston, RD (2002). The art and design of genetic screens: *Drosophila melanogaster*. Nature Rev. Genet. 3, 176–188

Stapleton M, Carlson J, Brokstein P, Yu C, Champe M, George R, Guarin H, Kronmiller B , Pacleb J, Park S, Wan K, Rubin GM and Celniker SE (2002)
A *Drosophila* full-length cDNA resource *Genome Biology* 3(12):research0080.1-0080.8

Strunkelnberg, M., Bonengel, B., Moda, L. M., Hertenstein, A., de Couet, H. G., Ramos, R. G. and Fischbach, K. F. (2001). rst and its paralogue kirre act redundantly during embryonic muscle development in *Drosophila*. Development 128, 4229-39.

Su, M. T., Fujioka, M., Goto, T. and Bodmer, R. (1999). The *Drosophila* homeobox genes *zfh-1* and *even-skipped* are required for cardiac-specific differentiation of a *numb*-dependent lineage decision. Development 126, 3241-51.

Tapanes-Castillo A, Baylies MK (2004) Notch signaling patterns *Drosophila* mesodermal segments by regulating the bHLH transcription factor *twist*. Development 131(10): 2359-2372.

Taylor MV (1995). Making *Drosophila* Muscle. Current Biology. 5(7):740-2

Taylor MV, Beatty KE, Hunter HK, Baylies MK (1995) *Drosophila* MEF2 is regulated by twist and is expressed in both the primordia and differentiated cells of the embryonic somatic, visceral and heart musculature. Mech Dev 50(1): 29-41.

Taylor MV (1996) Muscle development: a myogenic switch. Current Biol. 6:924–926

Taylor MV (2000) A novel *Drosophila*, mef2-regulated muscle gene isolated in a subtractive hybridization-based molecular screen using small amounts of zygotic mutant RNA. Dev Biol 220(1): 37-52.

Taylor, M. V. (2000). Muscle development: Molecules of myoblast fusion. Curr Biol 10, R646-8

Taylor, M. V. (2002). Muscle differentiation: how two cells become one. Curr Biol 12, R224-8.

Taylor, M. V. (2003). Muscle differentiation: signalling cell fusion. Curr Biol 13, R964-6.

Thibault ST SM, Miyazaki WY, Milash B, Dompe NA, Singh CM, Buchholz R,, Demsky M FR, Francis-Lang HL, Ryner L, Cheung LM, Chong A, Erickson C,, Fisher WW GK, Hartouni SR, Howie E, Jakkula L, Joo D, Killpack K, Laufer, A MJ, Smith RD, Stevens LM, Stuber C, Tan LR, Ventura R, Woo A,, Zakrajsek I ZL, Chen F, Swimmer C, Kopczynski C, Duyk G, Winberg ML, et al. (2004) A complementary transposon tool kit for *Drosophila melanogaster* using P and piggyBac. Nat Genet 36(3): 283-287.

Thisse, B., el Messal, M. and Perrin-Schmitt, F. (1987). The *twist* gene: isolation of a *Drosophila* zygotic gene necessary for the establishment of dorsoventral pattern. Nucleic Acids Res 15, 3439-53.

Thisse B, Stoetzel C, Gorostiza-Thisse C, Perrin-Schmitt F (1988) Sequence of the *twist* gene and nuclear localization of its protein in endomesodermal cells of early *Drosophila* embryos. Embo J 7(7): 2175-2183.

Thummel C (2001) Molecular mechanisms of developmental timing in *C. elegans* and *Drosophila*. Dev Cell 1(4): 453-465.

Venken KJT and Bellen HJ (2005) Emerging technologies for gene manipulation in *Drosophila melanogaster*. Nat. Revs. Genetics. 6: 167-178

Vafopoulou X SC (2006) Hormone nuclear receptor (EcR) exhibits circadian cycling in certain tissues,but not others, during development in *Rhodnius prolixus* (Hemiptera). Cell Tissue Res 323(3): 443-455.

Vigoreaux J (2001) Genetics of the *Drosophila* flight muscle myofibril: a window into the biology of complex systems. Bioessays 23(11): 1047-1063.

Vogler G, Urban J.(2008) The transcription factor Zfh1 is involved in the regulation of neuropeptide expression and growth of larval neuromuscular junctions in *Drosophila* melanogaster. Dev Biol. 1;319(1):78-85

Volk, T. and VijayRaghavan, K. (1994). A central role for epidermal segment border cells in the induction of muscle patterning in the *Drosophila* embryo. Development 120, 59-70.

Volk, T (1999) Singling out *Drosophila* tendon cells. TIG November 1999, volume 15, No. 11

Vorbruggen, G., and Jackle, H. (1997). Epidermal muscle attachment site-specific target gene expression and interference with myotube guidance in response to ectopic stripe expression in the developing *Drosophila* epidermis. Proc. Natl. Acad. Sci. USA *94*, 8606–8611.

Weigmann K, Klapper R, Strasser T, Rickert C, Technau G, Jäckle H, Janning W and Klämbt C (2003) FlyMove – a new way to look at development of *Drosophila.* Trends Genet 19, 310.

Williams, J. A., Bell, J. B. and Carroll, S. B. (1991). Control of *Drosophila* wing and haltere development by the nuclear *vestigial* gene product. Genes Dev 5, 2481-95.

Xie HB and Golic GK (2004) Gene deletions by ends-in targeting in *Drosophila melanogaster*. Genetics 168(3): 1477-1489.

Yarnitzky, T., Min, L., and Volk, T. (1997). The *Drosophila* neuregulin homolog Vein mediates inductive interactions between myotubes and their epidermal attachment cells. Genes Dev. *11*, 2691–2700.

Yin Z, Xu XL, Frasch M (1997) Regulation of the twist target gene *tinman* by modular cis-regulatory elements during early mesoderm development. Development 124(24): 4971-4982.

Yu YT, Breitbart RE, Smoot LB, Lee Y, Mahdavi V et al. (1992) Human myocyte-specific enhancer factor 2 comprises a group of tissue-restricted MADS box transcription factors. Genes Dev 6(9): 1783-1798.

Yu Y (1996). Distinct domains of myocyte enhancer binding factor-2A determining nuclear localization and cell type-specific transcriptional activity. J Biol Chem 271(40): 24675-24683.

Zimmermann G, Furlong E, Suyama K and Scott MP (2006) Mes2, a MADF-Containing Transcription Factor Essential for *Drosophila* Development. Developmental Dynamics 235:3387–3395, 2006

Zhang Z and Gerstein M (2003). Of mice and men: phylogenetic footprinting aids the discovery of regulatory elements. J Biol. 2 (2):11. Epub 2003 Jun 6

Websites

Tools :

Vista Genome Browser : http://pipeline.lbl.gov/cgi-bin/gateway2?bg=dm1
Match Transcription Factor binding site search software :
http://www.gene-regulation.com
InterProScan protein analysis : http://www.ebi.ac.uk/InterProScan/

Images :

www.sdbonline.org/fly/atlas/00atlas.htm
Hartenstein atlas of *Drosophila* Development
Fly Move - http://flymove.uni-muenster.de/
Fly Express - http://www.flyexpress.net/

Database :

Flybase : http://flybase.bio.indiana.edu/

Information :

Jeff Sekelsky Homologous Recombination Webpage :
http://sekelsky.bio.unc.edu/Research/Targeting/Targeting.html

Stocks :

Bloomington : http://fly.bio.indiana.edu/
Drosdel : http://www.drosdel.org.uk/
Exelixis : http://drosophila.med.harvard.edu/
Drosophila Genetic Resource Centre – Japan : http://www.dgrc.kit.ac.jp/en/
VDRC Vienna RNAi :
NIGFLY Japan RNAi : http://www.shigen.nig.ac.jp/fly/nigfly/index.jsp

Stapleton M, Carlson J, Brokstein P, Yu C, Champe M, George R, Guarin H, Kronmiller B , Pacleb J, Park S, Wan K, Rubin GM and Celniker SE (2002)
A *Drosophila* full-length cDNA resource *Genome Biology* 3(12):research0080.1-0080.8

Strunkelnberg, M., Bonengel, B., Moda, L. M., Hertenstein, A., de Couet, H. G., Ramos, R. G. and Fischbach, K. F. (2001). rst and its paralogue kirre act redundantly during embryonic muscle development in *Drosophila*. Development 128, 4229-39.

Su, M. T., Fujioka, M., Goto, T. and Bodmer, R. (1999). The *Drosophila* homeobox genes *zfh-1* and *even-skipped* are required for cardiac-specific differentiation of a *numb*-dependent lineage decision. Development 126, 3241-51.

Tapanes-Castillo A, Baylies MK (2004) Notch signaling patterns *Drosophila* mesodermal segments by regulating the bHLH transcription factor *twist*. Development 131(10): 2359-2372.

Taylor MV (1995). Making *Drosophila* Muscle. Current Biology. 5(7):740-2

Taylor MV, Beatty KE, Hunter HK, Baylies MK (1995) *Drosophila* MEF2 is regulated by twist and is expressed in both the primordia and differentiated cells of the embryonic somatic, visceral and heart musculature. Mech Dev 50(1): 29-41.

Taylor MV (1996) Muscle development: a myogenic switch. Current Biol. 6:924–926

Taylor MV (2000) A novel *Drosophila*, mef2-regulated muscle gene isolated in a subtractive hybridization-based molecular screen using small amounts of zygotic mutant RNA. Dev Biol 220(1): 37-52.

Taylor MV (2000). Muscle development: Molecules of myoblast fusion. Curr Biol 10, R646-8

Taylor MV (2002). Muscle differentiation: how two cells become one. Curr Biol 12, R224-8.

Taylor MV (2003). Muscle differentiation: signalling cell fusion. Curr Biol 13, R964-6.

Thibault ST SM, Miyazaki WY, Milash B, Dompe NA, Singh CM, Buchholz R,, Demsky M FR, Francis-Lang HL, Ryner L, Cheung LM, Chong A, Erickson C,, Fisher WW GK, Hartouni SR, Howie E, Jakkula L, Joo D, Killpack K, Laufer, A MJ, Smith RD, Stevens LM, Stuber C, Tan LR, Ventura R, Woo A,, Zakrajsek I ZL, Chen F, Swimmer C, Kopczynski C, Duyk G, Winberg ML, et al. (2004) A complementary transposon tool kit for *Drosophila melanogaster* using P and piggyBac. Nat Genet 36(3): 283-287.

Thisse, B., el Messal, M. and Perrin-Schmitt, F. (1987). The *twist* gene: isolation of a *Drosophila* zygotic gene necessary for the establishment of dorsoventral pattern. Nucleic Acids Res 15, 3439-53.